

TECHNISCHE UNIVERSITÄT MÜNCHEN

Lehrstuhl für Entwicklungsgenetik

Towards an Understanding of the Role of Apical Polarity Molecules in Neural Stem Cells and Neurogenesis

Franziska Weinandy

Vollständiger Abdruck der von der Fakultät Wissenschaftszentrum Weihenstephan für Ernährung, Landnutzung und Umwelt der Technischen Universität München zur Erlangung des akademischen Grades eines

Doktors der Naturwissenschaften

genehmigten Dissertation.

Vorsitzender: Univ.-Prof. Dr. A. Gierl

Prüfer der Dissertation:

1. Univ.-Prof. Dr. W. Wurst

2. Univ.-Prof. Dr. M. Götz

(Ludwig-Maximilians-Universität, München)

Die Dissertation wurde am 07.06.2010 bei der Technischen Universität München eingereicht und durch die Fakultät Wissenschaftszentrum Weihenstephan für Ernährung, Landnutzung und Umwelt am 09.12.2010 angenommen.

Table of Contents

| | |
|---|-----------|
| Table of Contents | I |
| Abbreviation | V |
| Abstract | IX |
| Zusammenfassung | XI |
| 1 Introduction | 1 |
| 1.1 ADHERENS JUNCTIONAL MOLECULES AND THEIR INTERACTING PARTNERS | 2 |
| 1.2 β-CATENIN DEPENDENT WNT SIGNALLING | 7 |
| 1.3 FIRST STEPS OF BRAIN DEVELOPMENT: FROM NEURULATION TO DISTINCT BRAIN STRUCTURES | 8 |
| 1.4 EMBRYONIC AND ADULT PROLIFERATIVE ZONES IN THE MOUSE CEREBRUM | 11 |
| 1.4.1 <i>Neural stem and progenitor cells in development</i> | 12 |
| 1.4.2 <i>The adult subependymal zone: origin and cellular composition</i> | 16 |
| 1.5 FUNCTION OF ADHERENS JUNCTIONAL AND APICAL PROTEINS IN NEUROGENESIS | 19 |
| 1.5.1 <i>Adherens junctions in embryonic neurogenesis</i> | 19 |
| 1.5.2 <i>Apical polarity complexes and embryonic neurogenesis</i> | 21 |
| 1.5.3 <i>β-Catenin dependent Wnt signalling in neurogenesis</i> | 22 |
| 1.6 REGIONAL HETEROGENEITY OF NEURAL STEM CELLS AND REGULATORS OF NEURONAL SUBTYPE SPECIFICATION | 25 |
| 1.6.1 <i>Neuronal fate determinants in dorsal and ventral forebrain development</i> | 25 |
| 1.6.2 <i>Generation of diverse olfactory bulb neurons</i> | 29 |
| 1.6.3 <i>Regional specification of postnatal and adult olfactory interneurons</i> | 30 |
| 1.7 AIM OF THE THESIS | 33 |
| 2 Materials | 35 |
| 2.1 COMMONLY USED BUFFERS | 35 |
| 2.2 BULK CHEMICALS | 35 |
| 2.3 KITS | 37 |
| 2.4 PROTEASE INHIBITORS | 37 |
| 2.5 TISSUE CULTURE REAGENTS | 38 |
| 3 Methods | 39 |
| 3.1 ANIMALS AND GENOTYPING | 39 |
| 3.1.1 <i>Animals</i> | 39 |
| 3.1.2 <i>Mouse tail DNA extraction</i> | 40 |
| 3.1.3 <i>Poly chain reactions</i> | 40 |
| 3.1.4 <i>Agarose gel electrophoresis of DNA</i> | 41 |
| 3.2 ANIMAL EXPERIMENTS | 41 |
| 3.2.1 <i>Anaesthesia</i> | 41 |
| 3.2.2 <i>BrdU administration</i> | 41 |

Table of Contents

| | | |
|------------|--|-----------|
| 3.2.3 | <i>Tamoxifen treatment</i> | 42 |
| 3.2.4 | <i>Perfusion and tissue preparation</i> | 42 |
| 3.3 | TISSUE CULTURE | 42 |
| 3.3.1 | <i>Preparation of coated cover slips</i> | 42 |
| 3.3.2 | <i>Preparation of primary embryonic cerebral cortical cell culture</i> | 42 |
| 3.3.3 | <i>Floating neurosphere cultures of the adult subependyma zone</i> | 43 |
| 3.3.4 | <i>Viral infection of floating neurosphere cultures</i> | 44 |
| 3.3.5 | <i>Colony forming neurosphere assay in collagen</i> | 44 |
| 3.4 | VIRUSES | 44 |
| 3.4.1 | <i>Viral expression plasmids</i> | 44 |
| 3.4.2 | <i>DNA preparation of viral plasmids</i> | 46 |
| 3.4.3 | <i>Retroviral production</i> | 46 |
| 3.4.4 | <i>Lentiviral production</i> | 47 |
| 3.4.5 | <i>Determination of viral titres</i> | 48 |
| 3.5 | IMMUNOCHEMISTRY | 48 |
| 3.5.1 | <i>General method</i> | 48 |
| 3.5.2 | <i>Antigen retrieval</i> | 49 |
| 3.5.3 | <i>Tyramide signal amplification</i> | 50 |
| 3.6 | IN-SITU HYBRIDISATION | 52 |
| 3.6.1 | <i>In vitro transcription: generation of digoxigenin labelled probes</i> | 52 |
| 3.6.2 | <i>In-situ hybridisation</i> | 52 |
| 3.7 | WESTERN BLOT ANALYSIS | 53 |
| 3.7.1 | <i>Tissue preparation</i> | 53 |
| 3.7.2 | <i>SDS-polyacrylamide gel electrophoresis (SDS-PAGE)</i> | 53 |
| 3.7.3 | <i>Transfer</i> | 54 |
| 3.7.4 | <i>Blocking, detection and scanning</i> | 54 |
| 3.7.5 | <i>Semi-quantitative western blot analysis</i> | 56 |
| 3.8 | SUBCELLULAR FRACTIONATION | 56 |
| 3.9 | β- GALACTOSIDASE REPORTER GENE ASSAY | 56 |
| 4 | Results | 58 |
| 4.1 | INFLUENCE OF CORTICAL α-E-CATENIN DEFICIENCY ON CELLULAR SIGNALLING | 58 |
| 4.1.1 | <i>Protein levels of α-E- and α-N-catenin in the <i>Emx1^{Cre}/α-catΔex2fl/fl</i> cortices</i> | 58 |
| 4.1.2 | <i>Influence of α-E-catenin loss on apical membrane proteins of the Par complex and Prominin-1</i> | 59 |
| 4.1.3 | <i>Loss of α-E-catenin does not change canonical Wnt signalling</i> | 64 |
| 4.1.4 | <i>Loss of α-E-catenin up-regulates the levels of GSK3β</i> | 66 |
| 4.1.5 | <i>Semi-quantitative analysis of α-E-catenin dependent candidate proteins</i> | 68 |
| 4.2 | ADHERENS JUNCTIONS AND PAR COMPLEX MOLECULES IN THE ADULT SUBEPENDYMAL ZONE | 70 |
| 4.2.1 | <i>Apical surface of the adult subependymal zone</i> | 70 |
| 4.2.2 | <i>Canonical Wnt signalling activity in the adult subependymal zone</i> | 71 |

| | | |
|------------|--|------------|
| 4.3 | FUNCTIONAL ANALYSIS OF ADHERENS JUNCTIONAL AND PAR COMPLEX MOLECULES IN NEUROSPHERE CULTURES | 74 |
| 4.3.1 | <i>Comparative analyses of the function of α- and β-catenin in neurosphere cultures...</i> | 74 |
| 4.3.2 | <i>Functional analysis of Par complex molecules in neurosphere cultures.....</i> | 80 |
| 4.4 | THE ROLE OF β-CATENIN IN ADULT NEUROGENESIS | 83 |
| 4.4.2 | <i>Maintenance of the pinwheel architecture of the adult SEZ despite loss of β-catenin</i> | 87 |
| 4.4.3 | <i>β-Catenin deletion does not change number of astrocytes in the lateral subependymal zone</i> | 87 |
| 4.4.4 | <i>Deletion of β-Catenin decreases the number of neuroblasts in the lateral ventricular wall.....</i> | 91 |
| 4.4.5 | <i>Loss of neuroblasts after β-Catenin deletion is caused by a decreasing stem cell pool in the lateral ventricular wall</i> | 92 |
| 4.4.6 | <i>β-Catenin is required for <i>Tbr2</i> expression in the RMS.....</i> | 92 |
| 4.4.7 | <i>The role of β-Catenin in neuronal subtype specification in the olfactory bulb.....</i> | 94 |
| 5 | Discussion | 104 |
| 5.1 | SUMMARY | 104 |
| 5.2 | α-E-CATENIN DEPENDENT SIGNALLING DURING CORTICAL NEUROGENESIS | 105 |
| 5.2.1 | <i>The loss of α-E-catenin causes only minor changes in polarity cues</i> | 105 |
| 5.2.2 | <i>α-E-Catenin does not control β-catenin signalling during early neurogenesis.....</i> | 106 |
| 5.2.3 | <i>Compensatory response of GSK3β to hyper-proliferation caused by loss of α-E-catenin from the cerebral cortex</i> | 108 |
| 5.3 | THE APICAL DOMAIN OF ADULT SEZ NEURAL STEM CELLS SHOWS CHARACTERISTIC FEATURES OF EMBRYONIC VENTRICULAR ZONE CELLS | 110 |
| 5.4 | THE PINWHEEL ORGANISATION OF THE ADULT SEZ DOES NOT DEPEND ON THE ADHESIVE FUNCTION OF β-CATENIN | 112 |
| 5.5 | THE ROLE OF ADHERENS JUNCTIONAL MOLECULES IN NEUROSPHERE CULTURES..... | 113 |
| 5.6 | THE ROLE OF THE PAR COMPLEX IN NEUROSPHERE CULTURES..... | 115 |
| 5.7 | THE DUAL ROLES OF β-CATENIN IN ADULT NEUROGENESIS <i>IN-VIVO</i>: MAINTENANCE OF THE NEURAL STEM CELL POOL AND CONTROL OF DORSAL PROGENITOR SUBTYPES | 116 |
| 5.7.1 | <i>The function of β-catenin in maintaining general adult neurogenesis.....</i> | 116 |
| 5.7.2 | <i>The prospective function of β-catenin in neural subtype specification.....</i> | 118 |
| 6 | References | 120 |
| 7 | Acknowledgements..... | 138 |
| | Curriculum Vitae | 139 |

Abbreviation

| | |
|------------------|--|
| % | Percent |
| °C | Degree Celsius |
| µg | Microgram(s) |
| µL | Microlitre(s) |
| AJ | Adherens Junction(s) |
| APC | Adenomatous Polyposis Coli |
| aPKC | Atypical Protein Kinase C |
| APS | Ammonium Peroxide Disulphate |
| bHLH | Basic helix-loop-helix |
| BLBP | Brain Lipid Binding Protein |
| BMP | Bone Morphogenetic Protein |
| BrdU | 5'-Bromo-2'-Deoxyuridine |
| BSA | Bovine Serum Albumin |
| CalB | Calbindin |
| CalR | Calretinin |
| cDNA | complementary DeoxyriboNucleic Acid |
| CFP | Cyan Fluorescent Protein |
| cm | Centimeter(s) |
| CNS | Central Nervous System |
| CO ₂ | Carbon Dioxide |
| CP | Cortical Plate |
| Cre | Cre Recombinase |
| Crib | Cdc42/Rac Interaction Binding |
| CSF | Cerebrospinal Fluid |
| Cux1/2 | Cut-Like homeoboX1/2 |
| DAPI | 4,6-diamidine-2-pheylidoleldihydrochloride |
| dATP | DeoxyAdenosine TriPhosphate |
| dCTP | DeoxyCytidine TriPhosphate |
| DCX | Doublecortin |
| dGTP | DeoxyGuanosine TriPhosphate |
| Dkk | Dickkopf |
| Dlx | Distal-Less homeoboX |
| DMEM | Dulbecco's Modified EageL Medium |
| DNA | DeoxyriboNucleic Acid |
| dNTP | DeoxyNucleoside TriPhosphate |
| dTTP | DeoxyThymidine TriPhosphate |
| e.g. | For example (Latin 'exempli gratia') |
| eCFP | enhanced Cyan Fluorescent Protein |
| EDTA | Ethylene-Diamine-tetra-Acetic-Acid |
| EGF | Epidermal Growth Factor |
| eGFP | enhanced Green Fluorescent Protein |
| Emx1 | Empty Spiracles Homeobox 1 |
| EPL | External Plexiform Layer |
| ER ^{T2} | estrogen ligand-binding domain |
| FCS | Fetal Calf Serum |
| FGF | Fibroblast growth factor |
| Fig. | Figure |
| Fzd | Frizzled |
| g | Gram(s) |

Abbreviation

| | |
|--------------|--|
| G | Gauge |
| G418 | Geneticin |
| GABA | γ -Amino Butyric Acid |
| GAD | Glutamic Acid Decarboxylase |
| GAPDH | GlycerAldehyde 3-Phosphate DeHydrogenase |
| GC | Granule Cells |
| GCL | Granule Cell Layer |
| GE | Ganglionic Eminence |
| GFAP | Glial Fibrillary Acidic Protein |
| GFP | Green Fluorescent Protein |
| GL | Glomerular Layer |
| GLAST | astrocyte-specific glutamate transporter |
| Gsh1/2 | GS Homeobox1/2 |
| GSK3 β | Glycogen synthase kinase 3 β |
| h | Hour(s) |
| HBSS | Hank's balanced salt solution |
| HCl | Hydrochloric acid |
| HEPES | 4-(2-Hydroxyethyl)-1-piperazineethanesulfonic acid |
| HERP | Hes Related Protein(s) |
| Hes | Hairy and Enhancer of Split |
| HESR | Hes Related |
| hGFAP | human Glial Fibrillary Acidic Protein |
| HIV1 | Human Immunodeficiency Virus Type 1 |
| i.e. | That is (Latin 'id est') |
| INM | Interkinetic Nuclear Migration |
| IPL | Internal Plexiform Layer |
| IRES | Internal Ribosomal Entry Site |
| ISH | In-Situ Hybridisation |
| IZ | Intermediate Zone |
| JGC | JuxtaGlomerular Cells |
| kDa | Kilodalton (molecular mass) |
| kg | Kilogram(s) |
| LDL | Low Density Lipoprotein |
| LEF | Lymphoid Enhancer binding Factor |
| LGE | Lateral Ganglionic Eminences |
| LGL | Lethal Giant Larvae |
| LRP | Receptor Related Protein |
| LTR | Long Terminal Repeat |
| LTR/SIN | Self-Inactivating Long Terminal Repeat |
| LV | Lateral Ventricle |
| M | Molar (mol/litre) |
| mA | Milliampere |
| MAPK | Mitogen Activated Protein Kinase |
| Mash1 | Mammalian Achaete Scute Homolog1 |
| Math1 | Mammalian Atonal Homolog |
| MCL | Mitral Cell Layer |
| mg | Milligram(s) |
| MGE | Medial Ganglionic Eminences |
| min | Minute(s) |
| mL | Millilitre(s) |
| mM | Millimolar |
| mm | Millimetre(s) |
| MMLV | Moloney Murine Leukemia Virus |
| mpi | Month Post Induction |
| mRNA | Messenger Ribonucleic Acid |

| | |
|---------|--|
| mTOR | Mammalian Target Of Rapamycin |
| NaCl | Sodium chloride |
| NCFC | Neural Colony Forming Cell |
| NeuroD1 | Neurogenic Differentiation1/2 |
| ng | Nanogram(s) |
| Ngn1/2 | Neurogenin1/2 |
| nm | Nanometre(s) |
| nM | Nanomolar |
| N-P40 | Nonidet-P40 |
| NSCL1/2 | Neuronal Stem Cell Leukemia1/2 |
| OB | Olfactory Bulb |
| Olig2 | Oligodendrocyte Transcription Factor 2 |
| ONL | Olfactory Nerve Layer |
| OSN | Olfactory sensory neurons |
| PAGE | Polyacrylamide Gel Electrophoresis |
| Par3/6 | Partitioning defective 3/6 homolog |
| Pax6 | Paired BoX gene 6 |
| PB1 | Phox/Bem1 |
| PBS | Phosphate Buffered Saline |
| PCNA | Proliferating Cell Nuclear Antigen |
| PCP | planer cell polarity |
| PCR | Poly chain reaction |
| PDL | Poly-D-Lysine |
| PDZ | PSD-95/Disclarge/ZO-1 |
| PFA | ParaFormAldehyde |
| PGC | PeriGlomerular Cells |
| PSA- | |
| NCAM | Polysialic Acid Neural Cell Adhesion Molecule |
| PVDF | PolyVinylidene Fluoride |
| RMS | rostral migratory stream |
| RNA | Ribonucleic Acid |
| RT | Room Temperature |
| SDS | Sodium dodecyl sulfate |
| sec | Second(s) |
| SEM | Standard Error of the Mean |
| Ser9 | Serine9 |
| SEZ | Subependymal Zone |
| sFRP | small Frizzeled Related Protein(s) |
| SGZ | SubGranular Zone |
| Shh | Sonic Hedgehog |
| shRNA | Small Hairpin Ribonucleic Acid |
| SV40 | Simian vacuolating Virus 40 promotor |
| SVZ | SubVentricular Zone |
| TAP | Transit Amplifying Precursor |
| TBE | Tris/Borate/EDTA, buffer solution containing mixture of Tris base, boric acid and EDTA |
| Tbr1/2 | T-box brain gene1/2 |
| TBS | Tris-buffered saline |
| TCF/LEF | T Cell Factor |
| TE | Tris/EDTA, buffer solution containing mixture of Tris base and EDTA |
| TEMED | TEtraMethylEthylenDiamine |
| TH | Tyrosine Hydroxlyase |
| TJ | Tight Junction(s) |
| UV | Ultraviolet |

Abbreviation

| | |
|-------|---|
| V | Volt |
| vGluT | vesicular Glutamate Transporter |
| VSVG | Vesicular Stomatitis Virus G |
| VZ | Ventricular Zone |
| WIF-1 | Wnt-inhibitory factor-1 |
| wpi | Weeks Post Induction |
| WPRE | Woodchuck Hepatitis Post-transcriptional Regulatory Element |
| WT | Wild-type(s) |
| x g | Times the acceleration of gravity (9.807 ms ²) |
| β-Gal | β-Galactosidase |

Abstract

Neurons are generated during both, embryonic development and adulthood. While embryonic neurogenesis occurs very widespread in the developing brain, it is restricted to fewer regions of the adult brain. One hallmark of embryonic and adult neural stem cells is their apical-basal polarity. This is characterised by the localisation of specialised molecules to structurally distinct membrane domains, referred to as apical and basal-lateral domain. Especially the apical, ventricular side of neural stem cells enriches proteins known to regulate morphogenesis and cell proliferation. Amongst them are the adherens junctional proteins α -E- and β -catenin, participating in the cell-to-cell contacts between neighbouring cells, as well as the Par complex members Par3 and Par6. The major aim of the present study was to investigate the role of these polarity molecules in embryonic and adult neurogenesis.

Loss of α -E-catenin during embryonic cortical development severely impairs the radial morphology of embryonic neural stem cells and induces a transient over-proliferation of the neural tissue. By using semi-quantitative western blot technique, I could demonstrate that although α -E-catenin has a major role in maintaining the radial morphology of embryonic neural stem cells it barely controls the protein levels of classical apical molecules. Moreover, the present study helped to rule out Wnt signalling as a potential cause of the proliferation phenotype seen upon loss of α -E-catenin in the developing cerebral cortex. Instead Western blot screening revealed GSK3 β as a possible molecular key player participating in the phenotype seen after α -E-catenin ablation in the dorsal telencephalon.

As still very little is known about the role of polarity molecules in adult neural stem cells, the second part of this work addresses this topic in more detail. While loss of α -E-catenin and over-expression of Par6 showed no obvious effect on the neurosphere forming capacity, deletion of β -catenin and knock-down of Par3 strongly impaired neurosphere formation. As the *in-vitro* analysis displayed the strongest phenotype after loss of β -catenin, I concentrated further on its function in the adult subependymal zone (SEZ) *in-vivo*. The SEZ lining the lateral ventricles is the largest neurogenic niche in the adult rodent brain that continuously generates young neurons migrating along the rostral-migratory stream (RMS) to the olfactory bulb (OB). Surprisingly, conditional deletion of β -catenin in adult neural stem cells using the GLAST::CreER^{T2} mouse line did not disturb the adherens junctional cell-cell-contacts in the SEZ. The molecular role of β -catenin is, however, not only limited to its structural tasks in cell-cell adhesion, but involves as well the canonical Wnt signalling. Monitoring of canonical Wnt signalling activity by BAT-gal reporter mice revealed specific labelling exclusively in the dorsal wall of the lateral ventricles, suggesting that this pathway is highly active in this region.

As glutamatergic interneurons produced during adult neurogenesis originate exclusively in the dorsal region of the SEZ, I examined the influence of loss of β -catenin mediated Wnt signalling on this subpopulation. Indeed, genetic deletion of β -catenin in the adult SEZ caused an almost complete loss of Tbr2⁺ progenitors specified to adopt glutamatergic fate. Interestingly, defects in neurogenesis continue to spread over time and manifest later in decreased number of adult neural stem cells in the lateral SEZ leading consequently to an overall reduced number of neuroblasts.

In conclusion, these data support a model of Wnt gradients specifying different neuronal progenitors reminiscent of the function of Wnt gradients during development. Moreover, despite this similarity in Wnt gradients, the present study revealed major differences in the junctional coupling between neural stem cells during development and adulthood.

Zusammenfassung

Nervenzellen werden sowohl während der Embryonalentwicklung, als auch im Erwachsenenalter gebildet. Während die embryonale Neurogenese in großen Teilen des sich entwickelnden Nervensystems stattfindet, ist sie im adulten Gehirn auf wenige Bereiche beschränkt. Ein besonderes Merkmal von embryonalen und adulten neuralen Stammzellen ist ihre apiko-basale Polarität. Diese ist durch spezifische Moleküle innerhalb strukturell abgegrenzter Membrandomänen geprägt. Die Membrandomänen werden in apikale und basolaterale unterschieden. Insbesondere die apikale, ventrikuläre Seite neuraler Stammzellen weist eine Ansammlung von Proteinen auf, die nachweislich Morphogenese und Zellproliferation kontrollieren. Zu ihnen zählen sowohl die Zelladhäsionsproteine α -E- und β -Catenin, als auch die Par-Komplex Bestandteile Par3 und Par6. Das Hauptziel der vorliegenden Arbeit war es, die Rolle dieser Polaritätsproteine in embryonaler und adulter Neurogenese zu untersuchen.

Der Verlust von α -E-Catenin während der embryonalen Hirnrindenenwicklung beeinträchtigt maßgeblich die radiale Morphologie embryonaler neuraler Stammzellen und bewirkt eine transiente Überproliferation des neuralen Gewebes. Mit Hilfe von semi-quantitativen Western Blot Analysen konnte ich zeigen, dass α -E-Catenin trotz seiner Hauptaufgabe in der Erhaltung der radialen Morphologie neuraler Stammzellen, nur einen geringfügigen Einfluss auf die Proteinmenge klassischer apikaler Moleküle hat. Weiterhin hat die vorliegende Arbeit dabei geholfen, den kanonischen Wnt-Signalweg als potentielle Ursache für die nach Entfernung von α -E-Catenin transient aufgetretene Überproliferation auszuschließen. Stattdessen gelang es mir, GSK3 β als ein mögliches Schlüsselmolekül in der Entstehung dieses Phänotyps ausfindig zu machen.

Über die Rolle von Polaritätsmolekülen in adulten neuralen Stammzellen ist bis heute ist kaum etwas bekannt. Deshalb widmet sich der zweite Teil meiner Arbeit diesem Thema ausführlicher. Während Verlust von α -E-Catenin und Überexpression von Par6 keine auffälligen Auswirkungen auf die Neurosphärenbildung hatte, führte sowohl die Deletion von β -Catenin als auch der Knockdown von Par3 zu einer starken Beeinträchtigung in der Generierung von Neurosphären. Da der Verlust von β -Catenin den stärksten Phänotyp in der *in-vitro* Analyse zeigte, habe ich außerdem die Funktion dieses Proteins *in-vivo*, in der adulten Subependymalzone (SEZ) untersucht. Die SEZ entlang der lateralen Hirnventrikel ist das größte Reservoir an Stammzellen im adulten Nagetierhirn. Tagtäglich generiert sie neue junge Neurone, die über den röhrenförmigen rostralen migratorischen Strom (RMS) zum Riechkolben migrieren. Mit Hilfe der GLAST::CreER^{T2} Mauslinie habe ich β -Catenin gezielt in

adulten neuralen Stammzellen deletiert. Überraschenderweise störte der Verlust von β -Catenin nicht die Adhäsionsverbindungen zwischen denjenigen Zellen der SEZ, die Kontakt zum Ventrikel haben. Jedoch ist die molekulare Funktion von β -Catenin nicht nur auf strukturelle Aufgaben innerhalb der Zell-Zell-Kontakte beschränkt, sondern auch eng mit dem kanonischen Wnt-Signalweg verknüpft. Die Analyse von BAT-gal-Reportermäusen, die das LacZ-Gen unter der Kontrolle eines Wnt/ β -Catenin-induzierbaren Promotors tragen, zeigte, dass lediglich eine Subpopulation innerhalb der dorsalen Wand der lateralen Ventrikel über Wnt-Responsivität verfügen. Da die adult entstehenden glutamatergen Interneurone ausschließlich der dorsalen SEZ entspringen, habe ich untersucht, ob der Verlust des Wnt/ β -Catenin-Signalweg diese Subpopulation beeinflusst. Tatsächlich führte die genetische Deletion von β -Catenin in der adulten SEZ zu einem fast vollständigen Verlust von $Tbr2^+$ Vorläuferzellen, welche dazu bestimmt sind zu glutamatergen Interneuronen zu differenzieren. Interessanterweise breitete sich der Defekt in der adulten Neurogenese mit fortschreitender Zeit weiter aus und manifestiert sich in einer geringern Anzahl an adulten neuralen Stammzellen in der lateralen SEZ. Folglich werden auch deutlich weniger Neuroblasten in der adulten SEZ gebildet.

Abschließend lässt sich sagen, dass die gewonnenen Daten ein Model unterstützen bei dem Wnt-Gradienten unterschiedliche neurale Vorläuferzellen spezifizieren. Dies erinnert stark an die Funktion von Wnt-Gradienten während der Embryonalentwicklung. Trotz der Ähnlichkeiten in Wnt-Gradienten, zeigt die vorliegende Studie auch, dass wesentliche Unterschiede in den Adhäsionsverbindungen zwischen neuralen Stammzellen während der Embryonalentwicklung und des Erwachsenenalters bestehen.

1 Introduction

The term neurogenesis describes the process by which neurons are newly generated from self-renewing and multipotent neural stem cells or from already more restricted progenitor cells. In most mammalian species, the main part of neurogenesis occurs during embryonic development. During this time, the majority of the neurons are produced that will later on contribute to complicated brain functions, such as processing sensory inputs, controlling body movements or performing higher mental activities. The formation of such a complex structure like the brain is therefore not a simple undertaking; it rather involves an integrated series of developmental steps that need to be coordinated and strictly regulated. A key point of this regulation is to define when a cell is allowed to proliferate and self-renew or when it needs to differentiate into a functionally mature unit. A number of molecules, of which some will be discussed later in this chapter, are known to control the behaviour of neural stem cells, but how these factors cooperatively act and which role they play at different stages within the neurogenic lineage is just starting to be appreciated.

In the present thesis, I have looked in detail at one key feature of neural stem cells *in-vivo*, namely their apical-basal polarity. In general, apical-basal polarity is characterised by the localisation of specialised molecules to structurally distinct membrane domains, termed apical and basal-lateral domain. The apical and basal-lateral membranes of neural stem cells are separated by adherens junctional complexes, which are mainly composed of three proteins: cadherin, α - and β -catenin. In the present study, I have used semi-quantitative Western blot analysis to find out how the loss of α -catenin in embryonic neural stem cells influences the protein expression levels of molecules shown to localise close to the adherens junctions. As some of these proteins are also known to control proliferation or differentiation, this analysis takes us a small step forward to achieving a detailed molecular view of the complex processes regulating embryonic neurogenesis.

Having studied polar signalling molecules in development, also prompted the investigation of their role in adult neural stem cells. In mammals, two specialised brain areas are known to contain the slow proliferating cells that generate neurons throughout life-time (Fig.1-6A): the subependymal zone (SEZ) lining the lateral ventricles (Altman, 1969, Lois & Alvarez-Buylla, 1993) and the subgranular zone (SGZ) of the dentate gyrus of the hippocampus (Altman & Das, 1965, Kaplan & Bell, 1984). It has been reported, that the stem cells of both regions exhibit polar morphologies characterised by a distinct basal process contacting blood vessels (Filippov *et al.*, 2003, Mirzadeh *et al.*, 2008, Tavazoie *et al.*, 2008, Shen *et al.*, 2008) and a specialised apical extension. In the case of subgranular stem cells, the apical process

spreads out in numerous small branches, which gives the cells a tree-like appearance (Filippov *et al.*, 2003, Fukuda *et al.*, 2003, Mignone *et al.*, 2004). In contrast, the stem cells of the SEZ just show a small apical endfoot having direct contact to the lateral ventricle. Although the morphological feature of the adult neural stem cells has been described extensively, still very little is known about the molecules contributing to this polarity and virtually no studies have been published as to if and how this apical-basal polarity influences adult neurogenesis. Thus, the second part of this thesis concentrates on characterising the apical surface of the SEZ. Furthermore, the function of those apical structures will be analysed using viral vector and transgenic mouse approaches.

The following sections will lead through the broad concept of neurogenesis by describing basic features of embryonic and adult neurogenic areas. But, before addressing these issues, I will focus on the molecular components being the centre of the present study: the adherens junctions.

1.1 ADHERENS JUNCTIONAL MOLECULES AND THEIR INTERACTING PARTNERS

The core of adherens junctions (AJ) is composed of intercellular interactions by transmembrane proteins of the cadherin family. Different family members are found in different tissues, but only epithelial (E), neural (N) and retinal (R) cadherins are participating in the contacts between embryonic neural stem cells (Matsunami & Takeichi, 1995, Redies & Takeichi, 1996, Stoykova *et al.*, 1997). In order to connect adjacent cells, cadherins form homodimers between each other in a calcium-dependent manner. In addition to their extracellular interactions, cadherins are at their intracellular side associated with cytoplasmic proteins that are directly or indirectly connected to the actin cytoskeleton. The intracellular tail of classical cadherins preferentially binds to p120-catenin and β -catenin (Perez-Moreno *et al.*, 2003, Yin & Green, 2004). Interestingly, under conditions where β -catenin is limited and/or modified, plakoglobin can act as a substitute (Lewis *et al.*, 1997, Miravet *et al.*, 2003, Perez-Moreno & Fuchs, 2006). In addition, β -catenin is known to interact with α -catenin. In mammals, two different α -catenins are expressed in the brain: α -E-catenin, which is most common in epithelial tissue, and α -N-catenin that is restricted to the brain (Perez-Moreno & Fuchs, 2006). Both proteins have been shown to form together with β -catenin and cadherin a complex at the plasma membrane of 1:1:1 stoichiometry (Hirano *et al.*, 1992, Aberle *et al.*, 1994, Watabe *et al.*, 1994). However, two collaborating laboratories have suggested that this ternary protein interaction is highly dynamic. In 2005, these groups published that α -catenin binds only as a monomer to β -catenin, while high local concentrations of α -catenin favour dimerisation (Drees *et al.*, 2005, Yamada *et al.*, 2005). Further analysis of those dimers revealed their role in actin filament bundling and suppression of Arp2/3-mediated actin polymerisation and branching (Drees *et al.*, 2005, Pokutta *et al.*, 2008).

Based on these findings, the formation of AJ can be discussed in a slightly new way (Fig.1-1A). The assembly of AJ starts with the targeted delivery of cadherin- β -catenin complexes to the most apical domain of the lateral plasma membrane. Nectin, another AJ transmembrane protein, plays an essential role for this process as it localises earlier at the apical-lateral side of the membrane and thereby recruits the cadherin-catenin complexes specifically to this region (Tachibana *et al.*, 2000). Subsequently, cadherin molecules of neighbouring cells establish primordial contacts in the intercellular space, while α -catenin proteins are recruited to the cytoplasmic side of the complex. Step by step transient contacts mature and expand in lateral directions by further extracellular clustering of cadherin molecules. This results finally in an accumulation and dimerisation of α -catenin molecules in the cytoplasm close to the plasma membrane, which in turn causes a rearrangement of the actin cytoskeleton at this side.

In addition to these central molecules, an extremely diverse group of proteins is also directed to the place of AJ assembly (Fig.1-1A). Two other adhesion molecules, vinculin and zonula occludens-1 (ZO-1), can bind to α -catenin (Itoh *et al.*, 1993, Watabe-Uchida *et al.*, 1998, Imamura *et al.*, 1999). Furthermore, small Rho GTPases such as Rac1, Cdc42 and RhoA, concentrate at the cadherin-mediated contacts and even modulate their formation (Braga *et al.*, 1997, Hordijk *et al.*, 1997, Kuroda *et al.*, 1997, Takaishi *et al.*, 1997, Zhong *et al.*, 1997, Cappello *et al.*, 2006, Perez-Moreno & Fuchs, 2006). In 2007, immunoelectron microscopy studies resolved that also the Notch inhibitor Numb localises next to the AJ of radial glia cells (Rasin *et al.*, 2007). Additionally, the partition defective (Par) complex, which is crucial for cell polarity, was discovered to be sorted to the apical membrane domain of embryonic neural stem cells which adjoins directly to the lateral AJ membrane (Manabe *et al.*, 2002, Imai *et al.*, 2006, Marthiens & French-Constant, 2009).

The mammalian Par complex, like its initially described invertebrate homologue in the nematode *Caenorhabditis elegans* or the fruit fly *Drosophila melanogaster*, is composed of two scaffold proteins, Par6 and Par3, and an atypical protein kinase C (aPKC) (Assemat *et al.*, 2008). Three Par6 proteins, encoded by three different genes, exist in mammals: Par6a, Par6b and Par6d, but only Par6a is expressed in the brain (Joberty *et al.*, 2000). Interestingly, the domain structure of the different Par6 proteins is highly conserved. All three contain the Phox/Bem1 (PB1), Cdc42/Rac interaction binding (Crib) and PSD-95/Disc-large/ZO-1 (PDZ) domain, which mediate the binding to other Par complex members (Bose & Wrana, 2006, see also Fig.1-1B). One direct interaction partner is aPKC, of which, upon binding, comes in close contact to its downstream effectors, such as Par3 and lethal giant larvae (LGL) (Yamanaka *et al.*, 2003). Strikingly, aPKC is the only member of the Par complex possessing an enzymatic activity that is exceptionally important for signal

transmission during complex cellular processes. Like Par6, also aPKC is encoded by more than one gene. In mammals, two different aPKC proteins have been identified: aPKC λ and aPKC ζ (Ono *et al.*, 1989, Selbie *et al.*, 1993). In contrast to conventional protein kinase Cs, aPKCs do not require calcium or diacylglycerol to become activated, but rather rely on specific protein-protein interactions (Hirano *et al.*, 2004). This is due to their lack of a C2 domain or a complete C1 domain. Instead, aPKCs exhibit a PB1 domain, which allows their binding to Par6. Two specific sites, Thr-411 and Thr-563, need to be phosphorylated for full enzymatic activation of aPKC. Its catalytic kinase domain is located in the C-terminal region and is known to phosphorylate Par3 (Akimoto *et al.*, 1994, Nagai-Tamai *et al.*, 2002). Intriguingly, this phosphorylation event has been shown to be crucial for Par3 localisation and the establishment of cell polarity (Hirose *et al.*, 2002, Nagai-Tamai *et al.*, 2002). From the Par3 gene family, only two isoforms (100kDa and 180kDa) of the Par3a locus are found to be predominantly expressed in the brain. All Par3a isoforms contain three PDZ domains, but the shortest isoform (100kDa) lacks the aPKC binding domain (Fig.1-1B). The first PDZ domain of Par3a protein was reported to bind directly the C-terminus of nectin-1 and -3, an interaction that was demonstrated to be very specific in murine radial glial cells having no typical tight but rather adherens junctions (Takekuni *et al.*, 2003). Whether nectin-1 and -3 with the help of Par3 direct Par6 and aPKC to the adherens junctions remains unknown and needs further investigation.

A key step towards the understanding how Par complex activity and consequently cell polarity is regulated came from the observation that the small Rho GTPase Cdc42 is a direct interactor of Par6a (Joberty *et al.*, 2000, Lin *et al.*, 2000). Cdc42 binds only in its active GTP-bound state to the Crib motive of Par6a, resulting in an auto-phosphorylation and activation of aPKC (Lin *et al.*, 2000, Yamanaka *et al.*, 2001, Henrique & Schweisguth, 2003, see also Fig.1-1B). However, the biochemical relationship between Par6a, Par3, aPKC and Cdc42 and the activation of the complex remains unclear. Another model suggests an inactive conformation of Par6 at the beginning of complex formation, while binding of aPKC or GTP•Cdc42 causes a conformational change, allowing the interaction of Par6 with Par3 (Gao *et al.*, 2002, Etienne-Manneville & Hall, 2003, see also Fig1-1B).

Taken together, significant progress has been made in the identification of key players involved in the establishment of AJ and cell polarity in epithelial cells. But, clearly we need to know more about the diverse functions of these proteins. In this regard, especially β -catenin deserves closer attention. Not only is β -catenin a critical component of the cadherin adhesion complex, but it is also part of the Wnt mediated pathway. The next section will first describe how the canonical Wnt signalling is activated and later focus on the protein families displaying key components of the pathway.

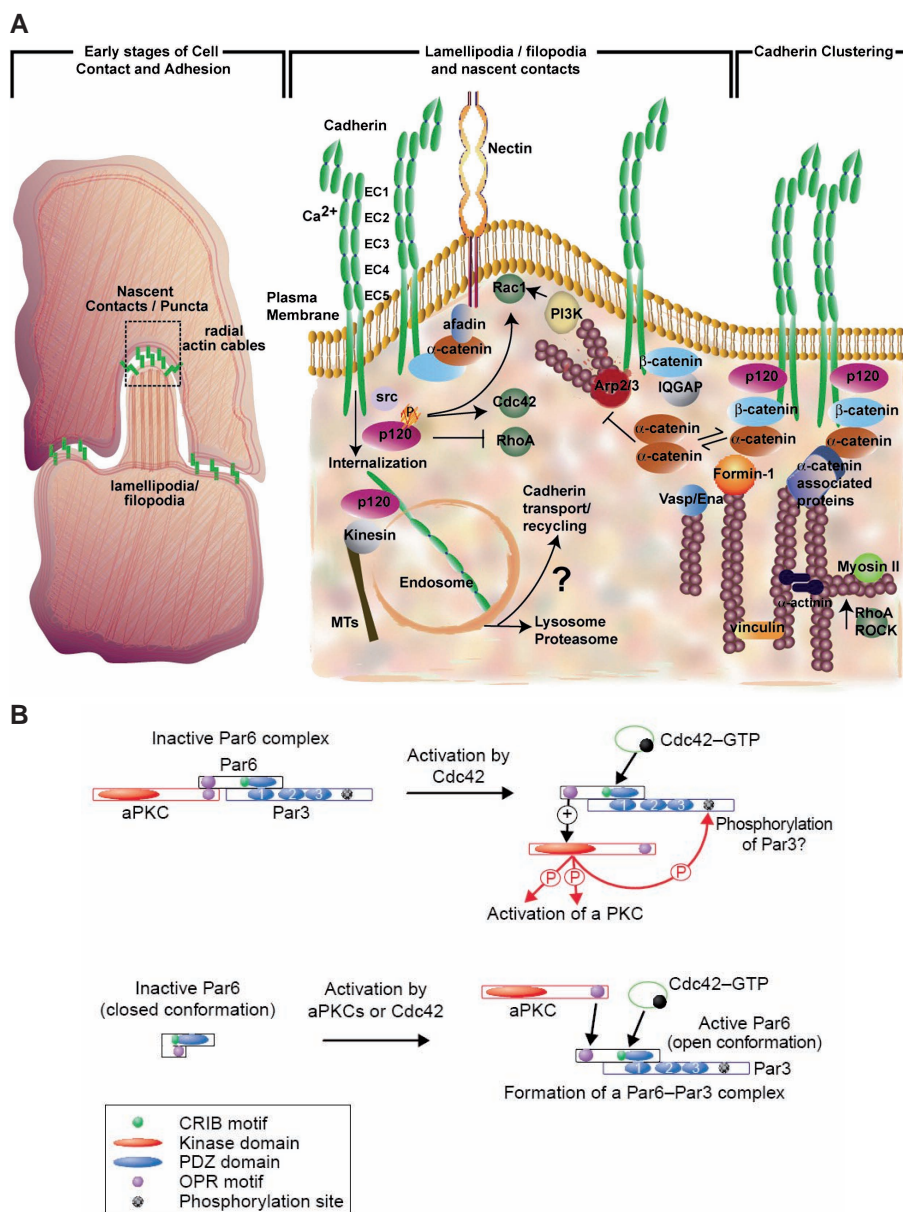


Figure 1-1. Summary of molecules contributing to the lateral and apical domain of polarised epithelial cells

A) Formation and maintenance of the adherens junctions are depicted. Adherens junction assembly is initiated by individual E-cadherin molecules from opposing cells that start to contact each other via their extracellular domain. Simultaneously, a number of molecules accumulate on the intracellular side of clustering cadherin proteins, such as β-catenin, α-catenin, p120, Cdc42, Rac, atypical protein kinase (aPKC), Par3 and Par6. Some of these proteins, like aPKC or Cdc42, are known to control adherens junction stabilisation. Moreover, activation of Rac or Cdc42 as well as dimerisation of α-catenin have been shown to regulate actin dynamics. *Adapted from Perez-Moreno and Fuchs, 2006.*

B) Two different models were suggested to underlie the activation of the Par complex. Starting point of the upper model is an inactive complex consisting of Par3, Par6 and aPKC that upon binding of GTP•Cdc42 becomes stimulated. Subsequent auto-phosphorylation of aPKC takes place, resulting in its catalytic activation. The second mechanism shown in the lower panel proposes, that Par6 is prevented from its closed confirmation by interacting with Par3, which in turn allows its binding to GTP•Cdc42 and aPKC. Thereby, aPKC becomes activated and phosphorylates important down-stream targets, like Lgl. *Adapted from Etienne-Manneville and Hall, 2003.*

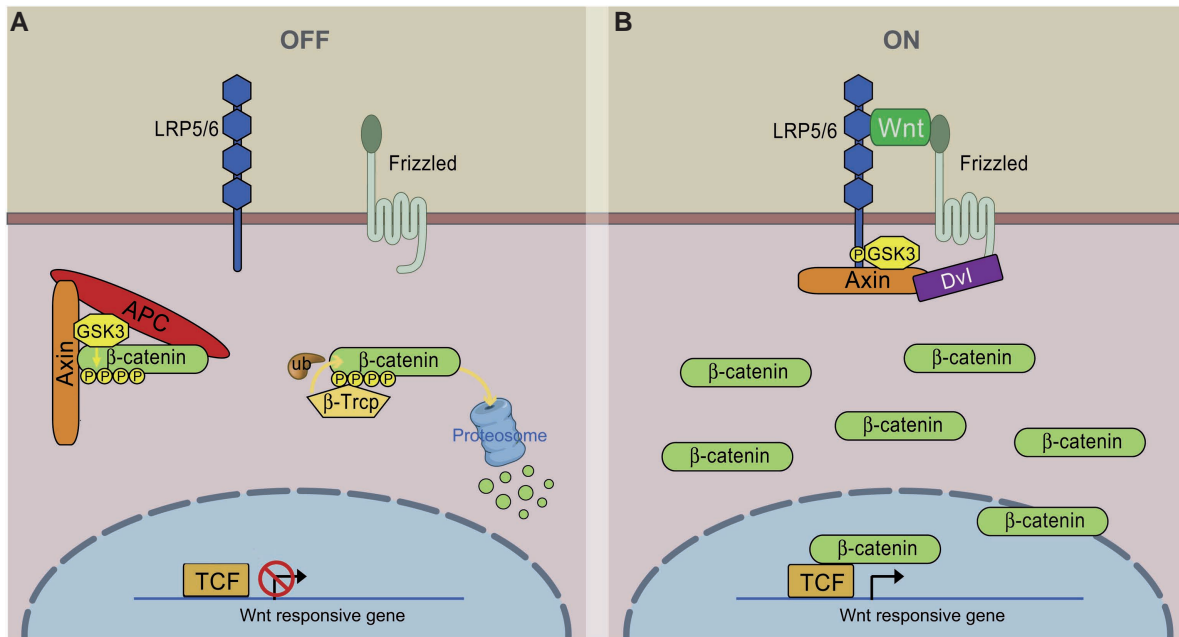


Figure 1-2. Overview of canonical β -catenin dependent Wnt signalling (Modified from MacDonald et. al, 2009)

A) In the absence of Wnt ligands, cytoplasmic β -catenin is kept in a complex with Axin, APC and GSK3 allowing its phosphorylation by GSK3 (yellow encircled Ps). Phosphorylated β -catenin is recognised by the E3 ubiquitin ligase β -Trcp, which targets β -catenin for proteosomal degradation. As a consequence, TCF/LEF dependent gene expression is repressed.

B) In the presence of soluble Wnt molecules, a receptor complex forms between frizzled and LRP5/6. Dishevelled (Dvl) recruitment by frizzled leads to recruitment of Axin and GSK3 to the intracellular side of the Wnt receptors. Subsequently, LRP5/6 gets phosphorylated by GSK3. On the other hand, GSK3-mediated phosphorylation and degradation of β -catenin is inhibited, allowing β -catenin to accumulate in the nucleus where it serves as a coactivator for TCF/LEF to activate Wnt-responsive genes.

APC: adenomatous polyposis coli, GSK3: glycogen synthase kinase 3, LRP5/6: low-density-lipoprotein receptor related proteins5/6, TCF/LEF: T cell factor/lymphoid enhancer binding factor

1.2 β -CATENIN DEPENDENT WNT SIGNALLING

In addition to its function in cell adhesion, β -catenin plays a major role in canonical Wnt signalling. This pathway is highly conserved between the different species and participates in multiple developmental events and adult tissue homeostasis (Cadigan & Nusse, 1997, Logan & Nusse, 2004). In general, activation of the canonical Wnt pathway occurs when soluble Wnt proteins bind to cell-surface receptors of the frizzled family (Fig.1-2). This interaction results in an activation of dishevelled family proteins, which in turn destabilises the Axin-glycogen synthase kinase 3β -adenomatous polyposis coli (Axin-GSK3 β -APC) complex, thereby preventing the GSK3 β from phosphorylating β -catenin (Rubinfeld *et al.*, 1996). The N-terminal phosphorylation of β -catenin normally promotes its proteolytic degradation (Aberle *et al.*, 1997, Salomon *et al.*, 1997, Behrens *et al.*, 1998). After the inhibition of the β -catenin destruction machinery, a pool of cytoplasmic β -catenin stabilises and subsequently enters the nucleus. Nuclear β -catenin interacts with DNA binding T cell factor/lymphoid enhancer binding factor (TCF/LEF) to turn on gene transcription. The vertebrate genome encodes four highly similar TCF/LEF proteins. Prominent canonical Wnt target genes are CyclinD1, Sox2, Sox9 and c-myc that all promote cell proliferation. Furthermore, genes involved in regulation of the Wnt pathway itself, like Axin, TCF1 or LEF1, have been demonstrated to be dependent on nuclear β -catenin signalling (see also: <http://www.stanford.edu/~rnusse/wntwindow.html>). It is worth mentioning, that in addition to the canonical, two non-canonical Wnt pathways have been identified: the planer cell polarity (PCP) pathway and calcium pathway (Montcouquiol *et al.*, 2006). In non-canonical signalling, Wnt ligands still bind to frizzled receptors in order to activate dishevelled, but the downstream targets do not involve GSK3 β or β -catenin.

The most widely recognised Wnt receptors are Frizzled proteins. Frizzled receptors are seven-pass transmembrane G-coupled protein receptors, which have cysteine-rich domains in their N-terminus which bind to Wnt proteins (Dann *et al.*, 2001). There are 10 reported mouse Frizzled receptors (Fzd1-10). In addition to Frizzled receptors, the canonical Wnt pathway requires single-span transmembrane co-receptors that belong to a subfamily of the low-density-lipoprotein (LDL) receptor related proteins (LRPs), the LRP5 and LPR6 (Tamai *et al.*, 2000),

Soluble Wnt molecules are lipid-modified glycoproteins that consist of usually 350-400 amino acids (Cadigan & Nusse, 1997). Sequencing of the mouse genome has revealed 19 genes encoding for different members of the Wnt family, which can be divided into 12 conserved Wnt subfamilies. The degree of similarity between the amino acid sequences of different Wnt

proteins is minimally 18%, including a conserved pattern of 23–24 cysteine residues (Cadigan & Nusse, 1997). However, some of the Wnt proteins, such as Wnt7a and Wnt7b are related closer to each other. According to their biological activities, Wnt molecules can also be divided into two functional classes: canonical and non-canonical Wnts. While Wnt-1, Wnt-3a, Wnt-8 and Wnt-10b have been shown to act via canonical signalling, Wnt-4, Wnt-5a and Wnt-11 are known effectors of the non-canonical pathways (Kuhl *et al.*, 2000).

Besides Wnt signalling agonists, a diverse group of extracellular Wnt inhibitors exists, including the secreted frizzled-related proteins (sFRP), Wnt-inhibitory factor-1 (WIF-1) and members of the Dickkopf (Dkk) family (Kawano & Kypta, 2003). The sFRPs consist of five Wnt-binding glycoproteins that resemble the membrane-bound Frizzled. The Dkk family is comprised of four structurally-related members (Dkk-1 to Dkk-4) and a unique Dkk3-related protein named soggy. Dkk proteins function as antagonists of canonical Wnt signalling by binding to LRP5/6, where in the example of Dkk1 interaction leads to the induction the rapid endocytosis of LRP5/6 (He *et al.*, 2004).

Since the discovery of the Wnt-1 gene 28 years ago (Nusse & Varmus, 1982), a complex Wnt signalling network far beyond a simple, linear cascade has emerged. By now it is clear, that canonical Wnt signalling involves many components displaying multiple distinct functions and acting in different cellular compartments. The stability of β -catenin plays a central role within canonical signalling and post-translational modifications. For example, phosphorylation and dephosphorylation of β -catenin probably regulate many crucial aspects of the Wnt pathway. Especially, the tight regulation of individual events within the Wnt pathway is fundamental for its proper function in embryonic and adult neural stem cells. However, before highlighting the known key aspects of Wnt/ β -catenin signalling in neural stem cells, I will first explain the origin and composition of the neurogenic areas being analysed in the present study. The starting point will be a brief introduction into the generation of the earliest recognisable manifestation of the developing vertebrate brain: the neural plate.

1.3 FIRST STEPS OF BRAIN DEVELOPMENT: FROM NEURULATION TO DISTINCT BRAIN STRUCTURES

Neural tissue originates from the ectoderm, an epithelium of polarised cells constituting one of the germ layers formed during early embryogenesis. The first step in the development of the vertebrate nervous system is the conversion of undifferentiated ectoderm to neuroectoderm (Fig.1-3A). Nearly 100 years ago Mangold and Spemann discovered that this conversion was initialised by a region within the mesodermal germ layer (Spemann & Mangold, 1924), now known as the Spemann's organiser in amphibians or the node in mice. Yet it took until the 1990s to identify mesodermal released factors that are responsible for the neural induction. Several studies have shown that suppression of the bone morphogenetic

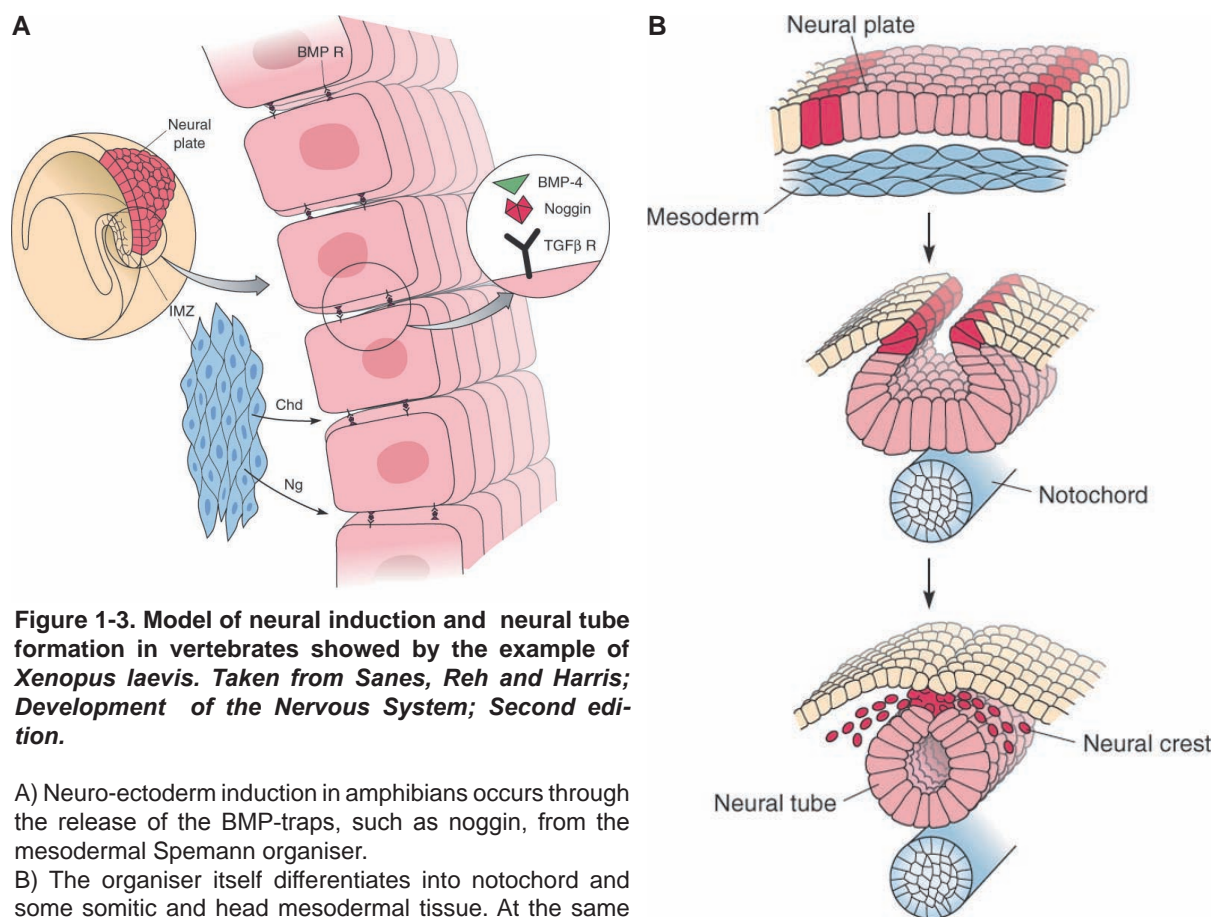


Figure 1-3. Model of neural induction and neural tube formation in vertebrates showed by the example of *Xenopus laevis*. Taken from Sanes, Reh and Harris; *Development of the Nervous System; Second edition*.

A) Neuro-ectoderm induction in amphibians occurs through the release of the BMP-traps, such as noggin, from the mesodermal Spemann organiser.

B) The organiser itself differentiates into notochord and some somitic and head mesodermal tissue. At the same time, the neuro-ectoderm forms the neural plate (light red), rolls up into a tube and delaminates from the rest of the ectoderm. A group of cells known as the neural crest (bright red) arises at the point of fusion of the neural tube. While the neural tube forms the central nervous system, the neural crest cells generate the peripheral nervous system.

BMP: bone morphogenetic protein, *BMP R*: bone morphogenetic protein receptor, *Chd*: chordin, *IMZ*: involuting marginal zone, *Ng*: noggin

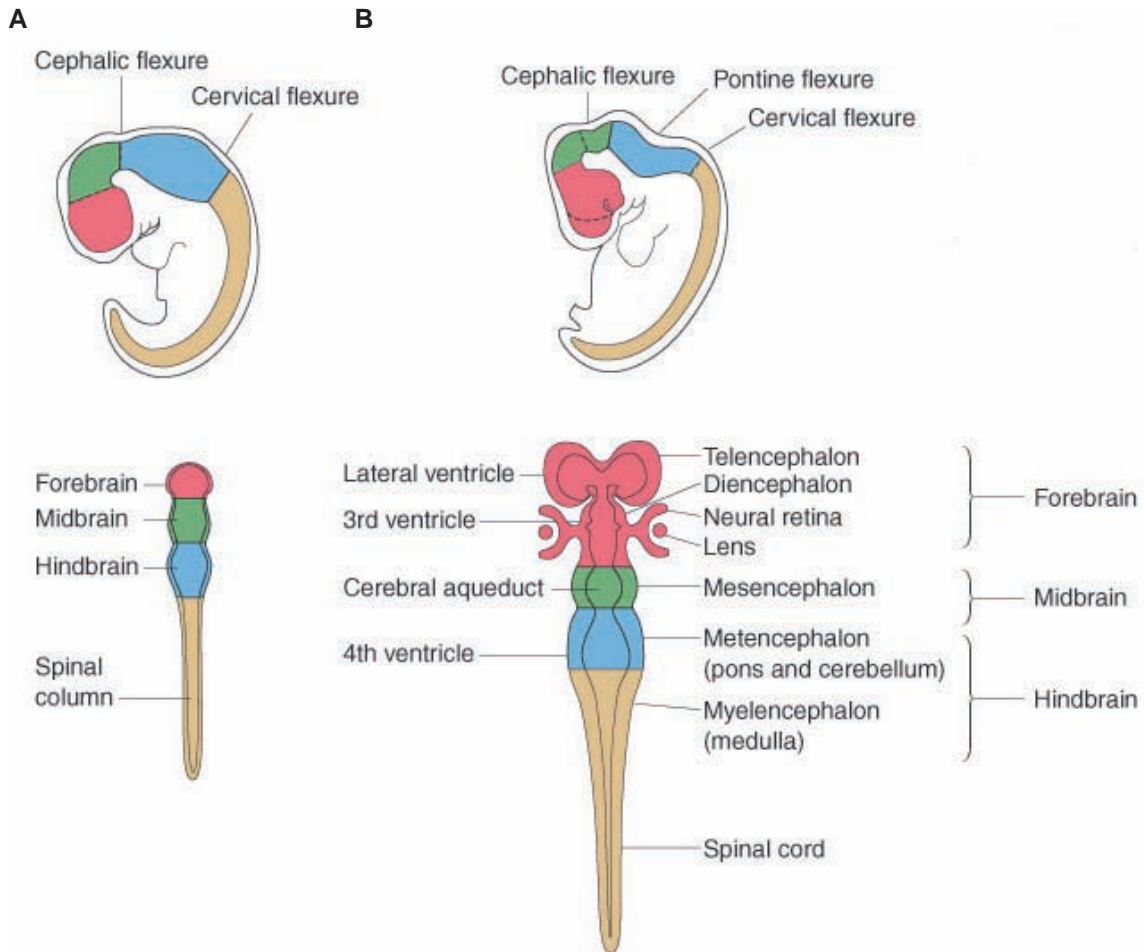


Figure 1-4. Development of primary and secondary brain vesicles using the example of a human embryo depicted here schematically in a lateral (top of the panels) and dorsal view (bottom of the panels). Taken from Sanes, Reh and Harris; *Development of the Nervous System; Second edition.*

A) The first structure to appear is the division of the embryonic brain into primary three brain vesicles, known as the forebrain (prosencephalon), midbrain (mesencephalon), and hindbrain (rhombencephalon).

B) In the next step the brain becomes further subdivided: the forebrain generates the paired telencephalic vesicles and the diencephalon, while the rhombencephalon splits into the metencephalon and the myelencephalon.

protein (BMP) signalling pathway, (Lamb *et al.*, 1993, Zimmerman *et al.*, 1996, Piccolo *et al.*, 1996, Fainsod *et al.*, 1997) allows the ectoderm to acquire neural properties and to form the neural plate. In contrast, ectoderm that exhibits BMP signalling gives rise to the epidermis of the skin.

Shortly after its formation, the neural plate begins to fold, creating the neural groove, which develops into a tubular structure called the neural tube (Fig.1-3B). This event is called neurulation and takes place between the embryonic days E7-9 in mice and three to four postovulatory weeks in humans. But, even before this process has completely finished in the posterior part of the tube, the most anterior portion starts to acquire brain specification. For that purpose, the most rostral part of the tube balloons into three primary vesicles (Fig.1-4A): forebrain (prosencephalon), midbrain (mesencephalon) and hindbrain (rhombencephalon). In a second step, the forebrain becomes subdivided into the anterior telencephalon and the more caudal diencephalon. The hindbrain further separates into a posterior myelencephalon, which form the pons and the cerebellum, and a more anterior metencephalon which forms the medulla oblongata (Melton *et al.*, 2004). The anterior-posterior regionalisation finally ends in the caudal part of the neural tube where it specifies the spinal cord (Fig.1-4B).

Furthermore, patterning takes place along the dorsal-ventral axis of the neural tube depending on the position within the tube results in different structures. In the telencephalon, for instance, the dorsal region mainly gives rise to the cerebral cortex (or pallium), while the ventral region generates the lateral and medial ganglionic eminences (LGE and MGE) resulting in the striatum and the pallidum, respectively (Fig.1-7). Interestingly, vast areas of the telencephalon are later in development populated by inhibitory interneurons that migrate all the way from the ganglionic eminences into the cerebral cortex (Wichterle *et al.*, 2001, for review see: Marin & Rubenstein, 2001, Stuhmer *et al.*, 2002).

1.4 EMBRYONIC AND ADULT PROLIFERATIVE ZONES IN THE MOUSE CEREBRUM

Before addressing the telencephalic neurogenic areas and its cellular components in more detail, it is necessary to specify the term neural stem cells further. As already briefly mentioned, multipotent stem cells are usually defined by two criteria: namely their self-renewal that is ideally maintained for an unlimited number of cell divisions and their potential to give rise to multiple, differentiated cell types (for review see: Götz & Huttner, 2005). In this work I will use the term neural stem cells to indicate primary progenitor cells at different developmental stages that expand into a limited number of lineages, generating differentiated neurons or glial cells.

1.4.1 Neural stem and progenitor cells in development

The mouse brain consists of approximately 75 million nerve cells and 25 million glia (Williams, 2000). The source of all these brain cells are the neuroepithelial cells, of which both the single layered neural plate and neural tube are composed. Neuroepithelial cells span the wall of the neural tube – namely the wall of the telencephalic vesicles – possessing both an apical (ventricular) and basal (pial) membrane domain. At their ventricular surface, neuroepithelial cells display a primary cilium and are attached to their neighbouring cells by adherens junctions (AJ), tight junctions (TJ) as well as gap junctions (Shoukimas & Hinds, 1978, Astrom & Webster, 1991, Aaku-Saraste *et al.*, 1996, for review see: Götz & Huttner, 2005). Divisions of the neuroepithelial cells occur at the side close to the ventricle. During interphase, the cells move their nucleus towards the basement membrane, and finally return to the apical surface where they will undergo mitosis again. This complex mitotic behaviour, known as interkinetic nuclear migration (INM), was first described in 1935 (Sauer, 1935) and causes the misleading impression that the neuroepithelium is stratified (hence referred to as pseudostratified epithelium). The cell layer containing the moving nuclei of embryonic neural stem cells is known as the ventricular zone (VZ).

Initially, neuroepithelial cells divide symmetrically, generating two radial daughter cells in order to amplify the pool of neural stem cells and to increase the surface area of the tissue by lateral expansion (Fig.1-5A). Moreover, later in development some neuroepithelial cells undergo also asymmetric divisions thereby producing the first neurons. In this regard, the division is considered asymmetric with respect to the ultimate fate of the daughter cells, because it results in a stem cell, which remains in the VZ, and a daughter cell which migrates along the radial glia outward to settle in the preplate (for review see: Casanova & Trippe, 2006). Thus, the epithelial tissue starts to grow in thickness, requiring the apical neural stem cells to further expand their radial process.

The onset of neurogenesis appears to be around E11 in the mouse telencephalon. By this time the transition of neuroepithelial cells to a different type of neural stem cell, i.e. the radial glial cell, takes place (Pinto & Götz, 2007). The transition does not happen rapidly and radial glia cells continue to share many characteristics of neuroepithelial cells. For example, radial glia maintain the radial bipolar morphology with a basal process touching the basal lamina and a single ciliated apical endfoot lining the ventricle. Moreover, radial glial cells undergo INM and divide at the ventricular surface. Only the movement of the radial glia nucleus is further limited than that of an epithelial cell, as it extends basally just to the boundary of the arising cortical neuronal layer.

However, the transition of neuroepithelial cells to radial glial cells is also marked by changes. The apical neural stem cells not only loose their functional TJ at the ventricular endfeet (Aaku-Saraste *et al.*, 1996), but they also upregulate a number of astroglial markers such as

vimentin, nestin, the β -subunit of S100 protein (S100 β) and the brain lipid-binding protein (BLBP) (Hartfuss *et al.*, 2001, Malatesta *et al.*, 2003). Furthermore, the cells start to build astrocyte-like specialised contacts with endothelial cells of the developing telencephalic vasculature (Takahashi *et al.*, 1990, Misson *et al.*, 1991). The mode of cell divisions occurring in the cerebral cortex changes dramatically over that time. Although, radial glial cells are still symmetrically self-renewing (about 30% in the dorsal telencephalon at E13.5, (Konno *et al.*, 2008)), the majority of cells tend to undergo asymmetric self-renewing divisions, generating directly or indirectly all remaining neurons in the developing cortex (Fig.1-5B). Indirect neurogenesis occurs via the production of another class of mitotic cells, the intermediate progenitors. Time-lapse imaging has revealed that those progenitors migrate away from their ventricular place of birth and populate a secondary proliferative layer (Noctor *et al.*, 2004, Miyata *et al.*, 2004). As this second progenitor zone forms basally directly adjacent to the VZ it is referred as subventricular zone (SVZ). The intermediate progenitors are also called basal progenitors as they are located at further basal positions. Importantly, the vast majority (~90%) of SVZ progenitors undergo symmetric terminal division by generating two neurons, while only ~10% of them produce a second generation of basal progenitors (Haubensak *et al.*, 2004, Noctor *et al.*, 2004, Wu *et al.*, 2005). Furthermore, in contrast to their apical mother cells, basal progenitors have a multipolar, rather than a radial, morphology. They show no distinct basal or apical processes, and are therefore both non-epithelial and unpolarised (Attardo *et al.*, 2008, Noctor *et al.*, 2008, Fish *et al.*, 2008). In addition, basal progenitors differ from neuroepithelial and radial glial cells by the expression of specific transcription factors such as T-box brain gene2 (Tbr2) (Englund *et al.*, 2005), Cux1 and Cux2 (Nieto *et al.*, 2004), Svet1 (Tarabykin *et al.*, 2001) and Neurogenin2 (Ngn2) (Miyata *et al.*, 2004).

The characteristic differences between those apical neural stem cells that are self-renewing and those basal progenitors that undergo mostly only one round of division raises the question as to how the proliferative behaviour of telencephalic cells is regulated. Therefore, I have concentrated the first part of my thesis work on a mouse mutant lacking the polarised morphology of radial glia as well as the proliferation control of the dividing cells within the developing cerebral cortex. One key problem was to analyse if the generation of naturally apical sorted proteins within radial glia cells is altered under these mutant conditions and how one may explain the over-proliferation phenotype observed.

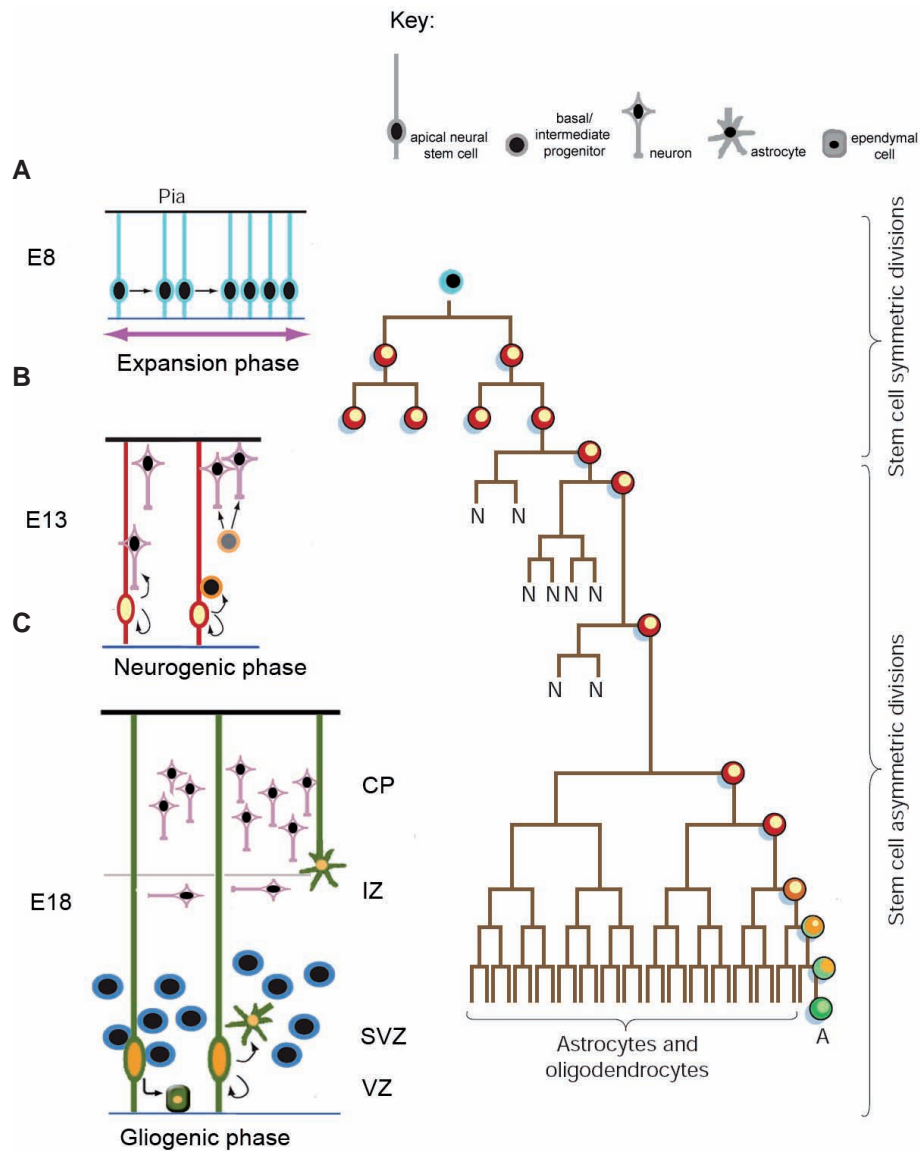


Figure 1-5. Model of neural stem cell behaviour at different developmental stages of the murine telencephalon (Modified from Temple, 2001 and Fish et al., 2008)

A) At embryonic day (E)8 neural stem cells (at this stage neuroepithelial cells) mainly self-renew by generating two apical daughter cells, and thus expand the tissue in lateral directions.

B) At mid-neurogenesis (around E14 in the cerebral cortex) all ventricular zone (VZ) cells are now radial glia. Some generate only radial glial cells by symmetric self-renewing divisions, while others are neurogenic, in which case they divide asymmetrically self-renewing and generate additionally a postmitotic neuron (N in the lineage tree) or basal progenitors. Basal progenitors, which accumulate in the subventricular zone (SVZ), in turn divide symmetrically producing mostly two neurons or rarely two neurogenic basal progenitors.

C) At late neurogenesis, from E18 on, mostly gliogenic radial glial cells remain. The majority divide asymmetrically by generating glial intermediate progenitors and another more restricted radial glia cell, which transforms eventually into an astrocyte or ependymal cell. However, a minority of radial glia cells retain apical contact, divide symmetrically and continue to function as neural stem cells in the neonates. A subpopulation of those will transform into adult neural stem cells (A in the lineage tree) of the subependymal zone, which will produce neurons throughout life-time.

A: adult neural stem cell; CP: cortical plate; IZ: intermediate zone; N: neuron; SVZ: subventricular zone; VZ: ventricular zone

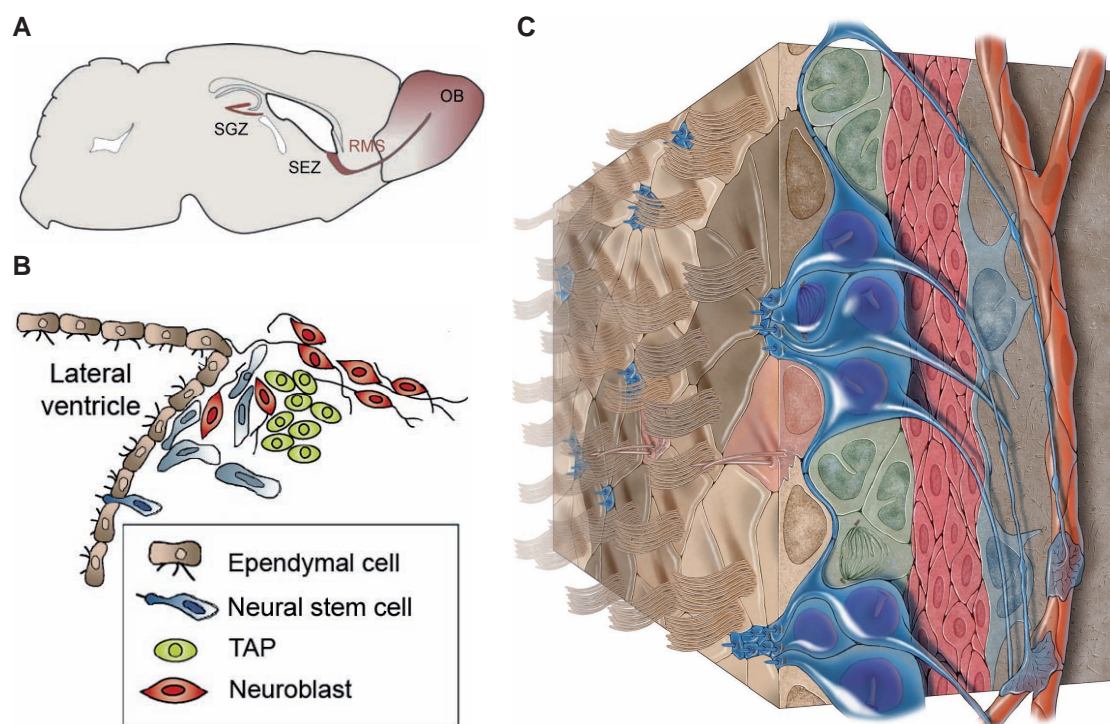


Figure 1-6. Adult neurogenic niches

A) Schematic illustration of a sagittal section through the adult mouse brain highlighting the regions of adult neurogenesis: the subependymal zone (SEZ) located at the lateral ventricle wall and the subgranular zone (SGZ) of the hippocampal dentate gyrus. Note also the rostral migratory stream (RMS), the migration route that newly generated neuroblasts take to travel from the SEZ to their final position in the olfactory bulb (OB). *Modified from Ma et al., 2009.*

B) The SEZ contains at least four distinct cell types: (1) the ependymal cells lining the ventricle; (2) the slow-proliferating neural stem cells with astroglia properties, that further give rise to (3) fast-proliferating transit-amplifying precursors (TAPs) and (4) neuroblasts which are generated by TAPs. *Modified from Ninkovic and Götz, 2007.*

C) Three-dimensional model of the adult subependymal neurogenic niche showing stem cells (blue), TAPs (green) and neuroblasts (red). Adult neural stem cells within the SEZ exhibit a striking apical-basal polarity characterised by a long basal process terminating on blood vessels (orange) and an apical endfoot at the ventricular surface. Ependymal cells (brown and peach) are arranged in a pinwheel-like structure (light and dark brown patterns) surrounding the apical surfaces of the stem cells. *Modified from Mirzadeh et al., 2008.*

1.4.2 The adult subependymal zone: origin and cellular composition

Neurons are not the only cells that need to be generated during brain development. Another very abundant cell type is obviously the neuroglia. Over the course of CNS development, a shift from neurogenesis to gliogenesis occurs, which is characterised by the generation of astrocytes, ependymal cells and oligodendrocytes (Fig.1-5C). Studies using retroviral labelling of SVZ progenitors suggest that radial glial cells generate oligodendrocytes through oligodendrocyte progenitor cells (Levison *et al.*, 1993, Levison & Goldman, 1993, Luskin & McDermott, 1994). In addition, some neonatal radial glia cells convert directly into ependymal cells, making up the walls of the CNS ventricles, whereas the remaining radial glia cells transform into astrocytes (Noctor *et al.*, 2008, for review see Kriegstein & Alvarez-Buylla, 2009). Thus, soon after birth, radial glia, basal progenitors and the two proliferative zones that they have built diminish.

However, a very restricted region along the walls of the lateral ventricles maintains neural stem cells until adulthood (Fig.1-6A). But, unlike embryonic neural stem cells, all cell bodies of the actively proliferating cells are now displaced subjacent to the newly formed ependymal layer. Therefore, this germinal region is referred to as subependymal zone (SEZ). Beside the cubical-shaped ependymal cells (type E cells) that line the walls of the postnatal and adult ventricles, three other cell types are resident in the SEZ as depicted in Fig.1-6B and C: the neural stem cells (type B cells), the transit-amplifying precursors (TAPs or type C cells) and the neuroblasts (type A cells). Interestingly, experiments using a Cre-lox-based strategy to specifically label neonatal radial glia have confirmed that postnatal/adult neural stem cells in the SEZ are direct descendants of VZ stem cells (Merkle *et al.*, 2004, Tramontin *et al.*, 2003, Alvarez-Buylla *et al.*, 2001).

Hence, it is not surprising, that adult and embryonic neural stem cells share characteristic properties like the expression of the marker antigens vimentin, nestin and RC2 (Doetsch *et al.*, 1999a, Doetsch *et al.*, 1999b). Moreover, adult neural stem cells are polarised like radial glia cells, possessing an apical endfoot with a primary cilium in direct contact to the ventricle and a long basal process that terminates on a blood vessel (Mirzadeh *et al.*, 2008, Shen *et al.*, 2008, Tavazoie *et al.*, 2008). The apical endfeet form junctional complexes between each other and with adjacent ependymal cells (Mirzadeh *et al.*, 2008). While at an ultrastructural level the connections between two adult neural stem cells appear almost identical to the symmetric discontinuous adherens junctions between radial glial cells, the tight and asymmetric adherens junctions found between adult neural stem cells and ependymal cells are different (Mirzadeh *et al.*, 2008). Another feature of the apical SEZ surface is its pinwheel organisation marked by the clustering of the thin apical neural stem cell processes in the centre, which are surrounded by the large somata of the ependymal cells (Mirzadeh *et al.*,

2008).

In addition to their radial glia properties, adult neural stem cells also show hallmarks of differentiated astrocytes, including the expression of the glial fibrillary acidic protein (GFAP). Furthermore, in sharp contrast to radial glia, adult neural stem cells are cycling very slowly. Therefore, they can be easily visualised by administration of the DNA-base analogue BrdU using the label-retaining approach. The basic principle of this method is that the DNA replication during S-phase allows the incorporation of BrdU into the genome of all dividing cells. As rapidly proliferating cells dilute the BrdU over time by incorporating new unlabelled DNA bases during following S-phases, and postmitotic cells migrate away, this mark will only remain within the slowly dividing adult neural stem cells in the SEZ (Carlen *et al.*, 2002, Colak *et al.*, 2008, Tavazoie *et al.*, 2008).

In 1992, Reynolds and Weiss showed that epidermal growth factor (EGF) and fibroblast growth factor2 (FGF2) function as mitogens to enhance the growth of adult neural stem cells and their progeny *in-vitro* (Reynolds & Weiss, 1992). Based on those findings, the scientists developed an *in-vitro* method for culturing and propagating neural stem cells isolated from neurogenic regions. In the presence of EGF and FGF2 these cells form non-adherent spherical clusters of proliferating cells with one sphere originating from a single progenitor or stem cell. This technique is referred to as the neurosphere assay and assesses the stem cell hallmarks of self-renewal and multipotency. The self-renewing capacity of neural stem cells is determined by number of passages, i.e. the respective rounds that a single stem cell can generate a new neurosphere. The multipotency is investigated by exposing neurosphere cells to differentiating conditions and analysing their fate. Upon withdrawal of EGF and FGF2, neurosphere cells deriving from multipotent neural stem cells differentiate into the three main cell types of the brain: neurons, astrocytes and oligodendrocytes.

It is worth noting, that recently many studies have questioned the clonality of the sphere assay (Singec *et al.*, 2006, Jessberger *et al.*, 2007, Mori *et al.*, 2007, Coles-Takabe *et al.*, 2008). It has been shown, that the high motility of neurosphere forming cells results frequently in the growth of chimeric neurospheres rather than the clonal expansion of single sphere-forming cells (Singec *et al.*, 2006, Jessberger *et al.*, 2007, Mori *et al.*, 2007, Coles-Takabe *et al.*, 2008). To overcome this problem more accurate techniques have been developed. One very elegant approach is the neural colony-forming cell (NCFC) assay, a semi-solid collagen-based assay (Louis *et al.*, 2008). This assay guarantees clonality of the sphere assay, as the very motile neurosphere forming cells stay separated from each other, do not cluster and therefore do not generate merged spheres. Moreover, it allows the investigation of neurosphere formation by neural stem cells lacking adherens junction molecules by capturing the neural stem cell progeny in close proximity to the cell generating

the colony. Another advantage of the collagen-based approach over the free-floating neurosphere assay is the ease with which one can discriminate, based on sphere-size, colonies originating from multipotent neural stem or bi- and uni-potent progenitor cells.

As already indicated above, the transit-amplifying progenitors represent another class of cycling cells within the SEZ. They originate directly from the relatively quiescent neural stem cells and are, in contrast to their mother cells, fast-proliferating. Thus, TAPs can be detected by a single BrdU pulse given one hour before sacrifice. Recent studies have proposed that the TAPs divide in close vicinity to blood vessels, often contact the vasculature (Tavazoie *et al.*, 2008) and express the EGF receptor (Morshead *et al.*, 1994, Seroogy *et al.*, 1995, Weickert *et al.*, 2000, Doetsch *et al.*, 2002). Like basal progenitors in embryonic development, the transit-amplifying cells do not directly contact the lateral ventricles and are thought to be already more restricted in their fate. At least two different lineages of the fast-proliferating intermediate progenitors have been identified within the SEZ: oligodendrocytic TAPs that generate oligodendrocytes migrating towards the white matter (Hack *et al.*, 2005, Marshall *et al.*, 2005, Menn *et al.*, 2006, Colak *et al.*, 2008) and the neurogenic TAPs that give rise to immature neuroblasts travelling via the rostral migratory stream (RMS) into the OB (Fig.1-6A and B) (Doetsch *et al.*, 2002, Parras *et al.*, 2004, Hack *et al.*, 2005, Menn *et al.*, 2006, Colak *et al.*, 2008).

Thousands of neuroblasts are born within the SEZ every day. During their journey through the RMS, which appears between white matter and striatum in rostral directions, they form a network of chains to move along each other. These chains are ensheathed by astrocytes (Jankovski & Sotelo, 1996, Lois *et al.*, 1996, Peretto *et al.*, 1997) that may secrete factors to enhance the migration of the new-born cells (Mason *et al.*, 2001). Notably, blood vessels running parallel in the RMS serve the moving neuroblasts as a scaffold and guidepost simultaneously (Bovetti *et al.*, 2007, Tavazoie *et al.*, 2008, Snayyan *et al.*, 2009). Neuroblasts migrate in a stepwise manner by extending first a prominent leading process tipped by a growth cone followed by translocation of their cell body (Kishi, 1987, Lois & Alvarez-Buylla, 1994, Wichterle *et al.*, 1997). Doublecortin (DCX), a microtubule-associated protein important for neuronal migration in the embryo (Francis *et al.*, 1999), is highly expressed in neuroblasts as well is the neural cell adhesion molecule being posttranslational modified by polysialic acid (PSA-NCAM) (consider rephrasing this sentence) (Bonfanti *et al.*, 1992, Seki & Arai, 1993). Even though neuroblasts show properties of already differentiated neurons, they continue to divide in the SEZ and on their way to the OB (Coskun & Luskin, 2002). Thus, they also appear positive for BrdU following a short pulse (Luskin, 1993).

After reaching the bulb, the neuroblast chains detach and cells start to migrate radially to various OB layers. In particular, reelin, the matrix glycoprotein tenascin-R and prokineticin-2 were shown to act as detachment signals for chain-migrating neuroblasts (Hack *et al.*, 2002,

Saghatelyan *et al.*, 2004, Ng *et al.*, 2005). Only a fraction of these cells survive to complete their differentiation into granule and periglomerular interneurons and their integration into the olfactory neuronal network, while approximately half of the newborn neurons fail and die after a few weeks (Petreanu & Alvarez-Buylla, 2002, Kempermann *et al.*, 2004).

The last cell type found within the ventricular wall, which gives the neurogenic region its name, are the ependymal cells. The main feature of these cells is a bundle of motile cilia on their apical surface (Doetsch *et al.*, 1997, Mirzadeh *et al.*, 2008) which extend into the cerebrospinal fluid (CSF) inside the ventricular lumen. Based on the number of cilia, at least two sorts of ependymal cells can be distinguished: E1 cells, possessing approximately 50 motile cilia, and E2 cells, having only two long cilia (Mirzadeh *et al.*, 2008). While the direct function of the E2 cells remains unknown, the beating activity of motile cilia was suggested to play a role in maintaining the flow of CSF through the ventricular system (Worthington & Cathcart, 1963, Cathcart & Worthington, 1964, Sawamoto *et al.*, 2006). Moreover, ependymal cells may supply the SEZ stem cells with nutrients and growth factors.

In 1999, it was proposed that ependymal cells themselves would act as slowly proliferating neural stem cells (Johansson *et al.*, 1999). But, this possibility could not be confirmed, since several groups were unable to isolate multipotent stem cells from purified ependymal cells (Chiasson *et al.*, 1999, Laywell *et al.*, 2000, Capela & Temple, 2002). However, after injury, differentiated ependymal cells are capable to enter the cell cycle and to proliferate. They produce scar-forming glial cells and oligodendrocytes after spinal cord injury (Meletis *et al.*, 2008) and give rise to neuroblasts and astrocytes in response to stroke (Carlen *et al.*, 2009). Overall, the above information indicates that the adult neurogenic niche along the wall of the lateral ventricle shares basic structural properties with the ventricular zone of the embryonic brain. Both regions contain highly polarised neural stem cells with direct contact to the ventricle, which allows the propagation of signals from the cerebrospinal fluid to the neural stem cells. By now many studies have been published identifying molecules that are essential to maintain the polarised structure of embryonic neural stem cells. Due to the importance of these data to the results reported in this thesis, I will now discuss those findings in more detail.

1.5 THE FUNCTION OF ADHERENS JUNCTIONAL AND APICAL PROTEINS IN NEUROGENESIS

1.5.1 Adherens junctions in embryonic neurogenesis

A variety of cadherin molecules are present in the vertebrate brain. Strikingly the expression pattern of different cadherin subtypes is region specific. For more than 20 years it has been

known that cells expressing different cadherins tend to segregate *in-vitro*, while those that possess the same cadherins tend to preferentially aggregate together (Nose *et al.*, 1988, for review see Halbleib & Nelson, 2006). Also, in the developing telencephalon the crucial role of Ca^{2+} dependent adhesion in cell sorting has been shown (Götz *et al.*, 1996).

Experiments affecting adherens junctional core proteins during cortical development have demonstrated that anchoring of VZ stem cells is crucial for tissue organisation and stem cell behaviour. For example, loss of N-cadherin in dorsal telencephalic neuroepithelial cells disrupted the adherens junctions (AJ) localised in their apical endfeet as well as their connections to the basement membrane (Kadowaki *et al.*, 2007). Furthermore, N-cadherin deficient cortices showed a scattered distribution of differentiated neurons throughout the tissue (Kadowaki *et al.*, 2007). Similar phenotypes were observed in the absence of α -E- or β -catenin from the forebrain, although these mutants showed additional dramatic changes in proliferation (Lien *et al.*, 2006, Machon *et al.*, 2003, Schmid, 2007). While loss of β -catenin during corticogenesis resulted in reduced proliferation (Machon *et al.*, 2003, Schmid, 2007), α -E-catenin deficient brains displayed hyperplasia induced by an increase in the number of mitotic cells (Lien *et al.*, 2006, Schmid, 2007). One can appreciate, that the two different catenins cause opposing cell cycling behaviours, by knowing the dual role of β -catenin in cell-cell adhesion as well as in the canonical Wnt pathway. Indeed, the prominent proliferative potential of Wnt signalling during cortical development was confirmed by a variety of different *in-vivo* approaches trying to specifically manipulate the signalling without interfering with the function of β -catenin in adhesion (Chenn & Walsh, 2002, Chenn & Walsh, 2003, Woodhead *et al.*, 2006). In general, over-activation of the canonical signalling resulted in decreased cell cycle exit and differentiation, whereas reduction of the signalling pathway caused the reverse phenotype (Chenn, 2008). After the next section more information on the role of canonical Wnt signalling in neurogenesis will be provided.

Contrary to β -catenin, which, as a central part of the Wnt signalling cascade, is linked in a straight line to transcriptional regulation of cell cycle behaviour, direct mechanisms underlying the proliferative control of α -catenin are not well understood. In regard to the over-proliferation phenotype observed after α -E-catenin deletion, multiple signalling pathways were suggested to be involved. For example, analysis of hyper-proliferating α -E-catenin deficient epidermal cells showed an increased activation of the Ras dependent mitogen-activated protein kinase (MAPK) pathway (Vasioukhin *et al.*, 2001). In addition, microarray profiling of α -E-catenin null keratinocytes determined up-regulation of NF κ B target genes (Kobielak & Fuchs, 2006). In contrast to hyperplasia in α -E-catenin lacking skin epithelium, the over-proliferation phenotype after α -E-catenin deletion in the brain has been related to an over-stimulation of the sonic hedgehog (Shh) pathway (Lien *et al.*, 2006). For a long time, Shh signalling has been known to be involved in stem cell maintenance and cancerogenesis

(Evangelista *et al.*, 2006). As α -catenin via its binding to β -catenin at the plasma membrane could also influence the amount of β -catenin that enters the nucleus, canonical Wnt signalling is another important pathway through which α -catenin may affect proliferation. Indeed, over-expression of α -catenin in cancer cell lines caused a decrease in β -catenin dependent transcription (Giannini *et al.*, 2000, Merdek *et al.*, 2004). Another interesting molecule that might contribute to the phenotype seen in α -E-catenin conditional knock-out brains is α -N-catenin. It is also expressed in ventricular cells (Stocker & Chenn, 2006) and may, in the absence of α -E-catenin, play a compensatory role in the process of AJ assembly and maintenance.

However, α -N-catenin, in contrast to α -E-catenin, is also present in differentiated neurons of the cortical plate (Stocker & Chenn, 2006). Accordingly, genetic deficiency of α -N-catenin resulted in a broader range of phenotypes than deletion of α -E-catenin. Besides the lack of an organised ventricular architecture, which is a common observation made in AJ protein mutants, α -N-catenin deficient brains displayed migration defects of Purkinje cell precursors in the cerebellum (Park *et al.*, 2002, Togashi *et al.*, 2002). Furthermore, impaired dendritic spine formation of hippocampal neurons, which later lead to unstable synaptic junctions was seen after loss of α -N-catenin (Togashi *et al.*, 2002, Abe *et al.*, 2004). Additionally α -N-catenin null neurons showed defects in axonal migration so that mutant fibres of the anterior commissure failed to cross the midline (Uemura & Takeichi, 2006).

Taken together, recent publications have helped to gain a better understanding of the role of the cadherin-catenin complex in brain development. Those studies showed clearer that one critical function of AJ core molecules is the maintenance of tissue integrity. Beside their conventional role as structure molecules these proteins are moreover part of multiple developmental pathways. Nevertheless, signalling cascades displaying how α -E-catenin at the spot of AJ would control those pathways remain to be identified. Therefore, one major aim of my thesis was to elucidate direct mechanisms explaining the mitotic potential of α -E-catenin in brain development.

1.5.2 Apical polarity complexes and embryonic neurogenesis

Analogous with other epithelial cells, the apical domain of mammalian VZ cells contains all members of the Par complex. Various loss- and gain-of function studies have helped to elucidate the role of those molecules in embryonic neurogenesis. For example, conditional deletion of $aPKC\lambda/1$ at a late stage of neurogenesis (E15 mouse cortex) disrupted junctional integrity and VZ architecture (Imai *et al.*, 2006). Importantly, no impact on fate decision and neurogenesis was seen in $aPKC\lambda/1$ deficient brains. As those mutant brains still expressed $aPKC\zeta$, a definitive answer to the problem of whether $aPKCs$ regulate neural differentiation is

only accessible by studies of aPKC λ /aPKC ζ double knock-outs (Imai et al., 2006). However, not all manipulations interfering with components of the apical neural stem cell domain leave cell fate unchanged. For example, cortical lack of Cdc42 during early neurogenesis caused an increase in the number of basal progenitors at the expense of Pax6 positive VZ cells (Cappello et al., 2006). Moreover, Cdc42 deficient cortices display gradual loss of adherens junctional and Par complex molecules from the ventricular surface (Cappello et al., 2006). Using both, loss- and gain-of-function experiments in the mouse telencephalon, two independent groups have demonstrated a crucial role of the Par protein complex in the maintenance of self-renewing VZ cells (Costa et al., 2008, Bultje et al., 2009). Remarkably, Bultje and colleagues showed that the subcellular Par3 localisation in radial glial cells is highly dynamic (Bultje et al., 2009). While Par3 largely co-localises with ZO-1 during interphase, it delocalises from the ZO-1 expressing junctions and becomes dispersed as soon as the cells enter mitosis (Bultje et al., 2009). Furthermore, the latter study suggests a mechanism by which daughter cells inheriting greater amounts of Par3 during neural stem cell mitoses develop high Notch signalling activity, resulting in their maintenance of a radial glia state (Bultje et al., 2009).

Besides the Par proteins, integral components of the apical plasma membrane also include the transmembrane protein Prominin-1 (Weigmann et al., 1997). In neuroepithelial and radial glia cells Prominin-1, also known as CD133, concentrates on the microvilli and the primary cilium, reaching into the ventricular lumen (Dubreuil et al., 2007). Although the exact function of Prominin-1 in neural stem cells has not yet been elucidated, recent data suggests a tight connection of this molecule to cell fate decisions. While neurogenic progenitors usually do not inherit the Prominin-1 positive apical domain, proliferative neural stem cells do (Kosodo et al., 2004). Consistent with that observation, VZ cells reduce the amount of Prominin-1 before undergoing neurogenic divisions by releasing parts of the Prominin-1 positive stem cell membrane microdomain (Marzesco et al., 2005, Dubreuil et al., 2007).

During the past few years, our knowledge about apical polarity cues and their function in embryonic mammalian neural stem cells has increased tremendously. But, clearly detailed investigations of the apical-lateral domain of adult neural stem cells and their functional relevance remain missing. Therefore, the present work characterises the apical domain of adult neural SEZ stem cells in analogy to well-characterised apical molecules expressed in embryonic VZ cells. Based on those observations, moreover, the role of Par complex proteins in adult SEZ cells will be evaluated.

1.5.3 β -Catenin dependent Wnt signalling in neurogenesis

During brain development Wnt/ β -catenin signalling regulates a wide variety of fundamental processes such as regional patterning, proliferation, cell survival, neuronal differentiation,

axon guidance or synaptic formation (for review see Chenn, 2008). One prominent source of Wnt ligands in the developing telencephalon is the cortical hem, a transient neuroepithelial structure located between the hippocampus anlage and the telencephalic choroid plexus epithelium (Grove *et al.*, 1998). The cortical hem mainly expresses Wnt-3a, -5a, -7b and -8b (Grove *et al.*, 1998). The adjacent developing cortex not only expresses distinct Wnt ligands, but moreover also the Wnt receptors. While the VZ exhibits a high abundance of Frizzled receptor 5/8, Wnt7a and β -catenin, Wnt7b is only expressed in the intermediate zone and the developing cortical plate (Kim *et al.*, 2001, Grove *et al.*, 1998, Chenn & Walsh, 2002, Funatsu *et al.*, 2004, Rubenstein *et al.*, 1999). Studies using different Wnt reporters have revealed canonical signalling activity mainly in the VZ of the developing dorsal telencephalon being high in early and low in late cortical neurogenesis (Machon *et al.*, 2007, Mutch *et al.*, 2009).

Consistent with that observation, manipulations of β -catenin dependent signalling at various developmental stages cause heterogeneous phenotypes. During early brain development, before the onset of neurogenesis (E8.5), canonical Wnt signalling mainly promoted the formation of dorsal telencephalic structures by inhibiting the expression of ventral markers in dorsal brain regions (Backman *et al.*, 2005). On the contrary, removal of β -catenin from neuroepithelial cells one day later (E9.5) showed a very different phenotype that is primarily characterised by apoptosis of embryonic neural stem cells, causing a substantial reduction of forebrain structures (Junghans *et al.*, 2005). D6-Cre mediated deletion of β -catenin in cortex and hippocampus anlage at E13.5 did not affect apoptosis, but decreased cell proliferation in both recombined brain regions by promoting premature cell-cycle exit (Machon *et al.*, 2003). As a consequence, the size of the adult cortex and the hippocampus was greatly reduced (Machon *et al.*, 2003). The central role of Wnt signalling in cell proliferation of hippocampal progenitors has been as well demonstrated by Wnt1/3 knock-out experiments (Ikeya *et al.*, 1997, Lee *et al.*, 2000) or over-expression analyses of dominant negative LEF1 (Galceran *et al.*, 2000). Beside loss-of-function studies, experiments ectopically activating canonical Wnt signalling have been performed. After CNS specific over-expression of stabilised β -catenin at the onset of neurogenesis, a dramatic enlargement of the forebrain was found (Chenn & Walsh, 2002). The overgrowth observed in this study was caused by an increased number of cells re-entering the cell cycle that subsequently expanded the proliferative zones (Chenn & Walsh, 2002).

In addition to its prominent role in proliferation, canonical Wnt signalling was also shown to instruct neuronal differentiation during cortical development (Hirabayashi *et al.*, 2004, Israsena *et al.*, 2004, Zhou *et al.*, 2006, Lyu *et al.*, 2008). For example, the abrogation of the Wnt/ β -catenin pathway in LRP6-deficient mice resulted in a thinner cortical plate due to a

reduced production rate of neurons (Zhou et al., 2006). Another study showed that expression of constitutive active β -catenin during mid-neurogenesis promoted neuronal differentiation in the neocortex, whereas inhibition of the canonical Wnt pathway at the same time point suppressed neuronal differentiation (Hirabayashi et al., 2004). In this context, the proneural genes neurogenin1/2 have been found to be direct targets for the β -catenin/TCF transcription complex in inducing neuronal differentiation (Hirabayashi et al., 2004, Israsena et al., 2004). Recently, it was published that canonical Wnt signalling not only promoted neuronal differentiation, but also influenced the laminar cell fate of the generated neurons dependent on β -catenin levels (Mutch et al., 2009). Over-expression of stabilised β -catenin by in-utero electroporation showed a reduction in the number of late-born (upper-layer) neurons, while over-expression of dominant negative TCF4 using the same technique resulted in the reverse effect (Mutch et al., 2009). Consequently, the decreasing activity of canonical Wnt signalling throughout cortical neurogenesis allowed the production of progressively more superficial layer neurons (Mutch et al., 2009).

Finally, the crucial role of canonical Wnt signalling in adult neurogenesis has been also demonstrated. *In-vitro* and *in-vivo* experiments revealed that Wnt-3 secreted by astrocytes of the dentate gyrus stimulates the neuronal fate commitment of adult neural stem cells and enhances the proliferation of neuroblasts (Lie et al., 2005). On a molecular level, Wnt signalling in adult hippocampal neurogenesis induced the activation of the transcription factor NeuroD1 (Kuwabara et al., 2009), which itself is shown to be an important proneurogenic factor in the adult brain (Gao et al., 2009). Furthermore, several recent *in-vitro* studies suggested that the proliferative control of Wnt signalling in adult neurogenesis is not only limited to the neuroblast population, but can also act on the neural stem cell pool (Yu et al., 2006, Hirsch et al., 2007). Moreover, experiments using pharmacological and retroviral approaches to interfere with canonical Wnt signalling in the adult SEZ showed that β -catenin signalling promotes proliferation of transit-amplifying progenitors (Adachi et al., 2007).

As the latter publication only provided a short-time analysis after acute interference with the canonical Wnt pathway, genetic approaches are still needed to specifically study the role of β -catenin in the long run in the adult SEZ. Therefore, the present work uses an inducible Cre line to specifically delete β -catenin in neural stem cells of adult mice. Due to the known function of canonical Wnt signalling in neuronal fate decision, one aspect of my thesis was to examine if β -catenin regulates neuronal fates and by this also influencing the transcriptional activity within the neuronal lineage. Thus, the following sections concentrate mainly on known transcriptional regulators specifying different neuronal phenotypes in distinct telencephalic regions and at several developmental and adult stages.

1.6 REGIONAL HETEROGENEITY OF NEURAL STEM CELLS AND REGULATORS OF NEURONAL SUBTYPE SPECIFICATION

1.6.1 Neuronal fate determinants in dorsal and ventral forebrain development

During development Notch signalling is one of the universal pathways inhibiting neuronal differentiation and maintaining self-renewal of the neural stem cells (Gaiano & Fishell, 2002). Specific targets of the Notch pathway are hairy and enhancer of split (Hes) genes, inhibitors of differentiation (Id) and HES-related (HESR or HERP) families (Abrous *et al.*, 2005). These effectors repress neuronal determination and differentiation by inhibiting the expression or activity of proneural basic helix-loop-helix (bHLH) transcription factors.

In the mammalian brain, two classes of proneural genes can be distinguished: (i) the determination factors, like mammalian achaete-scute homolog1 (Mash1), mammalian atonal homolog (Math1) and Neurogenin1 and 2 (Ngn1/2) and (ii) the differentiation factors including neurogenic differentiation1 and 2 (NeuroD1/2) and Math2 that are expressed in postmitotic cells (Fode *et al.*, 2000, Schuurmans *et al.*, 2004). Notably, different transcription factors are restricted to specific brain regions and control in those areas the generation of different neuronal subtypes. For example, Ngn1/2 and Mash1 have largely complementary expression patterns in the developing telencephalon. While high levels of Neurogenins are found in the cerebral cortex, Mash1 is up-regulated in the ventral ganglionic eminence (GE). The dorsal telencephalon is the region of all glutamatergic neurons in the cerebral cortex and the ventral telencephalon produces most γ -amino butyric acid (GABA)ergic neurons in the forebrain (Marin & Rubenstein, 2001, Gorski *et al.*, 2002).

Intriguingly, loss- and gain-of-function studies confirmed that Ngn1/2 induce a cerebral cortex specific differentiation course by promoting the sequential appearance of the differentiation factors NeuroD1/2, Math2/3 and neuronal stem cell leukemia1 and 2 (NSCL1/2) (Schuurmans *et al.*, 2004). In addition, the regulatory genes T-box brain1 and 2 (Tbr1/2), that are restricted in expression to the regions generating excitatory cortical neurons, also depend on the function of Ngn1/2 (Hevner *et al.*, 2001, Englund *et al.*, 2005, Schuurmans *et al.*, 2004, see also Fig1-6). However, Ngn1/2 were identified to be only required for the generation of early born neurons committed for deep cortical layers (Tarabykin *et al.*, 2001, Schuurmans *et al.*, 2004).

In line with its predominant ventral expression, Mash1 could be identified as an essential transcription factor driving the generation of GABAergic neurons in the developing forebrain (Porteus *et al.*, 1994, Guillemot *et al.*, 1993). In particular, Mash1-deficient mice show severe defects in the basal ganglia, cerebral cortex and olfactory bulb due to loss or reduction of the GABAergic neuronal subtypes (Casarosa *et al.*, 1999, Cau *et al.*, 2002). Mis-expression

studies of Mash1 in cortical neurons confirmed the proneural factor to be a direct inducer of the Dlx homeobox gene family (Fode *et al.*, 2000). Furthermore, Dlx2 has been shown to promote the expression of the biosynthetic enzyme glutamic acid decarboxylase (GAD) 67, which regulates the rate-limiting step in GABA synthesis (Anderson *et al.*, 1999). In order to do so, Dlx genes repress the transcription factor Olig2 and consequently an oligodendrocyte fate (Petryniak *et al.*, 2007).

Therefore, in mammals specification of a large variety of neuronal subtypes is not only dependent on the specific expression of proneural bHLH genes but also on the presence of homeobox genes like Dlx. Other well known members of the homeobox family are Pax6 or Gsh1/2. While Pax6 is mainly expressed in the radial glia of cerebral cortex, Gsh1 and Gsh2 are among the earliest markers of the ventral radial glial cells (Campbell & Götz, 2002). Pax6 is indispensable for the establishment of a correct glutamatergic phenotype (Schuurmans *et al.*, 2004, Kroll & O'Leary, 2005) and is furthermore a direct transcriptional regulator of Ngn2 (Scardigli *et al.*, 2001). But, independently of Ngn2, it specifies mainly upper-layer neurons (Tarabykin *et al.*, 2001, Schuurmans *et al.*, 2004). In contrast to Pax6, Gsh2 was shown to be crucial for the determination GABAergic neuronal fate. Lack of Gsh2 causes profound defects in telencephalic development, loss of early ventral markers and a delay in the appearance of GABAergic interneurons of the olfactory bulb (OB) (Corbin *et al.*, 2000, Stenman *et al.*, 2003).

The GE can be even further subdivided into the medial and lateral ganglionic eminences (MGE/LGE). Interestingly, GABAergic neurons that populate the cortex, the OB and the striatum originate in different proportions from these subdivisions of the ventral telencephalon. In addition to neurons, the subpallium is also a source of oligodendrocyte progenitors, while the earliest cortical oligodendrocytes arise from Nkx2.1-expressing precursor cells in the MGE. For better understanding, the most important genetic interactions underlying the regionalisation of the mammalian telencephalon are depicted in Fig.1-7.

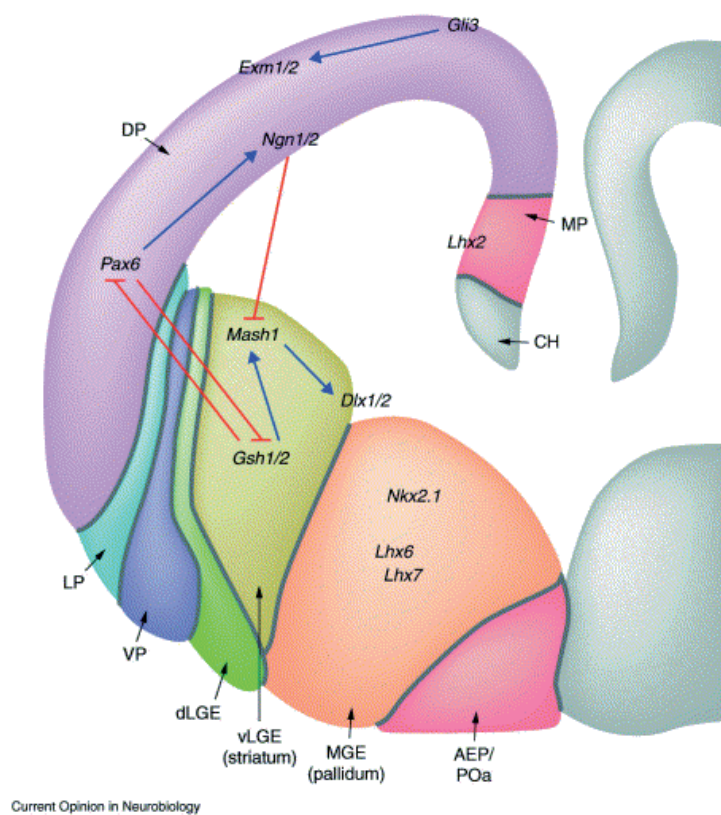


Figure 1-7. Summary of regionalised transcription factors in the developing forebrain. Adapted from Schuurmans and Guillemot, 2002.

Schematic coronal section through the telencephalic vesicles at E12.5 showing high expression levels of *Ngn1/2*, *Emx1*, *Emx2*, *Lhx2* and *Pax6* in the cortex. In contrast, the lateral ganglionic eminence (LGE) expresses *Mash1*, *Gsh1/2*, *Dlx1/2/5/6*. The LGE can be further subdivided into dorsal and ventral LGE due to higher levels of *Pax6*, *Gsh2*, *Dlx2* and *Mash1* in dLGE, and exclusive expression of *Gsh1* in the vLGE. In contrast, *Lhx6*, *Lhx7* and *Nkx2.1* are only present in the medial ganglionic eminence (MGE).

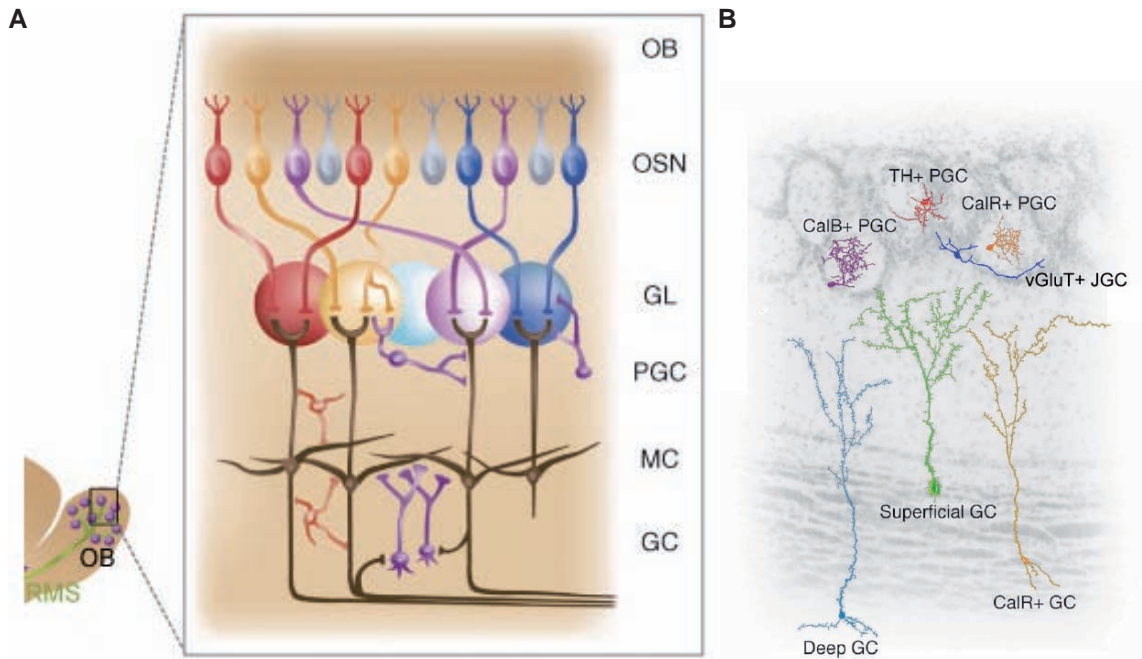


Figure 1-8. Schematic drawing of olfactory bulb (OB)

A) The diagram represents a sagittal section through the main olfactory bulb and depicts its neuronal networks: Olfactory sensory neurons (OSN) transport the primary sensory signal to mitral cells which project to the higher brain olfactory structures like the piriform cortex. Local interneurons, such as periglomerular cells (PGC), help to modify the incoming signal. *Modified from Lledo et al., 2009.*

B) Overview of interneurons generated in adult mouse brain. According to their neurochemical identity periglomerular neurons can be subdivided in calretinin (CalR)-, calbindin (CalB)- and tyrosine hydroxylase (TH)-positive cells. Lately, a new interneuronal subtype the glutamatergic juxtglomerular cells (JGC), being positive for expression of vesicular glutamate transporter (vGluT), was discovered to be produced in adulthood as well. Furthermore, two different types of granule cells (GC) can be distinguished based on their position into deep and superficial GC. A small subset of adult generated GC varies from the others by its expression of calretinin. *Modified from Alvarez-Buylla, 2009.*

CalB: calbindin; *CalR*: calretinin; *GC*: granule cells; *GL*: glomerular layer; *JGC*: juxtglomerular cells; *PGC*: periglomerular cells; *MC*: mitral cells; *TH*: tyrosine hydroxylase, *vGluT*: vesicular glutamate transporter

1.6.2 Generation of diverse olfactory bulb neurons

The development of the mouse main OB starts around E10.5 in the most rostral areas of the dorsal telencephalon that are already specified as an OB primordium at this stage (Lopez-Mascaraque *et al.*, 1996, Lopez-Mascaraque & de Castro, 2002). At E11, olfactory sensory neurons of the olfactory placode (the later olfactory epithelium) send initial axons to the primordium and may thereby induce the macroscopic evagination of the OB that takes place in mice around E12 (De Carlos *et al.*, 1995). The olfactory bulb is comprised of two types of neurons: (i) projection neurons including mitral and tufted cells that arise directly within the OB and (ii) interneurons originating mainly from the ventricular zone of the GE but also partially from the dorsal telencephalon (Toresson & Campbell, 2001, Wichterle *et al.*, 2001, Gorski *et al.*, 2002, Willaime-Morawek *et al.*, 2006, Kohwi *et al.*, 2007, Ventura & Goldman, 2007, Young *et al.*, 2007).

Thus, step by step, a complex anatomical structure forms, characterised by a distinct laminar organisation of the different neuronal cell types (Fig.1-8A). The most superficial layer of the OB is the olfactory nerve layer (ONL) which contains the thin and unmyelinated axons from the olfactory sensory neurons. Those neurons are the first station in the cascade of odour perception that obtain sensory signals from their odour receptors within the nasal cavities and transmit them to glomeruli in the glomerular layer (GL) of the main OB. Glomeruli are neuropil-rich spheroid structures which serve as input modules for the olfactory bulb (Pinching & Powell, 1971). Remarkably, they receive input from between 5,000 and 10,000 olfactory receptor cells, but their output only consists of dendrites of approximately 50 glutamatergic mitral and tufted cells. The GL, furthermore, consists of periglomerular interneurons that synapse on the dendrites of excitatory mitral cells in order to refine olfactory information. Periglomerular neurons can be morphologically classified into mainly GABAergic periglomerular cells and glutamatergic short axon cells that contact both apical and lateral dendrites of mitral cells (Price & Powell, 1970, Gheusi & Lledo, 2007). The GL is followed by the external plexiform layer (EPL) containing predominantly dendrites of mitral and tufted cells. The EPL contains additionally the cell bodies of the tufted cells that project to the internal plexiform layer (IPL). Directly underneath the EPL is the mitral cell layer (MCL) located which harbours the big cell bodies of the mitral cells, the principal output neurons of the bulb projecting to higher brain regions (i.e. olfactory cortex). In the centre of the OB is the granule cell layer (GCL) with its inhibitory interneurons that possess many short dendrites, forming dendro-dendritic synapses to the excitatory projection neurons (Lledo *et al.*, 2008).

As emphasised in the previous paragraph, precise odour discrimination in the olfactory system is only possible through complex networks of numerous neuronal subtype. Taking the

different origins of diverse OB neurons in account, it is not surprising that the very same transcription factors regulating telencephalic regionalisation are also involved in specification of the OB neurons. For example, projection neurons strongly express *Tbr1* and mice with a homozygous deficiency for this gene fail to form normal mitral and tufted cells (Bulfone *et al.*, 1998). Parallel studies in mice that are null-mutants for the mammalian homeobox genes *Dlx1* and *2*, have demonstrated the absence of OB interneurons (Bulfone *et al.*, 1998). Furthermore, in mutations of the homeobox gene *Emx2*, the olfactory nerve fails to build up an organised mitral cell layer (Yoshida *et al.*, 1997). The *Pax6^{Sey-/-}* mice, functional *Pax6* null mutants lacking the transactivation domain of *Pax6* do not even form an OB. Instead, these mice exhibit only an olfactory bulb like structure with mitral like cells and disorganised OB interneurons.

Having described the key molecular players of embryonic olfactory bulb neurogenesis, it is important to highlight again, that only olfactory interneurons are continuously produced during postnatal life and adulthood. In contrast, the generation of projection neurons is restricted to embryonic development. The next section will therefore discuss the characteristics of fate specification in adult neurogenesis that is to some extent different to processes taking place during development.

1.6.3 Regional specification of postnatal and adult olfactory interneurons

Since dorsal and ventral regions of the telencephalon contribute to the adult SEZ, adult neural stem cells are regionally specified and give rise to numerous subsets of olfactory interneurons (Hack *et al.*, 2005, Merkle *et al.*, 2007, Young *et al.*, 2007, Kohwi *et al.*, 2007). Traditionally, two principle types of continuously new-born interneurons were distinguished to integrate in the adult OB: (i) the periglomerular cells in the (GL) and (ii) the granule cells of the GCL (Fig.1-8B). Recently, Batista-Brito and colleagues suggested that a subpopulation of postnatally born interneurons are positive for parvalbumin integrates into the EPL (Batista-Brito *et al.*, 2008).

With respect to the expression of neurotransmitters or calcium-binding proteins, GABAergic periglomerular cells can be further subdivided into three non-overlapping populations: the dopaminergic tyrosine hydroxylase (TH)-positive, calretinin-positive and calbindin-positive cells (Kosaka *et al.*, 1995, Toida *et al.*, 2000, Panzanelli *et al.*, 2007, Parrish-Aungst *et al.*, 2007). Recently, our lab identified another class of adult generated periglomerular cells that are, in contrast to former described populations, glutamatergic (Brill *et al.*, 2009). Typically, these glutamatergic interneurons show morphological characteristics of short-axon cells (Brill *et al.*, 2009). According to their position within the GCL, granule cells can be further subdivided into deep and superficial interneurons (Shepherd, 1972). While the deep granule cells synapse predominantly with mitral cells, the upper granule neurons were shown to

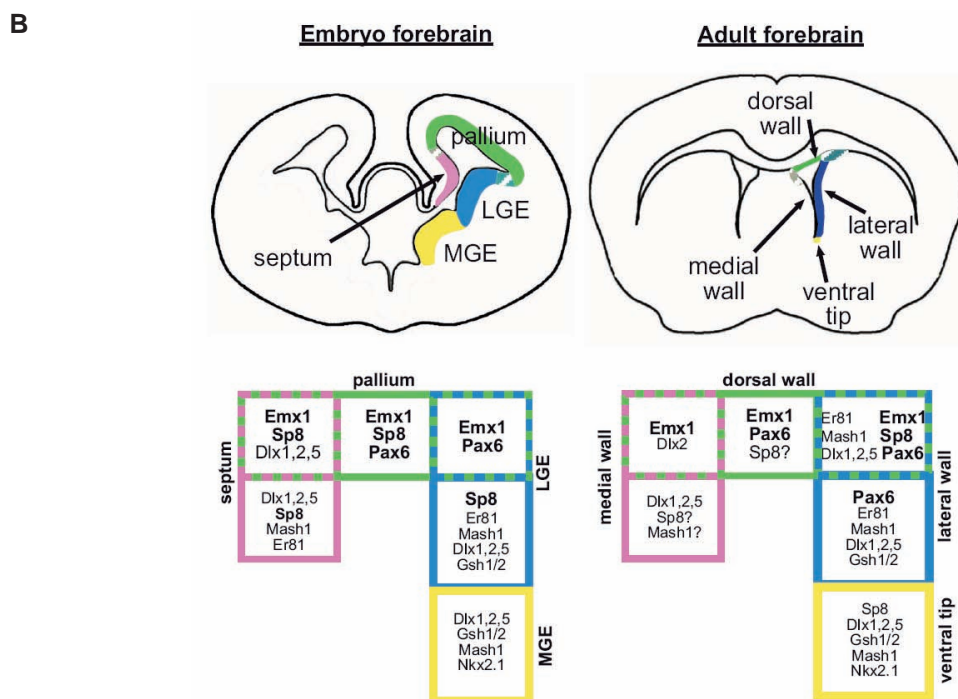
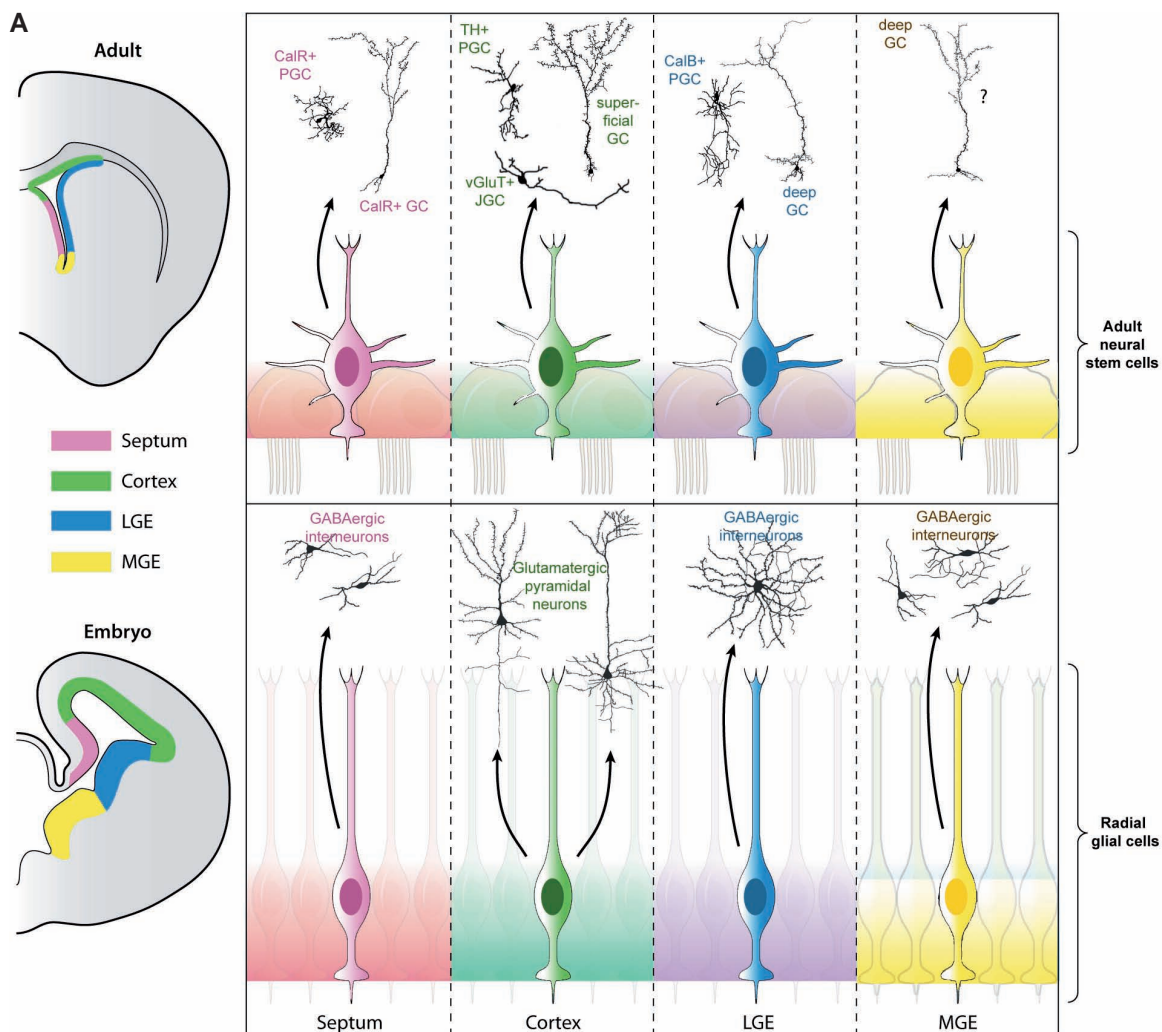


Figure 1-9. Heterogeneity of neural stem cells in the developing and adult forebrain as the origin of distinct neuronal subtypes

A) Summary of the four different subregions along the ventricular wall. Each area is known to be an origin of distinct neuronal subtypes during development (lower panel) and adulthood (upper panel). For example, ventral regions of the embryonic GE are mainly generating GABAergic interneurons, while the dorsal embryonic wall gives rise to glutamatergic pyramidal neurons. Moreover, region-specific production of various olfactory bulb interneurons is observed during postnatal and adult neurogenesis. Superficial granule cells (GC), tyrosine hydroxylase (TH)-positive periglomerular cells (PGC) and glutamatergic juxtglomerular cells are largely produced by dorsal neural stem cells. In contrast, lateral neural stem cells are the main source of calbindin (CalB)-positive PGC and deep GC. Note, that all zones surrounding the ventricle are contributing to the subependymal neurogenic areas in the adult brain. *Modified from Kriegstein and Alvarez-Buylla, 2009.*

B) Schematic drawing of a coronal hemisection through the developing and adult murine telencephalon showing region-specific expression patterns of transcription factors in the germinal zones. Sets of transcription factor, within each brain area are indicated by different colours and listed in the colour-corresponding boxes beneath.

Adapted from Alvarez-Buyalla, 2009

contact mostly tufted cells (Lledo *et al.*, 2008). In contrast to periglomerular cells, the majority of new-born GABAergic granule cells are negative for TH or calbindin. However, a small subset of adult generated glomerular cells express calretinin as well (Batista-Brito *et al.*, 2008, see also Fig.1-8B).

Although a wide variety of continuously born neurons have been described to exist in the OB, not until recently scientists have gained a better understanding of the molecular regulators specifying the interneuronal subtypes. Already in 2005, Pax6 was identified as a key factor in the general production of adult generated OB neurons, which can also specifically promote the fate of dopaminergic periglomerular cells (Hack *et al.*, 2005, Kohwi *et al.*, 2007). Pax6 is highly expressed in the RMS where it labels a large subpopulation of neuroblasts of which the majority are destined to become dopaminergic periglomerular neurons (Hack *et al.*, 2005). In contrast to maturing cortical neurons that during brain development derive from Pax6-positive radial glial cells and then down-regulate Pax6, most of the differentiating dopaminergic periglomerular neurons and a subpopulation of superficial granule neurons maintain Pax6 expression in the adult OB. Other important transcription factors that were also found in the neurogenic subpopulation of TAPs include Dlx1/2 and Mash1 (Doetsch *et al.*, 2002, Parras *et al.*, 2004, Hack *et al.*, 2005, Colak *et al.*, 2008, Brill *et al.*, 2008). Genetic fate mapping using an inducible Dlx2::CreErt2 mouse line confirmed that most OB interneurons are derived from a Dlx2-positive progeny (Batista-Brito *et al.*, 2008). Furthermore, retroviral vector mediated manipulations of Dlx2 expression in the adult SEZ revealed its major role in adult neurogenesis of virtually all OB interneurons (Brill *et al.*, 2008). The same study additionally showed that Dlx2 specifies adult-born periglomerular neurons towards a dopaminergic fate in a Pax6 dependent manner (Brill *et al.*, 2008).

Also, the generation of other olfactory interneurons is highly dependent on specific transcription factors. For example, the Sp8 zinc-finger transcription factor has been linked to the formation of the calretinin-positive cells in the OB (Waclaw *et al.*, 2006). Interestingly, Pax6 becomes up-regulated in the absence of Sp8 (Allen *et al.*, 2007), while over-expression of Pax6 or

Dlx2 decreases the production of calretinin-positive cells in proportion to all new-born neurons (Hack et al., 2005, Brill et al., 2008).

Like the embryonic forebrain, the adult SEZ expresses subtype-specific fate determinants only in restricted territories. Thus, adult neural stem cells in different regions around the lateral ventricles are already intrinsically limited to the generation of only a subset of different interneurons. Subsequent studies revealed the origin of different olfactory interneurons from particular SEZ sublocations (Hack et al., 2005, Merkle et al., 2007, Ventura & Goldman, 2007, Kohwi et al., 2007, Young et al., 2007). Young and colleagues performed fate-mapping experiments by expressing Cre recombinase under the control of transcription factors which are regionally restricted within the developing and postnatal ventricular walls. This analysis suggested that calbindin-positive periglomerular neurons are mostly derived from lateral Gsh2 positive SEZ regions (Young et al., 2007), while TH-positive cells originate from embryonic Emx1 expressing progenitors (Young et al., 2007, Kohwi et al., 2007). In addition, Ventura and Goldman specifically labelled postnatal dorsal radial glia and could show that those generate mostly TH-positive cells (Ventura & Goldman, 2007). Another study based on cell grafting experiments supported the idea that TH-positive OB neurons originate from dorsal regions (Merkle et al., 2007). Furthermore the same study showed that calbindin-positive neurons are produced in ventral regions, whereas calretinin-positive periglomerular cells and granular cells derive from the medial septum wall (Merkle et al., 2007). Interestingly, also the newly discovered olfactory glutamatergic interneurons originate exclusively from a dorsal neural stem cell population and it has been suggested that they follow the sequential expression from Pax6→Ngn2→Tbr2→Tbr1 during their maturation and differentiation (Brill et al., 2009).

Taken together, those studies emphasise that radial glia cells as well as adult neural stem cells are regionally heterogeneous and determined for the production of distinct neuronal subtypes. A schematic summarising this complicated process of area specification in the embryonic and adult brain is depicted in Fig.1-9. Although the cited analyses shed some light on region-restricted genetic fate determinants, still little is known about environmental factors that might regulate these transcription factors during adult neurogenesis. Therefore, I have examined in this work whether any signalling pathway is limited to the dorsal ventricular wall and hence may provide regionalised signals for the specification of Tbr2⁺ progenitors and thereby glutamatergic interneurons.

1.7 AIM OF THE THESIS

Given the distinct role of α -E-catenin in controlling proliferation during embryonic forebrain development (Lien et al., 2006, Schmid, 2007), one major aim of my thesis was to elucidate

direct mechanisms explaining the inhibitory mitotic potential of α -E-catenin in brain development. Many AJ associated proteins are known to influence cell proliferation. Especially the levels of such proteins are crucial for this process. Therefore, I decided to use semi-quantitative Western Blot analysis in order to detect potential changes in the levels of these signalling proteins.

As still very little is known about the role of adhesion and polarity molecules in adult neural stem cells, the second part of this work tested the following two questions:

- (1) Do adult neural stem cells and their ability to form neurospheres depend on the expression of adherens junctional and Par complex molecules *in-vitro* ?
- (2) What influence has loss of the canonical Wnt signalling molecule β -catenin on adult SEZ neurogenesis *in-vivo*? And how react adult neural stem cell to forced exclusion from the stem cell niche by interfering with the structural role of β -catenin in cell adhesion?

To answer these questions I used viral vector and transgenic mouse approaches and manipulated the discussed proteins of interest *in-vitro* and *in-vivo*.

2 Materials

2.1 COMMONLY USED BUFFERS

All aqueous solutions were prepared using filtered MilliQ water (Q-Gard 2 Purification Pack, Millipore, QGARD00D2) unless otherwise stated.

Phosphate-buffered saline (PBS)

| | |
|--|-------|
| <i>NaCl</i> | 137mM |
| <i>KCl</i> | 2.7mM |
| <i>Na₂HPO₄·7H₂O</i> | 8.3mM |
| <i>KH₂PO₄</i> | 1.4mM |

SDS electrophoresis buffer, 10x

| | |
|-----------------|-------|
| <i>Tris-HCl</i> | 250mM |
| <i>Glycine</i> | 1.92M |
| <i>SDS</i> | 1% |

Separating gel buffer (pH 8.8) for SDS-PAGE

| | |
|-----------------|------|
| <i>Tris-HCl</i> | 1.5M |
| <i>SDS</i> | 0.4% |

Stacking gel buffer (pH 6.8) for SDS-PAGE

| | |
|-----------------|------|
| <i>Tris-HCl</i> | 0.5M |
| <i>SDS</i> | 0.4% |

TBE (Tris/borate/EDTA) electrophoresis buffer, 10x

| | |
|-------------------|--------|
| <i>Tris base</i> | 890 mM |
| <i>Boric acid</i> | 890 mM |
| <i>EDTA</i> | 20 mM |

Tris-buffered saline (TBS)

| | |
|-------------------------|---------------|
| <i>Tris-HCl, pH 7.5</i> | 100 mM |
| <i>NaCl</i> | 0.9% (150 mM) |

TTBS (Tween-20/TBS)

0.1% Tween-20 in Tris-buffered saline (TBS)

2.2 BULK CHEMICALS

Table 2-1. Bulk chemicals.

| Chemical | Company | Ordering Number |
|--|---------|-----------------|
| 2-Hydroxypropyl- β -cyclodextrin | Sigma | H-107 |
| Acetone | Merck | 107021 |
| Agarose | Biozym | 870055 |
| Ammonium peroxide disulphate (APS) | Sigma | A-3678 |

Materials

| Chemical | Company | Ordering Number |
|---|--------------------------|------------------------|
| Ampicillin | Roth | K029 |
| Aqua Poly/Mount | Polyscience Inc. | 18606 |
| Boric acid | Roth | 6943 |
| Bovine serum albumin (BSA) | Sigma | A-9418 |
| BrdU (5'-bromo-2'-deoxyuridine) | Sigma | 16880 |
| DAPI (4,6-dasmindino-2-phenylindol) | AppliChem | A1001 |
| Diethyl ether | Merck | 1009211000 |
| Difco LB-Agar | Hartenstein Laborversand | 214010 |
| DNA Ladder (Generuler 1kb) | Fermentas | SM0311 |
| EDTA | Merck | 1084180250 |
| Ethanol | Merck | 107017 |
| Ethidium bromide | Roth | 7870 |
| Glycerol | Sigma | 3783 |
| Glycine | AppliChem | A4554 |
| HEPES | Roth | 9105 |
| Hydrochloric acid | Merck | 109057 |
| Hydrogen peroxides | Roth | 8070 |
| Isopropanol | Merck | 1096342500 |
| Mercaptoethanol | Merck | 805740 |
| Methanol | Merck | 822283 |
| Milk powder | Roth | T145 |
| n-Butanol | Merck | 100984 |
| Normal goat serum (NGS) | Vector Laboratories | S-1000 |
| N-P40 (Nonidet-P40) | ICN Biomedicals | 155942 |
| Orange G | Sigma | O-3756 |
| Paraformaldehyde (PFA) | Merck | 104005 |
| PCR buffer (10X Taq Buffer with (NH ₄) ₂ SO ₄) | Fermentas | B33 |
| PCR dNTP Mix (25mM each) | Fermentas | R1121 |
| PCR reagent: MgCl ₂ (25mM) | Fermentas | R0971 |
| Polyacrylamide (30%) | Sigma | A3699 |
| Ponceau S dye | Sigma | 141194 |
| Potassium chloride | Merck | 104936 |
| Potassium dihydrogen phosphate (KH ₂ PO ₄) | Merck | 104873 |
| Protein ladder (SeeBlue Plus2 Prestained Standard) | Invitrogen | LC5925 |
| Ringer infusion solution | Braun | 951 7170 |
| Sodium azide | Merck | 6688 |
| Sodium chloride | Fisher Bioreagents | BP358-212 |
| Sodium citrate | Merck | 6448 |
| Sodium deoxycholate | Sigma | D-6750 |
| Sodium dodecyl sulphate (SDS) | Roth | 2326 |
| Sodium hydroxide | Roth | P7101 |
| Sodium phosphate (Na ₂ HPO ₄ •7H ₂ O) | Merck | T876 |
| Taq DNA Polymerase | Fermentas | EP0281 |

| Chemical | Company | Ordering Number |
|-----------------|--------------------------|------------------------|
| TEMED | Sigma | T9281 |
| Tissue Tek | Hartenstein Laborversand | TTEK |
| Tris-HCl | Roth | 6683 |
| Triton-X100 | Roth | 3051 |
| Tween-20 | Sigma | P-1379 |

2.3 KITS

Table 2-2. General kits used in this work.

| Kit | Company | Ordering Number |
|---|----------------|------------------------|
| BCA Protein Assay Kit | Pierce | 23227 |
| ECL Western Blotting Detection Reagents (Amersham) | GE Healthcare | RPN2109 |
| Taq PCR Core Kit | Quiagen | 201223 |
| Tyramide Signal Amplification Kit (Fluorescein or Tetramethylrhodamine) | Perkin Elmer | NEL741/ NEL742 |
| β -Gal Reporter Gene Assay, chemiluminescent | Roche | 11 758 241 001 |

2.4 PROTEASE INHIBITORS

Table 2-3. Protease inhibitors used during tissue lysis.

| Protease inhibitor | Company | Ordering Number |
|--------------------------------------|----------------|------------------------|
| Complete Protease Inhibitor Cocktail | Roche | 4693116001 |
| Ocadaic acid | Alomone Labs | 0-900 |
| Sodium orthovanadate | Roche | 1697498 |

2.5 TISSUE CULTURE REAGENTS

Table 2-4. All reagents used for tissue culture experiments.

| Reagent | Company | Ordering Number |
|--|------------------------|-----------------|
| B-27 Serum-Free Supplement | Gibco (Invitrogen) | 17504044 |
| Bovine serum albumin (BSA) | Sigma | A-9418 |
| D-Glucose (Stock 45%) | Sigma | G-8769 |
| DMEM (Dulbecco's Modified Egel Medium) + 4.5g/mL glucose | Gibco (Invitrogen) | 41966 |
| DMEM (Dulbecco's Modified Egel Medium) + 4.5g/mL glucose and GlutaMAX | Gibco (Invitrogen) | 61965 |
| DMEM:F12 (Dulbecco's Modified Egel Medium:Nutrient Mixture F12) + GlutaMAX | Gibco (Invitrogen) | 31331 |
| DMSO | Sigma | D-2438 |
| EBSS (Earle's Balanced Salt Solution) | Gibco (Invitrogen) | 14155063 |
| EGF (Epidermal Growth Factor) | Roche | 855573 |
| FCS (Fetal Calf Serum) | Pan | 2602-P290705 |
| FGF2 (Fibroblast Growth Factor-2) | Roche | 10555400 |
| Geneticin (G418) | Invitrogen | 11811023 |
| HBSS (Hank's balanced salt solution) | Gibco (Invitrogen) | 24020 |
| Heparin | Sigma | H3393 |
| HEPES (1M) | Gibco (Invitrogen) | 15630 |
| Hyaluronidase | Sigma | H3884 |
| L-Glutamine (200mM) | Gibco (Invitrogen) | 25030 |
| Lipofectamine 2000 | Invitrogen | 12566014 |
| Magnesium chloride | Fluka | 63069 |
| Neurobasal | Gibco (Invitrogen) | 21103 |
| Neurocult Neural Colony Forming Cell Assay Kit | Stem Cell Technologies | 5740 |
| Opti-MEM + GlutaMAX | Invitrogen | 31985 |
| Penicillin/Streptomycin (Pen/Strep) | Gibco (Invitrogen) | 15140 |
| Poly-D-Lysine (PDL) | Sigma | P-0899 |
| Potassium chloride | Fluka | 60142 |
| Puromycin (2mg/mL) | Sigma | P-9620 |
| Sodium chloride | Sigma | S-6316 |
| Tetracycline (1mg/mL) | Sigma | T-3258 |
| Tris-HCl (1M) | Rockland | MB004 |
| Trypan Blue | Gibco (Invitrogen) | 0298 |
| Trypsin | Sigma | T-4665 |
| Trypsin (EDTA), 0.05% | Gibco (Invitrogen) | 25300 |

3 Methods

3.1 ANIMALS AND GENOTYPING

3.1.1 Animals

All animals used in this work were kept in the animal facility (Kleintierhaus) of the Helmholtz Zentrum München. They were maintained on a 12h light-dark cycle. The day of the vaginal plug was considered as embryonic day 0 (E0) and the day of birth as postnatal day 0 (P0). Experimental and control mice were maintained on several heterogeneous genetic backgrounds. The following mouse strains were used:

Table 3-1. Transgenic mice used in this work.

| Strain | Characteristics | Donating Investigator/ Supplier |
|--|--|--|
| Ctnnb1 ^{tm2^{Kem}} /KwJ | These mice possess <i>loxP</i> sites located in introns 1 and 6 of the β -Catenin gene. | Dr. Rolf Kemler (Brault <i>et al.</i> , 2001)/ The Jackson Laboratory |
| Ctnna1 ^{tm1^{Efu}} /J | These mice possess <i>loxP</i> sites on either side of exon 2 of the α -Catenin gene. | Dr. Elaine Fuchs (Vasioukhin <i>et al.</i> , 2001)/ The Jackson Laboratory |
| Cg-Tg(BAT-lacZ)3Picc | The BATGAL mice are a reporter strain that shows canonical Wnt signalling activity by expressing beta-galactosidase. Expression of the <i>lacZ</i> gene is under the control of seven consensus LEF/TCF-binding motifs upstream of the <i>Xenopus siamois</i> gene minimal promoter. | Dr. Stefano Piccolo (Maretto <i>et al.</i> , 2003)/ kind gift from Dr.Chichung Lie |
| Tg(hGFAP-GFP)Hket | The hGFAP::eGFP line labels astrocytes by the enhanced green fluorescent protein (eGFP) that is expressed under the control of the human glial fibrillary acidic protein (GFAP) promoter. | Dr. Helmut Kettenmann (Nolte <i>et al.</i> , 2001)/ kind gift from Dr. Frank Kirchhoff |
| Gt(ROSA)26Sor ^{tm1(ECFP)/Cos} | The R26R-CFP reporter mice contain an Enhanced Cyan Fluorescent Protein (ECFP) gene inserted into the <i>Gt(ROSA)26Sor</i> locus. Expression of the ECFP gene is blocked by a <i>loxP</i> -flanked STOP fragment. Only after successful Cre excision ECFP is expressed. | Dr. Frank Costantini (Srinivas <i>et al.</i> , 2001)/ kind gift from Dr. Frank Kirchhoff |
| Emx1 ^{tm1(Cre)} | This strain expresses Cre recombinase from the endogenous <i>Emx1</i> locus. | Dr. Shigeyoshi Itohara (Iwasato <i>et al.</i> , 2004)/ kind gift from Dr. Iwasato |
| Slc1a3 ^{tm1(CreErt2)Mgoe} | The inducible GLAST::CreER ^{T2} line expresses the CreER ^{T2} fusion protein under control of the <i>GLAST</i> promoter. Restricted to the cytoplasm, CreER ^{T2} can only enter the nucleus after exposure to tamoxifen. | Dr. Magdalena Götz (Mori <i>et al.</i> , 2006) |

| Strain | Characteristics | Donating Investigator/ Supplier |
|---------------------|--|--|
| Tg(Fos-lacZ)34Efu/J | The TOPGAL mice are like the BATGAL used as a canonical Wnt reporter strain. Expression of the <i>lacZ</i> gene is here under the control of three consensus LEF/TCF-binding motifs upstream of a minimal <i>c-fos</i> promoter. | Dr. Elaine Fuchs (DasGupta & Fuchs, 1999) / The Jackson Laboratory |

3.1.2 Mouse tail DNA extraction

Different crossings were set up for the different experiments presented in this thesis. To sort out animals of interest and to maintain the colonies mice were genotyped by PCR on tail DNA. Tail clips from ear-marked mice (3-4 weeks old) were incubated overnight at 55°C in 0.5mL of lysis buffer (1M Tris-HCl pH 8.5, 5mM EDTA, 0.2% SDS, 200mM NaCl and 1mg/mL proteinase K). The following day, hairs and tissue residues were removed by centrifugation at 16,000 x g for 10min. The supernatant was poured into 0.5mL isopropanol and mixed well. DNA precipitates were transferred in 300µl TE-buffer (10mM Tris-HCl pH8, 1mM EDTA). To solve the DNA, tubes were again rotated at 55°C for several hours.

3.1.3 Poly chain reactions

Poly chain reaction (PCR) for genotyping the *Ctnnb1^{tm2^{Kem}}/KmwJ*, the *Ctnna1^{tm1^{Efu}}/J*, the *Cg-Tg(BAT-lacZ)3Picc* and the *Tg(Fos-lacZ)34Efu/J* strain was performed according to protocols provided by The Jackson Laboratory.

Genotyping of the other mouse lines was done with a standard PCR mixture containing each required primer (0.2µM), 0.2mM of each dNTP (dATP, dGTP, dCTP, dTTP), 1.5 U of Taq DNA polymerase, 2.5µl 10xPCR buffer, and about 80ng of genomic DNA (~2µl) in a final volume of 25µl per sample.

PCR to detect the CreER^{T2} in the *Slc1a3^{tm1(CreErt2)/Mgoe}* knock-in mice employed the following primers: GLAST_Fwd (5'-GAG GCA CTT GGC TAG GCT CTG AGG A-3'), GLAST_Rew (5'-GAG GAG ATC CTG ACC GAT CAG TTG G-3') and CreER1 (5'-GGT GTA CGG TCA GTA AAT TGG ACA T-3'). Furthermore 5µL of 5xQ-solution was added per PCR sample. DNA was amplified for 35 cycles of denaturation at 94°C for 20sec, annealing at 55°C for 20sec and elongation at 72°C for 30sec. These primers generated two PCR products: 700bp for the wild-type allele and 400bp for the mutant allele.

For genotyping the *Emx1^{tm1(Cre)}* line the Emx1_Fwd (5'-GTG AGT GCA TGT GCC AGG CTT G-3'), the Emx1_Rew (5'-TGG GGT GAG GAT AGT TGA GCG C-3') and the Cre (5'-GCG GCA TAA CCA GTG AACAG C-3') primers were used. The thermocycling was performed for 10 cycles of denaturation at 95°C for 30sec, annealing at a starting point of 65°C for 30sec, whereas the temperature decreased 0.1°C per cycle, and elongation at 72°C for

1min. The PCR program was followed by another 30 cycles keeping the denaturation step, but changing annealing to 64.5°C for 30sec and elongation to 72°C for 30sec. The amplicon obtained from transgenic animals is 500bp and the wild-type amplicon is 200bp long.

The *Gt(ROSA)26Sor^{tm1(ECFP)/Cos}* reporter was genotyped using the R1 (5'-AAA GTC GCT CTG AGT TGT TAT-3'), the R2 (5'-GCG AAG AGT TTG TCC TCA ACC-3') and the R3 (GGA GCG GGA GAA ATG GAT ATG-3') primers. PCR was carried out for 40 cycles of denaturation at 94°C for 30sec, annealing at 50°C for 30sec and elongation at 72°C for 40sec. R1 and R2 amplify the mutant product at 250bp. R1 and R3 amplify the wild-type product at 500bp.

3.1.4 Agarose gel electrophoresis of DNA

To separate DNA fragments that were amplified in PCR, 1% agarose gel in TBE buffer with 10µg/mL ethidium bromide was used. Electrophoresis of DNA fragments in agarose gel was performed in horizontal chamber (Midi electrophoresis chamber type 30EL, Neolab, 857830000) in TBE buffer. DNA molecular weight standard and 20µl of samples obtained as described containing 1x Orange G sample buffer were loaded into the wells of the gel. Electrophoresis was conducted at constant 120mA amperage and at 10V per cm of gel length voltage. Results of separation were registered by the Gel Imaging and Documentation System (GeneFlash, Syngene), where the gel was illuminated with UV light and visualized by built-in software module.

3.2 ANIMAL EXPERIMENTS

3.2.1 Anaesthesia

For Perfusion animals were anesthetized by intraperitoneal injection of Ketamin (Ketaminhydrochlorid, 100mg per kg of body weight) and Rompun (Xylazinhydrochlorid, 20mg per kg of body weight).

3.2.2 BrdU administration

In this work 5'-bromo-2'-deoxyuridine (BrdU) pulses were used to label proliferating cells in vivo. BrdU is a thymidine analogue that incorporates during its bioavailability into the newly synthesized DNA of dividing cells. Continuous administration of BrdU for two weeks in drinking water (1mg BrdU per 1mL of a 2% sucrose solution) followed by a change over to normal water for another two weeks allowed the visualisation of slow-cycling cells.

3.2.3 Tamoxifen treatment

Mice carrying one *GLAST::CreER^{T2}* allele were treated with tamoxifen at an age of 8-11 weeks. In order to obtain a sufficient concentration of nuclear CreERT2 to deplete α - and β -Catenin respectively mice were fed with tamoxifen food (TAM 400, Lasvendi) was for 5 days, followed by a break of 7 days, and subsequent repeat of step 1.

3.2.4 Perfusion and tissue preparation

After different survival times the mice were anesthetized and perfused with 4% para-formaldehyde (PFA) in phosphate-buffered saline. Brains were removed and post-fixed at 4°C in the same fixative.

To perform vibratome sectioning, tissue was washed in PBS and directly embedded in 3% agarose (in PBS) in plastic moulds. After hardening of the agarose, brains were cut into 70 μ m thick slices and collected in PBS. For long-term storing vibratome sections were kept in PBS including 0.1% sodium azide.

Tissue following up cryostat sectioning was first incubated for 24h in 30% sucrose (in PBS), embedded in Tissue-Tek and snap-frozen in dry ice. The 20 μ m thick cut slices were directly collected on Superfrost glass slides and stored at -20°C before proceeding with immunohistochemical analyses.

3.3 TISSUE CULTURE

3.3.1 Preparation of coated cover slips

Glass cover slips were washed with acetone and boiled in ethanol containing 0.7% HCl for 30min. After washing two times in 100% ethanol, cover slips were dried at RT and autoclaved for 2h at 180°C. To each well of a 24-well plate one sterilized cover slip was added and pre-wetted with PBS. The PBS was replaced by 1% poly-D-lysine (PDL) dissolved in phosphate-buffered saline and plates were incubated for at least 2h at 37°C. The wells were washed three times using autoclaved MilliQ water. After drying plates for 2h in the laminar flow they were transferred to the fridge and stored at 4°C until needed.

3.3.2 Preparation of primary embryonic cerebral cortical cell culture

Time-pregnant mice were sacrificed by cervical dislocation; the embryos (E11) were removed and collected in ice-cold Solution A (HBSS containing 0.01M HEPES). The brains were dissected out and the meninges were carefully taken away. Dorsal telencephalon was cut off and separated from the olfactory bulb, the hippocampus anlagen and ganglionic eminences (GE). Cortices from each transgenic embryo were collected in separate tubes under sterile conditions in Solution A on ice. The tissue was then allowed to settle; the balanced salt solution was replaced by 0.05% trypsin (EDTA) and incubated for 15min at

37°C. The enzyme activity was stopped by the addition of twice the volume of DMEM (4.5g glucose, GlutaMAX) supplemented with 10% FCS and penicillin/streptomycin (100units/mL penicillin, 100units/mL streptomycin). The tissues were mechanically dissociated with a fire-polished Pasteur pipette coated with serum, centrifuged for 5min at 172 x g and resuspended in the FCS containing medium. Cells were plated on PDL coated cover slips in a 24-well plate. Each well contained 200,000 cells in 500µL medium. Incubation was performed at 37°C and 5% CO₂. Usually after 2 days *in-vitro*, 500µL preheated DMEM (4.5g glucose, GlutaMAX) containing 2% B-27 and 100units/mL of penicillin/streptomycin. Cells were fixed after 3 days *in-vitro* by replacing the medium to 500µL PBS, followed by incubation in 4% PFA (solved in PBS) for 15min.

3.3.3 Floating neurosphere cultures of the adult subependymal zone

Adult animals were killed by cervical dislocation and decapitated. The skull was opened; the brain removed and collected in ice-cold Solution A (HBSS containing 0.01M HEPES). The adult subependymal zone (SEZ) was dissected out in three steps: First, the brain was turned upside down, cut at level of the optic chiasm followed by the separation of the two hemispheres into halves. Second, the hippocampus was removed, thus underneath the adult SEZ became visible. Last, the SEZ was separated from the striatum and white matter by cutting out a thin layer of tissue. Afterwards the tissue was incubated in a dissociation solution (Solution A containing 1.33mg/mL trypsin and 0.7mg/mL hyaluronic acid) at 37°C for 15min, gently triturated and incubated for another 15min. To inactivate trypsin Solution B (EBSS solution including 4% BSA and 20mM HEPES) was added and cells were passed through a 70µm cell strainer. Next cells were centrifuged at 200 x g for 5 min and resuspended in 30% sucrose dissolved in 0.5x HBSS. Following another centrifugation step at 750 x g for 10 min, the cell pellet was taken up in 10mL of Solution B, and centrifuged again at 200 x g for 7 min. Finally, cells were resuspended in adult neurosphere medium consisting of DMEM:F12 (GlutaMAX), 8mM HEPES, 100units/mL of penicillin/streptomycin, 10ng/mL EGF/FGF2 and 1x B-27. Cell concentration was determined by Trypan Blue dye exclusion and primary sphere forming cells were seeded at a cell density of 5-10cells/µL. Incubation took place at 37°C with 95% air and 5% CO₂. Every second day fresh EGF and FGF2 were added at a final concentration of 10ng/mL. Cells were passaged once a week by centrifugation at 172 x g for 10 min, followed by enzymatic (0.05% trypsin [EDTA]) re-dissociation and re-plating in 50% neurosphere conditioned medium and 50% fresh adult neurosphere medium. From second passage on, cells were seeded at a clonal density of 1cell/µL. Usually, sphere forming cells were kept in cell culture flasks. However, to perform reliable quantifications of built spheres, cells were seeded in 24-well plates at a volume of 500µL medium per well.

For differentiation, grown spheres within neurosphere medium were transferred directly in a 24-well plate including PDL coated glass cover slips. One day later old medium was exchanged completely to Neurobasal medium containing 2mM L-glutamine and 1x B-27.

3.3.4 Viral infection of floating neurosphere cultures

Dissociated secondary neurosphere forming cells were plated in a 24-well plate at a clonal density of 1cell/ μ L. Cells were infected two hours after plating at a final concentration between 100 and 300 viral particles per well.

3.3.5 Colony forming neurosphere assay in collagen

Extraction and dissociation of primary neurosphere forming cells was performed as described above. In order to plate primary adult brain-derived cells under semi-solid conditions, dissociated cells were resuspended in complete proliferation medium. Complete proliferation medium was prepared as suggested in the technical manual of the NeuroCult neural colony-forming cell (NCFC) assay kit: per 1mL NCFC serum-free medium (provided by the NeuroCult kit) 66ng EGF, 33ng FGF2 and 192 μ L proliferation supplements (provided by the NeuroCult kit) were added. After resuspending cells completely, ice-cold collagen was added at a final concentration of 0.04%. Finally, the mixture was dispersed in a 24-well plate at a volume of 500 μ L per well. Cells were cultured at a concentration of 25cells/mL. Incubation took place for 21 days at 37°C, 5% CO₂ and 95% humidity. To avoid depletion of media, cultures were replenished by adding once a week 35 μ L of replenishment medium per well. Replenishment medium was made of 900 μ L Neurobasal medium, 50 μ L proliferation supplements (provided by the NeuroCult kit), 250ng FGF2, 500ng EGF and 0.01% Heparin. By day 21, plates were scanned using the Zeiss Axioplan2 light microscope with a 5x objective lens. Colonies were counted and classified by size.

3.4 VIRUSES

3.4.1 Viral expression plasmids

In order to knock down partition defective protein 3 (Par3, GeneID: 93742), two different 21bp long short-hairpin RNA (shRNA) sequences were used: Par3a (5'-GGA GAT CTT CGA AAC AGA AGA-3') and Par3b (5'GCA GCA AAC AAG GAG CAA TAT-3'). These two oligonucleotides targeting different regions of the Par3 mRNA (Fig. 3-1C) were cloned into the lentiviral pLVTH plasmid in which after deletion of the H1 promoter the expression of shRNA is regulated by the U6 promoter (Costa et al., 2008). However, as a control the empty pLVTH vector was used that still contained the H1 promoter (Wiznerowicz & Trono, 2003, Fig.3-1A).

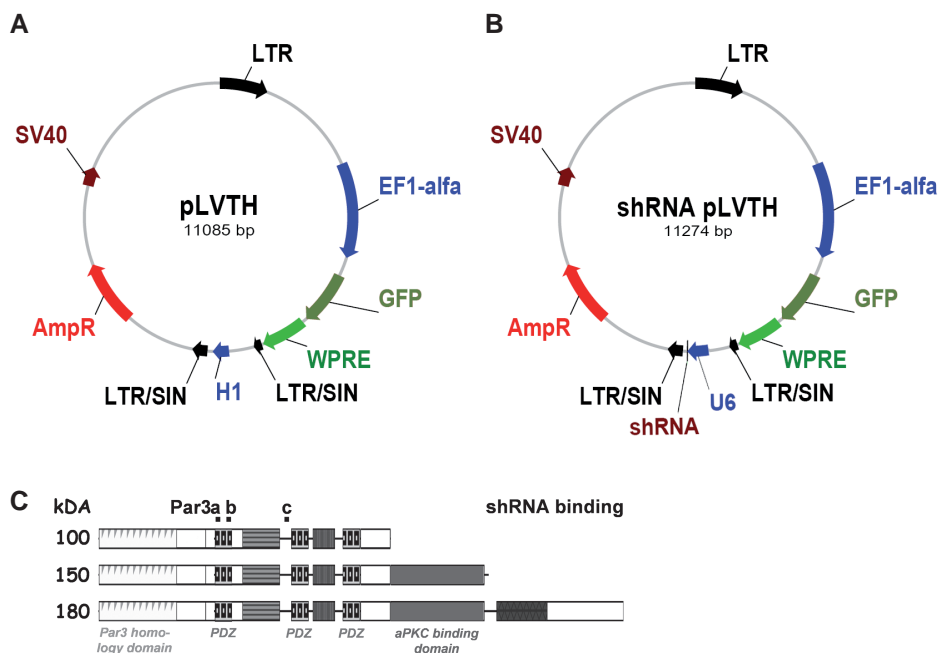


Figure 3-1. Schematic drawing of lentiviral plasmids used for the Par3 knockdown study

A) The empty pLVTH construct expressing GFP under the control of the human EF1- α promoter (Wiznerowicz & Trono, 2003) was used as a reference to exclude phenotypes caused by the infection itself. B) As described above, H1 promoter of the empty pLVTH plasmid was exchanged by U6 that regulated shRNA expression instead. Furthermore, the shRNA-pLVTH constructs allowed expression of GFP as well, so that the effect of RNAi could be analysed in a cell-autonomous manner. C) The domain organisation of Par3 and the regions in Par3 being targeted by the three different RNAi constructs Par3a, Par3b and Par3c.

AmpR: ampicillin resistance, *GFP*: green fluorescent protein, *LTR*: long terminal repeat, *LTR/SIN*: self-inactivating long terminal repeat, *SV40*: simian vacuolating virus 40 promoter, *WPRE*: woodchuck hepatitis post-transcriptional regulatory element

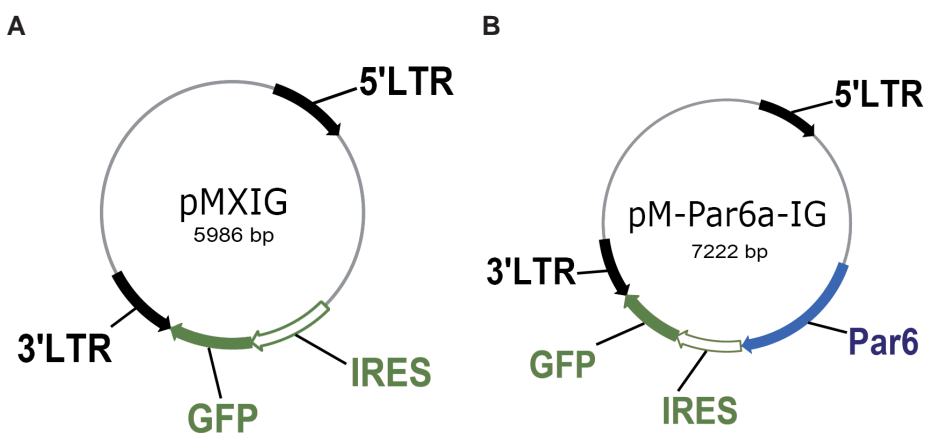


Figure 3-2. Schematic map of retroviral plasmids used for the Par6 over-expression study

A) The pMXIG vector allowed to visualise infected cells by GFP expression that was controlled via an internal ribosomal entry site. All over-expression experiments were normalised to infections using this empty construct. B) The Par6 α gene was subcloned between the upstream LTR sequence and the IRES-GFP.

GFP: green fluorescent protein, *IRES*: internal ribosomal entry site, *LTR*: long terminal repeat

To perform gain-of-function studies, full-length cDNA of Par6 α was cloned into the retroviral pMXIG plasmid (Mizuguchi *et al.*, 2001, Costa *et al.*, 2008, Fig.3-2).

3.4.2 DNA preparation of viral plasmids

All lentiviral constructs were purified using caesium chloride density gradient centrifugation in order to separate supercoiled plasmid DNA from linear and open-circular DNA. Per plasmid 250mL of transformed bacterial cells were used. First, bacteria were centrifuged at 5,000 x g for 20min and resuspended in 10mL Qiagen-Buffer1 containing RNase. Subsequently, cells were lysed by incubating suspension in 10mL of Qiagen-Buffer2 for 5min at RT. After mixing cell extract with 10mL ice-cold Qiagen-Buffer3 it was paper filtrated to remove cell debris. Finally, DNA was precipitated by adding 20mL isopropanol, followed by a centrifugation step at 8,000 x g for 1h at 4°C. The resulting DNA pellet was washed at 8,000 x g for 10min using 70% ethanol. Ethanol was removed and the pellet was air-dried until transparency before its resuspension in 8mL TE-buffer (10mM Tris-HCl pH8, 1mM EDTA). Furthermore, 8.80g CsCl were dissolved in the resuspension, followed by adding 800 μ L saturated Ethidium bromide. Samples were warmed up to 37°C for 15min and centrifuged at full speed in a swing out rotor for 10min. The supernatant was transferred into an 11.2 ml OptiSeal tube (Beckmann) and ultra-centrifuged at 80,000 x g for 5h followed by 30min at 100,000 x g at 20°C. Ethidium bromide intercalates between adjacent base pairs of the DNA molecules and causes the DNA to fluoresce. Thus, the position of the separated DNA bands can be seen by ultraviolet radiation. After the ultra-spin super-coiled DNA (lower band) was collected using a syringe with a 22G needle. Finally, Ethidium bromide was removed by adding an equal volume of n-butanol dissolved in TE-buffer to the collected DNA solution. Everything was spun down and the upper organic phase discarded. The extraction was repeated until lower aqueous phase was completely colourless. Then, an equal volume of diethyl ether was added, solutions mixed well and the upper, organic phase removed to exclude n-butanol from the water phase. Due to its low boiling point, ether is depleting itself over time. Another cleaning step was added. Therefore, DNA solution was diluted again with 2 volumes of sterile TE-buffer, 1/10 volume of 3M sodium acetate (pH 5.2) and another 2 volumes of ice-cold 100% ethanol. The solutions were mixed and incubated overnight at 4°C. Following a centrifugation step at 10,000 x g for 1h at 4°C, the resulting pellet was washed with 10mL ice-cold 100% ethanol and air-dried until transparency. DNA was dissolved in 500 μ L of sterile 10mM Tris-HCl (pH8) resulting in an average yield of 1mg pure DNA.

3.4.3 Retroviral production

Retroviral preparation was performed using the 293GPG cell line that expresses constantly genes encoding for viral proteins (Ory *et al.*, 1996). To overcome the problem of inefficient

packaging caused by cell propagation, these newly introduced genes also exhibit three different antibiotic selection sequences: Tetracycline represses the production of vesicular stomatitis virus G (VSVG) envelope protein. Puromycin selects for the integrated VSVG gene and the Tet repressor that regulates VSVG expression. Geneticin (G418) selects for integrated group antigens (gag) and the reverse transcriptase (pol) of the Moloney murine leukemia virus (MMLV) genome.

Packaging cells were cultured in basic medium A (DMEM containing 10% of heat inactivated FCS, 1mg/mL penicillin/streptomycin, 1µg/mL tetracycline, 2µg/mL puromycin and 0.3mg/mL Geneticin). They were passaged two times per week using diluted 0.25% Trypsin (1:5 in PBS) and split at a ratio of 1:3 to 1:5. In general, cells were kept in culture and passaged up to twenty times maximum until a new vial of frozen cells was defrosted.

For viral production 293GPG cells were plated into 10cm dishes in basic medium A without tetracycline, whereby VSVG expression is induced. The next day, a transfection mix of 12.5µg DNA, 30µL Lipofectamine2000 and 3mL Opti-MEM per one 10cm dish was prepared and incubated for 30min at RT. Meanwhile, the 80-90% confluent cells were washed twice using Opti-MEM with 10% FCS to remove all remaining antibiotics. In the last step washing medium was exchanged by adding carefully 3mL of the transfection mix to each plate. The following morning, transfection medium was replaced by packaging medium consisting of DMEM (4.5g glucose, GlutaMAX) supplemented with 10% FCS.

The first medium collection was performed 48h after transfection, followed by a second harvest 72h after transfection. To concentrate viral particles, culture medium was filtered through a pre-wetted low-protein binding 0.45µm PVDF filter and spun down at 50,000 x g for 90min at 4°C. Supernatant was discarded and transparent pellet was resuspended in TNE buffer (50mM Tris-HCl pH7.8, 130mM NaCl, 1mM EDTA). Viral aliquots of 5µL or 10µL were stored at -80°C.

3.4.4 Lentiviral production

Instead of the 293GPG packaging cell line the lentiviral production was performed using 292T cells. Therefore, additionally two viral packaging plasmids, pCMVΔ8.9 (Zufferey et al., 1997) and pVSVG, were required for the preparation. The pseudotyped pCMVΔ8.9 packaging construct contains all human immunodeficiency virus type 1 (HIV1) genes besides *vif*, *vpr*, *vpu* and *nef*. On the other hand the pVSVG envelope vector expresses the vesicular stomatitis virus glycoprotein under the control of the CMV promoter.

First, 292T cells were expanded in basic medium B (DMEM containing 10% of heat inactivated FCS and 0.3mg/mL Geneticin). At the day of transfection, cells were split, resuspended in Opti-MEM (GlutaMAX) including 10% heat inactivated serum. Meanwhile, the transfection mix containing 7.5µg of pCMVΔ8.9, 5µg of pVSVG, 3µg of the expression

plasmid, 36µL Lipofectamine2000 and 3mL Opti-MEM per one 10cm dish was prepared and incubated for 30min at RT. Resuspended cells were poured into transfection mix, seeded into 10cm dishes and incubated overnight. The next morning, transfection medium was exchanged by packaging medium described in the previous section.

Harvest and purification of lentiviruses was done in almost the same manner as the retroviral production. But in order to increase lentiviral titres, an additional concentration step was performed. Thus, two harvests of the same type of resuspended viral particles were combined, ultra-centrifuged at 80,000 x g for 90min at 4°C and resuspended in TBS-5 (50mM Tris-HCl pH7.8, 130mM NaCl, 10mM KCl and 5mM MgCl₂). Viral aliquots of 10µL were stored at -80°C.

3.4.5 Determination of viral titres

Viral vectors were added in serial dilution to primary embryonic (E14) cortical cell cultures. Cells were maintained 2 days *in-vitro* to allow the expression of the GFP. Then they were fixed in 4% PFA for 15min at RT and processed for GFP immunocytochemistry. The number of GFP⁺ colonies was counted per cover slip. As one infectious viral particle results in one clone and the applied volume of the viral solution is known, the exact number of viral particle per µL can be determined via this method.

3.5 IMMUNOCHEMISTRY

3.5.1 General method

In this work immunostaining was performed on fixed tissue culture samples (immunocytochemistry) and sectioned brain slices (immunohistochemistry) ranging from 20-200µm of thick-ness. As antibody dilutions and incubation times are highly dependent on thickness of the tissue and fixation method, all detailed information of primary antibody applications can be seen in table 3-2.

In general, antibodies were diluted in 0.1M PBS containing 0.5% Triton-X-100. Furthermore, 10% normal goat serum or 2% bovine serum albumin was added to the antibody solution in order to reduce non-specific binding. Antigen labelling was performed indirectly in following sequence: First, specimens were incubated with primary antibodies that recognise and bind to antigens of interest, followed by three wash steps in PBS. In order to visualise primary antibody binding, samples were exposed to subclass specific secondary antibodies conjugated to Alexa 488, Alexa 543, Alexa 633 (1:1000, Invitrogen) or Cy2, Cy3, Cy5 (1:400, Jackson Immuno Research).

Furthermore, detection of some antigens required (see table 3-2) signal amplification using Avidin-Biotin interactions. Thus, after primary antibody binding specimens were incubated with a biotinylated secondary antibody (1:200, Vector Laboratories) directed against the

immunoglobulins of the primary antibody. Finally, specimens were exposed to fluorochrome (Alexa 488, Alexa 543 or Alexa 633) - conjugated Streptavidin (1:1000, Invitrogen). Nuclei were visualised with DAPI (4', 6' Diamidino-2-phenylindole, Sigma) by incubating sections for 10 minutes with a concentration of 0.1µg/ml DAPI in PBS.

After completed labelling, samples were mounted in Aqua Poly/Mount, a glycerol-based mounting medium that enhances and retains fluorescent stains. Stainings were analyzed at the Zeiss Axioplan2 light microscope (Axiovision software 4.2) or the Olympus FV1000 laserscanning confocal microscope (Olympus Flouview Ver. 2.0b software) with optical sections of 1µm intervals.

3.5.2 Antigen retrieval

Antigen retrieval (or antigen recovery) is performed to expose or retrieve antigens which have become masked by the tissue fixation process. Several retrieval protocols are available; depending on the epitope (see table 3-2) the following methods have been used in this thesis.

Microwave oven heating

Shi and his colleagues developed in 1991 the first antigen unmasking technique based on microwave heating of tissue sections in the presence of metal solutions (Shi *et al.*, 1991). In order to recover binding to α -E-Catenin, Ki67, Pax6 or PCNA, sections were boiled 8min in 0.01M sodium citrate buffer (pH6). After the microwave treatment sections were usually transferred into PBS and washed three times before incubation with the first antibody. However, in the case of PCNA staining, sections were kept in the hot sodium citrate buffer for 20min until they cooled down. Then, sections were permeabilised with 0.3% Triton-X-100 in PBS for 30min and quenched with 0.1M glycine-Tris (pH 7.4) for 30min. After incubation with a blocking solution of 0.2% gelatine, 300mM NaCl and 0.3% Triton-X-100 in PBS an overnight incubation with the primary antibody at 4°C followed.

Autoclave heating

Detection of the Partitioning defective 3 homolog (Par3) in the adult brain was achieved on 10µm thick paraffin sections. After deparaffinisation and rehydration in PBS, slides were immersed in an autoclavable tray containing 0.01M sodium citrate buffer (pH6) and autoclave at 120°C for 10min. After cooling down the tray at room temperature, slides were washed three times in PBS before continuing immunostaining.

DNA denaturation

In order for the anti-BrdU antibody to access the 5'-bromo-2'-deoxyuridine (BrdU) that has incorporated into the genome denaturation of DNA is needed. Therefore, sections were incubated in 2N HCl for 30min. Afterwards the acid was neutralised by washing sections three times 10min in 0.1M sodium tetraborate buffer (pH 8.5). Finally, sections were rinsed once in PBS and incubated in the primary anti-BrdU antibody solution.

3.5.3 Tyramide signal amplification

Some antigens were detected by tyramide signal amplification (Perkin Elmer) that not only amplified weak signals but also allowed simultaneous detection of two proteins by two antibodies generated in the same species. Immunocytochemistry involving the tyramide kit was done as described in the tyramid signal amplification handbook (Perkin Elmer). In brief, specimens were washed three times in TNT wash buffer (0.1M Tris-HCl, pH 7.5, 0.15M NaCl, 0.05% Tween 20) before quenching endogenous peroxidase activity by incubating sections for 30min in 0.3% H₂O₂. After three washing steps, incubation of the primary antibody diluted in TNB Blocking Buffer (0.1M Tris-HCl, pH 7.5, 0.15M NaCl and 0.5% Blocking Reagent [provided by the kit]) at 4°C was performed followed by another incubation with the corresponding biotinylated secondary antibody (1:200, Vector Laboratories). Sections were washed again and incubated with a horseradish-peroxidase coupled Streptavidin (1:200, provided by the kit). Finally, the fluorophore tyramides (Fluorescein or Tetramethylrhodamine) diluted 1:100 in the provided amplification buffer were added to the specimens for 7min.

Table 3-2. Primary antibodies used for immunohistochemical analysis performed in this work.

| Antigen | Company, Ordering Number | Specie | Dilution | Antigen Retrieval, Blocking Reagent |
|---|---------------------------------|---------------|------------------------------|--|
| BrdU ((5'-bromo-2'-deoxyuridine) | Abcam, Ab-6326-250 | rat IgG2a | 1:200-1:500 | 30min HCl 2N, 3x10min Borate buffer pH8.5, 3x10min PBS |
| Doublecortin (DCX) | Millipore, AB5320 | guinea pig | 1:1000 | - |
| Doublecortin (DCX) | Abcam, AB18723 | rabbit | 1:500 | - |
| GFP | Aves Labs,Inc; GFP-1020 | chick | 1:700, 1:5000 (Tyramide Kit) | - |
| Glial Fibrillary Acidic Protein (GFAP) | Sigma, G3893 | mouse IgG1 | 1:100 | - |
| Glial Fibrillary Acidic Protein (GFAP) | DAKO, Z0334 | rabbit | 1:200 | - |
| Partitioning defective 3 homolog (Par3) | Millipore, 07-330 | rabbit | 1:100 (whole mounts) | Amplification needed or Paraffin sections (10µm), autoclaving in Citrate Buffer |
| Pax6 (polyclonal) | Covance, PRB-278P | rabbit | 1:500-1:700 | Bioling recommended, Amplification |
| Tbr2 | Abcam, ab23345-100 | rabbit | 1:1000 | - |
| Tyrosine hydroxylase (TH) | Millipore, AB9702 | rabbit | 1:200 | - |
| α-E-Catenin | BD Transd. Lab, 610193 | mouse, IgG1 | 1:100 | Boiling in Citrate Buffer |
| β-Catenin | BD Transd. Lab, 610153 | mouse, IgG1 | 1:200 | Blocking for 30 min in PBS (1%Tx, 2.5% NGS), Biotin amplification (whole mounts) |
| β-Catenin | Sigma, C2206 | rabbit | 1:2000 | 10% NGS |
| β-Galactosidase | Capell | rabbit | 1:10.000 (Tyramide Kit) | - |

3.6 IN-SITU HYBRIDISATION

In-situ hybridisation (ISH) was carried out on cryostat sections of 25µm thickness. In general, the *in-vitro* transcription and the ISH were carried out under semi-sterile conditions using sterile pipet tips and gloves. The ISH technique can be divided into two main steps: (i) generation of the antisense RNA specific probe by *in vitro* transcription, (ii) hybridisation of the RNA probe and its detection in the section.

3.6.1 *In vitro* transcription: generation of digoxigenin labelled probes

The cDNA containing the ISH plasmid was linearised by use of an enzyme at the end cDNA probe insert. Therefore, the RNA polymerase falls off the DNA strand at a defined point after transcribing the according cDNA into RNA. Linearisation of 1µg DNA was performed with 1µL of the according enzyme and 2µL 10xbuffer in a final volume of 20µL. After digestion DNA was purified by phenol extraction. Transcription was performed by using 1µg DNA, 2µL digoxigenin labelled dNTPs (Roche), 4µL 5xbuffer (Stratagene), 1µL RNase inhibitor (Roche) and 1µL of the according RNA polymerase (T3, T7, Sp6) (Stratagene). The mixture was kept for 2h at 37°C and RNA was cleaned over a RNA binding column (Qiagen). 1µL of the resulting RNA probe was examined on a gel for RNA presence. All probes were then tested on sections. As a rule of thumb 2µL per 100µL hybridisation buffer was used first until the optimal concentrations were determined.

3.6.2 *In-situ* hybridisation

Cryostat sections were incubated in chambers containing sterile water to avoid drying of the sections overnight. Per slide 150µL of hybridisation buffer (50% formamide, 4xSSC, 2% SDS, 50 µg/mL yeast tRNA (Roche), 2% blocking reagent (Roche), 50µg/mL Heparin in H₂O) were used. After adding the probe to the hybridisation buffer the mixture was heated up to 74°C for 4min to separate RNA strands and mixed again. Sections were incubated in an oven at 65°C overnight.

The next day the washing solution was pre-warmed in a water bath to 65°C. Sections were moved to a sterile washing chamber and incubated twice for 30min at 65°C in washing solution (50% formamide, 4xSSC, 0.1% Tween20 in H₂O) followed by two washing steps in 1x MABT (100mM maleic acid, 150mM NaCl, 0.1% Tween20, pH 7.5 in H₂O) for 30min at RT. Slides were blocked in ISH blocking buffer (1xMABT, 2% blocking reagent (Roche), 10% NGS). The blocking solution was discarded and replaced by antibody containing solution (anti-digoxigenin fab fragments 1:2500 in ISH blocking buffer) and covered by parafilm. Sections were incubated at 4°C overnight.

The next day, sections were washed 5 times in 1xMABT buffer and twice in freshly prepared AP staining buffer (100mM Tris (pH 9.5), 50mM MgCl₂, 200mM NaCl, 0.1% Tween20 in

H₂O). 3.5µL NBT (Roche) and BCIP (Roche) were added per 1mL AP buffer and put onto the sections until the desired staining intensity was reached. Reaction was stopped by washing the section in autoclaved water or sections were washed in PBS and processed for immunohistochemistry as described above.

3.7 WESTERN BLOT ANALYSIS

3.7.1 Tissue preparation

All embryonic brain samples were isolated from E11-E13 time pregnant transgenic mice as described in section 3.3.2. Tissue from the dorsal, ventral and lateral wall of the lateral brain ventricles was collected from adult male C57BL/6J mice. Therefore, adult mice were sacrificed by cervical dislocation, brains were promptly removed and tissue of interest extracted.

Before starting tissue lysis, collected samples were shock-frozen in liquid nitrogen and stored at -80°C. After determination of the genotype, embryonic cortical samples of the same genotype were pooled and homogenised in 1.5 volumes of ice-cold lysis buffer (20mM Tris-HCl, pH 7.4, 137mM NaCl, 10% glycerol, 0.1% sodium dodecyl sulphate (SDS), 0.5% sodium deoxycholate, 1% Triton-X-100 with the addition of Complete protease inhibitor cocktail, 100µM sodium orthovanadate and 100nM ocadaic acid) using a dounce homogeniser. After passing sample ten times through a pre-wetted 27G needle syringe, resulting homogenates were sonicated using a sonicator for 5sec with a power of 10% in order to cut DNA molecules and open all nuclei sufficiently. Samples were centrifuged at 16,000 x g for 10min at 4°C to remove cell debris and supernatant was collected. Proteins were quantified by the BCA method and diluted in 5x sample buffer (250mM Tris-HCl, pH6.8, 4% SDS, 10% glycerol, 2% β-mercaptoethanol, 0.006% bromphenol blue). Samples were boiled for 5min at 95°C and cooled down again prior to loading electrophoresis gel. Usually a total amount of 10-40µg protein was load per lane.

3.7.2 SDS-polyacrylamide gel electrophoresis (SDS-PAGE)

SDS-PAGE was performed using the vertical Mini-PROTEAN 3 Cell System (Biorad, 165-3301). Gels were polymerised in the corresponding gel casting system. First, the separating gel was poured. Per 10mL monomer solution 4mL separating gel buffer (see commonly used buffers), 1.8mL deionised water and 0.1% SDS were used. Depending on the size of the protein that was analysed, different percentages of acrylamide ranging from 6 to 14% were applied. Furthermore, immediately prior to casting the gel 0.08% ammonium peroxide disulphate (APS) and 8µL TEMED were added. To prevent air bubbles the poured gel was covered by a thin layer of isopropanol. When separating gel had set, isopropanol was

discarded and the gel was rinsed with deionised water. After removing the water from the polymerised separating gel, the loading gel was poured on top and a comb was placed to create the wells. Per 5mL loading gel solution 625 μ L stacking gel buffer (see commonly used buffers), 3.46mL deionised water, 0.1% SDS, 5% acrylamide, 0.08% APS and 6 μ L TEMED were used. After the gel had polymerised, the comb was removed, and the wells were rinsed thoroughly with running buffer (25mM Tris-HCl, pH 8.3, 192mM glycine and 0.1% SDS). In order to perform proper semi-quantitative Western blot analysis, gel duplicates loaded with the same samples were run with a constant current at 50mA and voltage at 200V. Usual running time was about 1.5h. Finishing the run, stacking gel was cut off and the separating gel was equilibrated for 10min in transfer buffer containing 25mM Tris base, 200mM glycine, 15% methanol and 0.1% SDS.

3.7.3 Transfer

In order to make the separated proteins accessible to antibody detection, they were moved from within the gel onto Immobilon-P membrane (Millipore, IPVH00010) made of polyvinylidene difluoride (PVDF). Membranes were pre-wetted with methanol, which was replaced stepwise by transfer buffer. The separating gel was placed on top of equilibrated membrane. This gel-membrane sandwich was positioned between a stack of six Whatman filter papers. The entire stack covered by transfer buffer was placed into the semi-dry blotting aperture (NeoLab, 7-0120) and per gel blotted at 120mA, 8V limited for 1.5h at RT.

3.7.4 Blocking, detection and scanning

Transfer efficiency was checked immediately after blotting by covering PVDF membrane with Ponceau S dye followed by rinsing it gently with deionised tap water. Non-specific binding was blocked by incubation with TTBS (see commonly used buffers) supplemented with 5% non-fat dry milk for 15min at RT. Primary antibodies (see table 3-3) were diluted in TTBS and membranes were incubated at 4°C overnight. After subsequent washes in TTBS, membranes were incubated for 2h at RT with a horseradish-peroxidase-linked secondary antibody (GE Healthcare, NA9310 and NA9340) diluted 1:5000 in TTBS and directed against the appropriate species. The blots were washed again three times in TTBS and proteins detected with the ECL Western Blotting Detection Reagents (GE Healthcare, RPN2109) and exposure to X-ray film prior to scanning. Developed X-ray films were digitalised using the CanoScan N670U (Canon) and the Adobe Photoshop CS3 software to generate 16-bit grey scale images with a spatial resolution of 400 dots per inch.

Table 3-3. Primary antibodies used for Western blot analysis performed in this work.

| Antigen | Company, Ordering Number | Specie | Dilution | Protein size in kDA |
|---|--------------------------|--------|--------------|---------------------|
| α -E-Catenin | BD Transd. Lab, 610193 | mouse | 1:250 | 102 |
| α -N-Catenin | Abcam, ab11347 | rabbit | 1:250 | 100, 105 |
| β -Actin | Sigma, A5441 | mouse | 1:20,000 | 42 |
| β -Catenin | BD Transd. Lab, 610153 | mouse | 1:500 | 92 |
| Atypical protein kinase <i>λ</i> /i aPKC <i>λ</i> /i | BD Transd. Lab, 610175 | mouse | 1:200 | 74 |
| Cdc42 | BD Transd. Lab, 610928 | mouse | 1:100 | 22 |
| Glycogen synthase kinase 3 <i>β</i> (GSK3 <i>β</i>) | Epitomics/Biomol, 1561-1 | rabbit | 1:500 | 47 |
| Partitioning defective 3 homolog (Par3) | Millipore, 07-330 | rabbit | 1:500-1:1000 | 100, 150, 180 |
| Par6 | Santa Cruz, sc-14405 | goat | 1:500-1:2000 | 37 |
| Paired box gene 6 (Pax6) | Chemicon, Ab5409 | rabbit | 1:500 | 47 |
| Ser9 phosphorylated GSK3 <i>β</i> (p-GSK3 <i>β</i>) | Cell Signaling, 9336 | rabbit | 1:500 | 48 |
| Thr410/403 phosphorylated aPKC <i>λ</i> /i and aPKC <i>ζ</i> (p-aPKC) | Cell Signaling, 9378 | rabbit | 1:500 | 76 |
| Prominin-1 (Cd133) | eBioscience, 14-1331 | rat | 1:500 | 97 |

3.7.5 Semi-quantitative Western blot analysis

In order to perform semi-quantitative Western blot analysis, the gel analysing tool of ImageJ was used. All lanes of interest were outlined using the rectangular selection tool of ImageJ. Thus, corresponding lane profiles plotting the signal intensity against its position within the gel/membrane were generated. The absolute intensity (AI) of each signal was calculated by determining the area under the peak at the position of the antibody signal and at three neutral positions in order to score the background as well. Furthermore, measurements of the corresponding α -Actin bands were included in order to normalise for the amount of proteins that were effectively loaded. The results of the α -catenin knock-out cortices were normalised to wild-type situation and calculated as fold changes in %. The average fold changes and standard errors of the mean (SEM) resulted from three independent experiments using three different sample sets.

3.8 SUBCELLULAR FRACTIONATION

Cortical tissue was isolated from wild-type and α -catenin knock-out embryos at E11, shock-frozen in liquid nitrogen and stored at -80°C . After determination of the genotype, ten embryonic cortical samples of the same genotype were pooled, resuspended in 200 μL of ice-cold hypotonic Buffer A (10mM HEPES, pH 7.9, 10mM KCl supplemented with Complete protease inhibitor cocktail, 100 μM sodium orthovanadate and 100nM ocadaic acid) and transferred to a douncer. Cell membranes were broken by moving the loose pistil ten times up and down. Subsequently the samples were passed through a pre-wetted 27G needle syringe ten times and N-P40 was added at final concentration of 0.1%. The cloudy solution was spun down at 1000 x g for 5min at 4°C . The supernatant (cytoplasm) was frozen at -20°C before continuing Western blot procedure.

The nuclei were resuspended in 150 μL ice-cold high-salt Buffer B (Buffer A containing 400mM NaCl) and sonicated using the sonicator for 5sec with a power of 10%. N-P40 was added at final concentration of 1% and nuclei were incubated for 40min on ice. Finally, lysate was spun down again at 3000 x g for 10min at 4°C to discard cell debris. The supernatant was frozen at -20°C before continuing Western blot analysis.

3.9 β -GALACTOSIDASE REPORTER GENE ASSAY

Canonical Wnt signalling activity was monitored by applying the β -galactosidase reporter gene assay to embryonic cortical tissue isolated from wild-type and α -catenin knock-out mice carrying as well the TOPGAL reporter gene. Therefore, cortices from twelve E11 embryos of the same genotype were pooled and homogenised in 400 μL of lysis reagent (provided by the

kit). Protein extract was spun down at 16,000 x g for 5min at 4°C to precipitate cellular debris. Supernatant was collected and protein concentration was determined by BCA assay. For internal standardisation, β -galactosidase positive control (provided by the kit) was resuspended by serial dilution steps in lysis reagent as well. Furthermore, wild-type cortices without the TOPGAL reporter were lysed as control. The protein concentration in all extracts was diluted to 0.7 and 1.4 μ g/ μ L. Then, 50 μ L of each sample was pipetted in triplicates into a white microplate and covered by 100 μ L of the substrate reagent (provided by the kit). Following an incubation time of 20min at RT, plate was transferred to a luminometer (Orion II Microplate Luminometer, Berthold Detection Systems) that injected automatically 50 μ L of the initiation reagent (provided by the kit). After a delay of 1sec, the luminometer measured the chemiluminescence signals of each well for 5sec and summarised it in the value relative light units [rlu/5sec].

4 Results

4.1 INFLUENCE OF CORTICAL α -E-CATENIN DEFICIENCY ON CELLULAR SIGNALLING

Loss of α -E-catenin during brain development has been reported to cause ectopic tissue expansion due to hyperproliferation (Lien et al., 2006, Schmid, 2007). In order to elucidate mechanisms explaining this phenotype, I used the $Emx1^{Cre/\alpha-cat\Delta ex2fl/fl}$ mice for biochemical analysis. These double transgenic animals were generated by crossing the $Ctnna1^{tm1Efu/J}$ mice (Vasioukhin et al., 2001), which possess loxP sites on either side of exon 2 of the targeted gene, to the $Emx1$ driven Cre line (Iwasato et al., 2004, Cappello et al., 2006). The $Emx1::Cre$ line expresses Cre recombinase in the developing cerebral cortex from E9.5 onwards (Iwasato et al., 2004, Cappello et al., 2006, Schmid, 2007), resulting in a decrease of α -E-catenin mRNA at E10 and loss of the α -catenin immunoreactivity at E11 (Schmid, 2007). Interestingly, hyper-proliferation seen in the $Emx1^{Cre/\alpha-cat\Delta ex2fl/fl}$ occurred in a narrow time window, starting shortly after α -E-catenin reduction at E11 and ending at E13 (Schmid, 2007). In order to explain the observed phenotype on a molecular level, I have concentrated my analysis on this time window by collecting samples from the developmental stages E11, E12 and E13. To assess the impact of α -E-catenin deletion on protein level of known α -E-catenin interactors Western blotting was applied using actin as internal control. Whole protein extracts were obtained from control or α -E-catenin deficient cortices dissected at the three developmental stages. Control animals (referred to as WT) carried none or only a single α -catenin floxed allele and were eventually heterozygous for the $Emx1::Cre$. Experimental animals were homozygous for the α -E-catenin floxed allele and heterozygous for the $Emx1::Cre$ (referred to as α -cat fl/fl x $Emx1::Cre$).

4.1.1 Protein levels of α -E- and α -N-catenin in the $Emx1^{Cre/\alpha-cat\Delta ex2fl/fl}$ cortices

In order to examine the loss of α -E-catenin after recombination at quantitative levels, I first performed Western blot analysis of cortical protein lysates obtained from all three developmental stages using an antibody recognising specifically α -E-catenin. A specific protein band at ~100kDa was detected in controls, while this band was not visible in α -E-catenin knock-out samples indicating the purity of my cortical preparations (Fig.4-1A).

Beside α -E-catenin also α -N-catenin is present in the developing cerebral cortex. Both α -catenin types are expressed in embryonic neural stem cells, but only α -N-catenin is also found in neurons (Stocker & Chenn, 2006). As α -N-catenin may play a compensatory role in the absence of α -E-catenin, I analysed control and mutant cortical lysates in the next step for its overall expression level. Surprisingly, protein amounts of α -N-catenin were not altered after loss of α -E-catenin (Fig.4-1B). Control and mutant lysates from E12 and E13 cortices resulted in two bands above ~98kDa at equal intensities (Fig.4-1B). These represent the two

reported α -N-catenin isoforms: α -N-catenin-I with a molecular weight of 100kDa and α -N-catenin-II having a molecular weight of 105kDa (Uchida *et al.*, 1994). Due to the very low expression levels of α -N-catenin in E11 cortices, only faint bands at the position of the α -N-catenin isoforms were obtained from control or mutant lysates. Additionally, when α -N-catenin was expressed at higher levels at E12 and E13 within the cortical tissue, no differences in expression levels could be seen between control and mutants.

In conclusion, depletion of α -E-catenin during cortical development does not up-regulate the levels of α -N-catenin. Thus, although both molecules are prominent members of the adherens junctional complex, one does not substitute the other.

4.1.2 Influence of α -E-catenin loss on apical membrane proteins of the Par complex and Prominin-1

Beside the unrestricted growth of the cerebral cortex, another prominent phenotype of α -E-catenin deficiency was related to the morphology of cells residing in the expanding tissue (Schmid, 2007). Conditional loss of α -E-catenin provoked a complete loss of the elongated morphology of embryonic neural stem cells, which as a consequence led to the disappearance of the cadherin- β -catenin band delineating the ventricular surface of the cortex (Schmid, 2007). Ultrastructural analysis revealed that adherens junctions (AJ) were still present, but irregularly distributed in mutant cortices (Schmid, 2007).

AJ also serve as an anchoring point for multiple other proteins including the Par complex molecules, which have been shown to control cell proliferation (Costa *et al.*, 2008, Bultje *et al.*, 2009, Nolan *et al.*, 2008). The redistribution of AJ in the α -E-catenin deficient cortex may influence the expression level of these proteins and therefore cause the observed over-proliferation of the cortical cells. To investigate this, I performed Western blot analysis of wild-type and $Emx1^{Cre/\alpha\text{-cat}\Delta\text{ex}2fl/fl}$ cortical lysates using antibodies recognising Par3, Par6, aPKC λ /I and the phosphorylated, activated form of aPKC (referred to as p-aPKC). The antibody against p-aPKC detects endogenous aPKC ζ only when phosphorylated at threonine 410, and endogenous aPKC λ /I only when phosphorylated at threonine 403. In agreement with the presence of AJ despite loss of α -E-catenin, also the three analysed proteins of the Par complex known to concentrate at the AJ were found in conditional knock-out lysates (Fig.4-2/4-3). Par3 appeared as two discrete protein bands, corresponding to the two prominent brain isoforms with a molecular weight of 100kDa and 180kDa (Fig.4-2A). While both Par3 isoforms seemed to be up-regulated especially in the mutant cortices at E11, no obvious difference was seen at the other developmental stages (Fig.4-2A). However, no apparent change in protein levels of Par6 (Fig.4-2B) or aPKC λ /I (Fig.4-3A) was observed upon loss of α -E-catenin. Western blots probed for Par6 with a molecular weight of 37kDa showed

one

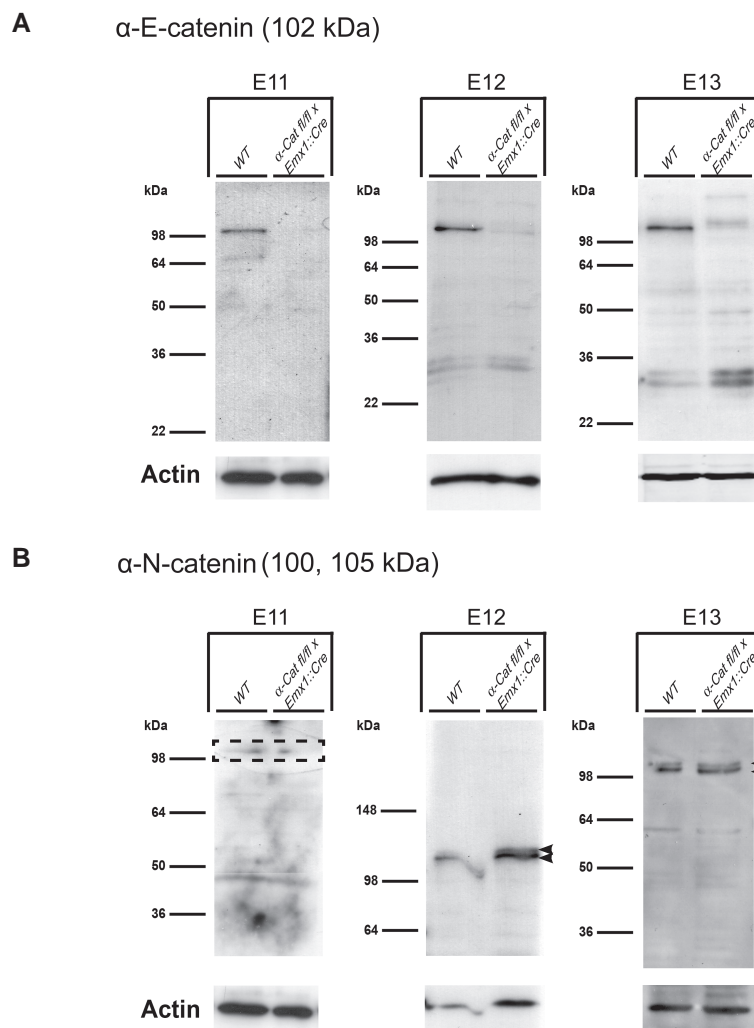


Figure 4-1. Protein levels of α -E- and α -N-catenin in $Emx1^{Cre/\alpha-cat\Delta ex2fl/fl}$ cortices

(A-B) Cortical protein lysates obtained from embryos of the indicated genotypes at developmental stages E11, E12 and E13 were analysed by Western blotting using an antibody recognising α -E- (A) or α -N-catenin (B). The positions of relative-molecular-mass markers are always shown to the left side of the two lanes comparing protein levels of wild-types (WT) to α -E-catenin mutants (α -Cat fl/fl x $Emx1::Cre$). The molecular weight (in kDa) of the proteins against the Western blots were probed is given in brackets in the upper left corner of each panel. Signals detected with β -actin antibody served as internal controls for protein loading. (A) Note, that the specific α -E-catenin protein band above ~98kDa is present in wild-type lysates, but is absent in α -E-catenin conditional knock-out lysates indicating efficient deletion by the Cre line. (B) While the specific bands of α -N-catenin were rarely detectable (dashed square) in wild-type and knock-out lysates at E11, two bands (arrowheads) running very close together were visible at later stages. The two bands correspond to the different α -N-catenin isoforms: α -N-catenin I (100kDa) and α -N-catenin II (105kDa). No obvious changes in α -N-catenin protein levels were seen between wild-type and α -E-catenin knock-out lysates.

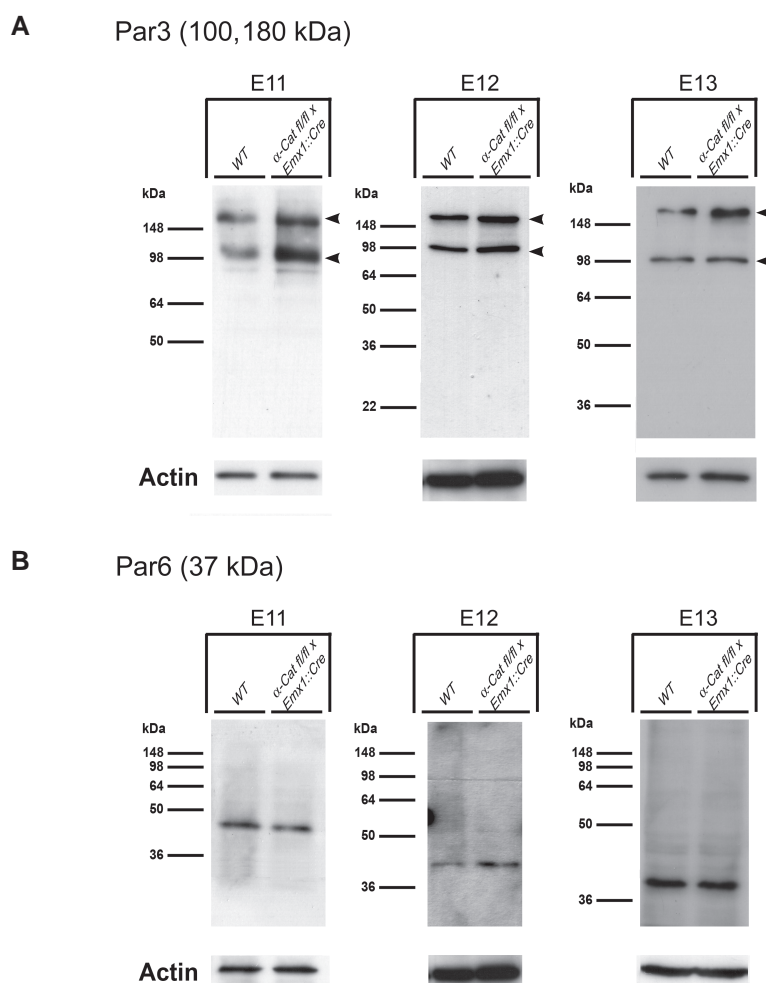


Figure 4-2. Par complex proteins are still present in α -E-catenin deficient cortices

(A-B) Endogenous expression of Par3 (A) and Par6 (B) in the cerebral cortex of wild-type (WT) or α -E-catenin deficient (α -Cat fl/fl x Emx1::Cre) embryos from E11 to E13 of mouse development. The positions of relative-molecular-mass markers are shown on the left of the individual Western blots. Anti- β -actin staining was used as an internal loading control. (A) Both, wild-type and α -E-catenin deficient cortices contain Par3 protein, that was present as two distinct protein bands (arrowheads). These bands probably correspond to the two different Par3 splice variants with a molecular mass of 100kDa and 180kDa. Note, that at E11 Par3 protein levels seem to be higher in knock-out cortices than the levels observed in wild-type tissue. (B) In contrast, similar amounts of Par6, represented by the single protein band between 36 and 50kDa, are present in wild-type and α -E-catenin deficient cortices.

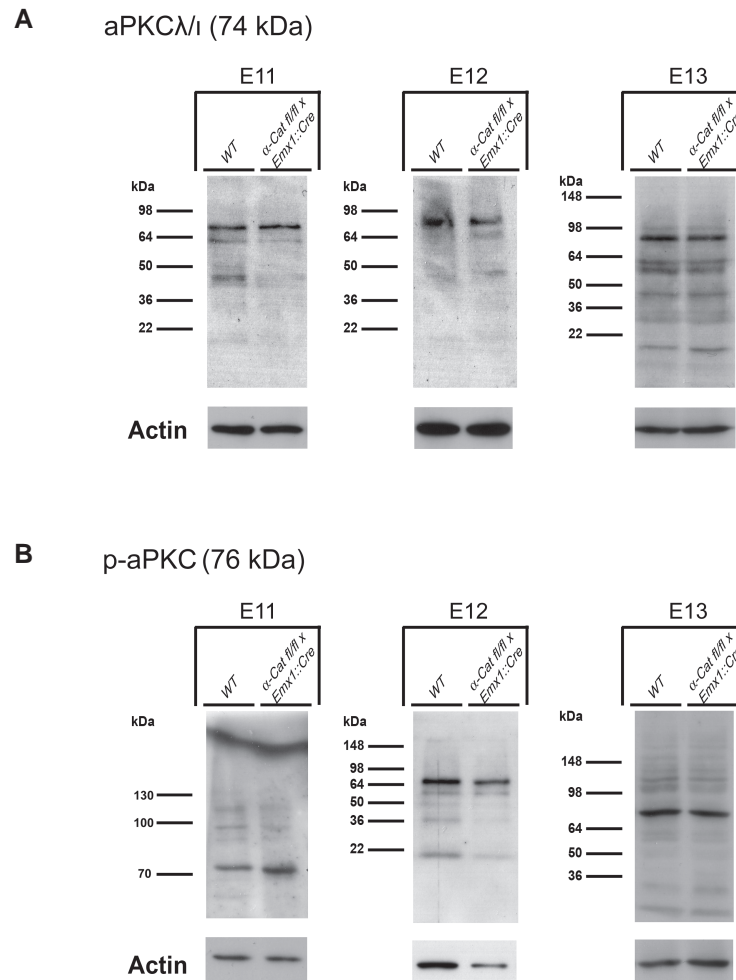


Figure 4-3. Loss of α -E-catenin in the cerebral cortex does not influence total levels of aPKC λ 1 or the amount of its activated form

(A-B) Western blot analysis performed to examine the total expression levels of aPKC λ 1 (A) and the amount of phosphorylated, active aPKC λ 1 and aPKC ζ (B, referred to as p-aPKC) in the cerebral cortex of wild-type (WT) or α -E-catenin deficient (α -Cat fl/fl x Emx1::Cre) mouse embryos from E11 to E13. The positions of relative-molecular-mass markers are shown on the left of the individual Western blots. Anti- β -actin staining was used as an internal loading control. (A) Western blotting using an antibody against aPKC λ 1 revealed similar protein levels in presence or absence of α -E-catenin. (B) Beside E11, where p-aPKC is slightly increased in α -E-catenin deficient cortices, the amount was not altered in later developmental stages.

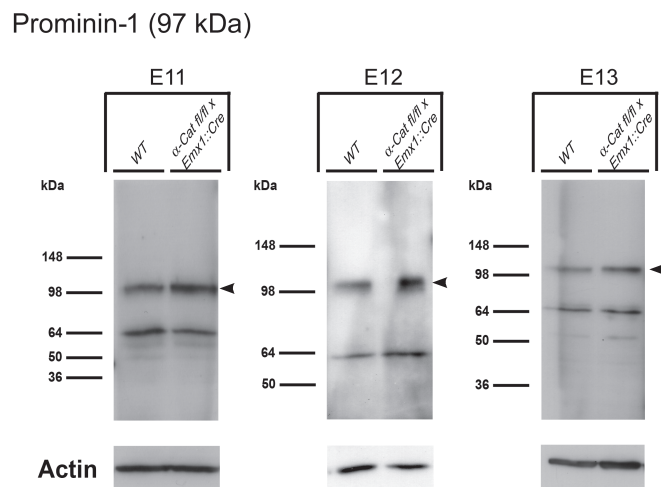


Figure 4-4. Prominin-1 levels are not altered in α -E-catenin deficient cortices

Western blot analysis for Prominin-1 (CD133) expression in wild-type (WT) or α -E-catenin deficient cortices (α -Cat fl/fl x Emx1::Cre) collected at E11, E12 and E13. β -actin expression was used to normalise for equal loading. The positions of molecular weight standards are shown on the left of the individual Western blots. The Prominin-1 specific protein band corresponding to its molecular weight of 97kDa is marked by arrowheads. Note, that the total amount of Prominin-1 is minimally changed upon loss of α -E-catenin.

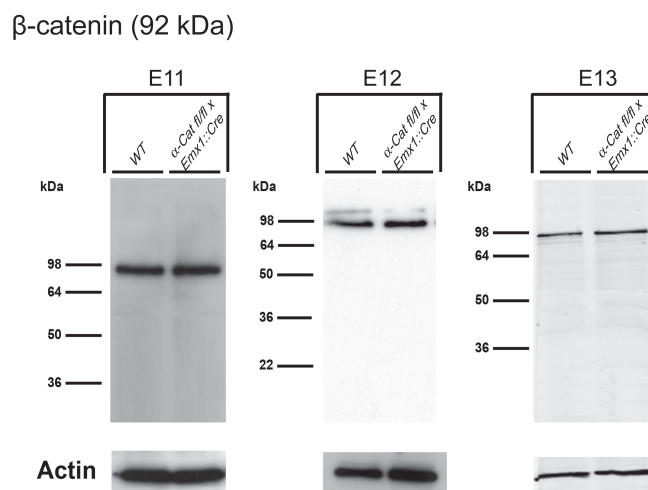


Figure 4-5. Depletion of α -E-catenin in the cerebral cortex has no major effect on the relative abundance of β -catenin

Total protein lysates from wild-type (WT) or α -E-catenin deficient (α -Cat fl/fl x Emx1::Cre) cortices from E11-E13 were analysed by Western blot with anti- β -catenin antibody. The positions of relative-molecular-mass markers are shown on the left of the individual blots. Anti- β -actin staining was used as an internal loading control. Note that although α -E-catenin becomes depleted from the β -catenin/cadherin complex at the adherens junctions, protein levels of β -catenin do not change in comparison to wild-type.

specific protein band between 36kDa and 50kDa (Fig.4-2B). aPKC λ /I having a molecular weight of 74kDa was present as a discrete protein band between 64kDa and 98kDa (Fig.4-3A). Also the levels of p-aPKC being present as a single band around the same size as aPKC λ /I was not altered between wild-type and mutant at the developmental stages E12 and E13 (Fig.4-3B). However, in similarity to Par3 the amount of p-aPKC was as well a bit increased at E11 after loss of α -E-catenin (Fig.4-3B).

While the Par complex proteins are localised adjajently to the AJ in the cell cortex underneath the apical plasma membrane, Prominin-1 is restricted exclusively to the apical membrane domain and the primary cilium emerging from it. To evaluate possible alterations of this protein, I examined its levels by western blotting. Western blot analysis revealed a specific Prominin-1 protein band at ~98kDa (Fig.4-4). However another unspecific band was detected at ~64kDa. Interestingly, also Prominin-1 is present in cortical tissue after loss of α -E-catenin and its protein levels are in comparison to wild-type lysates minimally up-regulated. Taken together these data imply that loss of α -E-catenin barely influences the protein levels of the Par complex members or Prominin-1. Only the amount of Par3 and p-aPKC is slightly increased at E11, the first time point showing a complete loss of α -E-catenin protein after recombination.

4.1.3 Loss of α -E-catenin does not change canonical Wnt signalling

β -Catenin has two key functions; it interacts with cadherin and α -E-catenin at the AJ and it mediates the canonical Wnt-signalling pathway (for review see: Cadigan & Nusse, 1997). As α -E-catenin is a major β -catenin-binding protein, over-expressed α -catenin inhibits the transcriptional activity of the β -catenin-TCF/LEF complex in the canonical Wnt signalling pathway (Hwang *et al.*, 2005). Thus, loss of α -E-catenin from the adherens junctional complex might increase the pool of unbound β -catenin and activate canonical Wnt signalling. To investigate the role of β -catenin dependent Wnt signalling in $Emx1^{Cre/\alpha-cat\Delta ex2fl/fl}$ mice, I first analysed potential changes in total levels of β -catenin in E11-E13 wild-type and α -E-catenin deficient cortices using Western blot analysis. Although α -E-catenin was depleted in the mutant brains, the total levels of β -catenin appearing as a distinct protein band at ~98kDa remained unchanged (Fig.4-5).

However, quantifications of total protein levels do not rule out that the nuclear β -catenin levels, which result in increased transcription of canonical Wnt target genes, did not change. To determine if loss of α -E-catenin increases the amount of β -catenin translocating to the nucleus, I performed cell fractionations of cortical wild-type and mutant lysates of embryonic stage E11 (Fig.4-6A-B). Cytoplasmic and nuclear compartments were efficiently separated as determined by probing nuclear fractions and cytoplasmic fractions for the nuclear protein Pax6 and the cytoplasmatic protein GAPDH respectively. The low levels of Pax6 in the

cytosol and GAPDH in the nuclear fractions suggested an efficient separation of cellular compartments (Fig.4-6B). I further demonstrated equal total protein loads by assessing total nuclear Pax6 and cytosolic GAPDH (Fig.4-6A). Both, wild-type and mutant cortices showed an accumulation of endogenous β -catenin in the cytosol and in the nucleus, but no difference in the total amount of cytosolic or nuclear β -catenin was observed (Fig.4-6A).

The analysis of cytoplasmic and nuclear β -catenin levels provides already good insights into potential changes in the β -catenin signalling pathway. However, subcellular fractions are only enriched rather than clearly separated from each other. Therefore this technique may be not sufficiently sensitive to see minimal changes. For this reason, I used another independent method and investigated the canonical Wnt signalling activity after loss of α -E-catenin applying the TOPGAL reporter mice (DasGupta & Fuchs, 1999). The TOPGAL reporter strain contains three consensus LEF/TCF-binding motifs in front of a minimal c-fos promoter to drive transcription of β -galactosidase. With the help of Dr. Marie-Theres Schmid, I crossed our α -E-catenin^{flox/flox}/Emx1::Cre mice with TOPGAL animals and generated triple transgenic mice. Immunostaining against β -galactosidase was performed by Dr. Marie-Theres Schmid on brain sections of wild-type and mutant embryos sacrificed at E11. The staining revealed a graduated pattern of reporter expression being high at caudal levels and low in rostral regions (Fig.4-6C-D). Strikingly, an almost identical pattern of staining was observed in E11 TOPGAL wild-type and TOPGAL mutant brains. Although staining of tissue sections for β -galactosidase is useful to determine the distribution of active β -catenin signalling in the brain, this is not a quantitative method. To assess quantitative differences in the activity of the enzyme, I performed a β -galactosidase reporter gene assay on cortical lysates of TOPGAL wild-type and TOPGAL mutant embryos obtained from embryos at E11. The reporter gene assay for the quantitative determination of β -galactosidase activity is based on chemiluminescent substrates, which upon β -galactosidase activity get cleaved and provide a light signal. Measurements of the relative light units obtained upon cleavage of the chemiluminescent β -galactosidase specific substrates revealed no significant difference in the overall levels of TOPGAL reporter activity between wild-type and mutant brains (Fig.4-6E).

In conclusion, α -E-catenin has no impact on β -catenin dependent signalling in the developing cortex. Neither the total nor the nuclear levels of β -catenin were affected after loss of α -E-catenin. Furthermore, the spatial localisation and the enzymatic activity representing the total levels of TCF/LEF dependent β -galactosidase reporters were not altered in the TOPGAL α -E-catenin deficient brains.

β -catenin (92 kDa)

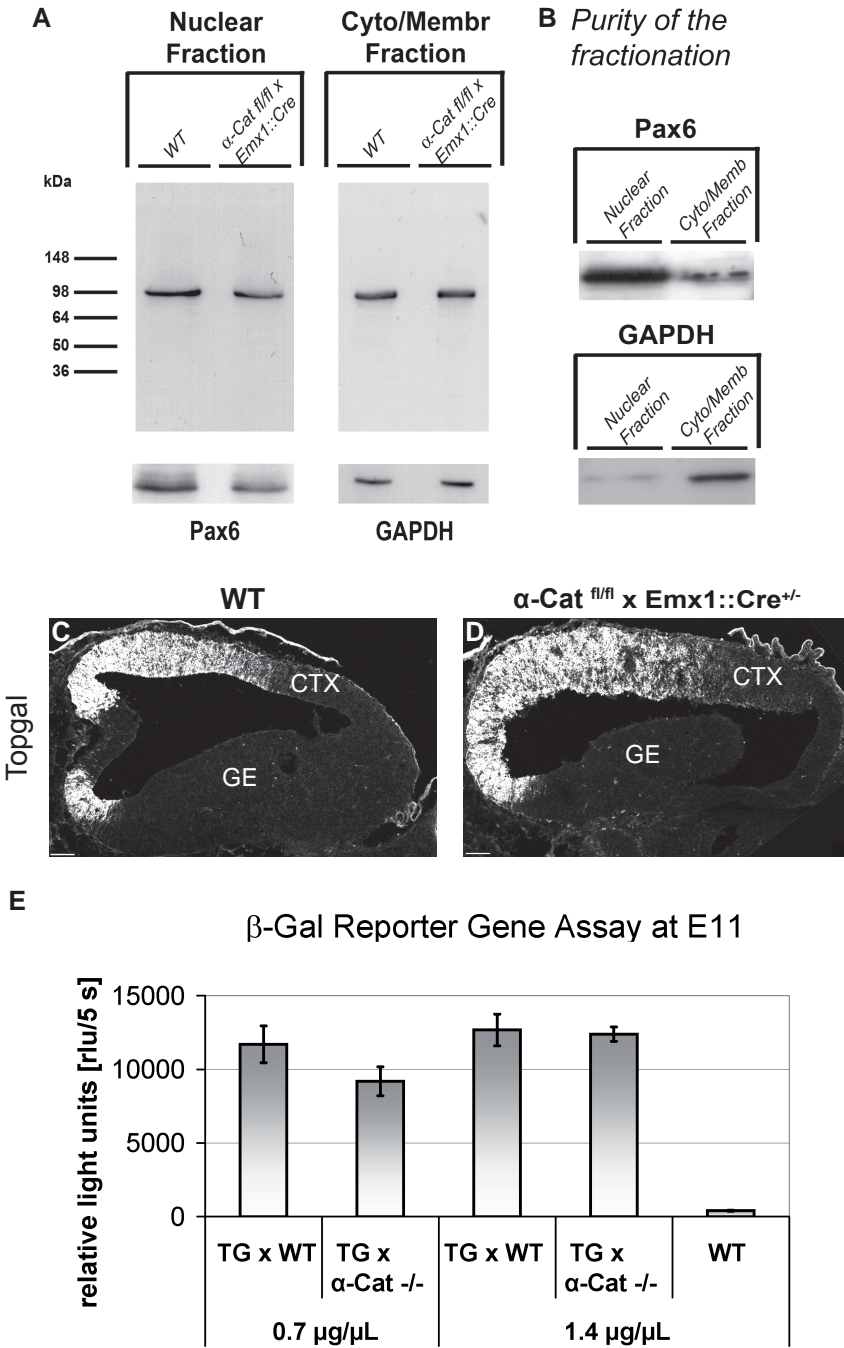


Figure 4-6. Canonical Wnt signalling activity is not changed in E11 cortices after loss of α -E-catenin

(A) Wild-type and mutant cortical lysates were fractionated into cytoplasmic and nuclear components and assessed for relative amounts of β -catenin using Western blot technology. Total protein loads were assessed by the abundance of Pax6 and GAPDH in nuclear and cytoplasmic fractions, respectively. Note, that loss of α -E-Catenin does not change the amount of nuclear or cytoplasmic β -catenin.

(B) Purity of the separation was monitored by probing cytoplasmic and nuclear fractions for the nuclear protein Pax6 or the cytoplasmic protein GAPDH.

(C-E) TOPGAL reporter for β -catenin transcriptional activity reveals no changes in α -E-catenin deficient cortices.

(C-D) Staining against β -galactosidase in the telencephalon of E11 wild-type (WT) and α -E-catenin knock-out (α -Cat^{fl/fl} x Emx1::Cre^{+/-}) embryos positive for TOPGAL transgene show similar intensity and distribution of the signal. (E) Quantitative analysis of β -galactosidase activity in lysates of TOPGAL wild-type (TG x WT) and TOPGAL α -E-catenin deficient (TG x α -cat^{-/-}) cortices at E11. Lysate of wild-type cortices lacking the Topgal reporter was used as a negative control.

Immunostainings and confocal images in C and D were done by Dr. Marie-Theres Schmid. Scale bars: 100 μ m Ctx: cortex; GE: ganglionic eminences

4.1.4 Loss of α -E-catenin up-regulates the levels of GSK3 β

Glycogen synthase kinase 3 β (GSK3 β) is a ubiquitous expressed multifunctional enzyme known to function in a variety of biological processes including proliferation, cell survival and metabolism (for review see: Rayasam *et al.*, 2009). The multifunctional role of GSK3 β can be explained by its involvement in many different signalling pathways such as canonical Wnt signalling, the classical MAP kinase cascade or the mTOR pathway (for review see: Frame & Cohen, 2001).

To examine if GSK3 β is regulated in response to loss of α -E-catenin, I performed Western blot analysis on wild-type and α -E-catenin lacking cortices. GSK3 β protein was detected with a specific antibody, visualising a band ~47kDa in control and knock-out brains (Fig.4-7A). While the levels of GSK3 β were comparable between wild-type and conditional knockouts at E11, I detected a clear increase in the protein amount of mutant cortices obtained from E12 (Fig.4-7A). This increase was still visible at E13, but tends to go back to normal levels at this developmental stage (Fig.4-7A).

The enzymatic activity of GSK3 β can be inhibited by phosphorylation of serine9 (Ser9) and thus plays an important role in regulation of GSK3 β function. In this regard it is important to bear in mind that Wnt mediated inactivation of GSK3 β does not involve its Ser9 phosphorylation (Ding *et al.*, 2000, McManus *et al.*, 2005). Interestingly, over-proliferating keratinocytes lacking the Par complex member Cdc42 showed up-regulated levels of Ser9 phosphorylated GSK3 β (Wu *et al.*, 2006). As the Cdc42 knock-out keratinocytes showed as well a reduction in adherens junction mediated cell adhesion, I tested the hypothesis, if phosphorylation of GSK3 β at Ser9 might be α -E-catenin dependent by Western blotting. An antibody specifically recognising GSK3 β phosphorylated at Ser9 (p-GSK3 β) was used to detect the endogenous levels of the inhibited kinase. Although the total cellular GSK3 β was increased in mutant embryos at E12 and E13, p-GSK3 β levels were unchanged in the cortices of α -E-catenin deficient embryos at all analysed developmental stages (Fig.4-7B).

Results

These experiments indicate that α -E-catenin regulates the total protein amounts of GSK3 β without affecting its kinase activity dependent on the phosphorylation of Ser9. Strikingly, the up-regulation of GSK3 β starts at E12, one day after the loss of α -E-catenin protein in the Cre expressing cortices and is counterbalanced already at E13, when the proportion of mitotic cortical cells was no longer increased (Schmid, 2007).

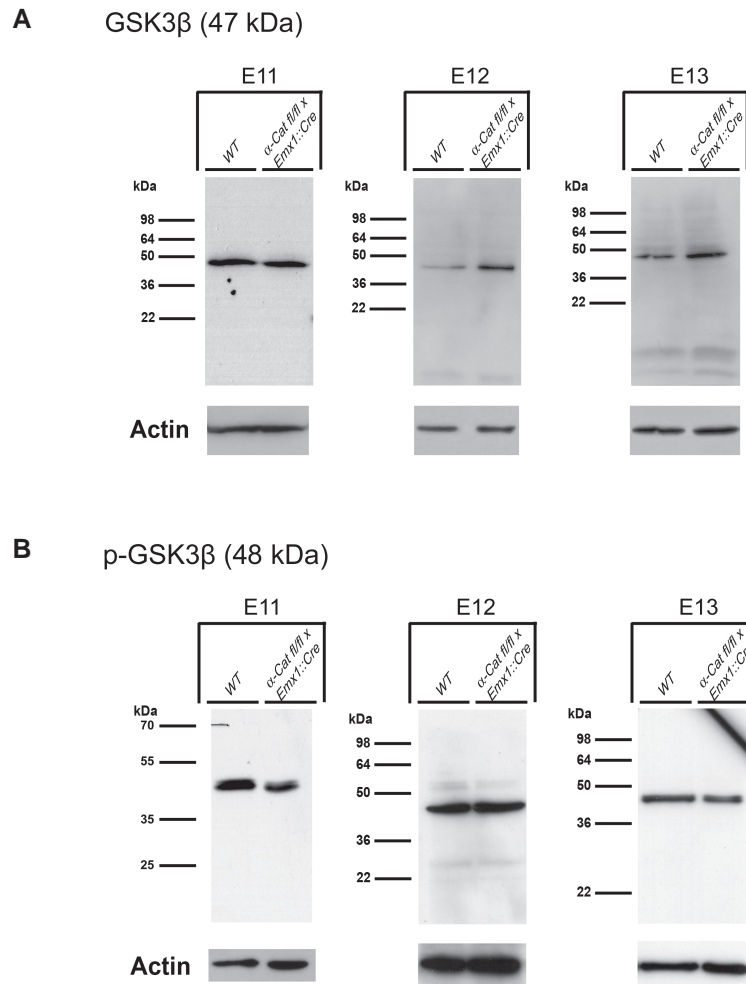


Figure 4-7. α -E-catenin controls protein levels of GSK3 β without affecting its phosphorylation at Ser9

Western blot was carried out of lysates from wild-type of α -E-catenin null cortices with the antibodies indicated at the upper side of each panel. The positions of relative-molecular-mass standards are shown on the left of the individual blots. β -actin served as an internal loading control. Note that the levels of GSK3 β are increased in E12 and E13 α -E-catenin null cortices, with the highest differences between wild-type and mutant seen at E12. In contrast, absence of α -E-catenin does not change the amount of Ser9 phosphorylated GSK3 β .

4.1.5 Semi-quantitative analysis of α -E-catenin dependent candidate proteins

The Western blot screen revealed two candidates which are up-regulated upon loss of α -E-catenin. To assess this in a more quantitative manner, I performed semi-quantitative analysis of the Western blot signals using the ImageJ software (see Methods). Signal intensity of immunoreactive bands predicted at the molecular masses of the analysed proteins was first corrected for background signal and then normalised per corresponding actin bands.

The quantitative analysis is depicted in figure 4-8. It revealed that loss of α -E-catenin causes an increase in the GSK3 β content at E12 (245.99% compared with control, n=1 embryo per genotype). Also one day later GSK3 β levels were increased in mutant cortices ($122.36 \pm 5\%$ of controls, n=7 embryos per genotype) even to statistical significance. Since this result equals a reduction by half in comparison to E12, the up-regulation of GSK3 β is only transient. In contrast, the effect of α -E-catenin deficiency on Par3 levels was not so dramatic, but more acute. While Par3 amounts at E11 come up to 171.37% \pm 41% of wild-type levels (n=3 embryos per genotype), the increase is only 124.23% at E12 (n=2 embryos per genotype). Already one day later the difference in Par3 protein levels between knock-out and wild-type animals has disappeared ($93.13\% \pm 26\%$ of controls, n=5 embryos per genotype). However, paired t-test analysis of the investigated Par3 blots demonstrated neither at E11 nor at E13 statistical significance indicating only a minor regulatory effect of α -E-catenin on Par3.

In summary, I could show that loss of α -E-catenin does not change the total level of proteins associated with the AJ or apical membrane domains. Furthermore, the intensive study of canonical Wnt signalling activity using various independent approaches ruled out the possibility that this pathway is contributing to the over-proliferation phenotype seen in α -E-catenin null cortices. However, Western blot screening revealed a role of α -E-catenin in controlling cortical levels of GSK3 β , a well-known master regulator of neural stem cell proliferation and differentiation.

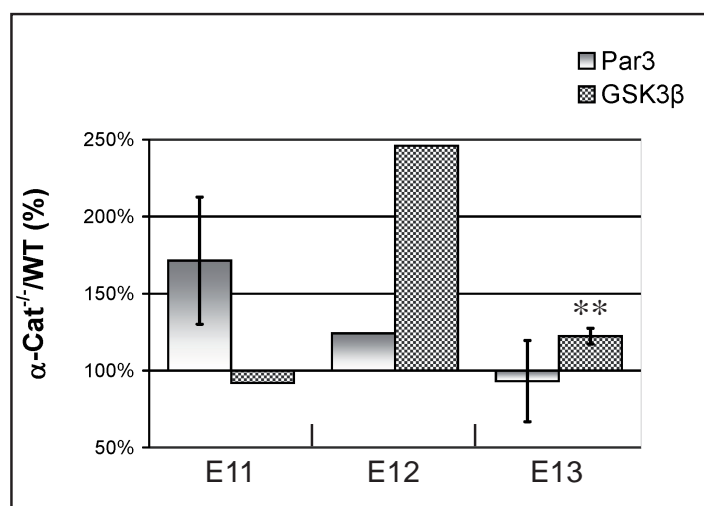


Figure 4-8. Semi-quantitative Western blot analysis of Par3 and GSK3 β

Histogram depicts the relative Par3 and GSK3 β protein levels after loss of α -E-catenin expressed as percentage of control. Semi-quantitative analysis confirmed a strong increase of GSK3 β levels at E12 to nearly 250%, while E13 lysates revealed an increase of only 122%. Paired t-test analysis revealed statistical significance for increase of GSK3 β levels at E13 (**p < 0.01). In contrast, response of α -E-catenin loss to Par3 levels was more acute, but not so strong. α -E-catenin deficiency resulted in ~170% increase of Par3 amounts at E11 and ~124% at E12.

Quantification results are represented as the mean \pm SEM (n=3 (Par3, E11), n=2 (Par3, E12), n=5 (Par3, E13); n=1 (Gsk3 β , E11), n=1 (Gsk3 β , E12), n=7 (Gsk3 β , E13); n represents the number of embryos per genotype).

4.2 ADHERENS JUNCTIONS AND PAR COMPLEX MOLECULES IN THE ADULT SUBEPENDYMAL ZONE

4.2.1 The apical surface of the adult subependymal zone

To evaluate the role of apical enriched molecules in adult neurogenesis, I first tested the adult subependymal zone (SEZ) for expression of proteins that have been discovered to localise at the ventricular surface of embryonic neural stem cells. Immunostaining of adult brain sections with antibodies against α -E- and β -catenin or Par3 revealed immunoreactivity along the medial, lateral and dorsal wall of the lateral ventricles (lateral wall Fig.4-9A-C, for overview see also Fig.4-13A). Staining of all three proteins primarily resembled the cuboid shape of the ependymal cells (Fig.4-9A-C). Moreover, when sections were co-immunostained with the anti-GFAP (Glial Fibrillary Acidic Protein) antibody in order to visualise astrocytes and adult neural stem cells, a subset of GFP⁺ cells were found to be expressing α - and β -catenin and Par3. Especially, GFP⁺ cells having close contact to the lateral ventricle, which were suggested to be the neural stem cells of the adult SEZ (Mirzadeh et al., 2008, Tripathi, 2009), were found to co-localise to the adherens junctional proteins and Par3 (Fig.4-9A-C).

In order to further elucidate the molecular composition of the apical membrane of ventricle-contacting cells, I decided to study whole mount preparations of the adult SEZ allowing an *en face* view of the ventricular surface. For this analysis, I used the hGFAP-eGFP (human GFAP promoter driven enhanced Green Fluorescent Protein) transgenic mouse line showing a strong eGFP signal in astrocytes and adult neural stem cells (Nolte et al., 2001, Tripathi, 2009). An advantage of the strong eGFP signal is that all cellular processes of a GFP⁺ cells including the thin apical processes of adult neural stem cells can be followed easily. *En face* confocal views of β -catenin immunolabelled whole mount preparations of the transgenic animals revealed two different cell types outlined by the AJ molecule: (1) GFP⁻ cells with large apical surfaces corresponding to ependymal cells; (2) GFP⁺ cells with a small apical surfaces, the presumable stem cells (Fig.4-9E). The same observation was made by analysing whole mounts of hGFAP-eGFP animals stained for α -E-catenin (Fig.4-9D) or Par3 (Fig.4-9F). As expected from the work of Mirzadeh and colleagues the ependymal cells at the ventricular SEZ surface are arranged in a pinwheel pattern surrounding one (Fig.4-9D-E) or more neural stem cells (Fig.4-9F).

To examine the expression of different Par3 isoforms and remaining Par complex members in the adult SEZ, I have probed Western blots of lysates from SEZ with antibodies raised against Par3, Par6, aPKC ζ and Cdc42. Par3 was present as two principle bands around and

above 98kDa (Fig.4-9G, first lane). The two bands correspond presumably to the two splice variants found to be predominantly expressed in the brain: 100kDa and 180kDa. The lane probed against Par6 revealed as well two bands: one prominent at ~36kDa corresponding to the molecular mass of Par6 and one thinner band above ~98kDa (Fig.4-9G, second lane). Interestingly, the upper band was never observed in lysates from the embryonic cortex (Fig4-2B). Furthermore, one specific band of aPKC ζ at its molecular mass of ~74kDa was detected (Fig.4-9G, third lane), as well as the specific band of Cdc42 at ~22kDa (Fig.4-9G, fourth lane).

After showing the presence of AJ and Par complex molecules in the adult SEZ, I was also interested in the cellular distribution of these molecules. Therefore, I performed double-immunostaining of α - with β -catenin and β -catenin with Par3 in SEZ whole mount preparations. While α - and β -catenin co-localised perfectly (Fig.4-9H), Par3 appeared to accumulate at more apical membrane positions and co-localised only partial with β -catenin (Fig.4-9I). As recently Par3 was found to localise to the cilia of polarised MDKC cells (Fan *et al.*, 2004), I have tested this possibility in adult SEZ whole mount preparations. Co-staining for Par3 and acetylated tubulin revealed punctuate Par3 marks at the acetylated tubulin⁺ cilia (Fig. 4-9K-K''), confirming the localisation of some Par3 molecules to the cilia.

4.2.2 Canonical Wnt signalling activity in the adult subependymal zone

To examine the second function of β -catenin, I next looked for canonical Wnt signalling activity in the adult SEZ. In order to monitor cells, which actively respond to Wnt ligands in a β -catenin dependent manner, I decided to use the BAT-gal transgenic mice (Maretto *et al.*, 2003) instead of the TOPGAL reporter mice. In contrast to the TOPGAL mice, the BAT-gal animals carry a reporter construct, which expresses β -galactosidase under the control of seven TCF/LEF and not only three promoter elements. Thus the expression level of β -galactosidase appears much

Figure 4- 9. Immunochemical analysis of adherens junctional and Par complex proteins in the adult SEZ

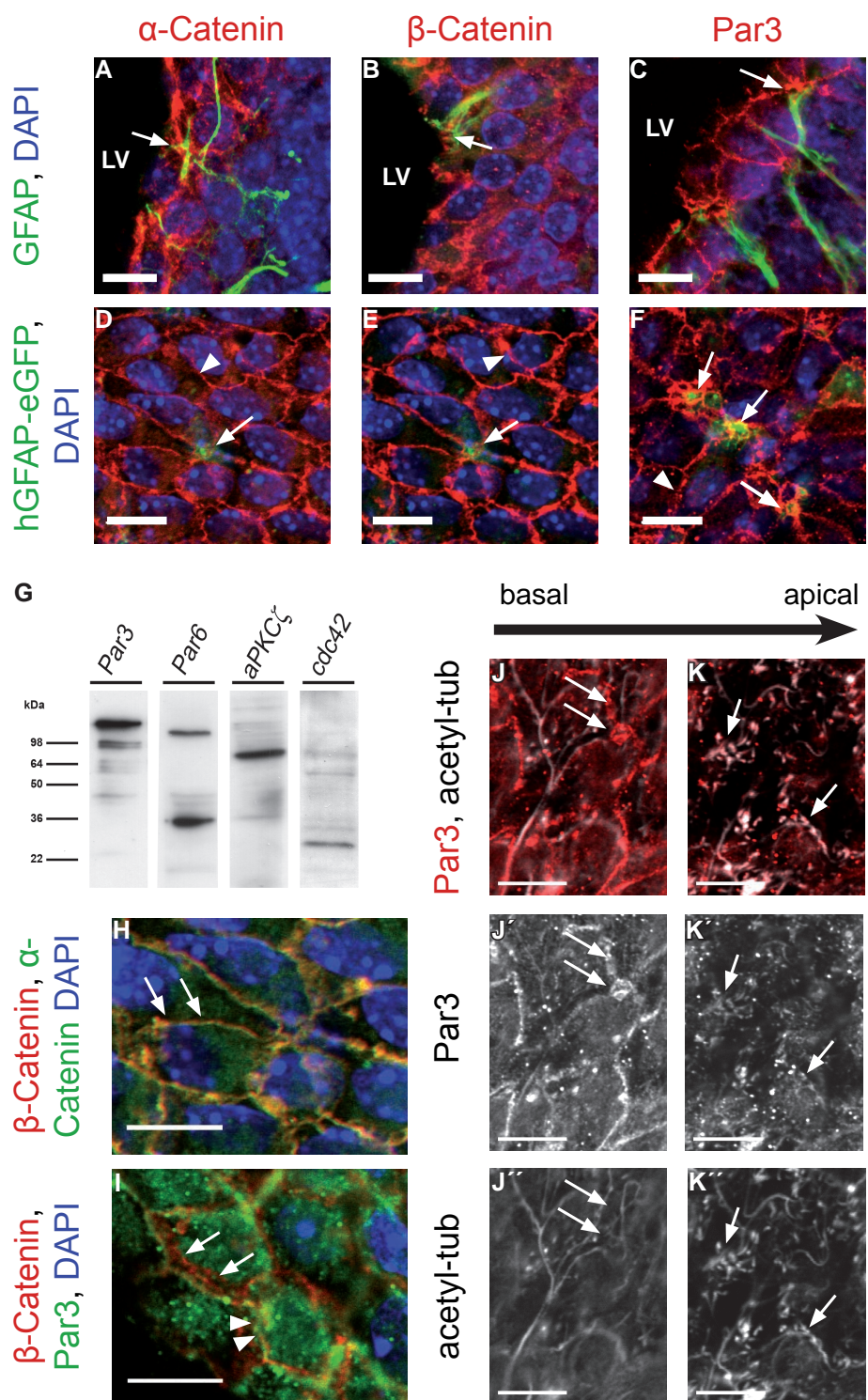
(A-C) Double immunolabelling of GFAP and α -E-catenin (A), β -catenin (B) or Par3 (C) was performed in sagittal sections through the adult SEZ. Confocal images revealed co-localisation (arrows) of the AJ molecules or Par3 with the endfeet of GFAP⁺ cells directly contacting the lateral ventricle (LV).

(D-F) Whole mount preparations of adult SEZ from hGFAP-eGFP transgenic mice were stained for α -E-catenin (D), β -catenin (E) or Par3 (F). Confocal images taken at the ventricular SEZ surface show that AJ molecules and Par3 locate at intercellular membranes outlining the small apical surfaces of GFP⁺ neural stem cells (arrows) and the big surfaces of GFP⁻ ependymal cells (arrowheads). Note the pinwheel architecture of the ventricular surface of the adult SEZ containing the thin apical neural stem cell processes in its centre.

(G) Western blot analysis confirm the presence of all Par complex members within adult SEZ lysates.

(H-K) The relative positioning of apical enriched molecules to each other was examined in en face views of adult SEZ whole mounts. (H) Note, that the two AJ molecules α -E- and β -catenin (arrows) co-localise perfectly. (I) In contrast, Par3 overlaps only with the most apical domain of β -catenin labelling (arrowheads), while it is excluded from basal β -catenin⁺ domains (arrows). (J-K) Staining for Par3 and acetylated tubulin was followed in z-axis for a given xy position. As shown before, Par3 locates at intercellular membranes (arrows) at basal positions (J-J''). Moreover, in apical positions (K-K'') it locates to the cilia of the SEZ cells as indicated by double labelling with acetylated tubulin (arrows).

Scale bars: 10 μ m. All nuclei were stained with 4,6-diamidino-2-phenylidolehydrochloride (DAPI). *Acetyl-tub*: acetylated tubulin; LV: lateral ventricle; SEZ: subependymal zone



stronger in the BAT-gal in comparison to the TOPGAL, helping to reveal also cells with lower canonical Wnt signalling activity (Maretto *et al.*, 2003).

Remarkably, immunostaining against β -galactosidase showed that only a subset of cells located at the dorsal wall of the lateral ventricle is subject to detectable levels of canonical Wnt signalling (Fig.4-10A). Moreover, a small number of β -galactosidase⁺ cells are found in the RMS (Fig.4-14B). Co-immunolabelling of the BAT-gal brain sections with antibodies against β -galactosidase and the astrocyte/neural stem cell marker GFAP showed that 52.43% of all β -galactosidase⁺ cells (n=82) are also positive for GFAP. Interestingly, some of the double-labelled cells had also direct contact to the ventricle, suggesting that these cells belong to the neural stem cell population (Fig. 4-10C-C''').

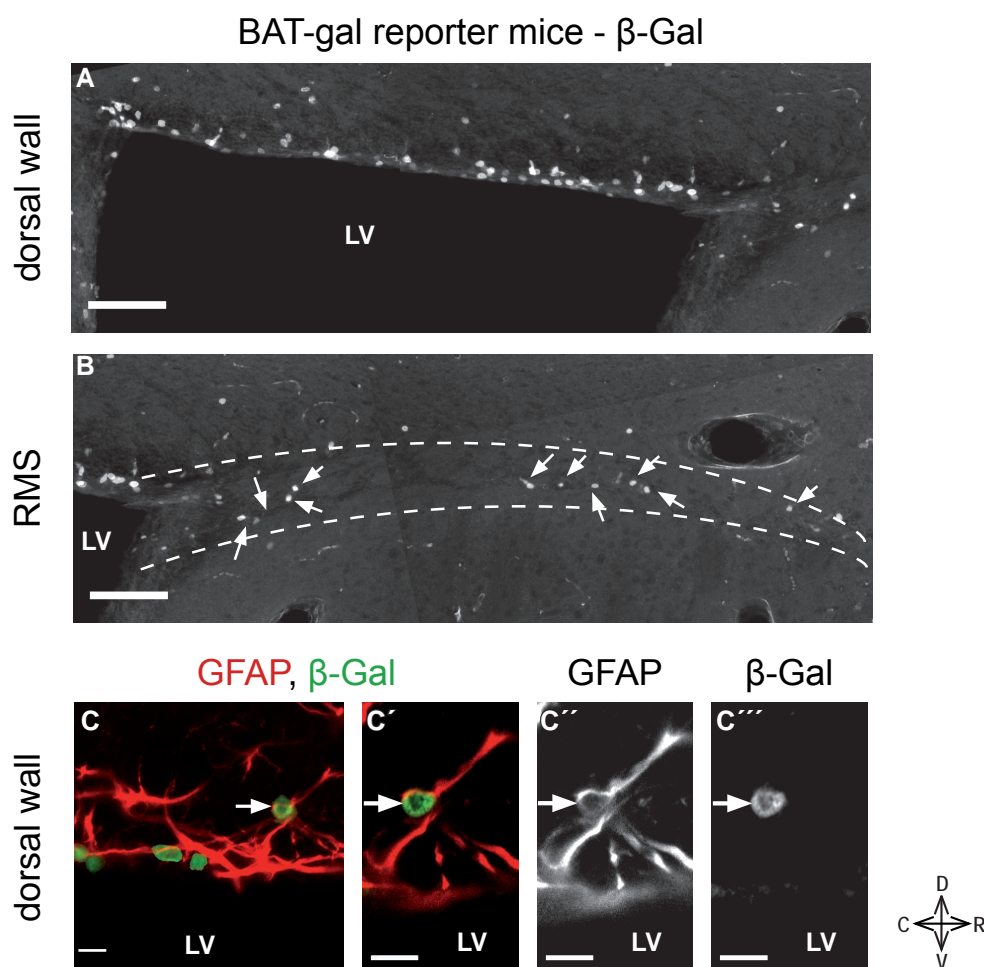


Figure 4- 10. Canonical Wnt signalling responsive cells in the adult subependymal zone

(A-B) Sagittal section of telencephalon of adult BAT-gal reporter mice stained against β -galactosidase (β -Gal) show a high immunoreactivity in the dorsal wall of the lateral ventricle (A). Moreover, a small fraction of β -Gal⁺ cells (arrows) are found in the rostral migratory stream (RMS) (B).

(C) At higher magnification β -Gal expressing cells in the dorsal wall of the lateral ventricle are found co-expressing GFAP. Note, that the β -Gal-GFAP double-positive cell has direct contact to the ventricle. For better resolution C'-C'''' display only a single optical section of 1 μ m, while C corresponds to a confocal stack with a thickness of 10 μ m.

Scale bars: 100 μ m in (A-B), 10 μ m in (C). Orientation of the sections is indicated by the cross in the lower right corner of the panel (C: caudal, D: dorsal, R: rostral, V: ventral). LV: lateral ventricle

4.3 FUNCTIONAL ANALYSIS OF ADHERENS JUNCTIONAL AND PAR COMPLEX MOLECULES IN NEUROSPHERE CULTURES

4.3.1 Comparative analyses of the function of α - and β -catenin in neurosphere cultures

The existence of adherens junctional molecules in adult neural stem cells, prompted me to examine the role of these proteins in adult neurogenesis. In order to analyse the influence of these molecules on the self-renewing capacity and multipotency of adult neural stem cells, the classical neurosphere assay of control and genetically manipulated neural stem cells served as a first read out (see also section 1.4.2). I used a transgenic inducible recombination system to conditionally delete α - and β -catenin specifically in adult neural stem cells. Therefore, I crossed the GLAST::CreER^{T2} mouse line (Fig.4-11C) to the *Ctnna1*^{tm1Efu/J} (described in section 4.1) and *Ctnnb1*^{tm2Kem/KnwJ} (Fig.4-11A) mouse line respectively. The *Ctnnb1*^{tm2Kem/KnwJ} mice possess loxP sites flanking exon 2-6 of the β -catenin gene (Brault et al., 2001). The GLAST::CreER^{T2} mice express CreER^{T2} fusion gene under control of the astrocyte-specific glutamate transporter (GLAST) promoter (Mori et al., 2006, Ninkovic *et al.*, 2007). The CreER^{T2} fusion protein consists of Cre recombinase fused to a mutant form of the human estrogen receptor, which does not bind its natural ligand (17 β -estradiol) at physiological concentrations, but will bind the synthetic estrogen receptor ligand tamoxifen. Restricted to the cytoplasm, CreER^{T2} can only gain access to the nucleus after exposure to tamoxifen (Fig.4-11D). For *in-vivo* studies later presented in this thesis, I additionally crossed in the R26R-CFP reporter line to be able to follow cells that underwent Cre recombination events in a mainly un-recombined environment (Srinivas et al., 2001, Fig.4-11B). Expression of the enhanced Cyan Fluorescent Protein (eCFP) is blocked by a loxP-flanked neomycin cassette inserted into the locus ROSA26. Therefore, Cre-mediated deletion of the stop signal results in constitutive expression of eCFP in all recombined cells. The present neurosphere experiments were performed with animals being heterozygous for the GLAST::CreER^{T2}. While control animals carried only a single α - or β -catenin floxed allele (referred to as α -cat^{fl/+} or β -cat^{fl/+}), experimental animals were homozygous for the floxed allele (referred to as α -cat^{fl/fl} or β -cat^{fl/fl}). It has been reported, that activity of the Cre recombinase due to mis-recombination and DNA damage can induce cell death (Forni *et al.*, 2006, Schmidt-Suppran & Rajewsky, 2007). The direct comparison of tamoxifen treated α -cat^{fl/+}/ β -cat^{fl/+} and α -cat^{fl/fl}/ β -cat^{fl/fl} animals in the present study excluded the possibility that the observed phenotypes on adult neurogenesis were caused by activity of the Cre recombinase or by the estrogen analogue tamoxifen. Tamoxifen treatment was done in adult mice at the age of 8-11 weeks.

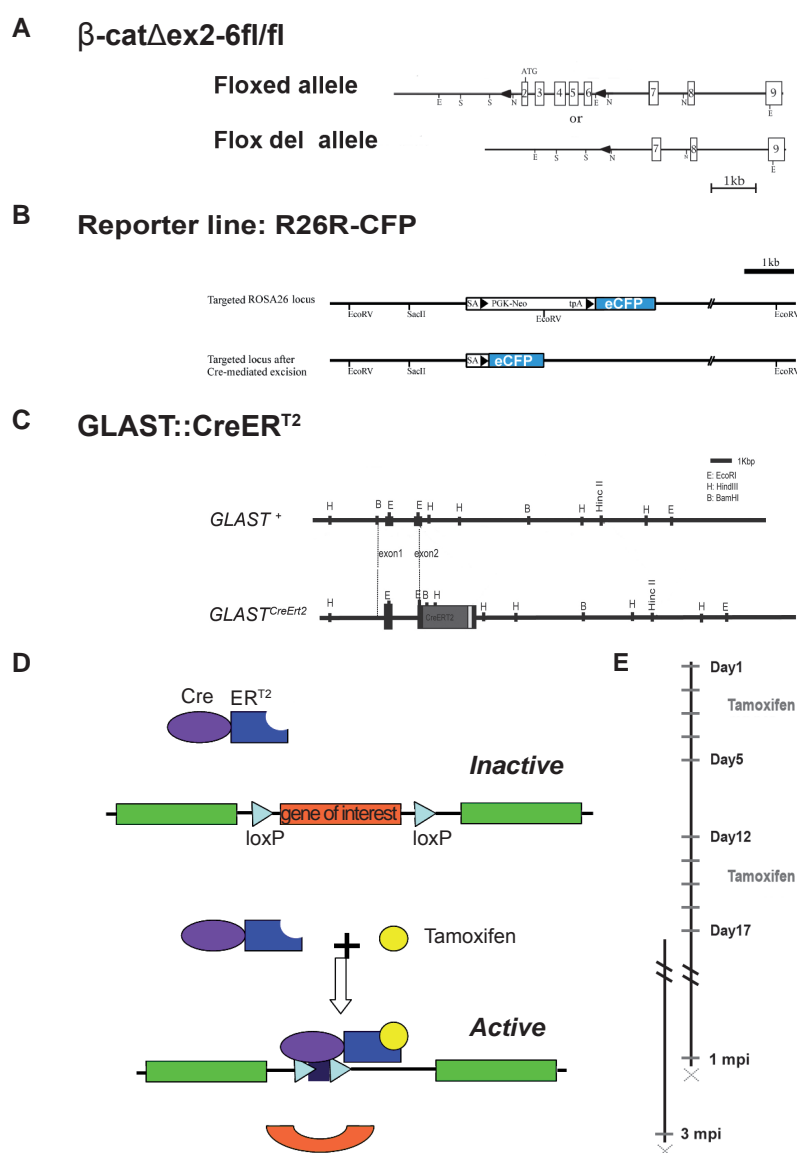


Figure 4-11. Experimental outline for conditional deletion of α - or β -catenin in the adult murine brain

(A) Restriction map of the modified β -catenin locus of B6.129-Ctnna1^{tm1Efu}/J transgenic mice. The floxed allele (upper panel) contains two loxP sites (black triangles) flanking exons 2-6 of the β -catenin gene. Deletion of the floxed segment is achieved by enzymatic activity of Cre recombinase and results in the flox del allele (lower panel). *Adapted from Maretto et al., 2003*

(B) Modified ROSA26 locus of the R26R-CFP reporter strain. The eCFP cDNA was inserted into the ROSA26 locus, preceded by a loxP-flanked transcriptional termination sequence (tpA). Cre-mediated excision of the floxed tpA leads to constitutive eCFP expression and allows tracing of all recombined cells. *Modified from Srinivas et al., 2001*

(C) Gene map showing the insertions site of the nucleotide sequence encoding for the fusion protein CreER^{T2} into the astrocyte and neural stem cell specific *GLAST* locus of the *Glact::CreER^{T2}* mouse line. *Modified from Mori et al., 2006*

(D) Scheme of tamoxifen based inducible Cre/loxP system. CreER^{T2} encodes a Cre recombinase (Cre) fused to a mutant estrogen ligand-binding domain (ER^{T2}). Upon administration of tamoxifen (an estrogen receptor antagonist), the CreER^{T2} is able to penetrate the nucleus and induce recombination.

(E) Experimental design. Tamoxifen food was administered to transgenic mice being heterozygous for *GLAST::CreER^{T2}* and carrying floxed allele for the gene of interest at the age of 8-10 weeks. Mice were killed either one (1mpi) or three months (3mpi) after end of tamoxifen induction.

1mpi: 1 month post induction; 3mpi: 3 months post induction

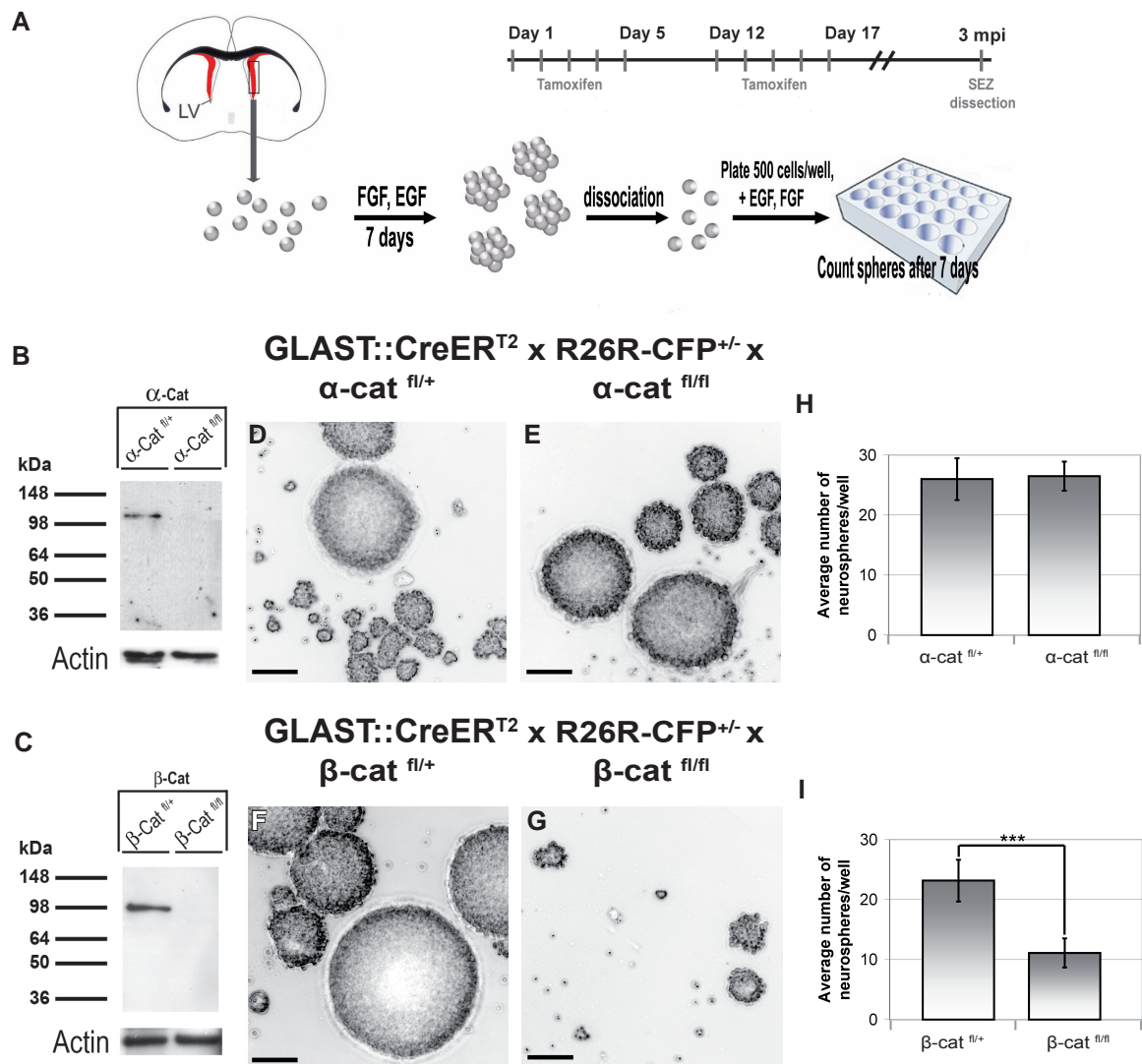


Figure 4-12. Secondary neurosphere formation is reduced after loss of β -catenin, but not altered after loss of α -E-catenin

(A) Schematic representation of the experimental design.

(B-C) Western blot confirming deletion of α -E-catenin and β -catenin in mutant neurosphere forming cells collected four days after plating.

(D-G) Representative bright-field images of secondary spheres obtained from control (*Glast::CreER^{T2} x α -Cat^{fl/+}* or *β -cat^{fl/+}*) and conditional knock-out animals (*Glast::CreER^{T2} x α -Cat^{fl/fl}* or *β -cat^{fl/fl}*). Note, that β -catenin deficient spheres (G) are lower in number and smaller than spheres obtained from control brains (F). In contrast, α -E-catenin deficient spheres (E) are comparable to control spheres (D).

(H-I) Histograms depicting the average number of spheres found per well of a 24-well plate. While loss of α -E-catenin has no effect on the secondary neurosphere forming capacity, β -catenin conditional knock-out cells form significantly lower number of secondary neurospheres.

Quantifications arise from one set of experiment performed with one animal per genotype (total number of spheres per 24-well plate: 624 (α -Cat^{fl/+}), 636 (α -Cat^{fl/fl}), 556 (β -cat^{fl/+}), 267 (β -cat^{fl/fl})). Error bars indicate SEM. Asterisks indicate a statistical difference between the individual wells that contained neurosphere forming cells of different genotypes (***) $p < 0.001$ in Student's t-test).

Scale bars: 100 μ m. LV: lateral ventricle; 3mpi: 3 months post induction

In order to evaluate the function of α - or β -catenin in neurosphere formation, the SEZ of GLAST::CreER^{T2} x α -cat^{fl/+} or β -cat^{fl/+} and GLAST::CreER^{T2} x α -cat^{fl/fl} or β -cat^{fl/fl} mice was dissected 3 months after the end of tamoxifen treatment and cultivated in the presence of EGF and FGF2 at a density of 5 cells/ μ L (Fig.4-12A). Successful deletion of the proteins was confirmed by Western blotting of cell lysates obtained four days after first plating (Fig.4-12B-C). To ensure reliable quantification of the remaining neurospheres, I passaged control and mutant neurospheres once after 7 days and dispersed the dissociated cells to 24-well plates (Fig.4-12A). While α -E-catenin deficient neural stem cells were not impaired in their ability to form secondary neurospheres, β -catenin lacking SEZ cells produced significantly fewer secondary colonies than heterozygous control cells (Fig.4-12D-I). Moreover the size of β -catenin conditional knock-out spheres appeared smaller than the size of control spheres (Fig.4-12F-G). Thus, β -catenin appears to be required for either proliferation or survival of neural stem cells or for proper cell adhesion.

To overcome the problem of mis-interpreting inadequate cell adhesion as proliferation defect, I grew the cells isolated from β -catenin deficient or control brains within a semi-solid collagen matrix as it prevents efficiently the neural stem cell progeny from floating away from the cell that generated the colony (see also section 1.4.2). To ensure that an impaired adhesion was not causing the absence of any phenotype in α -E-catenin deficient suspension cultures, I performed the neural colony forming cell (NCFC) assay as well with these genotypes. Within the collagen, single control cells grew to form spatially separated colonies of cells of different sizes. The size of the colonies is an indication for their ability to be passaged, i.e. to self-renew. While larger colonies can be passaged multiple times, spheres displaying a smaller diameter than <1mm do not form tertiary neurospheres.

The average number of primary neurospheres obtained from both, α -cat fl/+ and β -cat fl/+ animals was ~100 colonies per control dissected control SEZ. Interestingly, similar to the results obtained from secondary neurospheres cultured in suspension, also α -E-Catenin deficient primary neurospheres did not differ significantly in size or number from the control spheres (Fig.4-13). Conversely, loss of β -catenin caused the same phenotype seen in classical neurosphere assay after the first passage with a significant decrease in the number of primary colonies in comparison to control colonies (Fig.4-14). However, the strongly reduced number of colonies was still composed of a population of large, medium- sized and small colonies (Fig.4-14).

Taken together, the comparative functional analysis of the two adherens junctional molecules demonstrated an essential role of only β -catenin but not α -E-Catenin in the formation of neurospheres. As only the total number of spheres is decreased upon loss of β -catenin, but not the size composition, β -catenin is indispensable for progenitor and neural stem cell

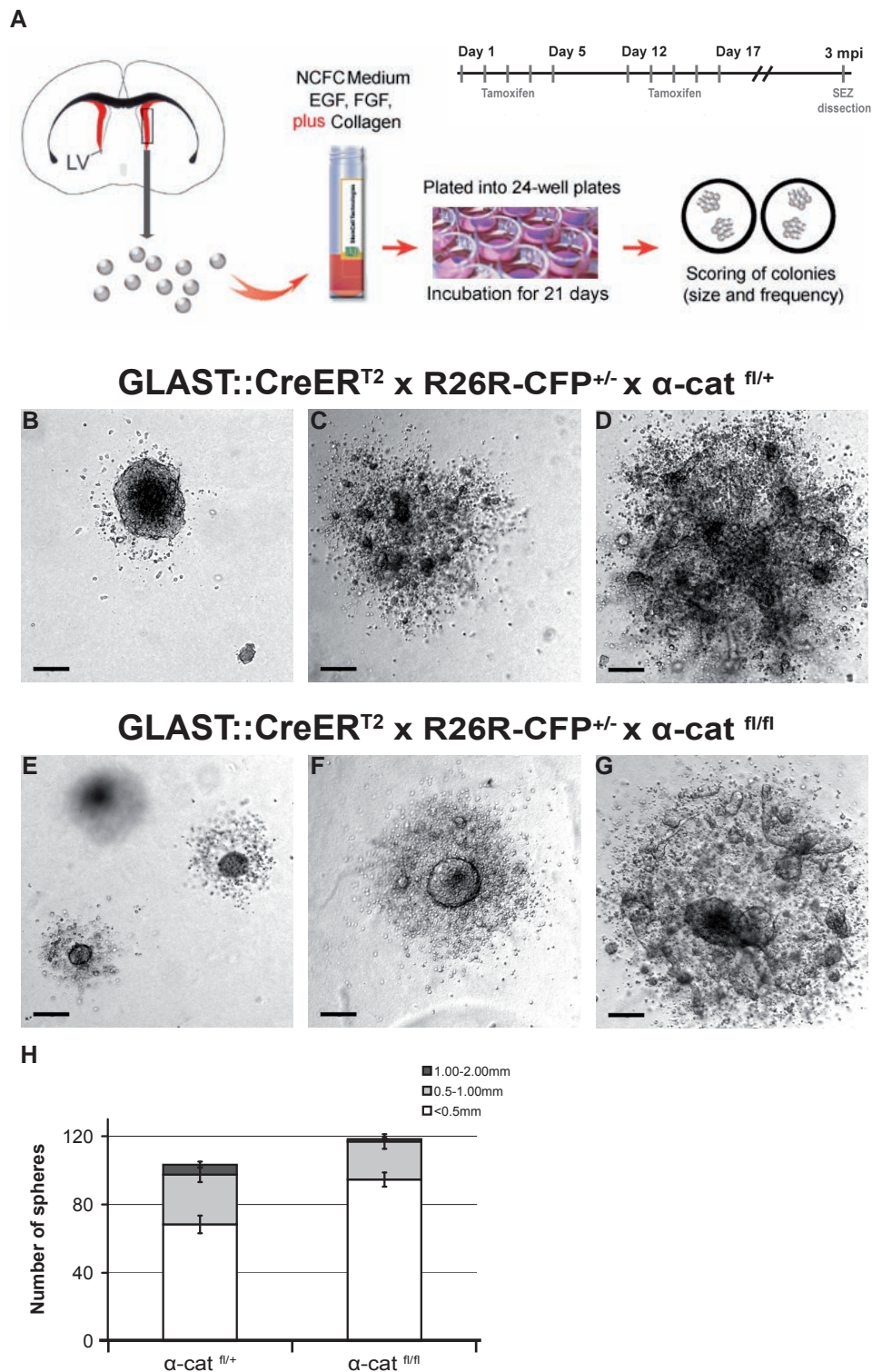


Figure 4-13. Loss of α -E-catenin does not affect primary neurosphere formation in collagen assay

(A) Work flow scheme summarising the collagen-based neural colony forming cell assay.

(B-G) Representative bright-field images of primary spheres of different size categories generated from control (Glast::CreER^{T2} x α -Cat^{fl/+}) and conditional knock-out brains (Glast::CreER^{T2} x α -Cat^{fl/fl}).

(H) Histogram shows the average number of primary spheres that were generated per animal of the indicated genotype per different size category. No statistical difference was determined between α -E-catenin deficient and control colonies regarding the total average number or average number of a size category.

Quantifications arise from three sets of experiments performed with three animal per genotype (total number of spheres: 412 (α -Cat^{fl/+}), 482 (α -Cat^{fl/fl})). Error bars indicate SEM.

Scale bars: 100 μ m. LV: lateral ventricle; 3mpi: 3 months post induction

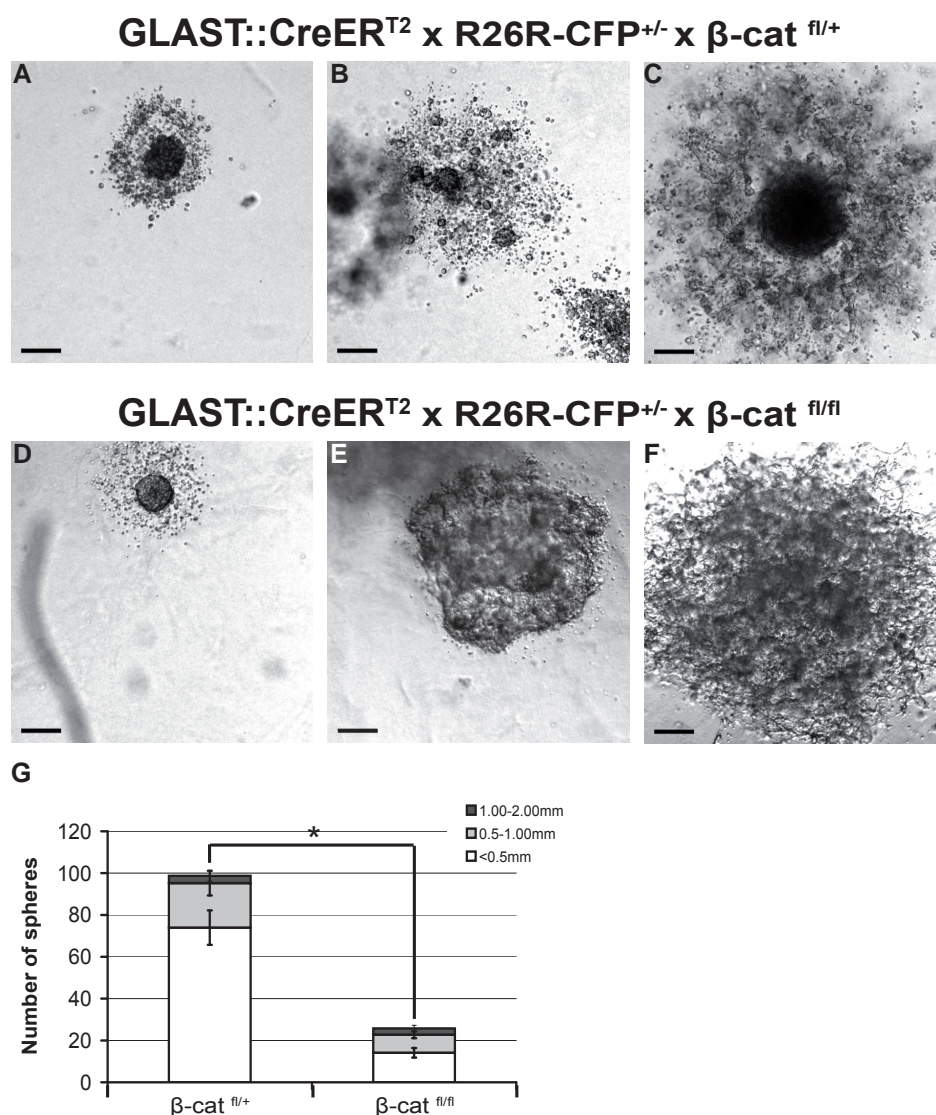


Figure 4-14. Loss of β -catenin decreases primary neurosphere formation in collagen assay

(B-F) Representative bright-field images of primary spheres of different size categories generated from control (Glast::CreER^{T2} x β -Cat^{fl/+}) and conditional knock-out brains (Glast::CreER^{T2} x β -Cat^{fl/fl}).

(H) Histogram shows the average number of primary spheres per size category obtained from animals of the indicated genotype. β -Catenin conditional knock-out SEZ cells generate a significant lower number of neurospheres without changing the size composition.

Quantifications arise from three sets of experiments performed with three animal per genotype (total number of spheres: 395 (β -Cat^{fl/+}), 103 (β -Cat^{fl/fl})). Error bars indicate SEM. Asterisk indicates a statistical difference between the total number of neurospheres obtained from different genotypes (* p <0.05 in Student's t-test).

Scale bars: 100 μ m.

proliferation or survival. In contrast loss of α -E-Catenin has no major effect on the behaviour of neural stem cells *in-vitro* suggesting a more prominent role of canonical Wnt signalling in the neurosphere generation, rather than an influence of cell-cell contacts during this process.

4.3.2 Functional analysis of Par complex molecules in neurosphere cultures

Although Par complex molecules have been implicated to play a crucial role in controlling the proliferative progenitor fate of embryonic neural stem cells, nothing is known about the function of these molecules in adult neural stem cells (Costa et al., 2008, Bultje et al., 2009). Therefore, I investigated how loss of Par3 protein influences neurosphere formation in suspension cultures. As a first step the presence of Par3 protein was confirmed in adult SEZ neurospheres using immunohistochemistry (Fig.4-15A).

In order to interfere with the members of the Par complex, I used a viral vector approach. Loss-of-function studies were performed with lentiviruses expressing two different short hairpin sequences against the Par3 protein: Par3a and Par3b (see section 3.4.1, Costa et al., 2008). Additionally, the empty pLVTH viral vector was used as a control (see section 3.4.1, Costa et al., 2008). Gain-of-function studies were done with the retroviral vectors: pM-Par6-IG expressing the full-length Par6a before the IRES-GFP protein and the empty pMXIG (Mizuguchi et al., 2001, Costa et al., 2008, see Fig.3-2). The major difference between retro- and lentiviruses is their way of integration. Due to their lack of any complex that would allow them to overcome nuclear membranes, retroviruses exclusively transduce cells during division. In contrast, lentiviruses have the capability to infect also non-mitotic cells. Before starting the neurosphere experiments, the titre of every virus was determined, so that the same number of viral particles for control and modified vectors could be applied. To manipulate Par3 expression in the culture, I mixed sphere forming wild-type cells obtained from the first passage of adult SEZ neurospheres with lentiviral control and Par3 shRNA vectors and plated them into 24-well plates at a density of 1cell/ μ L (Fig.4-15B). When infected neurosphere cells were examined seven days later, more than 75% of all neurospheres expressed GFP indicating a sufficient infection rate. While control spheres appeared healthy and contained colonies of different sizes, neurospheres were significantly reduced in number after transduction with Par3 shRNA constructs but without showing any difference in the size distribution of the spheres (Fig.4-15C-E). Consistent with data obtained from embryonic neural stem cells (Costa et al., 2008) Par3a proved to be most efficient shRNA construct. Par3a reduced the number of neurospheres to 62.42% of control levels, while Par3b showed only a reduction to 66.58% of control levels.

As the effects caused by the two different Par complex members are closely connected, I examine if Par6 gain-of function might have the opposite effect to Par3 shRNA mediated effects. Therefore, I transduced dissociated primary neurospheres from adult SEZ with

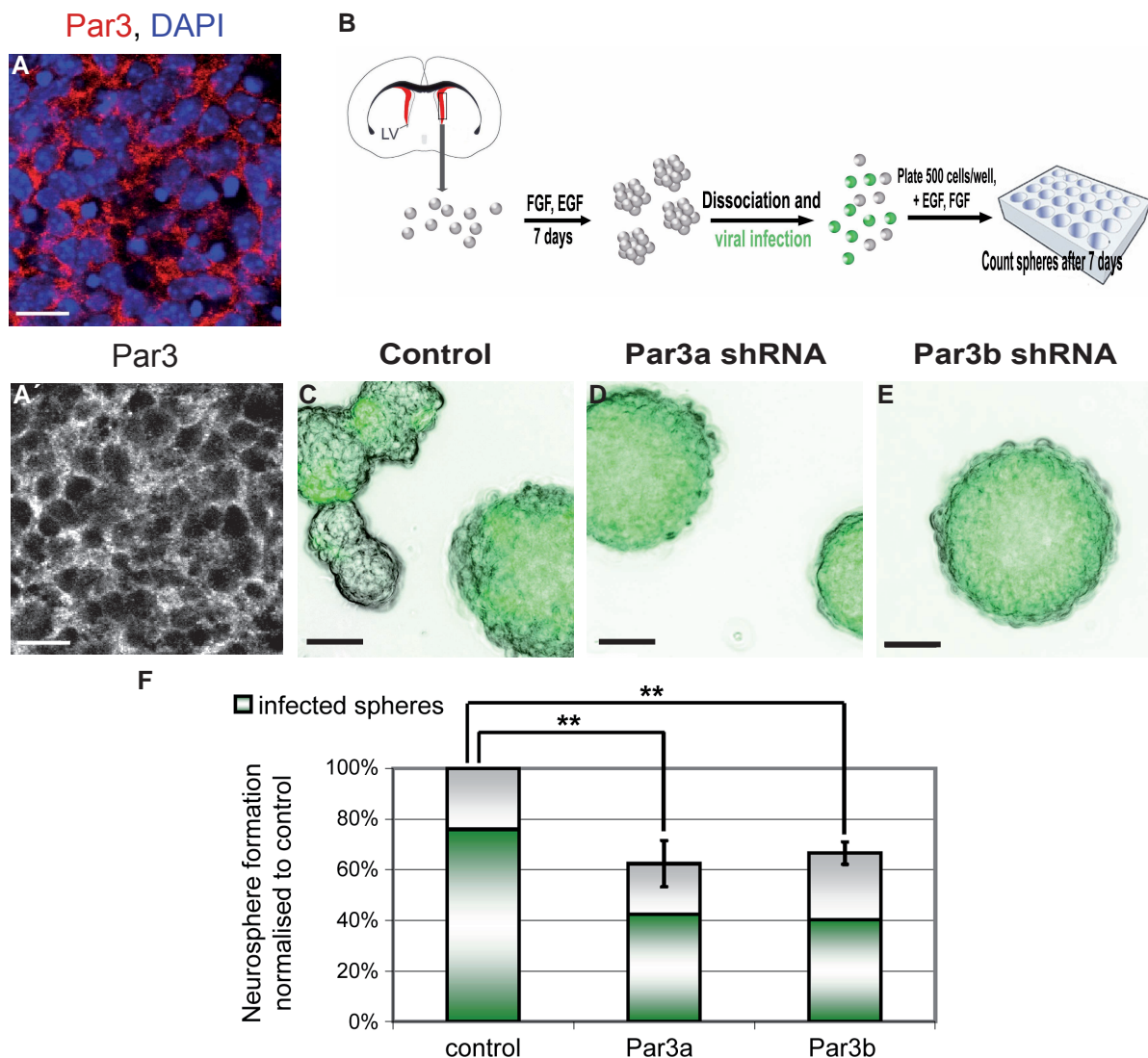


Figure 4-15. Reduced neurosphere formation after Par3 knock-down

(A-A') Fluorescence micrograph of a wild-type neurosphere grown from adult SEZ stained against Par3. Nuclei were stained with 4,6-diamidine-2-phenylidolehydrochloride (DAPI).

(B) Scheme summarising the experimental work-flow applied to reach sufficient viral infection of neurosphere forming cells.

(B-D) Representative bright-field images of neurospheres transduced with control or Par3 shRNA constructs (7 days after infection). Simultaneous overlay of the bright-field pictures with the GFP signal indicates successful viral infection.

(E) Bar chart showing the significant reduction in neurosphere generation after Par3 knock-down in comparison to control levels (7 days after infection). Note that the number of non-infected spheres remains stable between the three viral vectors, indicating only a loss of spheres showing a knock-down of the Par3 protein.

Quantifications arise from three sets of experiments (total number of spheres: 774 (pLVTH), 290 (Par3a), 480 (Par3b)). Error bars indicate SEM. Asterisks indicates a statistical difference between experimental (** $p < 0.005$ in Student's t-test).

Scale bars: 10 μ m (A), 50 μ m (C-E).

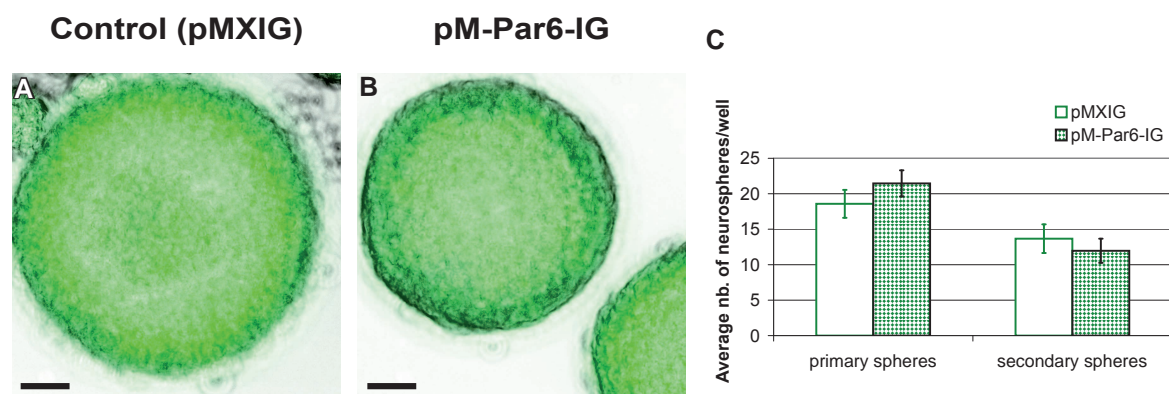


Figure 4-16. Over-expression of Par6 has no influence on the neurosphere capacity of adult neural stem cells

(A-B) Representative bright-field/GFP overlay images of neurospheres transduced with control or Par6 over-expression construct.

(C) Histogram depicting the average number of control and Par6 over-expressing spheres obtained per well of a 24 well plate. Statistic analysis revealed no significant difference between control and Par over-expression, neither at the level of primary, nor at the stage of secondary sphere formation.

Quantifications arise from three sets of experiments (total number of spheres: 646 (pMXIG, primary spheres), 715 (pM-Par6-IG, primary spheres), 528 (pMXIG, secondary spheres), 487 (pM-Par6-IG, secondary spheres)). Error bars indicate SEM.

Scale bars: 50 μ m.

retroviral vectors expressing the full-length Par6a with IRES GFP or as a control IRES GFP only. Notably the infection rate of the retroviral vectors, reaching nearly 100%, was much higher than that obtained by the lentiviral shRNA constructs. Surprisingly, however no difference between control and pM-Par6-IG infected cells was seen in their ability to form primary or secondary transduced neurospheres (Fig.4-16). The average number of colonies found per well was with both constructs ~20 at the level of primary spheres formation and ~13 after the second passage of the transduced sphere forming cells (Fig.4-16C).

These results therefore suggest that knock-down of Par3 by two independent shRNAs potentially reduces proliferation or cell-survival and as a consequence the self-renewing capacity of adult neural stem cells. In contrast overexpression of Par6 does not promote proliferation of the adult neural stem cells indicating that neurosphere proliferation is already at its maximum.

4.4 THE ROLE OF β -CATENIN IN ADULT NEUROGENESIS

As β -catenin showed a very striking phenotype in the neurosphere assay, I decided to investigate its role in adult neurogenesis further *in-vivo*. Therefore, I used animals being heterozygous for the GLAST::CreER^{T2} and the R26R-CFP reporter allele and carrying a single or two β -catenin floxed alleles. Figure 4-11E depicts the induction protocol used for all experiments shown in the following sections (Fig.4-11E).

4.4.1 Conditional deletion of β -catenin in the adult subependymal zone

In order to examine the efficiency of the recombination in the triple-transgenic animals, immunostaining against CFP was performed one month and three months after the end of tamoxifen administration (Fig.4-17). Strong reporter activity was seen along the dorsal, medial and lateral wall of the lateral ventricle (Fig.4-26) and due to the high density of cells in the lateral wall, this region showed a very broad band of CFP⁺ cells. The amount of reporter signal in animals carrying one or two β -catenin floxed alleles was comparable at both time-points of the analysis (Fig.4-17), suggesting a similar recombination rate in both.

Next, I confirmed the efficient deletion of β -catenin from the β -cat^{flox} x GLAST::CreER^{T2} x R26R-CFP mice one or three months post induction (1 or 3mpi) by immunohistochemistry (Fig.4-18). The SEZ of these animals showed a significant reduction of the β -catenin protein one month after the last tamoxifen injection in comparison to induced control animals (Fig.4-18A-B). Interestingly, the intensity of the β -catenin signal varied between different immunopositive cells within the conditional knock-out SEZ (Fig.4-18B). While some cells still expressed high amounts of β -catenin protein, others showed a much lower level (Fig.4-18B). Moreover, the disruption of the specific micromesh pattern of β -catenin staining, suggests that loss of the protein occurred also in ependymal cells (Fig.4-18B). However, co-immunolabelling of the sections with CFP revealed, that even 1mpi some reporter⁺ cells still contain β -catenin, indicating a very slow turn-over of the protein in adult SEZ cells (Fig.4-18E-E'). However three months after tamoxifen treatment a more pronounced reduction of the β -catenin protein was reached with all reporter⁺ cells lacking β -catenin immunoreactivity (Fig.4-18C, F-F').

To confirm that the deletion of β -catenin indeed abolished canonical Wnt signalling in the recombined cells, I also crossed the triple-transgenic mice to the BAT-gal reporter mouse line and analysed the expression of β -galactosidase in the dorsal ventricular wall using immunohistochemistry. In accordance with the gradual loss of the β -catenin protein from the adult SEZ of tamoxifen induced mutant animals, also the reduction of canonical Wnt responsive cells was proceeding by time (Fig.4-19). Surprisingly, both time points of the analysis showed CFP- β -galactosidase double-positive cells in the β -catenin deficient brains

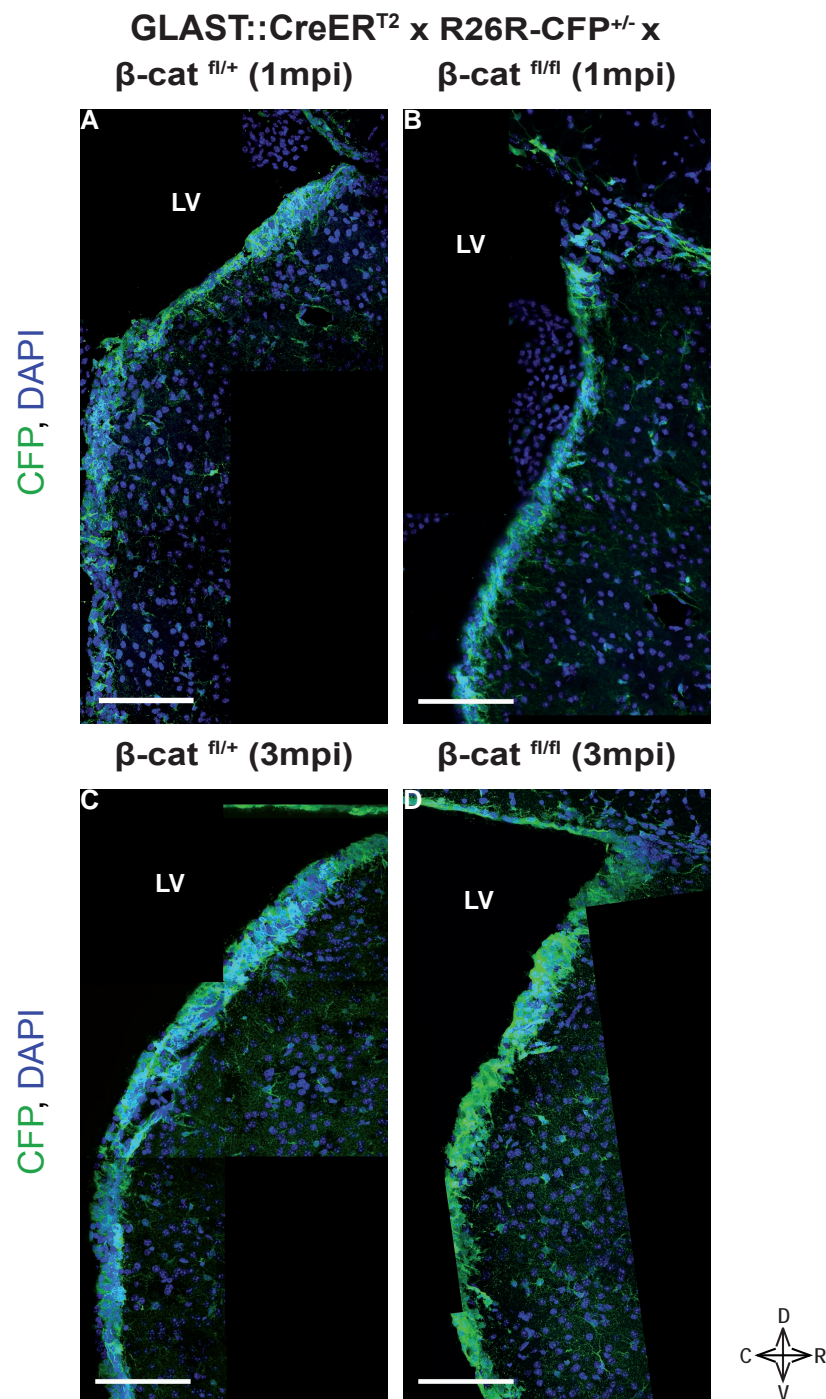


Figure 4-17. R26R-CFP reporter activity in the adult SEZ of GLAST::CreER^{T2} x R26R-CFP x β -cat^{fl/+} or β -cat^{fl/fl} mice

(A-D) Successful recombination of the Cre::ER^{T2} driven by the *GLAST* promoter was monitored by immunostaining for CFP one (A-B) or three months post tamoxifen induction (C-D). The Cre recombination efficiency, and thus the amount of reporter signal within the SEZ, was comparable between control and β -catenin conditional knock-out mice at both time points of analysis.

Scale bars: 100 μ m. All nuclei were stained with 4,6-diamidino-2-phenylindole dihydrochloride (DAPI). Orientation of the sections is indicated by the cross in the lower right corner of the panel (C: caudal, D: dorsal, R: rostral, V: ventral). LV: lateral ventricle; SEZ: subependymal zone; 1mpi: 1 month post induction; 3mpi: 3 months post induction

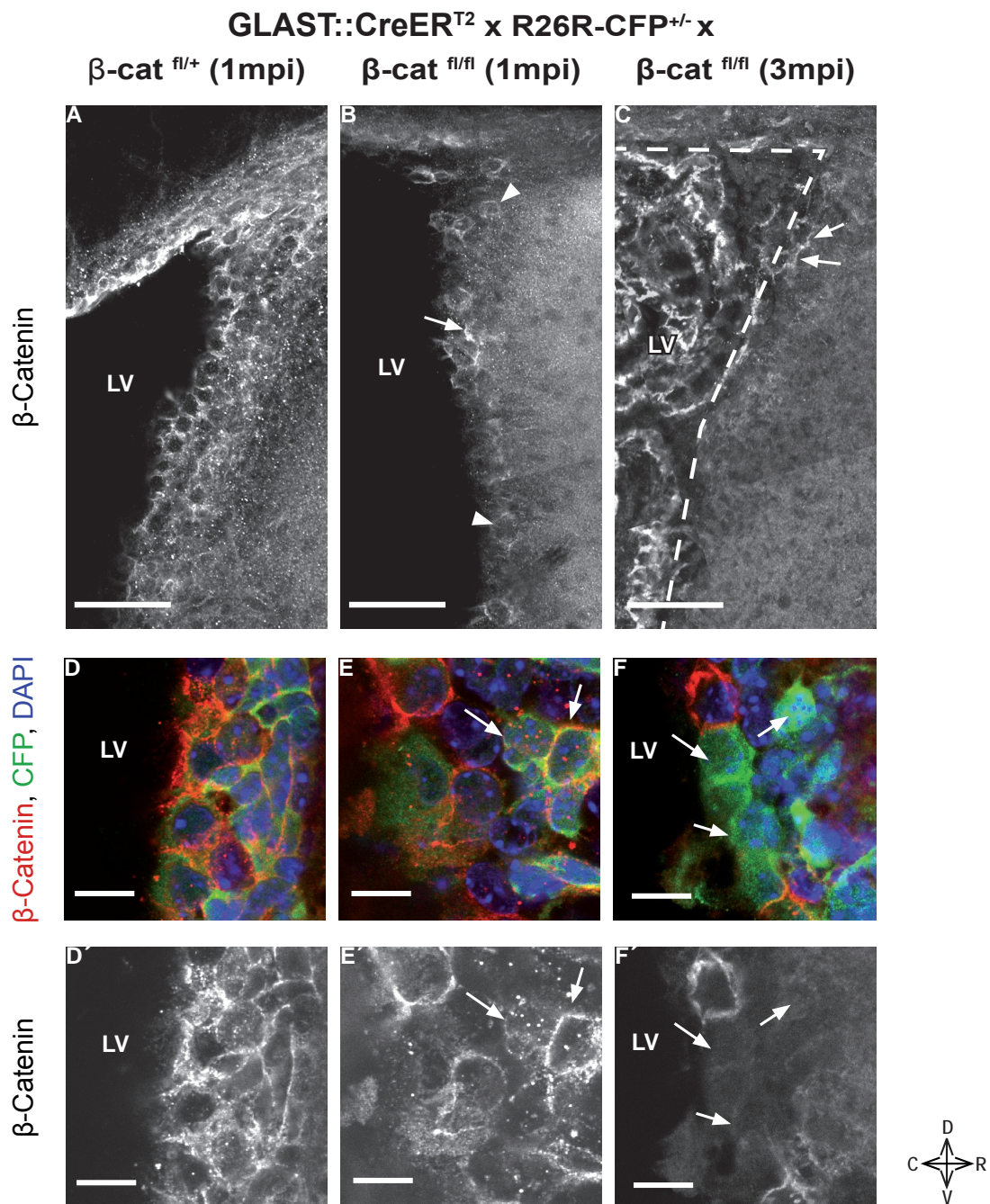


Figure 4-18. Loss of β -catenin in the adult SEZ using the GLAST::CreER^{T2} mouse model

(A-C) Immunostaining against β -catenin in the adult SEZ one (A-B) or three months (C) after activation of the CreER^{T2} expressed from the *GLAST* locus. Note the significant reduction of β -catenin protein at the two time points of the analysis in mice carrying two floxed β -catenin alleles. Arrows indicate cells containing high amounts of β -catenin and arrowheads point to cells being less immunoreactive for β -catenin (B-C). Interestingly, deletion of the protein progresses over time.

(C-F') While 1mpi still some reporter⁺ cells are immunoreactive for β -catenin (arrows in E-E'), virtually all reporter⁺ cells have lost the protein 3mpi (arrows in F-F').

Scale bars: 50 μ m in (A-C), 10 μ m in (D-F'). All nuclei were stained with 4,6-diamidino-2-phenylindole dihydrochloride (DAPI). Orientation of the sections is indicated by the cross in the lower right corner of the panel (C: caudal, D: dorsal, R: rostral, V: ventral). LV: lateral ventricle; SEZ: subependymal zone; 1mpi: 1 month post induction; 3mpi: 3 months post induction

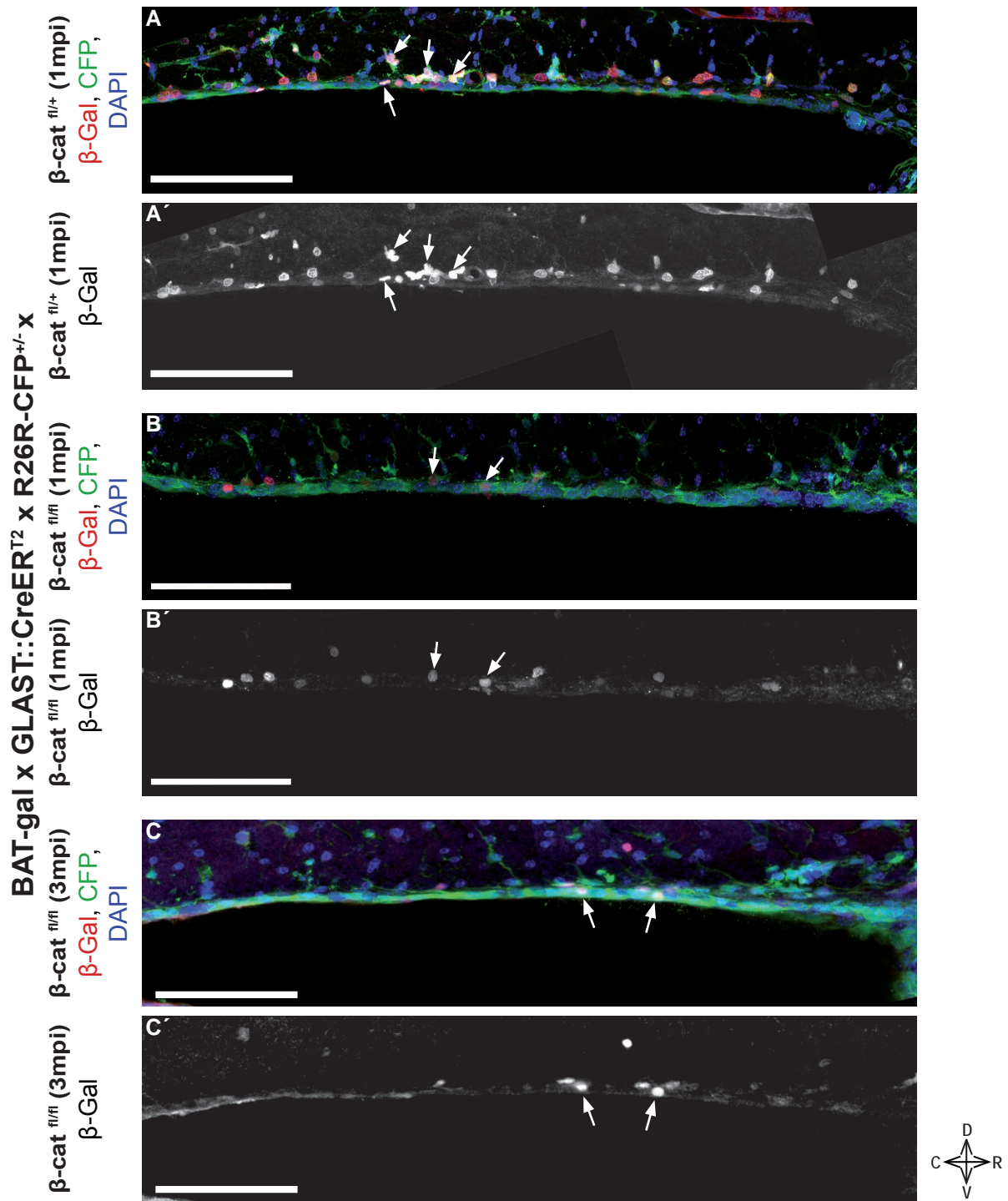


Figure 4-19. Reduced canonical Wnt signaling activity after loss of β -catenin in the ventricular dorsal wall

(A-C') Immunostaining against β -galactosidase (β -Gal) in BAT-gal reporter mice crossed to $GLAST^{CreERT2/R26R-CFP/\beta-cat^{\Delta ex2-6}/fl/fl}$ revealed strong reduction of immunoreactivity in the dorsal wall of the SEZ one (B-B') or three months after tamoxifen induction (C-C') in comparison to induced control animals (A-A'). Arrows indicate examples of recombined cells (CFP⁺) being also positive for β -Gal. Note, that some canonical Wnt responsive cells remain in β -Cat^{fl/fl} animals at both time points of the analysis. Interestingly, these cells are mostly located within the ependymal layer lining the ventricular wall (B-C').

Scale bars: 100 μ m. All nuclei were stained with 4,6-diamidine-2-phenylidole-dihydrochloride (DAPI). Orientation of the sections is indicated by the cross in the lower right corner of the panel (C: caudal, D: dorsal, R: rostral, V: ventral). LV: lateral ventricle; SEZ: subependymal zone; 1mpi: 1 month post induction; 3mpi: 3 months post induction

(Fig.4-19B-C'). While one month after induction the percentage of recombined cells showing as well β -galactosidase expression had dropped down to 44.79% of control levels (counted number of CFP⁺ cells: n=222 (control), n=254 (β -Cat^{f/f})), three months post induction this decrease reached 33.64% (n=186 (β -Cat^{f/f})) of control levels. Interestingly, the remaining double-positive cells were mainly located within the ependymal layer of the mutant brains (Fig.4-19B-C').

Taken together, I could confirm that the GLAST::CreER^{T2}-tamoxifen system allows the conditional deletion of β -catenin in the adult SEZ and an almost complete inhibition of canonical Wnt signalling associated with it. The conditional knock-out mutants were further analysed for gene specific alterations of adult SEZ neurogenesis.

4.4.2 Maintenance of the pinwheel architecture of the adult SEZ despite loss of β -catenin

As β -catenin is a major component of the AJ at the apico-lateral membrane of ependymal and adult neural stem cells, I first examined the state of the apical surface of these cells in β -catenin mutant brains. I decided to perform this analysis at a very late time point, namely nine months after tamoxifen treatment, in order to not miss phenotypes caused by the slow turn-over of the β -catenin protein. SEZ whole mount preparations of control and mutant animals were stained simultaneously with antibodies against with β -catenin and α -E-catenin or β -catenin and Par3 (Fig.4-20). Surprisingly, despite the complete loss of β -catenin protein, the staining pattern of α -E-catenin and Par3 did not indicate any obvious disturbance of cell-cell junctions between β -catenin deficient cells (Fig.4-20B'', D''). Moreover, no obvious change was noted in the pinwheel organisation of the neural stem cell niche on loss of β -catenin (Fig.4-20B''). However, membrane components accumulating α -E-catenin or Par3 in the β -catenin knock-out preparations appeared much broader than those seen in control whole mounts (Fig.4-20B'', D'').

Thus, β -catenin is not essential for the cellular organisation and integrity of the adult SEZ. Furthermore, these data suggest that despite loss of β -catenin cell-cell contacts are maintained.

4.4.3 β -Catenin deletion does not change the number of astrocytes in the lateral subependymal zone

As β -catenin was deleted in astrocytes and adult neural stem cells I examined this population in the lateral SEZ of β -cat^{f/+} x GLAST::CreER^{T2} x R26R-CFP and β -cat^{f/f} x GLAST::CreER^{T2} x R26R-CFP mice. Because β -catenin protein and Wnt signalling activity started to be reduced 1mpi, I analysed the phenotype at this time point. Furthermore, the analysis was repeated 3mpi, at a time point when virtually all reporter⁺ cells lost the β -catenin protein. As a first step,

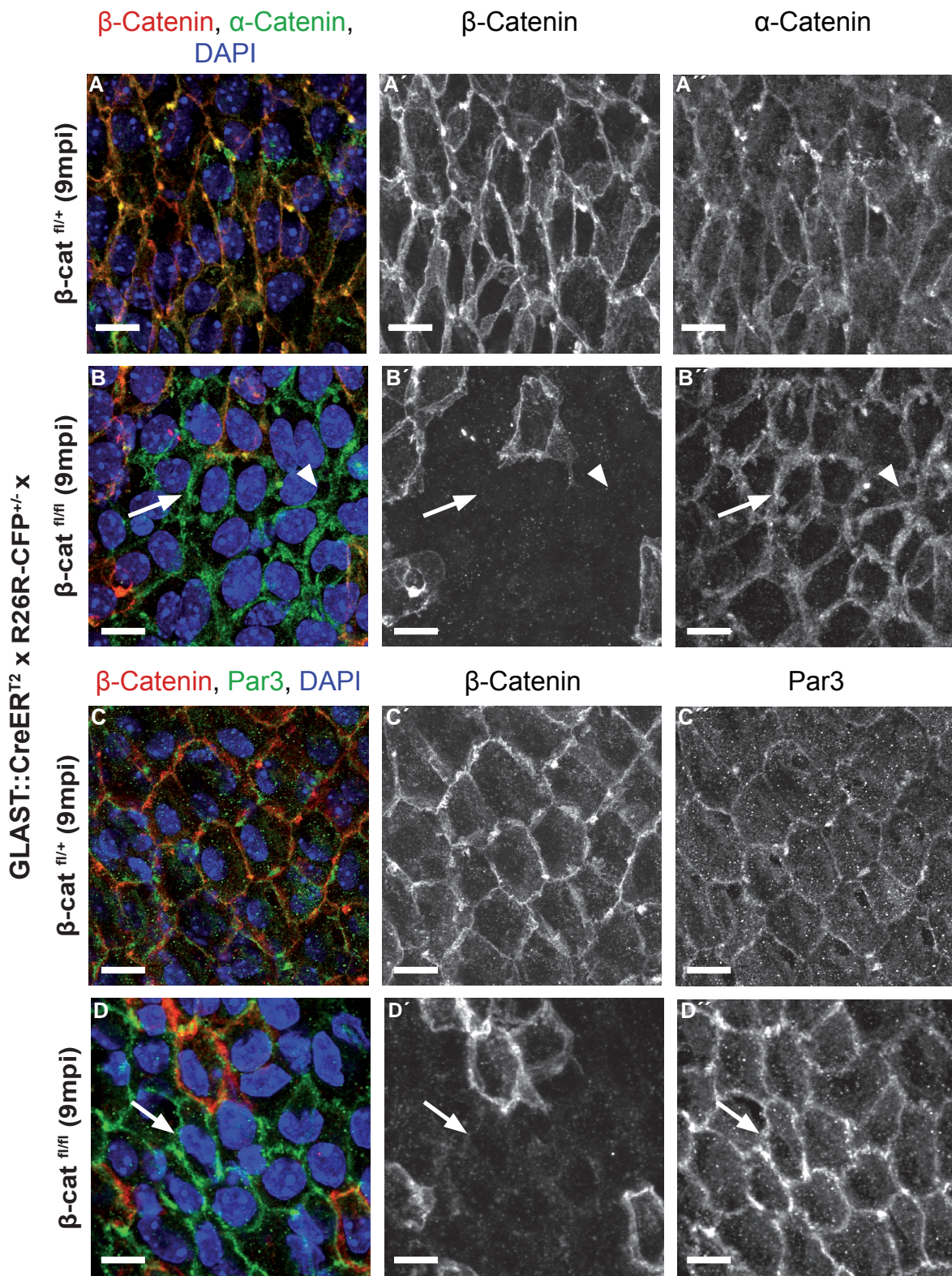


Figure 4-20. Despite loss of β -catenin apical proteins remain conserved in the adult SEZ

(A-D'') Whole mount preparations of adult SEZ from control and β -catenin deficient mice were stained for β -catenin (A-D'), α -E-catenin (A-B'') or Par3 (C-D''). En-face confocal images of the ventricular SEZ surface show that α -E-catenin and Par3 still locate at intercellular membranes outlining the apical surfaces of β -catenin deficient ependymal cells (arrows). Interestingly, both molecules appear more concentrated at the cell membrane of knock-out SEZ preparation in comparison to the control. (B, B'') Note, that α -E-catenin staining in the mutant SEZ surrounds as well a small apical surface, supposedly belonging to neural stem cells (arrowhead).

Scale bars: 10 μ m. All nuclei were stained with 4,6-diamidine-2-phenylidolehydrochloride (DAPI). SEZ: subependymal zone; 9mpi: 9 months post induction

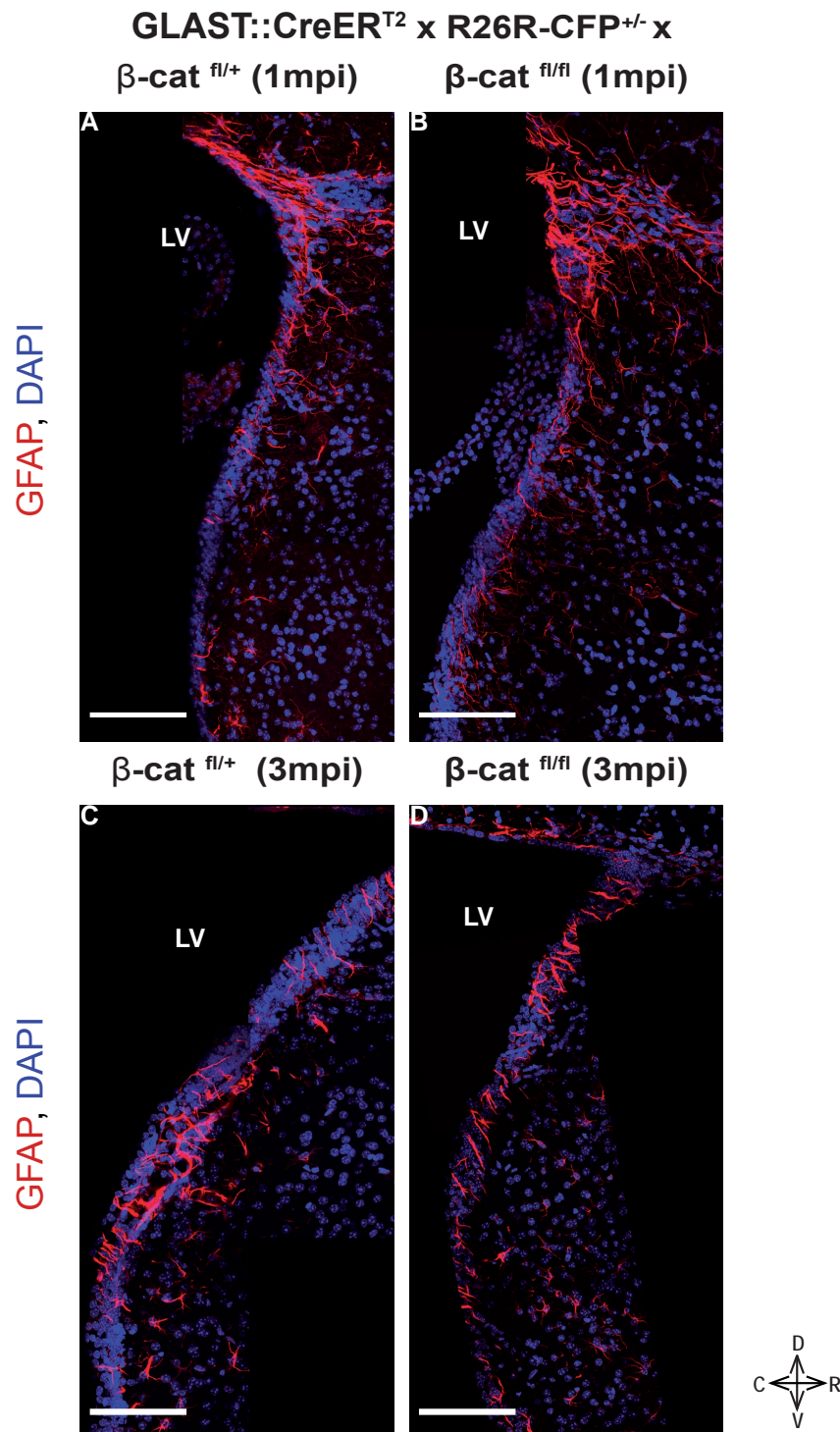


Figure 4-21. GFAP⁺ astrocytes and neural stem cells in adult SEZ after deletion of β -catenin

(A-D) GFAP immunostaining in adult SEZ one (A-B) or three months (C-D) after induction of Cre mediated recombination in β -Cat^{fl/+} or β -Cat^{fl/fl} mice. Note, that the amount of GFAP⁺ cells along the lateral wall of the ventricle looks similar between control and β -catenin deficient animals at both time points of the analysis.

Scale bars: 100 μ m. All nuclei were stained with 4,6-diamidino-2-phenylindole dihydrochloride (DAPI). Orientation of the sections is indicated by the cross in the lower right corner of the panel (C: caudal, D: dorsal, R: rostral, V: ventral). LV: lateral ventricle; SEZ: subependymal zone; 1mpi: 1 month post induction; 3mpi: 3 months post induction

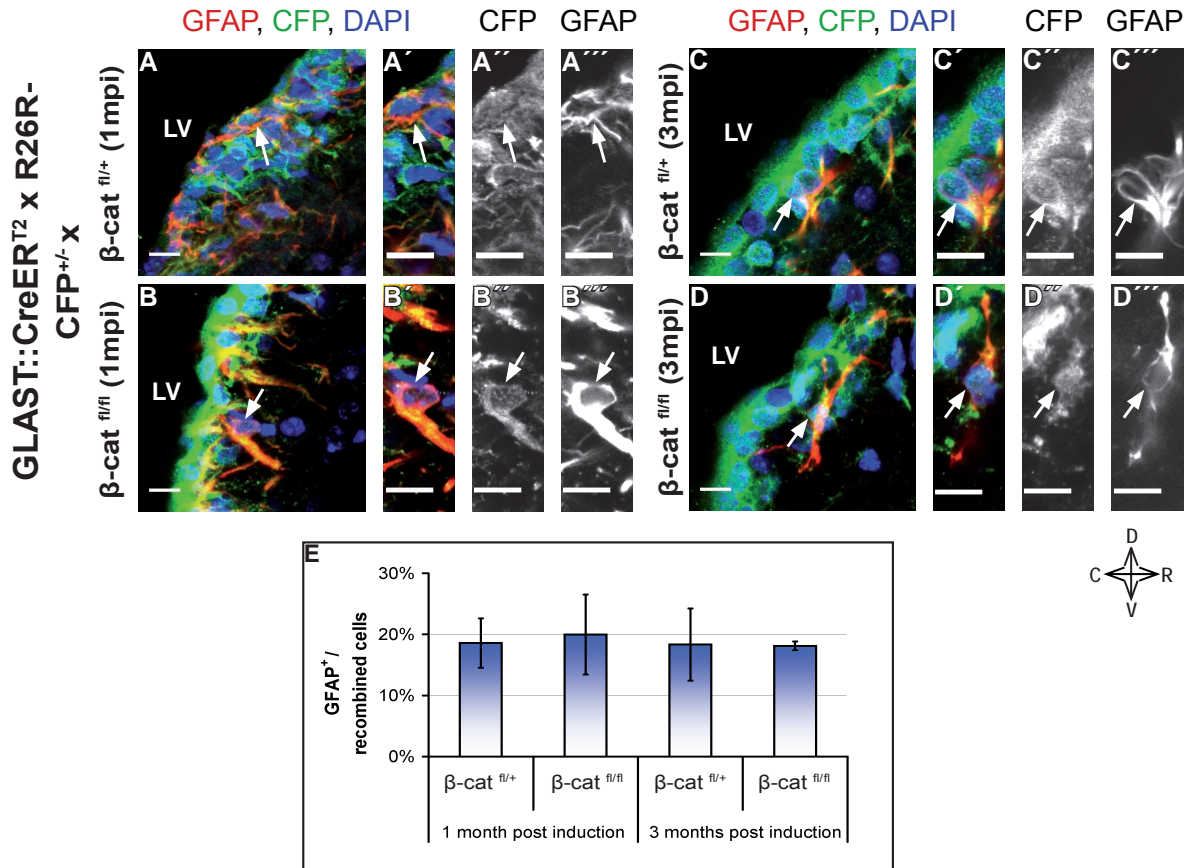


Figure 4-22. Quantitative analysis of GFAP⁺ cells in adult SEZ after loss of β -catenin

(A-D'') Fluorescent micrographs of CFP- and GFAP-immunostaining in the adult SEZ of GLAST::CreER^{T2} x R26R-CFP mice carrying one (A,C) or two floxed alleles of β -catenin gene (B,D). Animals were analysed one (A-B) or three months (C-D) after the last tamoxifen injection. (A, B, C, D) Pictures corresponds to a confocal stack with a thickness of 12 μ m. (A'-A''', B'-B''', C'-C''', D'-D''') Examples of CFP and GFAP double positive cells (arrows) that were found in control and β -catenin deficient mice 1mpi or 3mpi. For better co-localisation pictures display only a single optical section of 1 μ m.

(E) Histogram depicts the percentage of GFAP⁺ cells determined amongst all reporter⁺ cells. Quantitative analysis was done in the adult SEZ of GLAST::CreER^T x R26R-CFP x β -Cat^{fl/+} or ^{fl/fl} animals one or three months after tamoxifen induction. Means arise from quantifications performed in 3 animals respectively (total number of CFP⁺ cells analysed: 573 (control, 1mpi), 633 (β -cat^{fl/+}, 1mpi), 1263 (control, 3mpi), 1540 (β -cat^{fl/+}, 3mpi), 3 animals each). Error bars indicate SEM.

Scale bars: 10 μ m. All nuclei were stained with 4,6-diamidine-2-phenyldoleldihydrochloride (DAPI). Orientation of the sections is indicated by the cross in the lower right corner of the panel (C: caudal, D: dorsal, R: rostral, V: ventral). LV: lateral ventricle; SEZ: subependymal zone; 1mpi: 1 month post induction; 3mpi: 3 months post induction

I stained control and knock-out brain sections obtained from animals sacrificed at the two different time points with an antibody against GFAP (Fig.4-21). At first glance, the amount of GFAP⁺ cells found in the adult SEZ did not differ between control and knock-out animals at both time points of the study. Next, I performed double immunolabelling of GFAP and CFP on three control and three conditional knock-out brains per time-points and quantified the number of astrocytes amongst all reporter⁺ in SEZ found in the SEZ (Fig.4-22). Double-positive cells were found under all conditions (Fig.4-22A-D''). However, β -catenin deletion had no effect on the percentage of GFAP⁺ cells amongst all recombined cells counted in the SEZ neither at one nor at three months after tamoxifen treatment (Fig.4-22E). In all four experimental setups I found ~20% of all reporter⁺ cells being co-labelled for GFAP (Fig.4-22E).

However, because neural stem cells represent only a minority of all GFAP⁺ cells in the adult SEZ, these data do not exclude an influence of β -catenin deletion on adult neural stem cells.

4.4.4 Deletion of β -Catenin decreases the number of neuroblasts in the lateral ventricular wall

Before examining stem cells specifically, I analysed the neuroblasts in the lateral SEZ 1mpi and 3mpi. While DCX (Doublecortin) staining on the sections of control and conditional knock-out mice one month after end of tamoxifen treatment appeared quite similar (Fig.4-23A-B), the number of DCX⁺ cells in β -Cat^{fl/fl} x GLAST::CreER^{T2} x R26R-CFP was consistently reduced in comparison to control animals 3mpi (Fig.4-23C-D). For quantitative analysis, sections from three different control and conditional knock-out brains collected at the two different experimental time-points were co-immunolabelled with DCX and CFP (Fig.4-24). Double positive cells were seen in control and β -catenin deficient animals at both time-points of the analysis (Fig.4-24A-D''). However, I could immediately detect a pronounced reduction of DCX⁺ cells at 3mpi. Indeed, the percentage of DCX⁺ cells amongst all reporter⁺ cells in the lateral wall of β -Cat^{fl/fl} x GLAST::CreER^{T2} x R26R-CFP animals 3mpi was significant reduced by more than half in comparison to control values (Fig.4-24E, *p<0.05). Even 1mpi the amount of recombined cells being DCX⁺ was slightly reduced in the lateral SEZ of β -catenin deficient animals in comparison to control mice, although this difference was not significant (Fig.4-24E).

Taken together, these results indicate that the progressing loss of β -catenin results in a progressive reduction of the number of neuroblasts in the lateral wall of the ventricle.

4.4.5 Loss of neuroblasts after β -Catenin deletion is caused by a decreasing stem cell pool in the lateral ventricular wall

One possible explanation for the decreased number of neuroblasts found after β -catenin deletion is a loss or a decreased proliferative activity of neural stem cells in the adult SEZ. As discussed in the introduction, adult neural stem cells divide relatively slowly and their number can be estimated by assaying long-term BrdU retention. In order to label adult neural stem cells in the SEZ, mice were treated for two weeks with BrdU one month before sacrifice (Fig.4-25A). As the reduction of DCX⁺ cells was only significant in animals killed 3mpi, the label-retaining assay was performed within this time frame. Co-staining of forebrain sections from control and β -catenin conditional knock-out animals performed for BrdU and CFP revealed double positive cells in both cases (Fig.4-25F-G). However, quantifications determined a significant reduction of the number of label-retained cells amongst all reporter⁺ cells upon β -catenin deletion at 3mpi (Fig.4-25H, *** $p < 0.005$). While control animals showed 2.89% ($\pm 0.32\%$) slow dividing cells amongst recombined SEZ cells, conditional knock-out mice displayed only 1.47% ($\pm 0.15\%$) (Fig.4-25H).

These results suggest that deletion of β -catenin in the adult SEZ may lead to a decrease in the proliferation and/or survival of neural stem cells resident in the SEZ. Due to this decrease lower number of neuroblasts might be newly generated resulting in a final drop down of adult SEZ neurogenesis per se.

4.4.6 β -Catenin is required for Tbr2 expression in the RMS

Having analysed the function of β -catenin in the adult SEZ, prompted me to further investigate its role in the rostral migratory stream (RMS). As immunostaining for CFP labels also the progeny of recombined SEZ stem cells, I first took a closer look on reporter⁺ cells entering the RMS in control and mutant brains killed one month after tamoxifen treatment. Consistent with the unchanged numbers of neuroblasts in the SEZ at this time point of the analysis, no obvious difference was seen between the numbers of CFP⁺ cells being in the RMS of control or β -catenin deficient brains (Fig.4-26).

However, as shown by our and other groups (Hack et al., 2005, Kohwi et al., 2007, Brill et al., 2008, Brill et al., 2009), migrating neuroblasts within the RMS are no homogeneous population, but rather consist of a heterogeneous group of cells destined to acquire specific interneuronal fates. Subsequent studies showed that this heterogeneity arises in the SEZ, which contains different subsets of neural stem cells located in different areas along the lateral ventricle. The various stem cell subpopulations as well as their progeny are characterised by the expression of unique sets of transcription factors (see section 1.6.3, Fig.1-9). For example, Dlx2 is found in the GABAergic lineage that originates from the lateral wall of the lateral ventricle and accounts for the largest fraction of newly generated neurons

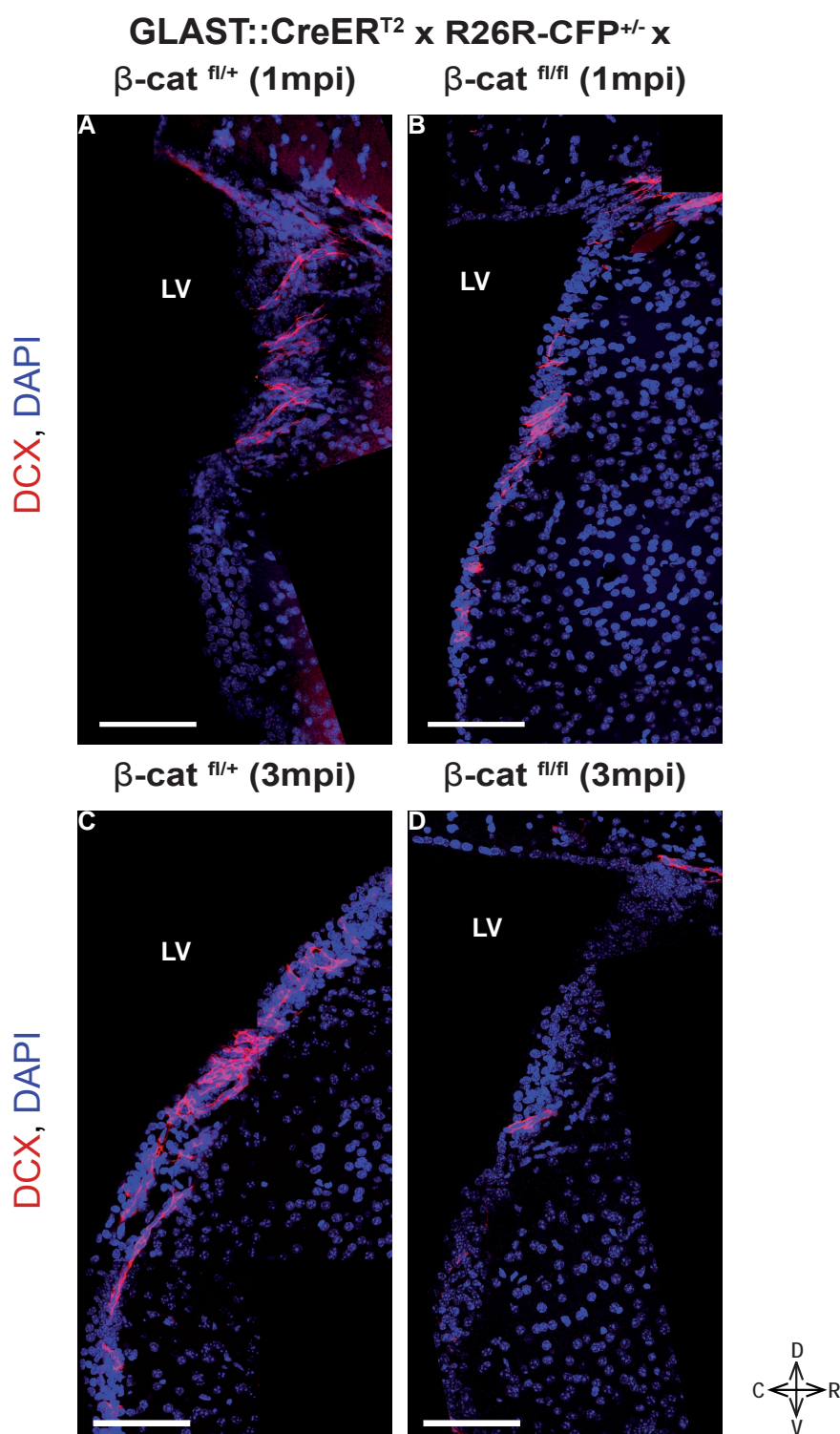


Figure 4-23. DCX⁺ neuroblasts in adult SEZ after deletion of β -catenin

(A-D) Fluorescent micrographs depicting DCX immunostaining labelling neuroblasts in the lateral wall of the ventricle one (A-B) or three months (C-D) after induction of Cre-mediated recombination in β -Cat^{fl/+} or β -Cat^{fl/fl} mice. While the number of DCX⁺ cells is comparable between control and mutant animals 1mpi, DCX expressing cells are obviously reduced 2 months later.

Scale bars: 100 μ m. All nuclei were stained with 4,6-diamidine-2-phenylidole-dihydrochloride (DAPI). Orientation of the sections is indicated by the cross in the lower right corner of the panel (C: caudal, D: dorsal, R: rostral, V: ventral). LV: lateral ventricle; SEZ: subependymal zone; 1mpi: 1 month post induction; 3mpi: 3 months post induction

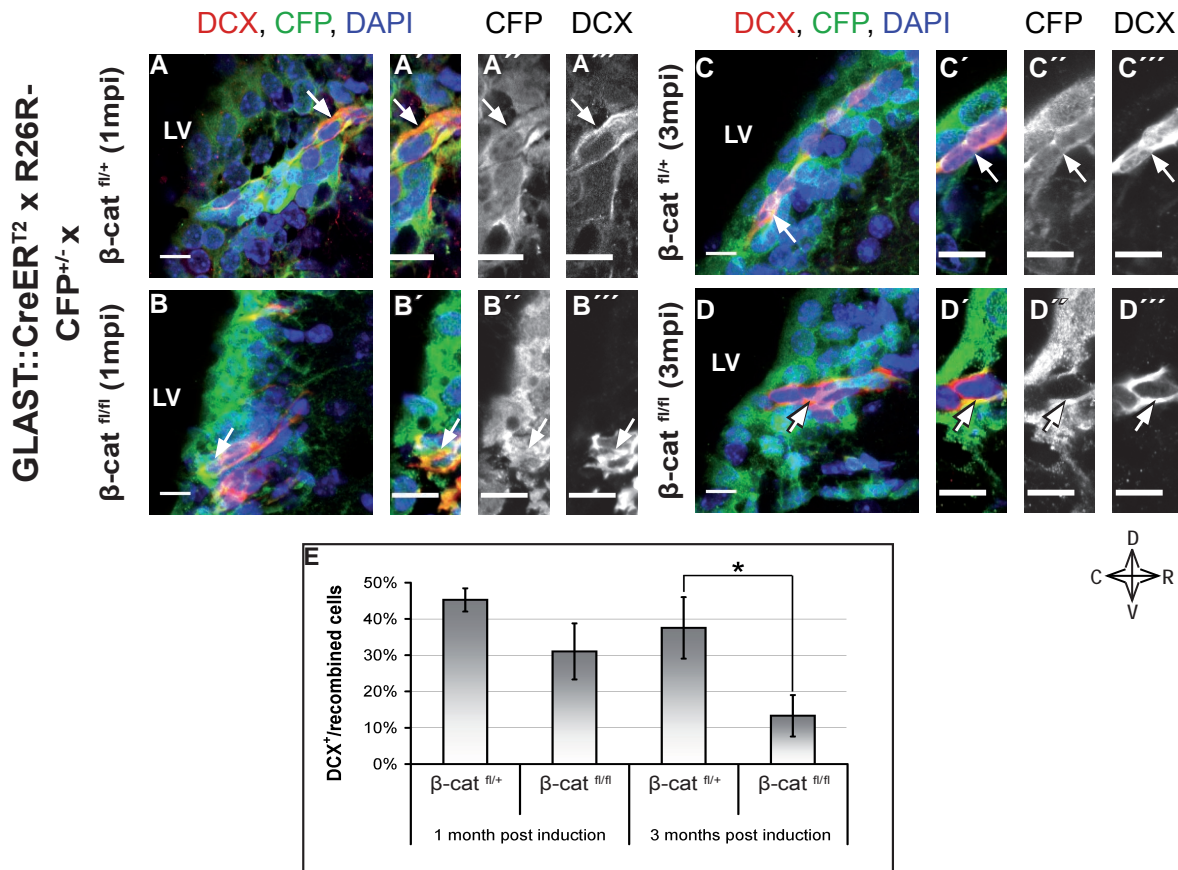


Figure 4-24. Loss of β -catenin decreases number of DCX⁺ neuroblasts in the lateral ventricular wall

(A-D'') CFP- and DCX-immunostaining in the adult SEZ of GLAST::CreERT² x R26R-CFP mice carrying one (A,C) or two floxed alleles of β -catenin gene one (A-B) or three months (C-D) after the last tamoxifen injection. (A, B, C, D) Pictures corresponds to a confocal stack with a thickness of 10 μ m. (A'-A'', B'-B'', C'-C'', D'-D'') Examples of CFP and DCX double positive cells (arrows) that were found in control and β -catenin deficient mice 1mpi or 3mpi. For better co-localisation pictures display only a single optical section of 1 μ m.

(E) Histogram depicts the percentage of DCX⁺ cells found amongst all reporter⁺ cells. Quantitative analysis was done in the adult SEZ of GLAST::CreERT² x R26R-CFP x β -Cat^{fl/+} or ^{fl/fl} animals one or three months after tamoxifen induction. Quantification revealed a significant reduction of neuroblast in β -catenin lacking cells of the lateral ventricular wall. Means arise from quantifications performed in 3 animals per genotype (total number of CFP⁺ cells analysed: 705 (control, 1mpi), 963 ($\beta\text{-cat}^{fl/+}$, 1mpi), 2229 (control, 3mpi), 1974 ($\beta\text{-cat}^{fl/+}$, 3mpi), 3 animals each). Error bars indicate SEM. Asterisk indicate a statistical difference between experimental groups (*p<0.05 in Student's t-test).

Scale bars: 10 μ m. All nuclei were stained with 4,6-diamidine-2-phenyldolehydrochloride (DAPI). Orientation of the sections is indicated by the cross in the lower right corner of the panel (C: caudal, D: dorsal, R: rostral, V: ventral). LV: lateral ventricle; SEZ: subependymal zone; 1mpi: 1 month post induction; 3mpi: 3 months post induction

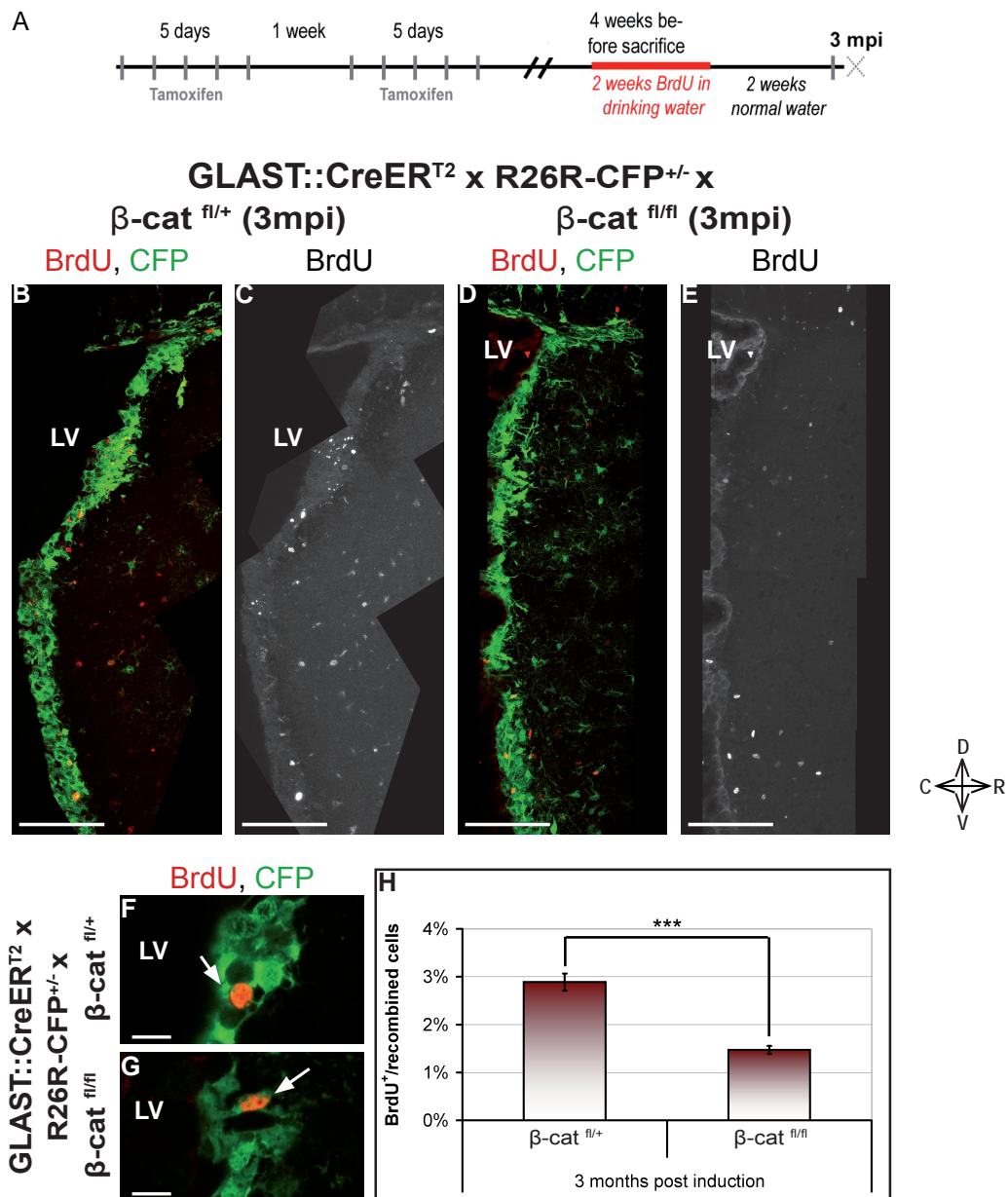


Figure 4-25. Deletion of β -catenin reduces neural stem cell self-renewal capacity

(A) Scheme of BrdU administration for marking label-retaining neural stem cells in the adult SEZ.

(B-G) Fluorescent images depicting reporter⁺ and label-retaining BrdU⁺ cells in the adult SEZ three months after induction of Cre mediated recombination in GLAST::CreER^{T2} x R26R-CFP mice carrying one (B, C, F) or two floxed alleles of β -catenin gene (D, E, G). Note, that the number of BrdU⁺ cells along the lateral wall of the ventricle is reduced in β -catenin deficient animals.

(H) Quantification of the percentage of label-retained BrdU⁺ cells amongst all reporter⁺ cells revealed a significant decrease in the number of slow-dividing cells found in β -catenin lacking cells. Means arise from quantifications performed in 3 control and 3 conditional knock-out animals (total number of CFP⁺ cells analysed: 2375 (control), 1962 (β -cat^{-/-})). Error bars indicate SEM. Asterisks mark a statistical difference between experimental groups (*** p <0.005 in Student's t-test)

Scale bars: 100 μ m in (B-E), 10 μ m in (F-G). Orientation of the sections is indicated by the cross in the lower right corner of the panel (C: caudal, D: dorsal, R: rostral, V: ventral). LV: lateral ventricle; SEZ: subependymal zone; 3mpi: 3 months post induction

integrating into the olfactory bulb (Doetsch et al., 2002, Brill et al., 2008). In contrast, a very small subpopulation of dorsally located neural stem cells generates glutamatergic juxtglomerular neurons, which arise from a lineage following the sequential expression of the transcription factors Pax6, Ngn2, Tbr2 and Tbr1 (Brill et al., 2009). Given that canonical Wnt signalling was highly active in the dorsal wall of the lateral ventricle (Fig.4-10) and that the β -catenin/TCF transcription complex was shown to directly target the proneural genes Ngn1/2 (Hirabayashi et al., 2004, Israsena et al., 2004), we hypothesised that the glutamatergic lineage might be especially affected by loss of β -catenin. To test this hypothesis, I performed Tbr2 staining in control and mutant brains sacrificed one month after tamoxifen treatment. A small number of Tbr2⁺ cells accumulating at the beginning of the descent arm of the RMS, i.e. where the RMS turns ventrally, was observed especially at medial section levels of control brains. (Fig.4-27A). Remarkably, Tbr2⁺ cells were missing at this position in the β -catenin deficient littermates (Fig.4-27B). Moreover, quantifications of the total number of Tbr2⁺ cells found per brain hemisphere revealed a reduction of 94% in β -Cat^{fl/fl} animals in comparison to controls (Fig.4-27C, n=138 (control), n=8 (β -Cat^{fl/fl})).

To examine, if β -catenin is as well required for the expression of the neurogenic factor Dlx2 being crucial for the generation of GABAergic interneurons, I performed in situ hybridisation with probes specific for Dlx2 mRNA in control and mutant animals killed one month after induction. As expected from the immunostaining against CFP displaying comparable levels of reporter⁺ cells along the lateral wall of the SEZ and in the RMS between conditional knock-outs and controls, also Dlx2 in situ did not show any obvious difference between the two genotypes (Fig.4-28). In control and β -catenin deficient brains, Dlx2 mRNA was abundantly expressed in the lateral wall of the lateral ventricle and in the RMS, but excluded from the dorsal or medial wall (Fig.4-28).

Another read-out for both, GABAergic and glutamatergic lineages is the neurogenic transcription factor Pax6. Pax6 was shown to be expressed in the dorsal SEZ as well as in the RMS co-localising with a large fraction of Dlx2⁺ cells, but also with a small fraction of Tbr1/2⁺ progenitors (Brill et al., 2008, Brill et al., 2009). Importantly, the Dlx2 transcription factor was never found to co-localise with Tbr1 (Brill et al., 2009). Even so the glutamatergic lineage is affected in the β -cat^{fl/fl} x GLAST::CreER^{T2} x R26R-CFP mice 1mpi, the majority of Pax6 expressing cells should be present in the RMS of these animals. Immunostaining against CFP and Pax6 in control and mutant mice confirmed this assumption and revealed equal numbers of double-positive cells in both genotypes (Fig.4-29).

In conclusion, these data suggest that loss of β -catenin and the resultant reduction of canonical Wnt signalling activity decrease the number of Tbr2 expressing cells in the RMS,

without strongly affecting the GABAergic lineage. Thus, β -catenin may play an instructive role in the specification of the dorsal SEZ progenitors towards a glutamatergic fate.

4.4.7 The role of β -Catenin in neuronal subtype specification in the olfactory bulb

Because the above results indicate a prominent role of β -catenin in neuronal subtype specification, I further examined different populations of the olfactory bulb neurons that were generated by stem cells manipulated within the SEZ. Given that loss of β -catenin had a pronounced effect on the $Tbr2^+$ progenitors destined to adopt glutamatergic fate, I first focused on this population. To do so, I combined in situ hybridisation using probes detecting mRNA of the vesicular glutamate transporters-2 (vGluT2) with the BrdU labelling protocol to visualise adult-generated cells. BrdU was given directly after end of tamoxifen treatment for two weeks in the drinking water followed by two weeks chase with BrdU free water to allow sufficient time for neurotransmitter differentiation (Fig.4-30A). In control and mutant animals some BrdU-positive cells were found in the glomerular cell layer of the OB, which as well showed intense vGluT2 mRNA signals (Fig.4-30A-B). Indeed, a small number of BrdU⁺ nuclei were surrounded by vGluT2 mRNA signal in the glomerular layer of the OB of control animals (4-30A). Surprisingly, double-positive neurons were also found in the OB of β -Cat^{fl/fl} animals (4-30B). Moreover quantifications revealed, that five weeks after tamoxifen treatment the proportion of BrdU⁺ cells amongst all vGluT2 expressing cells is barely altered between control and conditional knock-outs (control: 2.32%; β -Cat^{fl/fl}: 2.50%, see also Fig.4-30C). However, depletion of $Tbr2^+$ cells at 1mpi may only result in later reduction of vGluT2 expressing neurons.

As I observed a very high Wnt signalling activity in the dorsal SEZ, I next examined if the generation of the dopaminergic neurons, which as well originate from the dorsal ventricular wall, might be altered upon loss β -catenin 1mpi. I used two different markers to label this subpopulation of GABAergic periglomerular neurons: Pax6 and tyrosine hydroxylase (TH). Consistent with the fact that only ~7% of all 30 day old periglomerular neurons are dopaminergic (Kohwi et al., 2007), co-immunostaining against CFP and Pax6 revealed only a small number of double-positive cells, which, however, were present in both, wild-type and mutant animals (Fig.4-31). Furthermore, I also detected TH⁺ cells in the glomerular layer of control and β -Cat^{fl/fl} mice.

Taken together, these data demonstrate that β -catenin regulates the expression of $Tbr2$, but thus does not yet change the fate of the glutamatergic neurons at this early time point of the analysis. Furthermore, the fate of dopaminergic periglomerular neurons appears to be as well independent of β -catenin or canonical Wnt signalling.

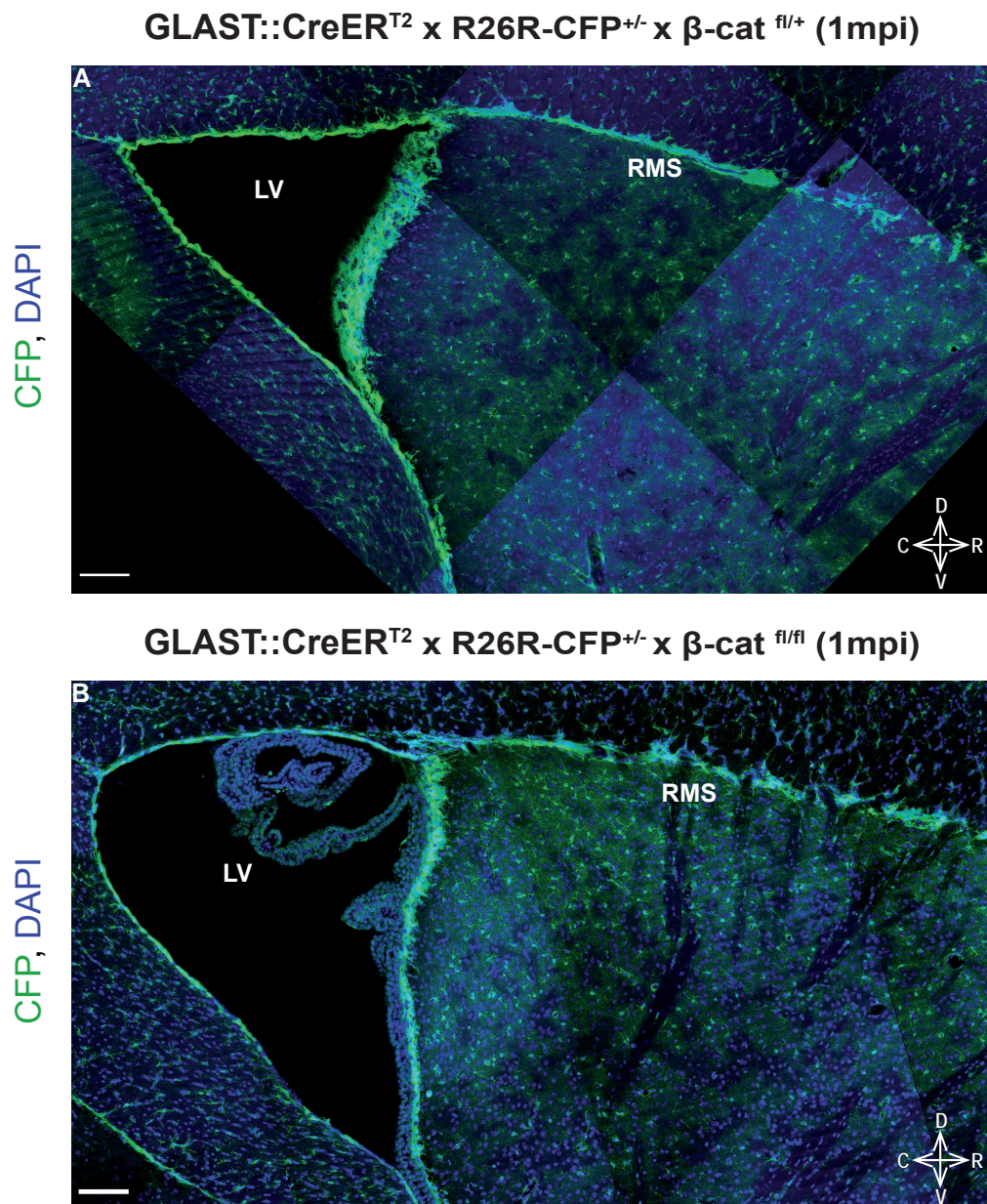


Figure 4-26. β -catenin deficient cells are able to migrate along the RMS

(A-B) Representative fluorescent photomicrographs comparing the spatial distribution of recombined CFP⁺ in the RMS in GLAST::CreER^{T2} x R26R-CFP mice carrying one (A) or two floxed alleles of β -catenin gene (B). The number of recombined cells migrating along the RMS is comparable between control and mutant animals.

Scale bars: 100 μ m. All nuclei were stained with 4,6-diamidino-2-phenylindole dihydrochloride (DAPI). Orientation of the sections is indicated by the cross in the lower right corner of the panel (C: caudal, D: dorsal, R: rostral, V: ventral). LV: lateral ventricle; RMS: rostral migratory stream; 1mpi: 1 months post induction

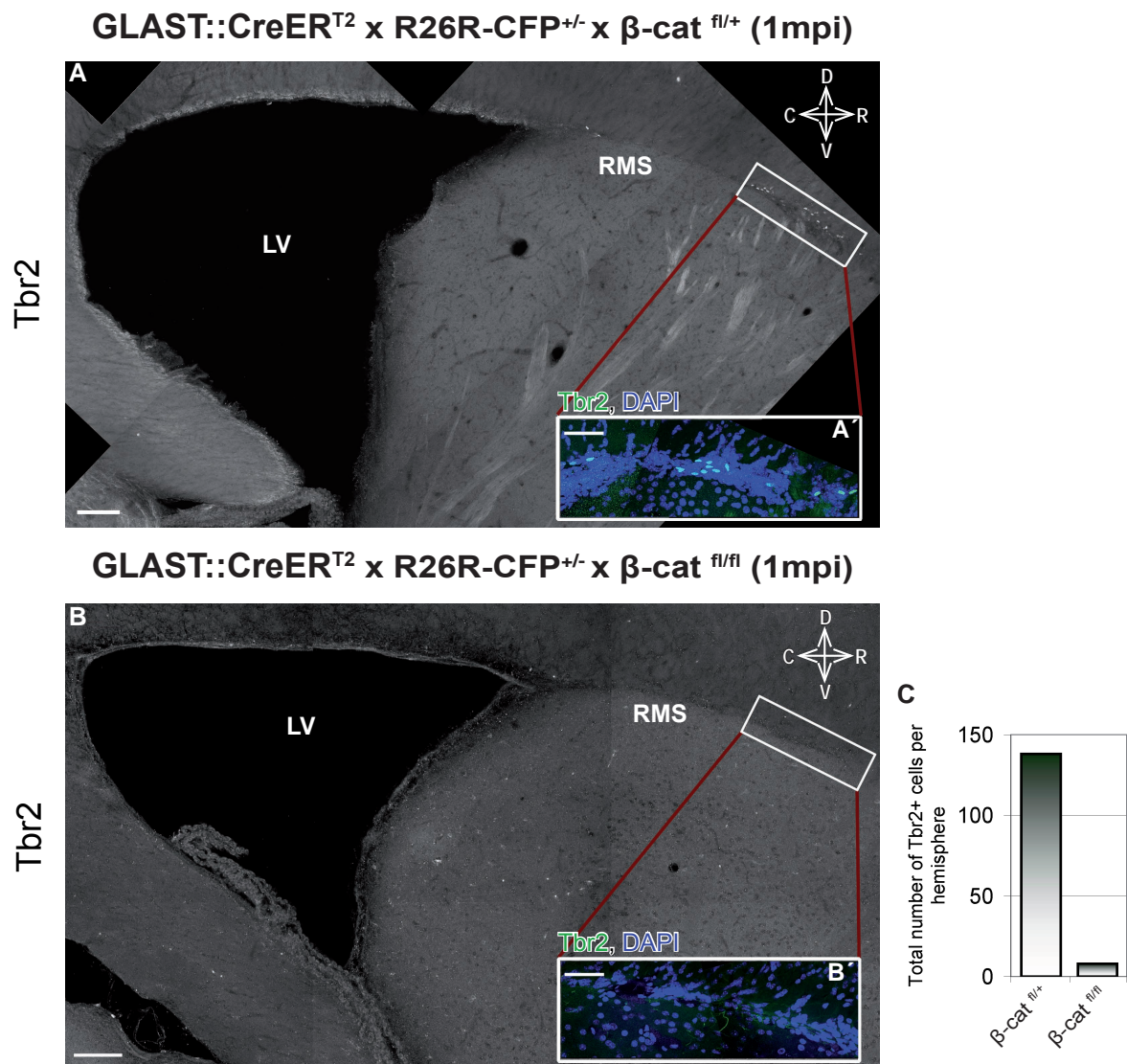


Figure 4-27. Tbr2 expressing cells in the RMS are lost in the absence of β -catenin

(A-B) Sagittal brain sections of control and β -catenin mutant brains were stained against Tbr2. Note the absence of Tbr2 expressing cells in brain section lacking β -catenin. (A'-B') Boxed areas are shown in higher magnifications demonstrating an accumulation of Tbr2⁺ cells in the control, but not in the mutant.

(C) Histogram showing the total number of Tbr2⁺ found per brain hemisphere in control and β -catenin deficient brains. Quantifications reveal a reduction of the Tbr2⁺ fraction in β -cat^{fl/fl} animals to 6% of control levels.

Scale bars: 100 μ m in (A, B), 20 μ m in (A', B'). Nuclei were stained with 4,6-diamidino-2-phenylindole dihydrochloride (DAPI). Orientation of the sections is indicated by the cross in the lower right corner of the panel (C: caudal, D: dorsal, R: rostral, V: ventral). LV: lateral ventricle; RMS: rostral migratory stream; 1mpi: 1 months post induction

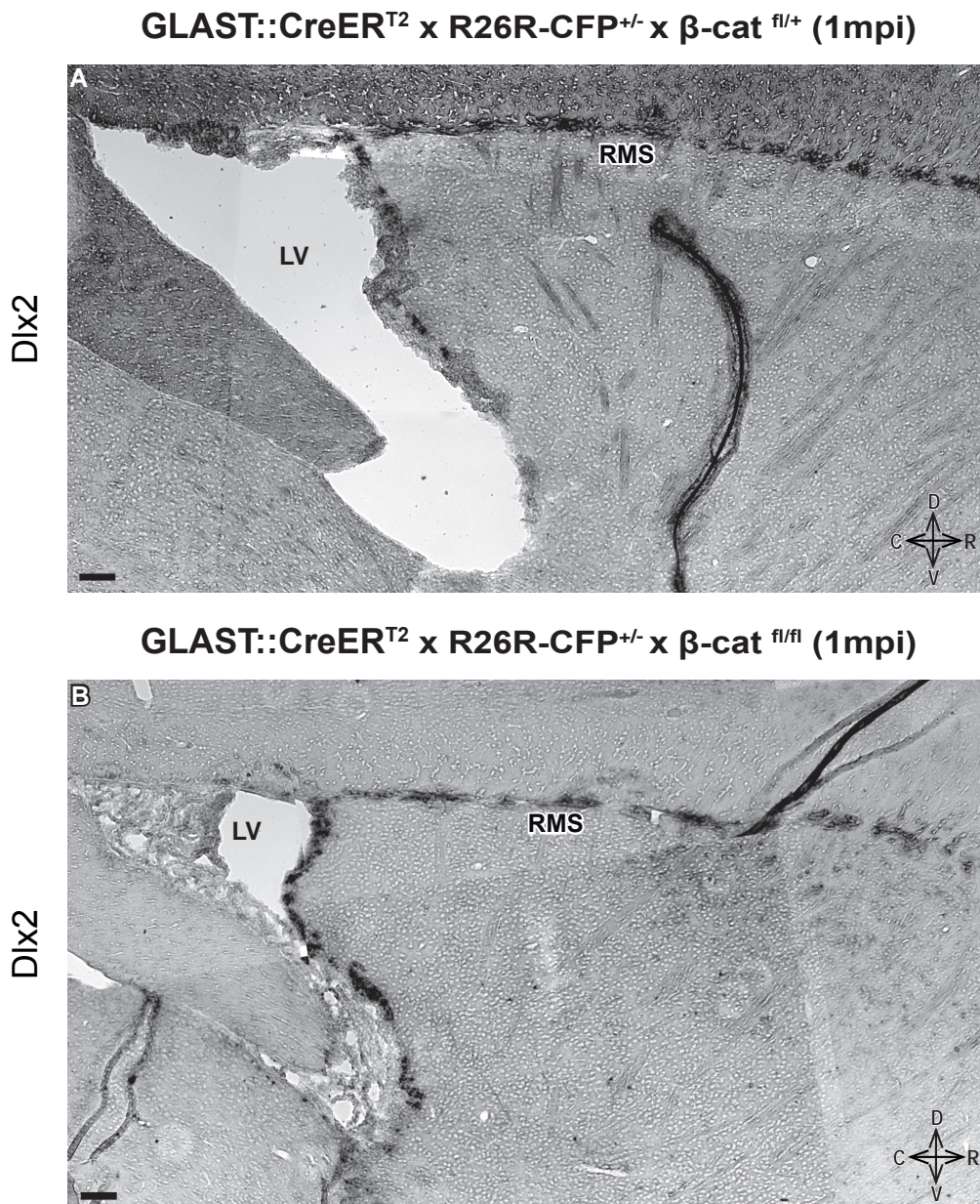


Figure 4-28. Expression pattern of Dlx2 transcription factor is not changed after loss of β -catenin

(A-B) In situ hybridization for Dlx2 shows intense mRNA signal in the lateral wall of the ventricle and in the RMS of control and mutant brains. The amount of in-situ signal is comparable between the two genotypes.

Scale bars: 100 μ m. Orientation of the sections is indicated by the cross in the lower right corner of the panel (C: caudal, D: dorsal, R: rostral, V: ventral). LV: lateral ventricle; RMS: rostral migratory stream; 1mpi: 1 months post induction

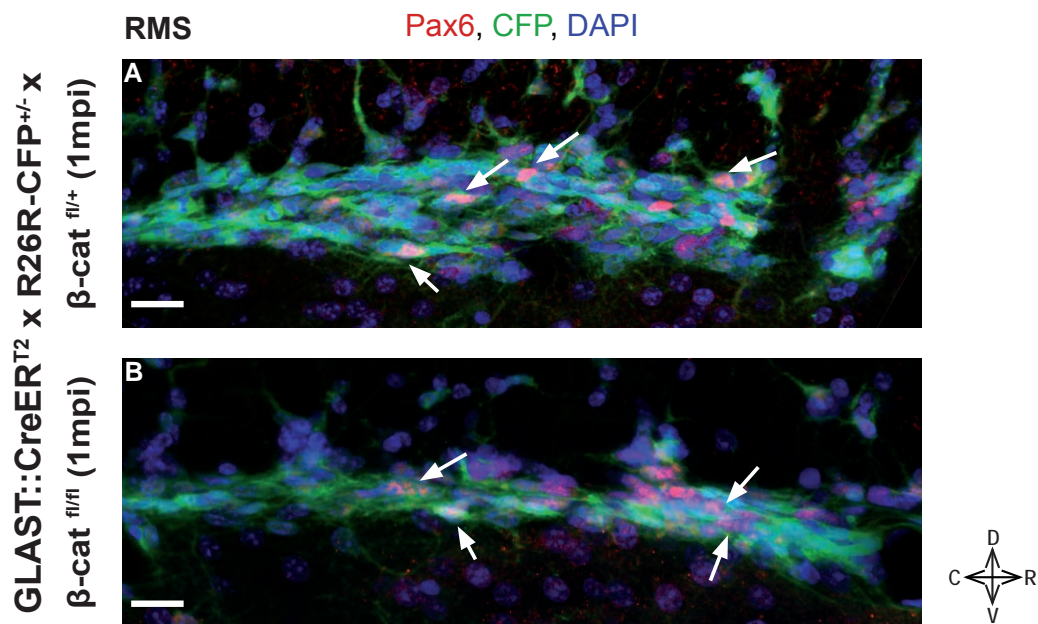


Figure 4-29. β-catenin deficient neuroblasts in the RMS express Pax6

(A-B) High magnification images of the rostral migratory stream (RMS) double stained for the reporter CFP and Pax6. Arrows indicate double-positive cells that are present in control and mutant brains.

Scale bars: 20μm. All nuclei were stained with 4,6-diamidine-2-phenylidolehydrochloride (DAPI). Orientation of the sections is indicated by the cross in the lower right corner of the panel (*C*: caudal, *D*: dorsal, *R*: rostral, *V*: ventral). *LV*: lateral ventricle; *RMS*: rostral migratory stream; *1mpi*: 1 months post induction

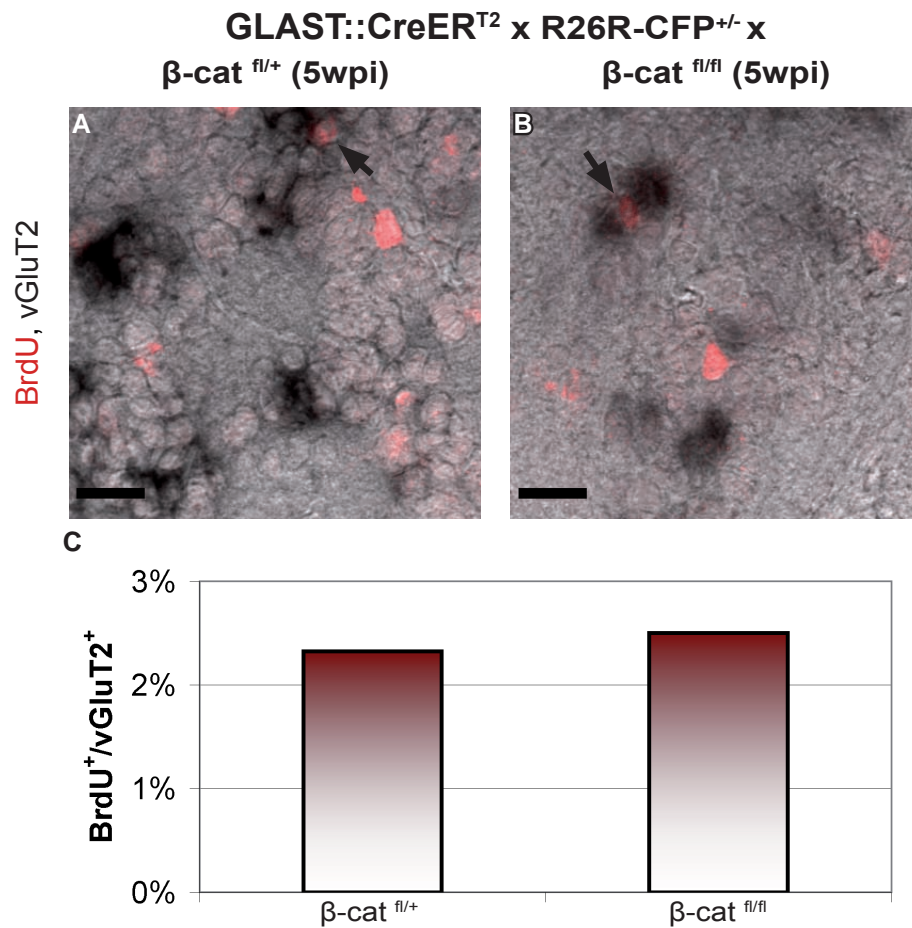


Figure 4-30. Detection of newborn glutamatergic neurons in GLAST::CreER^{T2} x R26R-CFP x β -cat^{fl/+} or β -cat^{fl/fl} mice

(A-B) To label newly generated glutamatergic neurons BrdU was given after the end of tamoxifen treatment for two weeks in drinking water followed by a chase of three weeks without BrdU. In-situ hybridisation for vGluT2 and immunohistochemistry for BrdU resulted in double-positive cells (arrows) in the glomerular layer of the adult olfactory bulb of control and mutant animals 5 weeks post induction (5wpi).

(C) Quantifications of the number of BrdU⁺ cells amongst all vGluT2⁺ cells revealed no difference between control and conditional knock-outs 5wpi.

Scale bars: 20 μ m.; 5wpi: 5 weeks post induction

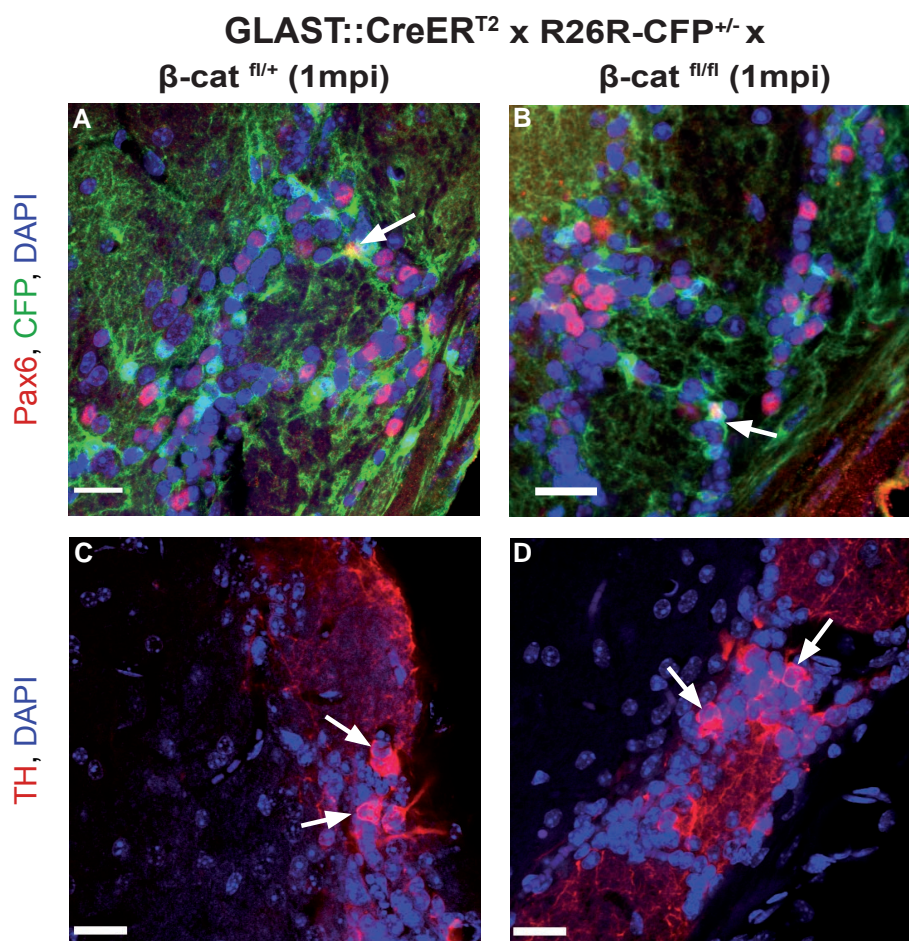


Figure 4-31. Newly generated dopaminergic neurons in the olfactory bulb of GLAST::CreER^{T2} x R26R-CFP x β -cat^{fl/+} or ^{fl/fl} mice

(A-D) Fluorescent micrographs showing representative examples of dopaminergic periglomerular neurons found in the olfactory bulb of control and β -Cat^{fl/fl} animals 1mpi. (A-B) Immunostaining against CFP and Pax6 revealed double-positive neurons in control and mutant brains (arrows). (C-D) Moreover, also immunoreactivity for tyrosine hydroxylase (TH) was present in the olfactory bulb of control and mutant brains (arrows).

Scale bars: 20 μ m. All nuclei were stained with 4,6-diamidine-2-phenylidole-dihydrochloride (DAPI). 1mpi: 1 months post induction

5 Discussion

5.1 SUMMARY

The global aim of the present study was to gain a better understanding of the role of stem cell polarity in neurogenesis. This general issue was addressed by (1) elucidating the impact of α -E-catenin on core cell-polarity proteins and its connection to proliferation pathways during embryonic corticogenesis by using a conditional loss-of-function approach, (2) comparing the influence of α -E-catenin, β -catenin, Par3 and Par6 on the mitotic behaviour of adult neural stem cell *in-vitro* and (3) providing a comprehensive analysis of the role of β -catenin in the adult SEZ-RMS-OB system *in-vivo*.

One remarkable finding of the first part of this work is that although α -E-catenin has a major role in maintaining the polarised radial morphology of cortical embryonic neural stem cells, it barely controls the expression levels of classical apical proteins. Moreover, the present study helped to rule out Wnt signalling as a potential cause of the proliferation phenotype seen upon loss of α -E-catenin in the developing cerebral cortex. Instead Western blot screening revealed GSK3 β as a possible molecular key player participating in the phenotype seen after α -E-catenin ablation in the dorsal telencephalon.

The second part of this thesis focused in detail on the molecular composition of the apical SEZ surface, and showed for the first time the presence and subcellular localisation of Par complex proteins in the largest adult neurogenic niche. Furthermore, data obtained from the neurosphere assay demonstrated the essential role of Par3 and β -catenin in neural stem cell proliferation/survival. As the *in-vitro* analysis displayed the strongest phenotype after loss of β -catenin, I concentrated further on its function *in-vivo*. Interestingly, loss of β -catenin in the adult SEZ did not interfere with its prominent role in cell adhesion, as the pinwheel organisation of the neural stem cells was still normal even several months after loss of the protein. The molecular role of β -catenin is, however, not only limited to its structural tasks in cell-cell adhesion, but involves as well the canonical Wnt signalling. Using the BAT-gal reporter line, I demonstrated that β -catenin-mediated Wnt signalling is predominantly active in the dorsal wall of the SEZ. My results show further, that genetic deletion of β -catenin in the adult SEZ leads to an almost complete loss of Tbr2⁺ progenitors originating exclusively in the dorsal region of the adult SEZ and specified to adopt glutamatergic fate. Interestingly, defects in neurogenesis continue to spread over the months and manifest in decreased number of adult neural stem cells in the lateral SEZ leading consequently to an overall reduced number of neuroblasts. My results therefore suggest a graded response to the loss of β -catenin. While the high levels of canonical Wnt signalling activity in dorsal neural stem cells might be essential for specification or maturation of glutamatergic interneurons, lower

levels of β -catenin dependent signalling which are not detectable by the BAT-gal reporter line are needed to maintain the stem cell pool.

5.2 α -E-CATENIN DEPENDENT SIGNALLING DURING CORTICAL NEUROGENESIS

5.2.1 The loss of α -E-Catenin causes only minor changes in polarity cues

One key challenge of polarised epithelial cells is to control the identity and distribution of functionally and structurally unique plasma membrane domains. The localisation of AJ to the apical-most domain of the lateral membrane and sorting of the Par complex to the subapical domain are tightly connected events in the establishment of the orientation of polarised cells. Several studies suggested that the formation of primordial cell-cell contacts is the initiating cue for recruitment of polarity proteins in close neighbourhood to the spot of AJ (Nelson & Chen, 2003, Perez-Moreno *et al.*, 2003). In contrast, other analyses demonstrated that Par3 preceded AJ formation (Harris & Peifer, 2004, Afonso & Henrique, 2006) and that Cdc42, aPKC as well as Par6 are indispensable for the maintenance of AJ (Georgiou *et al.*, 2008, Imai *et al.*, 2006, Harris & Tepass, 2008).

Consistent with the observation that Par3 acts upstream of AJ during the establishment of apico-basal polarity my Western blot data demonstrate that the expression of Par complex molecules is largely independent of α -E-catenin in the cerebral cortex. In this regard it is, however, worth noting that immunohistochemical and EM studies of our lab revealed that α -E-catenin deficient cortical cells are still able to form cell-cell contacts (Schmid, 2007). Furthermore, Par3 protein was not randomly distributed throughout the mutant cells, but concentrated closely to the cadherin/ β -catenin positive membrane spots (Schmid, 2007). Therefore, the present study does not figure out the hierarchy between the recruitment of other AJ proteins than α -E-catenin and Par complex molecules during the process of cell polarisation. Definitely, detailed analyses of conditional cadherin mutants lacking all cadherin types (E-, N- and R-cadherin) expressed in embryonic neural stem cells are needed to further illuminate this issue.

Another remarkable finding of the present study was, that the total levels of Prominin-1, a protein, which is exclusively enriched at the most apical membrane domain and the primary cilium of embryonic neural stem cells (Marzesco *et al.*, 2005, Marthiens & ffrench-Constant, 2009), are barely altered after loss of α -E-catenin. Immunostaining against Prominin-1 showed that the protein in similarity to Par3 was localised unidirectional within the α -E-catenin deficient cortical cells (Schmid, 2007). Together these data imply that α -E-catenin neither controls cell-cell contact formation nor asymmetric distribution of polarity cues within individual cells, but rather the overall polarity of the tissue.

However, aPKC provides the main biochemical output of the Par complex as it is the only member of the complex showing an enzymatic activity (Assemat *et al.*, 2008). The activity of this kinase is not only regulated by the interaction with the Par molecules or Cdc42, but also by lipid-derived second messengers generated by receptor-mediated events (Fields *et al.*, 2007). Not surprisingly, aPKC has been linked to other signalling cascades including the oncogenic Ras signalling (Bjorkoy *et al.*, 1997, Kampfer *et al.*, 2001) or the NF- κ B survival pathway (Lu *et al.*, 2001). My Western blot analyses show that the protein levels of activated, phosphorylated aPKC were only slightly altered in the mutant brains. Therefore an involvement of the enzyme in the hyper-proliferation phenotype caused by disruption of the α -E-catenin gene is very unlikely.

As the Western blot analyses give no information about the identity of the mutant cells containing the polar proteins, it is tempting to speculate that the polarity proteins might be mis-expressed in the basal progenitor population that usually down-regulates these proteins. However, the fact that the relative proportion of Pax6⁺ radial glia population and the Tbr2⁺ basal progenitor population in the Emx1^{Cre/ α -Cat Δ ex2fl/fl} brains remained at control levels (Schmid, 2007) argues against this hypothesis. On the other hand this raises the question which transcription factors actually regulate the expression of Par complex molecules. Until today the exact mechanisms involved in this process are poorly understood. Clearly, new research will be necessary to reveal the transcriptional key player in the complex process of cell polarity establishment and maintenance.

5.2.2 α -E-Catenin does not control β -catenin signalling during early neurogenesis

Deletion of α -E-catenin often leads to increased cell proliferation. This has been not only observed after loss of α -E-catenin from the brain (Lien *et al.*, 2006, Schmid, 2007), but also in α -E-catenin deficient skin (Vasioukhin *et al.*, 2001) or in cancer cell lines (Watabe *et al.*, 1994). One possible mechanism explaining this phenotype is based on the idea, that the intrinsic binding of α -E-catenin to β -catenin at the plasma membrane prevents β -catenin to enter the nucleus and function as a transcriptional co-activator of canonical Wnt target genes. Indeed over-expression of α -E-catenin in cancer cell lines and non-cancerous chondrocytes resulted in decreased β -catenin dependent transcriptional activity (Giannini *et al.*, 2000, Merdek *et al.*, 2004, Hwang *et al.*, 2005), while partial deletion of α -E-catenin in chondrocytes showed increased β -catenin/TCF signalling (Hwang *et al.*, 2005). In contrast to the previous analyses, recently a publication demonstrated that focal reduction of α -E-catenin in the developing cerebral cortex does not cause increased, but reduced β -catenin mediated signalling (Stocker & Chenn, 2009).

To clarify the potential role of β -catenin signalling in the Emx1^{Cre/ α -Cat Δ ex2fl/fl} cortices, a number of independent approaches were used in this work including the comparison of total, nuclear

and cytoplasmic β -catenin levels between wild-type and mutant cortices. Moreover, activity of β -catenin signalling was monitored by quantitative determination of β -galactosidase activity in the TOPGAL reporter background. All of these different methods did not reveal any significant changes between wild-type and mutant animals indicating no impact of α -E-catenin on β -catenin signalling during early neurogenesis. Supportively, similar results were previously published, when mutants lacking α -E-catenin in the entire CNS were analysed in detail for β -catenin mediated signalling (Lien *et al.*, 2008).

However, there are several reasons explaining the disparity between findings of the Vasioukhin or our lab and previously published works that did detect changes in β -catenin/TCF signalling. In regard to the cell culture experiments (Giannini *et al.*, 2000, Merdek *et al.*, 2004, Hwang *et al.*, 2005) one has to emphasize that direct comparisons between *in-vitro* and *in-vivo* studies are difficult. In contrast to cell culture systems that are supplied with defined nutrients and growth factors, living organs exhibit complex signalling mechanisms that depend on the tissue homeostasis or developmental stages. However, one explanation for the differences seen between the cell culture experiments and the developing brain is the existence of α -N-catenin in neural tissue, which could compensate for the loss of α -E-catenin (Stocker & Chenn, 2006). It is known that both α -E- and α -N-catenin are able to interact with the E-cadherin- β -catenin complex and therefore participate comparably in the process of AJ formation (Hirano *et al.*, 1992). But as I did not observe any change in the total levels of α -N-catenin in mutant brains compared to the control, this possibility is very unlikely. Moreover, the already discussed EM and immunohistochemical data show an existence of cell-cell contacts despite loss of α -E-catenin and capture of β -catenin at cadherin positive membrane spots (Schmid, 2007). These observations argue much more for an essential role of cadherin and not α -E-catenin in regulating the pool of free β -catenin molecules. The latter idea is furthermore supported by the finding that α -E-catenin was demonstrated to favour homodimerisation, when it is present in high local concentrations (Drees *et al.*, 2005). This data further demonstrate that there is no constant binding between α -E-catenin and β -catenin at the mature adherens junctions, but only in the process of AJ formation. Taken together, my data fit to this model that α -E-catenin proteins prefer homodimerisation, hence loss of α -E-catenin protein had no major influence on β -catenin protein levels.

While attractive, the above hypothesis does not provide an adequate explanation for why focal elimination of α -E-catenin using electroporation caused a reduction in β -catenin signalling (Stocker & Chenn, 2009). Obviously one major difference between the *in-vivo* work of Stocker and colleagues (Stocker & Chenn, 2009) and my analysis is the method applied to delete α -E-catenin from the embryonic neural stem cells. While the electroporation approach done by the Chenn lab targets only a subset of cells (Stocker & Chenn, 2009), the

conditional knock-out model used in this work eliminates α -E-catenin in the entire cerebral cortex. The widespread deletion of α -E-catenin can lead to non-cell-autonomous effects on the developing cortex that might obscure changes in β -catenin/TCF signalling seen due to focal deletion of the protein. Another difference between study of Stocker and colleagues (Stocker & Chenn, 2009) and the present analysis is time point of α -E-catenin deletion and the possible changing function of the protein over the course of neurogenesis. While recombination of the electroporated embryos began at E13.5 (Stocker & Chenn, 2009), the *Emx1* driven recombination starts already at E9.5. Indeed, usage of the hGFAP-Cre line (Malatesta et al., 2003) to delete α -E-catenin at later developmental stages (E13) showed also a much milder phenotype than this seen in the *Emx1*^{Cre/ α -Cat Δ ex2fl/fl} brains with no increase in proliferation (Schmid et al., in preparation). Taken together, it remains difficult to understand the influence of α -E-catenin on Wnt/ β -catenin signalling at mid-neurogenesis and further analyses are needed to complete our knowledge about the specific roles of α -E-catenin at different developmental stages.

5.2.3 Compensatory response of GSK3 β to hyper-proliferation caused by loss of α -E-catenin from the cerebral cortex

GSK3 β was discovered 30 years ago and named as one of several protein kinases that phosphorylate and inactivate glycogen synthase (Embi *et al.*, 1980). Despite involvement in metabolism, GSK3 β has been linked with a number of fundamental functions including transcription control, oncogenesis and neurological diseases (Woodgett, 2001). Strikingly the enzyme has been also implicated to play an essential role in regulating proliferation and differentiation of neural stem cells (Maurer *et al.*, 2005, Kim *et al.*, 2009). By examining control and *Emx1*^{Cre/ α -Cat Δ ex2fl/fl} cortices I found a notable increase in the GSK3 β protein levels in the α -E-catenin deficient cortices. Interestingly, this up-regulation appeared to be a transient effect, which was most prominent at E12 and nearly compensated at E13. Since GSK3 β up-regulation became prominent only one day after elimination of α -E-catenin protein, these events are probably not directly coupled to each other. This observation rather implies that GSK3 β is responding indirectly to the tissue-wide changes caused by α -E-catenin ablation. The most striking change seen in the *Emx1*^{Cre/ α -Cat Δ ex2fl/fl} mice was a temporary increase in cell proliferation starting at E11 and normalising again at E13. As the increased levels of GSK3 β are less pronounced at E13 than at E12, the kinase might play a compensatory role in the mutant cortices by inhibiting the over-proliferation caused by loss of α -E-catenin. Indeed, conditional deletion of both the α and β forms of GSK3 in the developing murine CNS, markedly enhanced progenitor proliferation (Kim et al., 2009), while over-expression of a constitutively active form of GSK3 β in pancreatic beta cells *in-vivo* significantly reduced number of mitotic active beta cells (Liu *et al.*, 2008). In contrast,

pharmacological inhibition of GSK3 β was shown to reduce the proliferation rate of neurosphere forming cells (Maurer et al., 2005) or cultured ventral mesencephalic precursors (Castelo-Branco *et al.*, 2004) by simultaneously increasing the rate of neuronal differentiation.

In contrast to many other protein kinases, one key feature of GSK3 β is, that it is by default enzymatically active and inhibited in response to several distinct pathways (Woodgett, 2001). Inhibition of the kinase can be achieved by its phosphorylation at Ser9; and various kinases, linking GSK3 β to multiple signalling pathways, have been identified to participate in this phosphorylation event. For example, MAPK-activated protein kinase1 and protein kinase B are able to mediate phosphorylation of GSK3 β at Ser9 in response to insulin or growth factors (Shaw & Cohen, 1999). Furthermore, the p70 ribosomal S6 kinase-1, activated by mTOR, a key regulator of cell growth, is known to phosphorylate GSK3 β at Ser9 (Grimes and Jope, 2001). Remarkably, the present study did not show any changes in GSK3 β activity that would dependent on the phosphorylation state of Ser9 residue. These findings additionally support the role of active GSK3 β in antagonising the increased proliferation observed in the α -E-catenin deficient cortices. Given that degradation of β -catenin is as well regulated by GSK3 β activity, and my Western blot data did not show decreased levels of the canonical Wnt signalling protein this result appears confusing. Interestingly, the activity of GSK3 β during canonical Wnt signalling does not involve its Ser9 phosphorylation (Ruel *et al.*, 1999, Ding et al., 2000), but the binding of FRAT (frequently rearranged in advanced T-cell lymphomas) proteins (Li *et al.*, 1999). The interaction of FRAT and dishevelled, a key regulator of the Wnt pathway, disrupts the β -catenin destruction complex and prevents β -catenin from its degradation. Thus, up-regulation of FRAT in the α -E-catenin lacking brains might inhibit increased β -catenin reduction. However, a more likely possibility is that the maintained interactions of cadherin and β -catenin at the plasma membrane of the mutant cortical cells rescue β -catenin from being degraded.

But how does GSK3 β inhibit the over-proliferation phenotype caused by loss of α -E-catenin? A number of diverse GSK3 β substrates were implicated to influence cell proliferation. One very prominent substrate is of course β -catenin that, as just discussed, was not changed at E11 between control and mutant brains. Other molecules known to be catalysed by GSK3 β include the carcinogenic transcription factor c-myc (Sears *et al.*, 2000) or the cell cycle promoting protein cyclinD1 (Diehl *et al.*, 1998). Phosphorylation of c-myc or cyclinD1 targets the proteins for proteolytic degradation and thus reduces their half-life (Alt *et al.*, 2000, Sears et al., 2000). While no change in the c-myc mRNA levels was seen after loss of α -E-catenin, mRNA levels of cyclinD1 were shown to be up-regulated at E11 (Schmid, 2007). The latter discovery furthermore supports the assumption that GSK3 β gets up-regulated at E12 in order

to compensate for the increased levels of cyclinD1 by promoting its phosphorylation and consequently its degradation.

Together these data highlight the cross-talk between the different signalling pathways and the ability of a multi-cellular organ to react fast to severe changes during development. However, at present, it remains unanswered, which molecules act as a molecular sensor detecting the over-proliferation of cortical cells. Therefore, future experiments assessing this problem are needed to fully understand the present findings.

5.3 THE APICAL DOMAIN OF ADULT SEZ NEURAL STEM CELLS SHOWS

CHARACTERISTIC FEATURES OF EMBRYONIC VENTRICULAR ZONE CELLS

Since the discovery of ongoing neurogenesis in the SEZ of adult mice (Lois & Alvarez-Buylla, 1993), a lot of effort has been done to characterise structure and cellular composition of the largest adult neurogenic niche (Kriegstein & Alvarez-Buylla, 2009). Recently, Mirzadeh and colleagues revealed the pinwheel organisation of the ventricular SEZ surface with the thin apical endfeet of adult neural stem cells in its centre surrounded by the cell bodies of the ependymal cells (Mirzadeh et al., 2008). My study could confirm these findings by showing that the two AJ molecules, α - and β -catenin, encircle the ventricular surfaces of ependymal and adult neural stem cells in the predicted pattern. Strikingly, the present work revealed, that the adult SEZ expresses also all Par complex members known to establish and maintain cellular polarisation (Assemat et al., 2008). Moreover, immunohistochemical analysis detected that Par3 protein locates to the apical cell cortex of ependymal and adult neural stem cells, as well as to their cilia. The cellular localisation of apical SEZ molecules identified in the present work is summarised in Fig.5-1. In agreement with the analysis of Mirzadeh and colleagues (Mirzadeh et al., 2008) this work underlines that adult neural stem cells retain basic epithelial properties of embryonic neural stem cells including the expression of important polarity cues.

The plasma membrane of embryonic neural stem cells can be divided into three distinct micro-domains (Marthiens & ffrench-Constant, 2009). The polarity proteins, Par3 and aPKC are located in the most apical domain; the two junctional proteins, ZO1 and afadin, are positioned more laterally followed by the adherens junctional proteins in a slightly more basal position (Marthiens & ffrench-Constant, 2009). Surprisingly, my study suggests that adult neural stem cells in contrast to their embryonic ancestors show not only Par3 staining at the apical, but also partially at the lateral membrane domain containing AJ molecules. However, as the lateral and apical membrane domain of polarised epithelial cells are distinctly separated from each other (Rodriguez-Boulan & Nelson, 1989) this finding is very unlikely and probably results from the limited confocal resolution applied during my analysis. While Marthiens and colleagues could only resolve the three micro-domains by analysing *en face*

stacks of confocal images acquired at 0.12 μ m (Marthiens & French-Constant, 2009), my microscopic study was based on images taken at 0.6 μ m intervals. Clearly, high-resolution microscopic analysis is needed to further clarify the separation of the micro-domains in the adult SEZ cells.

Remarkably, the present work could reveal that Par3 protein localises to the cilia of SEZ cells. Cilia are conserved microtubule-based protrusions of the cell surface that originate from the basal bodies, a centrosome-derived structure (Eggenchwiler & Anderson, 2007). Recent findings suggest that the primary cilium functions as a complex signalling centre mediating Shh (Huangfu *et al.*, 2003, Corbit *et al.*, 2005, Huangfu & Anderson, 2005, Liu *et al.*, 2005, Breunig *et al.*, 2008, Han *et al.*, 2008) and Wnt signalling (Gerdes & Katsanis, 2008). Both signalling pathways are known key regulators of adult neural stem cell proliferation (Yu *et al.*, 2006, Hirsch *et al.*, 2007, Palma *et al.*, 2005, Han *et al.*, 2008). As Par3 protein was implicated to play a crucial role in ciliogenesis (Sfakianos *et al.*, 2007) this finding strongly suggests a function of Par3 in adult neural stem cells, either in cilia formation or in cell polarity or in cilia-mediated signalling.

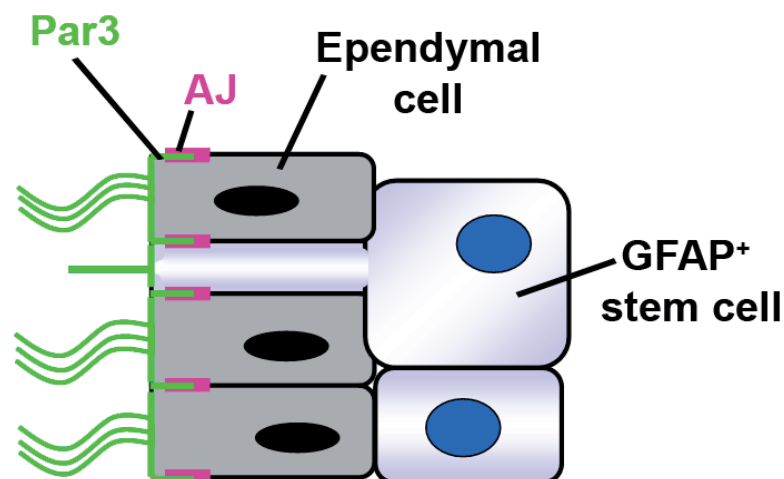


Figure 5-1. Model of apical membrane domain of ependymal and neural stem cells in the adult SEZ

The cell polarity Par complex, consisting of Par3, Par6 and aPKC localises to the apical membrane of the ependymal and adult neural stem cells. Furthermore, Par3 molecules are located along their cilia. In contrast, the adherens junctions (AJ), which form the cell-cell contacts between ependymal and adult neural stem cells, are positioned at the most apical side of the lateral membrane.

The Par molecules are highly conserved homologues to invertebrate key components needed for asymmetric cell divisions. Given the apical localisation of the Par complex in adult neural stem cells, raises the possibility that these proteins may also regulate the asymmetric cell division of adult neural stem cells. In analogy to neuroblast divisions seen in *Drosophila melanogaster*, already the discovery of these molecules in embryonic neural stem cells brought the hypothesis about the asymmetric segregation of polarity cues during their mitosis causing a different fate of the two daughter cells (Götz & Huttner, 2005, Zhong & Chia, 2008, Knoblich, 2008, Kosodo & Huttner, 2009). Indeed, aPKC was shown to be inherited by both daughter cells on symmetric proliferative divisions of radial glia cells and by only one of the daughter cells on an asymmetric neurogenic division (Marthiens & French-Constant, 2009). As the frequency of adult neural stem cell divisions is very low, such studies in the adult telencephalon are not a simple undertaking. Obviously, advanced live imaging methods allowing the analysis of an area of interest over several weeks are needed to clarify these processes in the adult brain. For now, imaging of Par complex molecule distribution during adult neural stem cells divisions is very much limited to cell culture experiments. Nevertheless such *in-vitro* studies in combination with manipulations of the proteins will help to get a first insight into this problem and provide a better understanding of the functional role of the protein complex in adult neurogenesis.

5.4 THE PINWHEEL ORGANISATION OF THE ADULT SEZ DOES NOT DEPEND ON THE ADHESIVE FUNCTION OF β -CATENIN

β -Catenin is a central structural component of the adherens junctional complex and was shown to play a crucial role in maintaining the cellular organisation of complex tissues and organs. For example, β -catenin null-mutant embryos, show severe adhesion defects at the gastrulation stage characterised by ectodermal cell detachment and dispersion of these cells into the proamniotic cavity (Haegel *et al.*, 1995). Also conditional loss of β -catenin during lens development resulted in a dramatic defect of lens morphogenesis due to the disintegration of the epithelial cells (Smith *et al.*, 2005). Furthermore, β -catenin was reported to be indispensable for maintaining the integrity of neuroepithelial and radial glial cells during cortical development (Machon *et al.*, 2003, Junghans *et al.*, 2005, Schmid, 2007). Therefore it was rather surprising, that in the present study loss of β -catenin in the ependyma and adult neural stem cells did not disturb the adherens junctional cell-cell-contacts, so that the pinwheel organisation of the adult SEZ was maintained.

The latter findings suggest that the junctional complexes beside the above discussed similarities also show some differences between embryonic and adult neural stem cells. But on which molecular components might be these differences in the cell-cell contacts based? Interestingly, it has been shown, that plakoglobin, which is the closest relative of β -catenin in

the armadillo protein family, can take over the function of β -catenin in cell adhesion (Huelsenken *et al.*, 2000, Posthaus *et al.*, 2002, Zhou *et al.*, 2007). This happens, for instance, in the early mouse embryo (Huelsenken *et al.*, 2000), in the epidermis (Posthaus *et al.*, 2002), or in the heart (Zhou *et al.*, 2007). These findings indicate that junctional complexes in the adult SEZ may contain in addition to β -catenin also plakoglobin, which until now was not shown to be expressed in embryonic neural stem cells of the murine brain.

However, in most instances plakoglobin appears to be not localised in the AJ but rather in the desmosomes, probably due to its higher affinity for desmosomal cadherins than for E-cadherin (Garrod & Chidgey, 2008). Strikingly, a comparative transcriptome analysis between purified adult neural SEZ stem cells and astrocytes/ependymal cells revealed, that desmosomal genes are especially enriched in the adult neural stem cells including desmoglein-2 and plakophilin-2 (Tripathi *et al.*, in preparation). Desmoglein-2 belongs to the family of desmosomal cadherins, which represent the membrane spanning constituents of desmosomes (Garrod & Chidgey, 2008). Plakophilin-2 is like β -catenin and plakoglobin a member of the armadillo family that participate in linking desmosomal cadherins to intermediate filaments in the cytoskeleton (Garrod & Chidgey, 2008). Especially, the interaction of these molecules with the intermediate filaments is the major reason for the extraordinary strength of desmosomal junctional complexes (Garrod & Chidgey, 2008). Therefore, these junctions are particularly abundant in tissues, such as epidermis and myocardium, which are continually exposed to mechanical forces (Garrod & Chidgey, 2008). Furthermore it is worth noting, that desmogleins were found to also contribute to the so-called composite junctions, an atypical junctional hybrid complex containing both desmosomal and AJ proteins (Franke *et al.*, 2009). Thus, it might be well possible, that adult neural stem cells do not contain the typical AJ, but rather these atypical junctional complexes.

In conclusion, the increased strength of cell-cell contacts containing both AJ molecules and desmosomal proteins may guarantee the maintenance of organised cell-cell contacts even after loss of β -catenin.

5.5 THE ROLE OF ADHERENS JUNCTIONAL MOLECULES IN NEUROSPHERE CULTURES

One general role of adherens junctional core proteins during cortical development is their involvement in anchoring of VZ stem cells and maintenance of tissue organisation (Machon *et al.*, 2003, Lien *et al.*, 2006, Schmid, 2007, Kadowaki *et al.*, 2007). Moreover, loss of both α -E- and β -catenin influences proliferation behaviour of cortical progenitors during early neurogenesis (Schmid, 2007). In order to discriminate between adhesion dependent and

independent phenotypes in α -E- and β -catenin deficient neurosphere forming cells obtained from adult SEZ, I performed the classical free floating neurosphere assay and the collagen based approach. Interestingly, both methods revealed the same results: While loss of α -E-catenin had no obvious effect on neurosphere forming capacity, lack of β -catenin reduced the number of generated colonies significantly.

Thus, neurosphere formation appears to be independent of α -E-catenin mediated adhesion or its anti-mitogenic potential. In this regard it is worth noting, that I also did not see an increase in proliferation, when I plated primary cells of E11 $Emx1^{Cre/\alpha-Cat\Delta ex2fl/fl}$ cortices. In conclusion, these observations emphasises one more the difference between *in-vitro* and *in-vivo* studies.

In contrast, β -catenin regulates the neural stem cell behaviour also dramatically *in-vitro*. Since the free-floating and the collagen based neurosphere assay revealed the same effect, the phenotype seen after loss of β -catenin can not be allocated to adhesion defects, but rather lack of canonical Wnt signalling. In fact, canonical Wnt signalling was shown to promote neural stem cell proliferation during embryonic brain development (for review see Chenn, 2008). Furthermore recent investigations demonstrated that over-expression of canonical Wnt-3a in neonatal neural stem cells increases neurosphere formation capacity (Yu et al., 2006). Additionally, Increased cell proliferation was observed, when neonatal forebrain cells cultured as monolayer in the presence of EGF were treated with recombinant Wnt-3a (Hirsch et al., 2007).

In this regard it is noteworthy that loss of β -catenin also decreased the number of BrdU label-retaining cells to half of control levels as presented in my *in-vivo* study of animals analysed 3mpi. Since I started to perform the collagen based assay with a reduced number of neural stem cells, it is not surprising that I obtained smaller numbers of colonies after loss of β -catenin. Remarkably, the number of spheres was not only reduced by 50% but by 80% of control levels. Thus, my work shows for the first time that canonical Wnt signalling is needed for the expansion of neurospheres obtained from adult neural stem cells.

Beside an impairment of neural stem cell proliferation another reason for the reduced number of β -catenin deficient neurospheres, might be an increase in apoptosis. Indeed loss of β -catenin has been associated with an enhancement of cell death during early brain development (Junghans et al., 2005). Interestingly, this work discusses the apoptotic phenotype as a result of misplaced neuroepithelial cells, and not lack of canonical Wnt signalling (Junghans et al., 2005). However, as I did not perform a detailed cell death analysis, future experiments will have to determine the role of β -catenin on the survival of adult neural stem cells.

In summary, my results show that β -catenin, but not α -catenin, is required for the maintenance of adult neural stem cells, as well as for the expansion of neurosphere forming

cells. I propose, that neither α - nor β -catenin mediated adhesion is needed for these processes, but rather the function of β -catenin in regulation of TCF/LEF dependent gene transcription.

5.6 THE ROLE OF THE PAR COMPLEX IN NEUROSPHERE CULTURES

Much of our knowledge on the role of polarity molecules in neurogenesis is derived from studies of the developing telencephalon. Previous work had established a crucial role of the small Rho-GTPase Cdc42 (Cappello et al., 2006) and the Par proteins (Costa et al., 2008, Bultje et al., 2009) in controlling the fate of embryonic neural stem cells. It has been shown that loss of Cdc42 resulted in an increased number of mitoses occurring basally and in a higher production of neurons (Cappello et al., 2006). Also loss of Par3 caused premature neurogenesis, whereas over-expression of Par3 or Par6 promoted proliferation of radial glia cells (Costa et al., 2008, Bultje et al., 2009). Intriguingly, the mitotic capacity of Par6 was also demonstrated in mammary epithelial cells, which upon Par6 over-expression increased their cell proliferation through activation of MAPK (Nolan et al., 2008).

In contrast, Par6 over-expression in the present work did not reveal any difference in the neurosphere formation capacity. The simplest explanation for the absence of increased proliferation may be the culture conditions. One of the key downstream pathways of both growth factors, EGF and FGF, include phosphorylation and activation of MAPK. As the neurosphere cultures contain very high levels of these growth factors, a high proportion, if not all MAPK molecules are already activated during neurosphere formation. Thus, higher levels of Par6 can simply not activate further MAPK molecules. For that reason an interesting experiment would be to grow the Par6 over-expressing SEZ cells without adding EGF and FGF to the medium. Perhaps neurosphere formation is induced by over-expression of Par6 in adult SEZ cells.

The present work showed, moreover, that knock-down of Par3 in isolated adult neural stem cells reduces significantly the number of generated neurospheres. Like already discussed for the case of β -catenin deficiency, two different mechanisms may explain this phenotype: First, Par3 depletion may decrease proliferation or second, increase cell death of neurosphere forming cells. The work from embryonic radial glia cells (Costa et al., 2008, Bultje et al., 2009) would support the hypothesis that neurosphere forming cells undergo premature differentiation and therefore result in a reduced number of colonies. However, I did not observe differentiated neurons, oligodendrocytes or astrocytes on the bottom of cell culture dish. Since the neurosphere assay is selecting for proliferating cells, Par3 deficient differentiating cells may simply die during the culture. Interestingly, some virally infected cells were able to generate neurospheres or fail to be maintained. Given that lentiviruses can integrate several times, the knock-down efficiency may differ between the neurosphere

forming cells. It might therefore be that low levels of Par3 allow neurosphere formation, while further loss of the protein may completely inhibit this process.

In contrast to the suggested model, silencing of Par3 during mammalian gland morphogenesis was shown to increase proliferation and simultaneously enhance cell death (McCaffrey & Macara, 2009). As the function of a protein is highly dependent on the tissue and culture system context, it remains to be studied to which extent proliferation and apoptosis contribute to the observed phenotype. For example, proliferation can be easily monitored by BrdU incorporation experiment or immunohistochemical analyses using an antibody against Ki67. Furthermore, apoptotic behaviour needs to be assessed by performing TUNEL labelling or staining against cleaved Caspase-3.

Taken together, my study is just the starting point in understanding the complex role of Par3 and Par6 during adult neurogenesis. Nevertheless, the present analysis showed for the first time, that loss of Par3 inhibits expansion of neurosphere forming cells. Therefore this work provides the basis for future *in-vitro*, but also *in-vivo* analyses that are clearly needed to further investigate the function of these molecules in adult neurogenesis.

5.7 THE DUAL ROLES OF β -CATENIN IN ADULT NEUROGENESIS *IN-VIVO*:

MAINTENANCE OF THE NEURAL STEM CELL POOL AND CONTROL OF DORSAL PROGENITOR SUBTYPES

5.7.1 The function of β -catenin in maintaining general adult neurogenesis

Recent studies suggest that β -catenin signalling is capable of regulating neural stem cell proliferation and the size of the cerebral cortex during embryonic neurogenesis. Transgenic mice over-expressing a stabilised form of β -catenin in neural progenitors had an abnormally large number of neural precursor cells caused by an increased rate of proliferation (Chenn & Walsh, 2002). Moreover, transgenic animals expressing relatively lower levels of stabilised β -catenin in embryonic neural stem cells develop enlarged forebrains and a greatly expanded SEZ in the adult brain (Chenn & Walsh, 2003). In contrast, β -catenin deletion during embryonic neurogenesis leads to reduced proliferation of neural progenitors (Machon et al., 2003, Schmid, 2007) supporting the mitogenic function of canonical Wnt signalling during embryonic neurogenesis.

Despite the growing numbers of studies on β -catenin in embryonic neurogenesis, relatively little is known about the functional effect of this molecule and its signalling in the adult neurogenesis. Only one analysis based on pharmacological and retroviral approaches has so far attempted to evaluate the role of canonical Wnt signalling in the adult SEZ (Adachi et al., 2007). Adachi and colleagues demonstrated that over-expression of stabilised β -catenin increased the number of transit-amplifying progenitors (TAPs) two days after retroviral

infection, while over-expression of DKK-1, an antagonist of the Frizzled receptor and negative regulator of canonical Wnt signalling, caused the opposite effect (Adachi et al., 2007). Together with the data obtained from the pharmacological inhibition of GSK3 β , this group concluded that β -catenin dependent signalling promotes the proliferation of TAPs and increases the number of newly generated neurons integrating into the olfactory bulb (Adachi et al., 2007). Further support for the idea that canonical Wnt signalling has a crucial role in adult neurogenesis comes from experiments demonstrating that Wnt-3 secreted by astrocytes of the dentate gyrus stimulates the neuronal fate commitment of adult neural stem cells and enhances the proliferation of neuroblasts in the adult hippocampus (Lie et al., 2005).

My study revealed that β -catenin is highly expressed in the adult neural stem cell of the SEZ. In order to manipulate the protein expression at the earliest stages of the neurogenic lineage and not like Adachi and colleagues only at the stage of TAPs and neuroblasts, I used a transgenic approach to delete β -catenin specifically in the neural stem cell population. A novel finding of my analyses is that already the neural stem cells of the adult SEZ are primarily dependent on the presence of β -catenin, which guarantees their maintenance. Moreover, I could demonstrate that also the neuroblast population is decreased upon loss of β -catenin. Taking my *in-vitro* neurosphere data and the published work manipulating Wnt signalling during adult neurogenesis (Lie et al., 2005, Adachi et al., 2007) in consideration, the most likely explanation is that both, the decreased stem cell pool and the decreased proliferation of their progeny would contribute to the lower number of neuroblasts. However, my observation that loss of β -catenin reduces the neuroblast population contradicts the findings of Adachi and colleagues. The group showed that although Dkk-1 over-expression decreased the number of TAPs, it increased in the numbers of neuroblasts (Adachi et al., 2007). These results suggest that the reduced proliferation of TAPs promotes the cells to enter the next step of the neuronal lineage. Two different reasons can be taken in account in order to explain the different outcomes of the two studies. First, since β -catenin in the present work was depleted slowly over a long period of time, it is well possible that my two time point analyses simply missed this transient increase in the neuroblast population. Second, the gradual loss of the protein argues for a non-synchronised depletion of β -catenin. Therefore, not all TAPs start to lack the protein at the same time and only subpopulations of TAPs would be driven to the neuroblast lineage at on particular time point. If this is the case, it is impossible to detect this small increase in the number of neuroblast amongst all recombined cells.

Until this time point of the discussion, I did not further comment on the molecular functions of β -catenin that would trigger the observed behaviour of the adult SEZ cells. As discussed in

the previous section, the adhesion and the pinwheel architecture of the SEZ were not obviously disturbed after loss of β -catenin. Therefore it is very unlikely that deficient adhesion would cause the observed phenotype, but rather the role of β -catenin in the canonical Wnt pathway. However, the BAT-gal reporter analysis demonstrated that β -catenin-mediated Wnt signalling is predominantly active in the dorsal and not in the lateral wall of the SEZ, the place showing a decreased number of stem cell and neuroblasts after loss of the protein. Interestingly, analysis of a different canonical Wnt reporter line expressing the Axin-d2EGFP transgene revealed that β -catenin-mediated signalling is as well present along the lateral wall of the ventricle (Adachi et al., 2007). The discrepancy between the two Wnt reporter lines might be interpreted as a difference in the detection sensitivity. While the BAT-gal line detects only high levels of Wnt signalling activity, the Axin-d2EGFP transgene may detect also lower levels. One possibility to further look into this problem would be to compare the levels of nuclear β -catenin in the dorsal and lateral ventricular wall using the nuclear fractionation technique.

Taken together, I propose that the lateral SEZ displays low levels of canonical Wnt signalling activity, which are crucial to maintain adult neural stem cells and consequently the overall neurogenesis of the SEZ-RMS system.

5.7.2 The prospective function of β -catenin in neuronal subtype specification

A particularly interesting aspect of my work is that loss of β -catenin caused an almost complete loss of the Tbr2⁺ progenitor population. This very recently discovered progenitor pool is originating from the dorsal region of the adult SEZ and was shown to produce a novel type of olfactory interneurons, which in contrast to the majority of newly generated neurons is glutamatergic and not GABAergic (Brill et al., 2009). During the process of adult neurogenesis this lineage follows a conserved sequence of transcription factors (Pax6→Ngn2→Tbr2→Tbr1) commonly observed during the generation of glutamatergic neurons in the cortex, cerebellum or hippocampus (Hevner *et al.*, 2006, Brill et al., 2009).

Strikingly, the proneural genes Ngn1/2 were shown to be direct targets for the β -catenin/TCF transcription complex (Hirabayashi et al., 2004, Israsena et al., 2004). Moreover, disruption of β -catenin in neural crest cells was shown to block the development of Ngn2-dependent sensory neurons (Hari *et al.*, 2002). This evidences when combined with my findings suggest a role for β -catenin mediated Wnt signalling in promoting Ngn2 expression, which in turn regulate Tbr2. In agreement with the proposed model the Guillemot lab showed that loss of Ngn1 and 2 during embryonic cortical neurogenesis reduced the expression of the T-box transcription factors, Tbr1 and 2 (Schoorjans et al., 2004). Furthermore, this hypothesis is supported by my own findings revealing high levels of Wnt signalling activity in the dorsal wall of SEZ, being the origin of the glutamatergic OB interneurons.

In general, two kinds of factors can control the fate of stem or progenitor cells during adult neurogenesis: intrinsic fate determinants or extrinsic environmental cues. In contrast to my work, a study based on homo- and heterotypical cell grafting experiments supported the idea that adult neural stem cells of the SEZ are primed to adopt a specific fate and do not get rapidly re-specified by environmental factors (Merkle et al., 2007). However, these experiments analysed how the diverse GABAergic lineages react to the changed environmental cues, but not how the newly discovered glutamatergic lineages would behave in a different environment. Therefore, this study does not exclude that the generation of glutamatergic neurons would depend on canonical Wnt signalling.

In this regard it is also worth noting, that my analysis did not show that loss of Tbr2 causes a reduction in the number of newly generated glutamatergic OB interneurons. This observation can be interpreted in two different ways. First, I only looked for the newborn neurons one week after I observed a reduction in Tbr2⁺ progenitor pool. As I don't know at which time point the number of Tbr2⁺ cells starts to be reduced in the β -catenin deficient brain, I clearly have not waited long enough to see an effect on the newly integrated neurons. Second, deletion of Tbr2 does not necessarily mean that the fate of the glutamatergic lineage would be changed at all. In order to discriminate these two possibilities, an analysis of newly generated vGlut2⁺ neurons at a later time point is needed.

In conclusion my data suggest an essential role of high canonical Wnt signalling activity in dorsal neural stem cells for the regulation of the T-box transcription factor2, which consequently may be crucial in the specification or maturation of glutamatergic interneurons. Furthermore my work emphasises, that neural stem cells in the developing and adult brain, besides the described similarities, display also major differences.

6 References

- Aaku-Saraste, E., A. Hellwig & W. B. Huttner, (1996) Loss of occludin and functional tight junctions, but not ZO-1, during neural tube closure--remodeling of the neuroepithelium prior to neurogenesis. *Dev Biol* **180**: 664-679.
- Abe, K., O. Chisaka, F. Van Roy & M. Takeichi, (2004) Stability of dendritic spines and synaptic contacts is controlled by alpha N-catenin. *Nat Neurosci* **7**: 357-363.
- Aberle, H., A. Bauer, J. Stappert, A. Kispert & R. Kemler, (1997) beta-catenin is a target for the ubiquitin-proteasome pathway. *EMBO J* **16**: 3797-3804.
- Aberle, H., S. Butz, J. Stappert, H. Weissig, R. Kemler & H. Hoschuetzky, (1994) Assembly of the cadherin-catenin complex in vitro with recombinant proteins. *J Cell Sci* **107 (Pt 12)**: 3655-3663.
- Abrous, D. N., M. Koehl & M. Le Moal, (2005) Adult neurogenesis: from precursors to network and physiology. *Physiol Rev* **85**: 523-569.
- Adachi, K., Z. Mirzadeh, M. Sakaguchi, T. Yamashita, T. Nikolcheva, Y. Gotoh, G. Peltz, L. Gong, T. Kawase, A. Alvarez-Buylla, H. Okano & K. Sawamoto, (2007) Beta-catenin signaling promotes proliferation of progenitor cells in the adult mouse subventricular zone. *Stem Cells* **25**: 2827-2836.
- Afonso, C. & D. Henrique, (2006) PAR3 acts as a molecular organizer to define the apical domain of chick neuroepithelial cells. *J Cell Sci* **119**: 4293-4304.
- Akimoto, K., K. Mizuno, S. Osada, S. Hirai, S. Tanuma, K. Suzuki & S. Ohno, (1994) A new member of the third class in the protein kinase C family, PKC lambda, expressed dominantly in an undifferentiated mouse embryonal carcinoma cell line and also in many tissues and cells. *J Biol Chem* **269**: 12677-12683.
- Allen, Z. J., 2nd, R. R. Waclaw, M. C. Colbert & K. Campbell, (2007) Molecular identity of olfactory bulb interneurons: transcriptional codes of periglomerular neuron subtypes. *J Mol Histol* **38**: 517-525.
- Alt, J. R., J. L. Cleveland, M. Hannink & J. A. Diehl, (2000) Phosphorylation-dependent regulation of cyclin D1 nuclear export and cyclin D1-dependent cellular transformation. *Genes Dev* **14**: 3102-3114.
- Altman, J., (1969) Autoradiographic and histological studies of postnatal neurogenesis. IV. Cell proliferation and migration in the anterior forebrain, with special reference to persisting neurogenesis in the olfactory bulb. *J Comp Neurol* **137**: 433-457.
- Altman, J. & G. D. Das, (1965) Autoradiographic and histological evidence of postnatal hippocampal neurogenesis in rats. *J Comp Neurol* **124**: 319-335.
- Alvarez-Buylla, A., J. M. Garcia-Verdugo & A. D. Tramontin, (2001) A unified hypothesis on the lineage of neural stem cells. *Nat Rev Neurosci* **2**: 287-293.
- Anderson, S., M. Mione, K. Yun & J. L. Rubenstein, (1999) Differential origins of neocortical projection and local circuit neurons: role of Dlx genes in neocortical interneuronogenesis. *Cereb Cortex* **9**: 646-654.
- Assemat, E., E. Bazellieres, E. Pallesi-Pocachard, A. Le Bivic & D. Massey-Harroche, (2008) Polarized complex proteins. *Biochim Biophys Acta* **1778**: 614-630.
- Astrom, K. E. & H. D. Webster, (1991) The early development of the neopallial wall and area choroidea in fetal rats. A light and electron microscopic study. *Adv Anat Embryol Cell Biol* **123**: 1-76.
- Attardo, A., F. Calegari, W. Haubensak, M. Wilsch-Brauninger & W. B. Huttner, (2008) Live imaging at the onset of cortical neurogenesis reveals differential appearance of the neuronal phenotype in apical versus basal progenitor progeny. *PLoS One* **3**: e2388.

- Backman, M., O. Machon, L. Mygland, C. J. van den Bout, W. Zhong, M. M. Taketo & S. Krauss, (2005) Effects of canonical Wnt signaling on dorso-ventral specification of the mouse telencephalon. *Dev Biol* **279**: 155-168.
- Batista-Brito, R., J. Close, R. Machold & G. Fishell, (2008) The distinct temporal origins of olfactory bulb interneuron subtypes. *J Neurosci* **28**: 3966-3975.
- Behrens, J., B. A. Jerchow, M. Wurtele, J. Grimm, C. Asbrand, R. Wirtz, M. Kuhl, D. Westlich & W. Birchmeier, (1998) Functional interaction of an axin in homolog, conductin, with beta-catenin, APC, and GSK3beta. *Science* **280**: 596-599.
- Bjorkoy, G., M. Perander, A. Overvatn & T. Johansen, (1997) Reversion of Ras- and phosphatidylcholine-hydrolyzing phospholipase C-mediated transformation of NIH 3T3 cells by a dominant interfering mutant of protein kinase C lambda is accompanied by the loss of constitutive nuclear mitogen-activated protein kinase/extracellular signal-regulated kinase activity. *J Biol Chem* **272**: 11557-11565.
- Bonfanti, L., S. Olive, D. A. Poulain & D. T. Theodosis, (1992) Mapping of the distribution of polysialylated neural cell adhesion molecule throughout the central nervous system of the adult rat: an immunohistochemical study. *Neuroscience* **49**: 419-436.
- Bose, R. & J. L. Wrana, (2006) Regulation of Par6 by extracellular signals. *Curr Opin Cell Biol* **18**: 206-212.
- Bovetti, S., Y. C. Hsieh, P. Bovolenta, I. Perroteau, T. Kazunori & A. C. Puche, (2007) Blood vessels form a scaffold for neuroblast migration in the adult olfactory bulb. *J Neurosci* **27**: 5976-5980.
- Braga, V. M., L. M. Machesky, A. Hall & N. A. Hotchin, (1997) The small GTPases Rho and Rac are required for the establishment of cadherin-dependent cell-cell contacts. *J Cell Biol* **137**: 1421-1431.
- Brault, V., R. Moore, S. Kutsch, M. Ishibashi, D. H. Rowitch, A. P. McMahon, L. Sommer, O. Boussadia & R. Kemler, (2001) Inactivation of the beta-catenin gene by Wnt1-Cre-mediated deletion results in dramatic brain malformation and failure of craniofacial development. *Development* **128**: 1253-1264.
- Breunig, J. J., M. R. Sarkisian, J. I. Arellano, Y. M. Morozov, A. E. Ayoub, S. Sojitra, B. Wang, R. A. Flavell, P. Rakic & T. Town, (2008) Primary cilia regulate hippocampal neurogenesis by mediating sonic hedgehog signaling. *Proc Natl Acad Sci U S A* **105**: 13127-13132.
- Brill, M. S., J. Ninkovic, E. Winpenny, R. D. Hodge, I. Ozen, R. Yang, A. Lepier, S. Gascon, F. Erdelyi, G. Szabo, C. Parras, F. Guillemot, M. Frotscher, B. Berninger, R. F. Hevner, O. Raineteau & M. Götz, (2009) Adult generation of glutamatergic olfactory bulb interneurons. *Nat Neurosci* **12**: 1524-1533.
- Brill, M. S., M. Snapyan, H. Wohlfrom, J. Ninkovic, M. Jawerka, G. S. Mastic, R. Ashery-Padan, A. Saghatelian, B. Berninger & M. Götz, (2008) A *dlx2*- and *pa6*-dependent transcriptional code for periglomerular neuron specification in the adult olfactory bulb. *J Neurosci* **28**: 6439-6452.
- Bulfone, A., F. Wang, R. Hevner, S. Anderson, T. Cutforth, S. Chen, J. Meneses, R. Pedersen, R. Axel & J. L. Rubenstein, (1998) An olfactory sensory map develops in the absence of normal projection neurons or GABAergic interneurons. *Neuron* **21**: 1273-1282.
- Bultje, R. S., D. R. Castaneda-Castellanos, L. Y. Jan, Y. N. Jan, A. R. Kriegstein & S. H. Shi, (2009) Mammalian Par3 regulates progenitor cell asymmetric division via notch signaling in the developing neocortex. *Neuron* **63**: 189-202.
- Cadigan, K. M. & R. Nusse, (1997) Wnt signaling: a common theme in animal development. *Genes Dev* **11**: 3286-3305.
- Campbell, K. & M. Götz, (2002) Radial glia: multi-purpose cells for vertebrate brain development. *Trends Neurosci* **25**: 235-238.

References

- Capela, A. & S. Temple, (2002) LeX/sse a-1 is expressed by adult mouse CNS stem cells, identifying them as nonependymal. *Neuron* **35**: 865-875.
- Cappello, S., A. Attardo, X. Wu, T. Iwasato, S. Itohara, M. Wilsch-Brauninger, H. M. Eilken, M. A. Rieger, T. T. Schroeder, W. B. Huttner, C. Brakebusch & M. Götz, (2006) The Rho-GTPase cdc42 regulates neural progenitor fate at the apical surface. *Nat Neurosci* **9**: 1099-1107.
- Carlen, M., R. M. Cassidy, H. Brismar, G. A. Smith, L. W. Enquist & J. Frisen, (2002) Functional integration of adult-born neurons. *Curr Biol* **12**: 606-608.
- Carlen, M., K. Meletis, C. Goritz, V. Darsalia, E. Evergren, K. Tanigaki, M. Amendola, F. Barnabe-Heider, M. S. Yeung, L. Naldini, T. Honjo, Z. Kokia, O. Shupliakov, R. M. Cassidy, O. Lindvall & J. Frisen, (2009) Forebrain ependymal cells are Notch-dependent and generate neuroblasts and astrocytes after stroke. *Nat Neurosci* **12**: 259-267.
- Casanova, M. F. & J. Trippie, 2nd, (2006) Regulatory mechanisms of cortical laminar development. *Brain Res Rev* **51**: 72-84.
- Casarosa, S., C. Fode & F. Guillemot, (1999) Mash1 regulates neurogenesis in the ventral telencephalon. *Development* **126**: 525-534.
- Castelo-Branco, G., N. Rawal & E. Arenas, (2004) GSK-3beta inhibition/beta-catenin stabilization in ventral midbrain precursors increases differentiation into dopamine neurons. *J Cell Sci* **117**: 5731-5737.
- Cathcart, R. S., 3rd & W. C. Worthington, Jr., (1964) Ciliary Movement in the Rat Cerebral Ventricles: Clearing Action and Directions of Currents. *J Neuropathol Exp Neurol* **23**: 609-618.
- Cau, E., S. Casarosa & F. Guillemot, (2002) Mash1 and Ngn1 control distinct steps of determination and differentiation in the olfactory sensory neuron lineage. *Development* **129**: 1871-1880.
- Chenn, A., (2008) Wnt/beta-catenin signaling in cerebral cortical development. *Organogenesis* **4**: 76-80.
- Chenn, A. & C. A. Walsh, (2002) Regulation of cerebral cortical size by control of cell cycle exit in neural precursors. *Science* **297**: 365-369.
- Chenn, A. & C. A. Walsh, (2003) Increased neuronal production, enlarged forebrains and cytoarchitectural distortions in beta-catenin overexpressing transgenic mice. *Cereb Cortex* **13**: 599-606.
- Chiasson, B. J., V. Tropepe, C. M. Morshead & D. van der Kooy, (1999) Adult mammalian forebrain ependymal and subependymal cells demonstrate proliferative potential, but only subependymal cells have neural stem cell characteristics. *J Neurosci* **19**: 4462-4471.
- Colak, D., T. Mori, M. S. Brill, A. Pfeifer, S. Falk, C. Deng, R. Monteiro, C. Mummery, L. Sommer & M. Götz, (2008) Adult neurogenesis requires Smad4-mediated bone morphogenetic protein signaling in stem cells. *J Neurosci* **28**: 434-446.
- Coles-Takabe, B. L., I. Brai n, K. A. Purpura, P. Kaprowicz, P. W. Zandstra, C. M. Morshead & D. van der Kooy, (2008) Don't look: growing clonal versus nonclonal neural stem cell colonies. *Stem Cells* **26**: 2938-2944.
- Corbin, J. G., N. Gaiano, R. P. Machold, A. Langston & G. Fishell, (2000) The Gsh2 homeodomain gene controls multiple aspects of telencephalic development. *Development* **127**: 5007-5020.
- Corbit, K. C., P. Aanstad, V. Singla, A. R. Norman, D. Y. Stainier & J. F. Rieper, (2005) Vertebrate Smoothed functions at the primary cilium. *Nature* **437**: 1018-1021.
- Coskun, V. & M. B. Luskin, (2002) Intrinsic and extrinsic regulation of the proliferation and differentiation of cells in the rodent rostral migratory stream. *J Neurosci Res* **69**: 795-802.
- Costa, M. R., G. Wen, A. Lepier, T. Schroeder & M. Götz, (2008) Par-complex proteins promote proliferative progenitor divisions in the developing mouse cerebral cortex. *Development* **135**: 11-22.

- Dann, C. E., J. C. Hsieh, A. Rattner, D. Sharma, J. Nathans & D. J. Leahy, (2001) Insights into Wnt binding and signalling from the structures of two Frizzled cysteine-rich domains. *Nature* **412**: 86-90.
- DasGupta, R. & E. Fuchs, (1999) Multiple roles for activated LEF/TCF transcription complexes during hair follicle development and differentiation. *Development* **126**: 4557-4568.
- De Carlos, J. A., L. Lopez-Mascaraque & F. Valverde, (1995) The telencephalic vesicles are innervated by olfactory placode-derived cells: a possible mechanism to induce neocortical development. *Neuroscience* **68**: 1167-1178.
- Diehl, J. A., M. Cheng, M. F. Roussel & C. J. Sherr, (1998) Glycogen synthase kinase-3beta regulates cyclin D1 proteolysis and subcellular localization. *Genes Dev* **12**: 3499-3511.
- Ding, V. W., R. H. Chen & F. McCormick, (2000) Differential regulation of glycogen synthase kinase 3beta by insulin and Wnt signaling. *J Biol Chem* **275**: 32475-32481.
- Doetsch, F., I. Caille, D. A. Lim, J. M. Garcia-Verdugo & A. Alvarez-Buylla, (1999a) Subventricular zone astrocytes are neural stem cells in the adult mammalian brain. *Cell* **97**: 703-716.
- Doetsch, F., J. M. Garcia-Verdugo & A. Alvarez-Buylla, (1997) Cellular composition and three-dimensional organization of the subventricular germinal zone in the adult mammalian brain. *J Neurosci* **17**: 5046-5061.
- Doetsch, F., J. M. Garcia-Verdugo & A. Alvarez-Buylla, (1999b) Regeneration of a germinal layer in the adult mammalian brain. *Proc Natl Acad Sci U S A* **96**: 11619-11624.
- Doetsch, F., L. Petreanu, I. Caille, J. M. Garcia-Verdugo & A. Alvarez-Buylla, (2002) EGF converts transit-amplifying neurogenic precursors in the adult brain into multipotent stem cells. *Neuron* **36**: 1021-1034.
- Drees, F., S. Pokutta, S. Yamada, W. J. Nelson & W. I. Weis, (2005) Alpha-catenin is a molecular switch that binds E-cadherin-beta-catenin and regulates actin-filament assembly. *Cell* **123**: 903-915.
- Dubreuil, V., A. M. Marzocco, D. Corbeil, W. B. Huttner & M. Wilsch-Brauninger, (2007) Midbody and primary cilium of neural progenitors release extracellular membrane particles enriched in the stem cell marker prominin-1. *J Cell Biol* **176**: 483-495.
- Eggenschwiler, J. T. & K. V. Anderson, (2007) Cilia and developmental signaling. *Annu Rev Cell Dev Biol* **23**: 345-373.
- Embi, N., D. B. Rylatt & P. Cohen, (1980) Glycogen synthase kinase-3 from rabbit skeletal muscle. Separation from cyclic-AMP-dependent protein kinase and phosphorylase kinase. *Eur J Biochem* **107**: 519-527.
- Englund, C., A. Fink, C. Lau, D. Pham, R. A. Daza, A. Bulfone, T. Kowalczyk & R. F. Hevner, (2005) Pax6, Tbr2, and Tbr1 are expressed sequentially by radial glia, intermediate progenitor cells, and postmitotic neurons in developing neocortex. *J Neurosci* **25**: 247-251.
- Etienne-Manneville, S. & A. Hall, (2003) Cell polarity: Par6, aPKC and cytoskeletal crosstalk. *Curr Opin Cell Biol* **15**: 67-72.
- Evangelista, M., H. Tian & F. J. de Sauvage, (2006) The hedgehog signaling pathway in cancer. *Clin Cancer Res* **12**: 5924-5928.
- Fainsod, A., K. Deissler, R. Yelin, K. Marom, M. Epstein, G. Pillemer, H. Steinbeisser & M. Blum, (1997) The dorsalizing and neural inducing gene follistatin is an antagonist of BMP-4. *Mech Dev* **63**: 39-50.
- Fan, S., T. W. Hurd, C. J. Liu, S. W. Straight, T. Weimbs, E. A. Hurd, S. E. Domino & B. Margolis, (2004) Polarity proteins control ciliogenesis via kinesin motor interactions. *Curr Biol* **14**: 1451-1461.
- Fields, A. P., L. A. Frederick & R. P. Regala, (2007) Targeting the oncogenic protein kinase C-1alpha signalling pathway for the treatment of cancer. *Biochem Soc Trans* **35**: 996-1000.

References

- Filippov, V., G. Kronenberg, T. Pivneva, K. Reuter, B. Steiner, L. P. Wang, M. Yamaguchi, H. Kettenmann & G. Kempermann, (2003) Subpopulation of nestin-expressing progenitor cells in the adult murine hippocampus shows electrophysiological and morphological characteristics of astrocytes. *Mol Cell Neurosci* **23**: 373-382.
- Fish, J. L., C. Dehay, H. Kennedy & W. B. Huttner, (2008) Making bigger brains-the evolution of neural-progenitor-cell division. *J Cell Sci* **121**: 2783-2793.
- Fode, C., Q. Ma, S. Casarosa, S. L. Ang, D. J. Anderson & F. Guillemot, (2000) A role for neural determination genes in specifying the dorsoventral identity of telencephalic neurons. *Genes Dev* **14**: 67-80.
- Forni, P. E., C. Scuoppo, I. Imayoshi, R. Taulli, W. Dastru, V. Sala, U. A. Betz, P. Muzzi, D. Martinuzzi, A. E. Vercelli, R. Kageyama & C. Ponzetto, (2006) High levels of Cre expression in neuronal progenitors cause defects in brain development leading to microencephaly and hydrocephaly. *J Neurosci* **26**: 9593-9602.
- Frame, S. & P. Cohen, (2001) GSK3 takes centre stage more than 20 years after its discovery. *Biochem J* **359**: 1-16.
- Francis, F., A. Koulakoff, D. Boucher, P. Chafey, B. Schaar, M. C. Vinet, G. Friocourt, N. McDonnell, O. Reiner, A. Kahn, S. K. McConnell, Y. Berwald-Netter, P. Denoulet & J. Chelly, (1999) Doublecortin is a developmentally regulated, microtubule-associated protein expressed in migrating and differentiating neurons. *Neuron* **23**: 247-256.
- Franke, W. W., S. Rickelt, M. Barth & S. Pieperhoff, (2009) The junctions that don't fit the scheme: special symmetrical cell-cell junctions of their own kind. *Cell Tissue Res* **338**: 1-17.
- Fukuda, S., F. Kato, Y. Tozuka, M. Yamaguchi, Y. Miyamoto & T. Hisatsune, (2003) Two distinct subpopulations of nestin-positive cells in adult mouse dentate gyrus. *J Neurosci* **23**: 9357-9366.
- Funatsu, N., T. Inoue & S. Nakamura, (2004) Gene expression analysis of the late embryonic mouse cerebral cortex using DNA microarray: identification of several region- and layer-specific genes. *Cereb Cortex* **14**: 1031-1044.
- Gaiano, N. & G. Fishell, (2002) The role of notch in promoting glial and neural stem cell fates. *Annu Rev Neurosci* **25**: 471-490.
- Galceran, J., E. M. Miyashita-Lin, E. Devaney, J. L. Rubenstein & R. Grosschedl, (2000) Hippocampus development and generation of dentate gyrus granule cells is regulated by LEF1. *Development* **127**: 469-482.
- Gao, L., G. Joberty & I. G. Macara, (2002) Assembly of epithelial tight junctions is negatively regulated by Par6. *Curr Biol* **12**: 221-225.
- Gao, Z., K. Ure, J. L. Aboody, D. C. Lagace, K. A. Nave, S. Goebbels, A. J. Eisch & J. Hsieh, (2009) Neurod1 is essential for the survival and maturation of adult-born neurons. *Nat Neurosci* **12**: 1090-1092.
- Garrod, D. & M. Chidgey, (2008) Desmosome structure, composition and function. *Biochim Biophys Acta* **1778**: 572-587.
- Georgiou, M., E. Marinari, J. Burden & B. Baum, (2008) Cdc42, Par6, and aPKC regulate Arp2/3-mediated endocytosis to control local adherens junction stability. *Curr Biol* **18**: 1631-1638.
- Gerdes, J. M. & N. Katsanis, (2008) Ciliary function and Wnt signal modulation. *Curr Top Dev Biol* **85**: 175-195.
- Gheusi, G. & P. M. Lledo, (2007) Control of early events in olfactory processing by adult neurogenesis. *Chem Senses* **32**: 397-409.
- Giannini, A. L., M. Vivanco & R. M. Kypta, (2000) alpha-catenin inhibits beta-catenin signaling by preventing formation of a beta-catenin/T-cell factor-DNA complex. *J Biol Chem* **275**: 21883-21888.

- Gorski, J. A., T. Talley, M. Qiu, L. Puelles, J. L. Rubenstein & K. R. Jones, (2002) Cortical excitatory neurons and glia, but not GABAergic neurons, are produced in the Emx1-expressing lineage. *J Neurosci* **22**: 6309-6314.
- Götz, M. & W. B. Huttner, (2005) The cell biology of neurogenesis. *Nat Rev Mol Cell Biol* **6**: 777-788.
- Götz, M., A. Wizenmann, S. Reinhardt, A. Lumsden & J. Price, (1996) Selective adhesion of cells from different telencephalic regions. *Neuron* **16**: 551-564.
- Grove, E. A., S. Tole, J. Limon, L. Yip & C. W. Ragsdale, (1998) The hem of the embryonic cerebral cortex is defined by the expression of multiple Wnt genes and is compromised in Gli3-deficient mice. *Development* **125**: 2315-2325.
- Guillemot, F., L. C. Lo, J. E. Johnson, A. Auerbach, D. J. Anderson & A. L. Joyner, (1993) Mammalian achaete-scute homolog 1 is required for the early development of olfactory and autonomic neurons. *Cell* **75**: 463-476.
- Hack, I., M. Bancila, K. Loulier, P. Carroll & H. Cremer, (2002) Reelin is a detachment signal in tangential chain-migration during postnatal neurogenesis. *Nat Neurosci* **5**: 939-945.
- Hack, M. A., A. Saghatelian, A. de Chevigny, A. Pfeifer, R. Ashery-Padan, P. M. Lledo & M. Götz, (2005) Neuronal fate determinants of adult olfactory bulb neurogenesis. *Nat Neurosci* **8**: 865-872.
- Haegel, H., L. Larue, M. Ohsugi, L. Fedorov, K. Herrenknecht & R. Kemler, (1995) Lack of beta-catenin affects mouse development at gastrulation. *Development* **121**: 3529-3537.
- Halbleib, J. M. & W. J. Nelson, (2006) Cadherins in development: cell adhesion, sorting, and tissue morphogenesis. *Genes Dev* **20**: 3199-3214.
- Han, Y. G., N. Spassky, M. Romaguera-Ros, J. M. Garcia-Verdugo, A. Aguilar, S. Schneider-Maunoury & A. Alvarez-Buylla, (2008) Hedgehog signaling and primary cilia are required for the formation of adult neural stem cells. *Nat Neurosci* **11**: 277-284.
- Hari, L., V. Brault, M. Kleber, H. Y. Lee, F. Ille, R. Leimeroth, C. Paratore, U. Suter, R. Kemler & L. Sommer, (2002) Lineage-specific requirements of beta-catenin in neural crest development. *J Cell Biol* **159**: 867-880.
- Harris, K. P. & U. Tepass, (2008) Cdc42 and Par proteins stabilize dynamic adherens junctions in the Drosophila neuroectoderm through regulation of apical endocytosis. *J Cell Biol* **183**: 1129-1143.
- Harris, T. J. & M. Peifer, (2004) Adherens junction-dependent and -independent steps in the establishment of epithelial cell polarity in Drosophila. *J Cell Biol* **167**: 135-147.
- Hartfuss, E., R. Galli, N. Heins & M. Götz, (2001) Characterization of CNS precursor subtypes and radial glia. *Dev Biol* **229**: 15-30.
- Haubensak, W., A. Attardo, W. Denk & W. B. Huttner, (2004) Neurons arise in the basal neuroepithelium of the early mammalian telencephalon: a major site of neurogenesis. *Proc Natl Acad Sci U S A* **101**: 3196-3201.
- He, X., M. Semenov, K. Tamai & X. Zeng, (2004) LDL receptor-related proteins 5 and 6 in Wnt/beta-catenin signaling: arrows point the way. *Development* **131**: 1663-1677.
- Henrique, D. & F. Schweisguth, (2003) Cell polarity: the ups and downs of the Par6/aPKC complex. *Curr Opin Genet Dev* **13**: 341-350.
- Hevner, R. F., R. D. Hodge, R. A. Daza & C. E. Ngund, (2006) Transcription factors in glutamatergic neurogenesis: conserved programs in neocortex, cerebellum, and adult hippocampus. *Neurosci Res* **55**: 223-233.

References

- Hirabayashi, Y., Y. Itoh, H. Tabata, K. Nakajima, T. Akiyama, N. Masuyama & Y. Gotoh, (2004) The Wnt/beta-catenin pathway directs neuronal differentiation of cortical neural precursor cells. *Development* **131**: 2791-2801.
- Hirano, S., N. Kimoto, Y. Shimoyama, S. Hirohashi & M. Takeichi, (1992) Identification of a neural alpha-catenin as a key regulator of cadherin function and multicellular organization. *Cell* **70**: 293-301.
- Hirano, Y., S. Yoshinaga, K. Ogura, M. Yokochi, Y. Noda, H. Sumimoto & F. Inagaki, (2004) Solution structure of atypical protein kinase C PB1 domain and its mode of interaction with ZIP/p62 and MEK5. *J Biol Chem* **279**: 31883-31890.
- Hirose, T., Y. Izumi, Y. Nagashima, Y. Tamai-Nagai, H. Kurihara, T. Sakai, Y. Suzuki, T. Yamamoto, A. Suzuki, K. Mizuno & S. Ohno, (2002) Involvement of ASIP/PAR-3 in the promotion of epithelial tight junction formation. *J Cell Sci* **115**: 2485-2495.
- Hirsch, C., L. M. Campano, S. Wöhrle & A. Hecht, (2007) Canonical Wnt signaling transiently stimulates proliferation and enhances neurogenesis in neonatal neural progenitor cultures. *Exp Cell Res* **313**: 572-587.
- Hordijk, P. L., J. P. ten Klooster, R. A. van der Kammen, F. Michiels, L. C. Oomen & J. G. Collard, (1997) Inhibition of invasion of epithelial cells by Tiam1-Rac signaling. *Science* **278**: 1464-1466.
- Huangfu, D. & K. V. Anderson, (2005) Cilia and Hedgehog responsiveness in the mouse. *Proc Natl Acad Sci U S A* **102**: 11325-11330.
- Huangfu, D., A. Liu, A. S. Rakeman, N. S. Murcia, L. Niswander & K. V. Anderson, (2003) Hedgehog signalling in the mouse requires intraflagellar transport proteins. *Nature* **426**: 83-87.
- Huelsken, J., R. Vogel, V. Brinkmann, B. Erdmann, C. Birchmeier & W. Birchmeier, (2000) Requirement for beta-catenin in anterior-posterior axis formation in mice. *J Cell Biol* **148**: 567-578.
- Hwang, S. G., S. S. Yu, J. H. Ryu, H. B. Jeon, Y. J. Yoo, S. H. Eom & J. S. Chun, (2005) Regulation of beta-catenin signaling and maintenance of chondrocyte differentiation by ubiquitin-independent proteasomal degradation of alpha-catenin. *J Biol Chem* **280**: 12758-12765.
- Ikeya, M., S. M. Lee, J. E. Johnson, A. P. McMahon & S. Takada, (1997) Wnt signalling required for expansion of neural crest and CNS progenitors. *Nature* **389**: 966-970.
- Imai, F., S. Hirai, K. Akimoto, H. Koyama, T. Miyata, M. Ogawa, S. Noguchi, T. Sasaoka, T. Noda & S. Ohno, (2006) Inactivation of α PKC λ results in the loss of adherens junctions in neuroepithelial cells without affecting neurogenesis in mouse neocortex. *Development* **133**: 1735-1744.
- Imamura, Y., M. Itoh, Y. Maeno, S. Tsukita & A. Nagafuchi, (1999) Functional domains of alpha-catenin required for the strong state of cadherin-based cell adhesion. *J Cell Biol* **144**: 1311-1322.
- Israsena, N., M. Hu, W. Fu, L. Kan & J. A. Kessler, (2004) The presence of FGF2 signaling determines whether beta-catenin exerts effects on proliferation or neuronal differentiation of neural stem cells. *Dev Biol* **268**: 220-231.
- Itoh, M., A. Nagafuchi, S. Yonemura, T. Kitani-Yasuda & S. Tsukita, (1993) The 220-kD protein colocalizing with cadherins in non-epithelial cells is identical to ZO-1, a tight junction-associated protein in epithelial cells: cDNA cloning and immunoelectron microscopy. *J Cell Biol* **121**: 491-502.
- Iwasato, T., R. Nomura, R. Ando, T. Ikeda, M. Tanaka & S. Itohara, (2004) Dorsal telencephalon-specific expression of Cre recombinase in PAC transgenic mice. *Genesis* **38**: 130-138.
- Jankovski, A. & C. Sotelo, (1996) Subventricular zone-olfactory bulb migratory pathway in the adult mouse: cellular composition and specificity as determined by heterochronic and heterotopic transplantation. *J Comp Neurol* **371**: 376-396.
- Jessberger, S., G. D. Clementson, Jr. & F. H. Gage, (2007) Spontaneous fusion and nonclonal growth of adult neural stem cells. *Stem Cells* **25**: 871-874.

- Joberty, G., C. Petersen, L. Gao & I. G. Macara, (2000) The cell-polarity protein Par6 links Par3 and atypical protein kinase C to Cdc42. *Nat Cell Biol* **2**: 531-539.
- Johansson, C. B., S. Momma, D. L. Clarke, M. Risling, U. Lendahl & J. Frisen, (1999) Identification of a neural stem cell in the adult mammalian central nervous system. *Cell* **96**: 25-34.
- Junghans, D., I. Hack, M. Frotscher, V. Taylor & R. Kemler, (2005) Beta-catenin-mediated cell-adhesion is vital for embryonic forebrain development. *Dev Dyn* **233**: 528-539.
- Kadowaki, M., S. Nakamura, O. Machon, S. Krauss, G. L. Radice & M. Takeichi, (2007) N-cadherin mediates cortical organization in the mouse brain. *Dev Biol* **304**: 22-33.
- Kampfer, S., M. Windegger, F. Hochholdinger, W. Schwaiger, R. G. Pestell, G. Baier, H. H. Grunicke & F. Uberall, (2001) Protein kinase C isoforms involved in the transcriptional activation of cyclin D1 by transforming Ha-Ras. *J Biol Chem* **276**: 42834-42842.
- Kaplan, M. S. & D. H. Bell, (1984) Mitotic neuroblasts in the 9-day-old and 11-month-old rodent hippocampus. *J Neurosci* **4**: 1429-1441.
- Kawano, Y. & R. Kypta, (2003) Secreted antagonists of the Wnt signaling pathway. *J Cell Sci* **116**: 2627-2634.
- Kempermann, G., L. Wiskott & F. H. Gage, (2004) Functional significance of adult neurogenesis. *Curr Opin Neurobiol* **14**: 186-191.
- Kim, A. S., D. H. Lowenstein & S. J. Pleasure, (2001) Wnt receptors and Wnt inhibitors are expressed in gradients in the developing telencephalon. *Mech Dev* **103**: 167-172.
- Kim, W. Y., X. Wang, Y. Wu, B. W. Doble, S. Patel, J. R. Woodgett & W. D. Snider, (2009) GSK-3 is a master regulator of neural progenitor homeostasis. *Nat Neurosci* **12**: 1390-1397.
- Kishi, K., (1987) Golgi studies on the development of granule cells of the rat olfactory bulb with reference to migration in the subependymal layer. *J Comp Neurol* **258**: 112-124.
- Knoblich, J. A., (2008) Mechanisms of asymmetric stem cell division. *Cell* **132**: 583-597.
- Kobielak, A. & E. Fuchs, (2006) Links between alpha-catenin, NF-kappaB, and squamous cell carcinoma in skin. *Proc Natl Acad Sci U S A* **103**: 2322-2327.
- Kohwi, M., M. A. Petryniak, J. E. Long, M. Ekker, K. Obata, Y. Yanagawa, J. L. Rubenstein & A. Alvarez-Buylla, (2007) A subpopulation of olfactory bulb GABAergic interneurons is derived from Emx1- and Dlx5/6-expressing progenitors. *J Neurosci* **27**: 6878-6891.
- Konno, D., G. Shioi, A. Shitamukai, A. Mori, H. Kiyonari, T. Miyata & F. Matsuzaki, (2008) Neuroepithelial progenitors undergo LGN-dependent planar divisions to maintain self-renewal ability during mammalian neurogenesis. *Nat Cell Biol* **10**: 93-101.
- Kosaka, K., Y. Aika, K. Toida, C. W. Heizmann, W. Hunziker, D. M. Jacobowitz, I. Nagatsu, P. Streit, T. J. Visser & T. Kosaka, (1995) Chemically defined neuron groups and their subpopulations in the glomerular layer of the rat main olfactory bulb. *Neurosci Res* **23**: 73-88.
- Kosodo, Y. & W. B. Huttner, (2009) Basal process and cell divisions of neural progenitors in the developing brain. *Dev Growth Differ* **51**: 251-261.
- Kosodo, Y., K. Roper, W. Haubensack, A. M. Marzese, D. Corbeil & W. B. Huttner, (2004) Asymmetric distribution of the apical plasma membrane during neurogenic divisions of mammalian neuroepithelial cells. *EMBO J* **23**: 2314-2324.
- Kriegstein, A. & A. Alvarez-Buylla, (2009) The glial nature of embryonic and adult neural stem cells. *Annu Rev Neurosci* **32**: 149-184.

References

- Kroll, T. T. & D. D. O'Leary, (2005) Ventralized dorsal telencephalic progenitors in Pax6 mutant mice generate GABA interneurons of a lateral ganglionic eminence fate. *Proc Natl Acad Sci U S A* **102**: 7374-7379.
- Kuhl, M., L. C. She Idahl, M. Park, J. R. Miller & R. T. Moon, (2000) The Wnt1/Ca²⁺ pathway: a new vertebrate Wnt signaling pathway takes shape. *Trends Genet* **16**: 279-283.
- Kuroda, S., M. Fukata, K. Fujii, T. Nakamura, I. Izawa & K. Kaibuchi, (1997) Regulation of cell-cell adhesion of MDCK cells by Cdc42 and Rac1 small GTPases. *Biochem Biophys Res Commun* **240**: 430-435.
- Kuwabara, T., J. Hsieh, A. Muotri, G. Yeo, M. Warashina, D. C. Lie, L. Moore, K. Nakashima, M. Asashima & F. H. Gage, (2009) Wnt-mediated activation of NeuroD1 and retro-elements during adult neurogenesis. *Nat Neurosci* **12**: 1097-1105.
- Lamb, T. M., A. K. Knecht, W. C. Smith, S. E. Stachel, A. N. Economides, N. Stahl, G. D. Yancopoulos & R. M. Harland, (1993) Neural induction by the secreted polypeptide noggin. *Science* **262**: 713-718.
- Laywell, E. D., P. Rakic, V. G. Kulkarni, E. C. Holland & D. A. Steindler, (2000) Identification of a multipotent astrocytic stem cell in the immature and adult mouse brain. *Proc Natl Acad Sci U S A* **97**: 13883-13888.
- Lee, S. M., S. Tole, E. Grove & A. P. McMahon, (2000) A local Wnt-3a signal is required for development of the mammalian hippocampus. *Development* **127**: 457-467.
- Levison, S. W., C. Chuang, B. J. Abramson & J. E. Goldman, (1993) The migrational patterns and developmental fates of glial precursors in the rat subventricular zone are temporally regulated. *Development* **119**: 611-622.
- Levison, S. W. & J. E. Goldman, (1993) Both oligodendrocytes and astrocytes develop from progenitors in the subventricular zone of postnatal rat forebrain. *Neuron* **10**: 201-212.
- Lewis, J. E., J. K. Wahl, 3rd, K. M. Sass, P. J. Jensen, K. R. Johnson & M. J. Wheelock, (1997) Cross-talk between adherens junctions and desmosomes depends on plakoglobin. *J Cell Biol* **136**: 919-934.
- Li, L., H. Yuan, C. D. Weaver, J. Mao, G. H. Farr, 3rd, D. J. Sussman, J. Jonkers, D. Kimelman & D. Wu, (1999) Axin and Frat1 interact with Dvl and GSK, bridging Dvl to GSK in Wnt-mediated regulation of LEF-1. *EMBO J* **18**: 4233-4240.
- Lie, D. C., S. A. Colamarino, H. J. Song, L. DeSire, H. Mira, A. Consiglio, E. S. Lein, S. Jessberger, H. Lansford, A. R. Dearie & F. H. Gage, (2005) Wnt signalling regulates adult hippocampal neurogenesis. *Nature* **437**: 1370-1375.
- Lien, W. H., O. Klezovitch, T. E. Fernandez, J. Delrow & V. Vasioukhin, (2006) alphaE-catenin controls cerebral cortical size by regulating the hedgehog signaling pathway. *Science* **311**: 1609-1612.
- Lien, W. H., O. Klezovitch, M. Null & V. Vasioukhin, (2008) alphaE-catenin is not a significant regulator of beta-catenin signaling in the developing mammalian brain. *J Cell Sci* **121**: 1357-1362.
- Lin, D., A. S. Edwards, J. P. Fawcett, G. Mbamalu, J. D. Scott & T. Pawson, (2000) A mammalian PAR-3-PAR-6 complex implicated in Cdc42/Rac1 and aPKC signalling and cell polarity. *Nat Cell Biol* **2**: 540-547.
- Liu, A., B. Wang & L. A. Niswander, (2005) Mouse intraflagellar transport proteins regulate both the activator and repressor functions of Gli transcription factors. *Development* **132**: 3103-3111.
- Liu, Z., K. Tanabe, E. Bernal-Mizrachi & M. A. Permutt, (2008) Mice with beta cell overexpression of glycogen synthase kinase-3beta have reduced beta cell mass and proliferation. *Diabetologia* **51**: 623-631.
- Lledo, P. M., F. T. Merkle & A. Alvarez-Buylla, (2008) Origin and function of olfactory bulb interneuron diversity. *Trends Neurosci* **31**: 392-400.

- Logan, C. Y. & R. Nusse, (2004) The Wnt signaling pathway in development and disease. *Annu Rev Cell Dev Biol* **20**: 781-810.
- Lois, C. & A. Alvarez-Buylla, (1993) Proliferating subventricular zone cells in the adult mammalian forebrain can differentiate into neurons and glia. *Proc Natl Acad Sci U S A* **90**: 2074-2077.
- Lois, C. & A. Alvarez-Buylla, (1994) Long-distance neuronal migration in the adult mammalian brain. *Science* **264**: 1145-1148.
- Lois, C., J. M. Garcia-Verdugo & A. Alvarez-Buylla, (1996) Chain migration of neuronal precursors. *Science* **271**: 978-981.
- Lopez-Mascaraque, L., J. A. De Carlos & F. Valverde, (1996) Early onset of the rat olfactory bulb projections. *Neuroscience* **70**: 255-266.
- Lopez-Mascaraque, L. & F. de Castro, (2002) The olfactory bulb as an independent developmental domain. *Cell Death Differ* **9**: 1279-1286.
- Louis, S. A., R. L. Rietze, L. Deleyrolle, R. E. Wagey, T. E. Thomas, A. C. Eaves & B. A. Reynolds, (2008) Enumeration of neural stem and progenitor cells in the neural colony-forming cell assay. *Stem Cells* **26**: 988-996.
- Lu, Y., L. Jamieson, A. R. Brasier & A. P. Fields, (2001) NF-kappaB/RelA transactivation is required for atypical protein kinase C iota-mediated cell survival. *Oncogene* **20**: 4777-4792.
- Luskin, M. B., (1993) Restricted proliferation and migration of postnatally generated neurons derived from the forebrain subventricular zone. *Neuron* **11**: 173-189.
- Luskin, M. B. & K. McDermott, (1994) Divergent lineages for oligodendrocytes and astrocytes originating in the neonatal forebrain subventricular zone. *Glia* **11**: 211-226.
- Lyu, J., V. Yamamoto & W. Lu, (2008) Cleavage of the Wnt receptor Ryk regulates neuronal differentiation during cortical neurogenesis. *Dev Cell* **15**: 773-780.
- Machon, O., M. Backman, O. Machonova, Z. Kozmik, T. Vacik, L. Andersen & S. Krauss, (2007) A dynamic gradient of Wnt signaling controls initiation of neurogenesis in the mammalian cortex and cellular specification in the hippocampus. *Dev Biol* **311**: 223-237.
- Machon, O., C. J. van den Bout, M. Backman, R. Kemler & S. Krauss, (2003) Role of beta-catenin in the developing cortical and hippocampal neuroepithelium. *Neuroscience* **122**: 129-143.
- Malatesta, P., M. A. Hack, E. Hartfuss, H. Kettenmann, W. Klinkert, F. Kirchhoff & M. Götz, (2003) Neuronal or glial progeny: regional differences in radial glia fate. *Neuron* **37**: 751-764.
- Manabe, N., S. Hirai, F. Imai, H. Nakanishi, Y. Takai & S. Ohno, (2002) Association of ASIP/mPAR-3 with adherens junctions of mouse neuroepithelial cells. *Dev Dyn* **225**: 61-69.
- Maretto, S., M. Cordenonsi, S. Dupont, P. Braghetta, V. Broccoli, A. B. Hassan, D. Volpin, G. M. Bressan & S. Piccolo, (2003) Mapping Wnt/beta-catenin signaling during mouse development and in colorectal tumors. *Proc Natl Acad Sci U S A* **100**: 3299-3304.
- Marin, O. & J. L. Rubenstein, (2001) A long, remarkable journey: tangential migration in the telencephalon. *Nat Rev Neurosci* **2**: 780-790.
- Marshall, C. A., B. G. Novitsch & J. E. Goldman, (2005) Olig2 directs astrocyte and oligodendrocyte formation in postnatal subventricular zone cells. *J Neurosci* **25**: 7289-7298.
- Marthiens, V. & C. French-Constant, (2009) Adherens junction domains are split by asymmetric division of embryonic neural stem cells. *EMBO Rep* **10**: 515-520.

References

- Marzesco, A. M., P. Janich, M. Wilsch-Brauninger, V. Dubreuil, K. Langenfeld, D. Corbeil & W. B. Huttner, (2005) Release of extracellular membrane particles carrying the stem cell marker prominin-1 (CD133) from neural progenitors and other epithelial cells. *J Cell Sci* **118**: 2849-2858.
- Mason, H. A., S. Ito & G. Corfas, (2001) Extracellular signals that regulate the tangential migration of olfactory bulb neuronal precursors: inducers, inhibitors, and repellents. *J Neurosci* **21**: 7654-7663.
- Matsunami, H. & M. Takeichi, (1995) Fetal brain subdivisions defined by R- and E-cadherin expressions: evidence for the role of cadherin activity in region-specific, cell-cell adhesion. *Dev Biol* **172**: 466-478.
- Maurer, M. H., R. E. Feldmann, Jr., J. O. Bromberg & A. Klenke, (2005) Comparison of statistical approaches for the analysis of proteome expression data of differentiating neural stem cells. *J Proteome Res* **4**: 96-100.
- McCaffrey, L. M. & I. G. Macara, (2009) The Par3/aPKC interaction is essential for end bud remodeling and progenitor differentiation during mammary gland morphogenesis. *Genes Dev* **23**: 1450-1460.
- McManus, E. J., K. Sakamoto, L. J. Armit, L. Ronaldson, N. Shpiro, R. Marquez & D. R. Alessi, (2005) Role that phosphorylation of GSK3 plays in insulin and Wnt signalling defined by knockin analysis. *EMBO J* **24**: 1571-1583.
- Meletis, K., F. Barnabe-Heider, M. Carlen, E. Evergren, N. Tomilin, O. Shupliakov & J. Frisen, (2008) Spinal cord injury reveals multilineage differentiation of ependymal cells. *PLoS Biol* **6**: e182.
- Melton, K. R., A. Iulianella & P. A. Trainor, (2004) Gene expression and regulation of hindbrain and spinal cord development. *Front Biosci* **9**: 117-138.
- Menn, B., J. M. Garcia-Verdugo, C. Yaschine, O. Gonzalez-Perez, D. Rowitch & A. Alvarez-Buylla, (2006) Origin of oligodendrocytes in the subventricular zone of the adult brain. *J Neurosci* **26**: 7907-7918.
- Merdek, K. D., N. T. Nguyen & D. Toksoz, (2004) Distinct activities of the alpha-catenin family, alpha-catenin and alpha-catenin, on beta-catenin-mediated signaling. *Mol Cell Biol* **24**: 2410-2422.
- Merkle, F. T., Z. Mirzadeh & A. Alvarez-Buylla, (2007) Mosaic organization of neural stem cells in the adult brain. *Science* **317**: 381-384.
- Merkle, F. T., A. D. Tramontin, J. M. Garcia-Verdugo & A. Alvarez-Buylla, (2004) Radial glia give rise to adult neural stem cells in the subventricular zone. *Proc Natl Acad Sci U S A* **101**: 17528-17532.
- Mignone, J. L., V. Kukekov, A. S. Chiang, D. Steindler & G. Enikolopov, (2004) Neural stem and progenitor cells in nestin-GFP transgenic mice. *J Comp Neurol* **469**: 311-324.
- Miravet, S., J. Piedra, J. Castano, I. Raurell, C. Franci, M. Dunach & A. Garcia de Herreros, (2003) Tyrosine phosphorylation of plakoglobin causes contrary effects on its association with desmosomes and adherens junction components and modulates beta-catenin-mediated transcription. *Mol Cell Biol* **23**: 7391-7402.
- Mirzadeh, Z., F. T. Merkle, M. Soriano-Navarro, J. M. Garcia-Verdugo & A. Alvarez-Buylla, (2008) Neural stem cells confer unique pinwheel architecture to the ventricular surface in neurogenic regions of the adult brain. *Cell Stem Cell* **3**: 265-278.
- Misson, J. P., C. P. Austin, T. Takahashi, C. L. Cepko & V. S. Caviness, Jr., (1991) The alignment of migrating neural cells in relation to the murine neopallial radial glial fiber system. *Cereb Cortex* **1**: 221-229.
- Miyata, T., A. Kawaguchi, K. Saito, M. Kawano, T. Muto & M. Ogawa, (2004) Asymmetric production of surface-dividing and non-surface-dividing cortical progenitor cells. *Development* **131**: 3133-3145.
- Mizuguchi, R., M. Sugimori, H. Takebayashi, H. Kosako, M. Nagao, S. Yoshida, Y. Nabeshima, K. Shimamura & M. Nakafuku, (2001) Combinatorial roles of olig2 and neurogenin2 in the coordinated induction of pan-neuronal and subtype-specific properties of motoneurons. *Neuron* **31**: 757-771.

- Montcouquiol, M., E. B. Crenshaw, 3rd & M. W. Kelley, (2006) Noncanonical Wnt signaling and neural polarity. *Annu Rev Neurosci* **29**: 363-386.
- Mori, H., T. Fujitani, Y. Kanemura, M. Kino-Oka & M. Taya, (2007) Observational examination of aggregation and migration during early phase of neurosphere culture of mouse neural stem cells. *J Biosci Bioeng* **104**: 231-234.
- Mori, T., K. Tanaka, A. Buffo, W. Wurst, R. Kuhn & M. Götz, (2006) Inducible gene deletion in astroglia and radial glia--a valuable tool for functional and lineage analysis. *Glia* **54**: 21-34.
- Morshead, C. M., B. A. Reynolds, C. G. Craig, M. W. McBurney, W. A. Staines, D. Morassutti, S. Weiss & D. van der Kooy, (1994) Neural stem cells in the adult mammalian forebrain: a relatively quiescent subpopulation of subependymal cells. *Neuron* **13**: 1071-1082.
- Mutch, C. A., N. Funatsu, E. S. Monuki & A. Chenn, (2009) Beta-catenin signaling levels in progenitors influence the laminar cell fates of projection neurons. *J Neurosci* **29**: 13710-13719.
- Nagai-Tamai, Y., K. Mizuno, T. Hirose, A. Suzuki & S. Ohno, (2002) Regulated protein-protein interaction between aPKC and PAR-3 plays an essential role in the polarization of epithelial cells. *Genes Cells* **7**: 1161-1171.
- Nelson, C. M. & C. S. Chen, (2003) VE-cadherin simultaneously stimulates and inhibits cell proliferation by altering cytoskeletal structure and tension. *J Cell Sci* **116**: 3571-3581.
- Ng, K. L., J. D. Li, M. Y. Cheng, F. M. Leslie, A. G. Lee & Q. Y. Zhou, (2005) Dependence of olfactory bulb neurogenesis on prokineticin 2 signaling. *Science* **308**: 1923-1927.
- Nieto, M., E. S. Monuki, H. Tang, J. Imiola, N. Habast, S. J. Khoury, J. Cunningham, M. Gotz & C. A. Walsh, (2004) Expression of Cux-1 and Cux-2 in the subventricular zone and upper layers II-IV of the cerebral cortex. *J Comp Neurol* **479**: 168-180.
- Ninkovic, J., T. Mori & M. Gotz, (2007) Distinct modes of neuron addition in adult mouse neurogenesis. *J Neurosci* **27**: 10906-10911.
- Noctor, S. C., V. Martinez-Cerdeno, L. Ivic & A. R. Kriegstein, (2004) Cortical neurons arise in symmetric and asymmetric division zones and migrate through specific phases. *Nat Neurosci* **7**: 136-144.
- Noctor, S. C., V. Martinez-Cerdeno & A. R. Kriegstein, (2008) Distinct behaviors of neural stem and progenitor cells underlie cortical neurogenesis. *J Comp Neurol* **508**: 28-44.
- Nolan, M. E., V. Aranda, S. Lee, B. Lakshmi, S. Basu, D. C. Allred & S. K. Muthuswamy, (2008) The polarity protein Par6 induces cell proliferation and is overexpressed in breast cancer. *Cancer Res* **68**: 8201-8209.
- Nolte, C., M. Matyash, T. Pivneva, C. G. Schipke, C. Ohlemeyer, U. K. Hahnisch, F. Kirchhoff & H. Kettenmann, (2001) GFAP promoter-controlled EGF P-expressing transgenic mice: a tool to visualize astrocytes and astrogliosis in living brain tissue. *Glia* **33**: 72-86.
- Nose, A., A. Nagafuchi & M. Takeichi, (1988) Expressed recombinant cadherins mediate cell sorting in model systems. *Cell* **54**: 993-1001.
- Nusse, R. & H. E. Varmus, (1982) Many tumors induced by the mouse mammary tumor virus contain a provirus integrated in the same region of the host genome. *Cell* **31**: 99-109.
- Ono, Y., T. Fujii, K. Ogita, U. Kikkawa, K. Igarashi & Y. Nishizuka, (1989) Protein kinase C zeta subspecies from rat brain: its structure, expression, and properties. *Proc Natl Acad Sci U S A* **86**: 3099-3103.
- Ory, D. S., B. A. Neugeboren & R. C. Mulligan, (1996) A stable human-derived packaging cell line for production of high titer retrovirus/vesicular stomatitis virus G pseudotypes. *Proc Natl Acad Sci U S A* **93**: 11400-11406.

References

- Palma, V., D. A. Lim, N. Dahmane, P. Sanchez, T. C. Brionne, C. D. Herzberg, Y. Gitton, A. Carleton, A. Alvarez-Buylla & A. Ruiz i Altaba, (2005) Sonic hedgehog controls stem cell behavior in the postnatal and adult brain. *Development* **132**: 335-344.
- Panzanelli, P., J. M. Fritschy, Y. Yanagawa, K. Obata & M. Sassoe-Pognetto, (2007) GABAergic phenotype of periglomerular cells in the rodent olfactory bulb. *J Comp Neurol* **502**: 990-1002.
- Park, C., W. Falls, J. H. Finger, C. M. Longo-Guess & S. L. Ackerman, (2002) Deletion in *Catn2*, encoding alpha N-catenin, causes cerebellar and hippocampal lamination defects and impaired startle modulation. *Nat Genet* **31**: 279-284.
- Parras, C. M., R. Galli, O. Britz, S. Soares, C. Galichet, J. Battiste, J. E. Johnson, M. Nakafuku, A. Vescovi & F. Guillemot, (2004) Mash1 specifies neurons and oligodendrocytes in the postnatal brain. *EMBO J* **23**: 4495-4505.
- Parrish-Aungst, S., M. T. Shipley, F. Erdelyi, G. Szabo & A. C. Puche, (2007) Quantitative analysis of neuronal diversity in the mouse olfactory bulb. *J Comp Neurol* **501**: 825-836.
- Peretto, P., A. Merighi, A. Fasolo & L. Bonfanti, (1997) Glial tubes in the rostral migratory stream of the adult rat. *Brain Res Bull* **42**: 9-21.
- Perez-Moreno, M. & E. Fuchs, (2006) Catenins: keeping cells from getting their signals crossed. *Dev Cell* **11**: 601-612.
- Perez-Moreno, M., C. Jamora & E. Fuchs, (2003) Sticky business: orchestrating cellular signals at adherens junctions. *Cell* **112**: 535-548.
- Petreanu, L. & A. Alvarez-Buylla, (2002) Maturation and death of adult-born olfactory bulb granule neurons: role of olfaction. *J Neurosci* **22**: 6106-6113.
- Petryniak, M. A., G. B. Potter, D. H. Rowitch & J. L. Rubenstein, (2007) Dlx1 and Dlx2 control neuronal versus oligodendroglial cell fate acquisition in the developing forebrain. *Neuron* **55**: 417-433.
- Piccolo, S., Y. Sasai, B. Lu & E. M. De Robertis, (1996) Dorsoventral patterning in *Xenopus*: inhibition of ventral signals by direct binding of chordin to BMP-4. *Cell* **86**: 589-598.
- Pinching, A. J. & T. P. Powell, (1971) The neuropil of the glomeruli of the olfactory bulb. *J Cell Sci* **9**: 347-377.
- Pinto, L. & M. Götz, (2007) Radial glial cell heterogeneity--the source of diverse progeny in the CNS. *Prog Neurobiol* **83**: 2-23.
- Pokutta, S., F. Drees, S. Yamada, W. J. Nelson & W. I. Weis, (2008) Biochemical and structural analysis of alpha-catenin in cell-cell contacts. *Biochem Soc Trans* **36**: 141-147.
- Porteus, M. H., A. Bulfone, J. K. Liu, L. Puelles, L. C. Lo & J. L. Rubenstein, (1994) DLX-2, MASH-1, and MAP-2 expression and bromodeoxyuridine incorporation define molecularly distinct cell populations in the embryonic mouse forebrain. *J Neurosci* **14**: 6370-6383.
- Posthaus, H., L. Williamson, D. Baumann, R. Kemler, R. Caldelari, M. M. Suter, H. Schwarz & E. Muller, (2002) beta-Catenin is not required for proliferation and differentiation of epidermal mouse keratinocytes. *J Cell Sci* **115**: 4587-4595.
- Price, J. L. & T. P. Powell, (1970) The mitral and short axon cells of the olfactory bulb. *J Cell Sci* **7**: 631-651.
- Rasin, M. R., V. R. Gazula, J. J. Breunig, K. Y. Kwan, M. B. Johnson, S. Liu-Chen, H. S. Li, L. Y. Jan, Y. N. Jan, P. Rakic & N. Sestan, (2007) Numb and Numbl are required for maintenance of cadherin-based adhesion and polarity of neural progenitors. *Nat Neurosci* **10**: 819-827.
- Rayasam, G. V., V. K. Tulasia, R. Sodhi, J. A. Davis & A. Ray, (2009) Glycogen synthase kinase-3: more than a namesake. *Br J Pharmacol* **156**: 885-898.

- Redies, C. & M. Takeichi, (1996) Cadherins in the developing central nervous system: an adhesive code for segmental and functional subdivisions. *Dev Biol* **180**: 413-423.
- Reynolds, B. A. & S. Weiss, (1992) Generation of neurons and astrocytes from isolated cells of the adult mammalian central nervous system. *Science* **255**: 1707-1710.
- Rodriguez-Boulan, E. & W. J. Nelson, (1989) Morphogenesis of the polarized epithelial cell phenotype. *Science* **245**: 718-725.
- Rubenstein, J. L., S. Anderson, L. Shi, E. Miyashita-Lin, A. Bulfone & R. Hevner, (1999) Genetic control of cortical regionalization and connectivity. *Cereb Cortex* **9**: 524-532.
- Rubinfeld, B., I. Albert, E. Porfiri, C. Fiol, S. Munemitsu & P. Polakis, (1996) Binding of GSK3 β to the APC-beta-catenin complex and regulation of complex assembly. *Science* **272**: 1023-1026.
- Ruel, L., V. Stambolic, A. Ali, A. S. Manoukian & J. R. Woodgett, (1999) Regulation of the protein kinase activity of Shaggy(Zeste-white3) by components of the wingless pathway in Drosophila cells and embryos. *J Biol Chem* **274**: 21790-21796.
- Saghatelian, A., A. de Chevigny, M. Schachner & P. M. Lledo, (2004) Tenascin-R mediates activity-dependent recruitment of neuroblasts in the adult mouse forebrain. *Nat Neurosci* **7**: 347-356.
- Salomon, D., P. A. Sacco, S. G. Roy, I. Simcha, K. R. Johnson, M. J. Wheelock & A. Ben-Ze'ev, (1997) Regulation of beta-catenin levels and localization by overexpression of plakoglobin and inhibition of the ubiquitin-proteasome system. *J Cell Biol* **139**: 1325-1335.
- Sauer, F. C., (1935) Mitosis in the neural tube. *J. Comp. Neur.* **62**: 377-405.
- Sawamoto, K., H. Wichterle, O. Gonzalez-Perez, J. A. Cholfin, M. Yamada, N. Spassky, N. S. Murcia, J. M. Garcia-Verdugo, O. Marin, J. L. Rubenstein, M. Tessier-Lavigne, H. Okano & A. Alvarez-Buylla, (2006) New neurons follow the flow of cerebrospinal fluid in the adult brain. *Science* **311**: 629-632.
- Scardigli, R., C. Schuurmans, G. Gradwohl & F. Guillemot, (2001) Crossregulation between Neurogenin2 and pathways specifying neuronal identity in the spinal cord. *Neuron* **31**: 203-217.
- Schmid, M. T., (2007) Comparative analysis of the function of alpha- and beta-catenin in cerebral cortical development, Dissertation *Media TUM*: 1-140.
- Schmid, M. T., F. Weinaudy, M. Wilsch-Bräuninger, M. Irmeler, J. Beckers, W. B. Huttner, L. Godinho & M. Götz, (in preparation) The role of α -E-catenin in cortical development: stem cell-specific effects on cell proliferation
- Schmidt-Suppran, M. & K. Rajewsky, (2007) Vagaries of conditional gene targeting. *Nat Immunol* **8**: 665-668.
- Schuurmans, C., O. Armant, M. Nieto, J. M. Stenman, O. Britz, N. Klenin, C. Brown, L. M. Langevin, J. Seibt, H. Tang, J. M. Cunningham, R. Dyck, C. Walsh, K. Campbell, F. Polleux & F. Guillemot, (2004) Sequential phases of cortical specification involve Neurogenin-dependent and -independent pathways. *EMBO J* **23**: 2892-2902.
- Sears, R., F. Nuckolls, E. Haura, Y. Taya, K. Tamai & J. R. Nevins, (2000) Multiple Ras-dependent phosphorylation pathways regulate Myc protein stability. *Genes Dev* **14**: 2501-2514.
- Seki, T. & Y. Arai, (1993) Highly polysialylated NCAM expression in the developing and adult rat spinal cord. *Brain Res Dev Brain Res* **73**: 141-145.
- Selbie, L. A., C. Schmitz-Peiffer, Y. Sheng & T. J. Biden, (1993) Molecular cloning and characterization of PKC iota, an atypical isoform of protein kinase C derived from insulin-secreting cells. *J Biol Chem* **268**: 24296-24302.

References

- Seroogy, K. B., C. M. Gall, D. C. Lee & H. I. Kornblum, (1995) Proliferative zones of postnatal rat brain express epidermal growth factor receptor mRNA. *Brain Res* **670**: 157-164.
- Sfakianos, J., A. Togawa, S. Maday, M. Hull, M. Pypaert, L. Cantley, D. Toomre & I. Mellman, (2007) Par3 functions in the biogenesis of the primary cilium in polarized epithelial cells. *J Cell Biol* **179**: 1133-1140.
- Shaw, M. & P. Cohen, (1999) Role of protein kinase B and the MAP kinase cascade in mediating the EGF-dependent inhibition of glycogen synthase kinase 3 in Swiss 3T3 cells. *FEBS Lett* **461**: 120-124.
- Shen, Q., Y. Wang, E. Kokovay, G. Lin, S. M. Chuang, S. K. Goderie, B. Roysam & S. Temple, (2008) Adult SVZ stem cells lie in a vascular niche: a quantitative analysis of niche cell-cell interactions. *Cell Stem Cell* **3**: 289-300.
- Shepherd, G. M., (1972) Synaptic organization of the mammalian olfactory bulb. *Physiol Rev* **52**: 864-917.
- Shi, S. R., M. E. Key & K. L. Kalra, (1991) Antigen retrieval in formalin-fixed, paraffin-embedded tissues: an enhancement method for immunohistochemical staining based on microwave oven heating of tissue sections. *J Histochem Cytochem* **39**: 741-748.
- Shoukimas, G. M. & J. W. Hinds, (1978) The development of the cerebral cortex in the embryonic mouse: an electron microscopic serial section analysis. *J Comp Neurol* **179**: 795-830.
- Singec, I., R. Knöth, R. P. Meyer, J. Maciaczyk, B. Volk, G. Ninkovic, M. Frotscher & E. Y. Snyder, (2006) Defining the actual sensitivity and specificity of the neurosphere assay in stem cell biology. *Nat Methods* **3**: 801-806.
- Smith, A. N., L. A. Miller, N. Song, M. M. Taketo & R. A. Lang, (2005) The duality of beta-catenin function: a requirement in lens morphogenesis and signaling suppression of lens fate in periodic ectoderm. *Dev Biol* **285**: 477-489.
- Snapyan, M., M. Lemasson, M. S. Brill, M. Blais, M. Massouh, J. Ninkovic, C. Gravel, F. Berthod, M. Götz, P. A. Barker, A. Parent & A. Saghatelian, (2009) Vasculature guides migrating neuronal precursors in the adult mammalian forebrain via brain-derived neurotrophic factor signaling. *J Neurosci* **29**: 4172-4188.
- Spemann, H. & H. Mangold, (1924) Über die Induktion von Embryonalanlagen durch Implantation artfremder Organisatoren. - Induction of embryonic primordia by implantation of organizers from a different species. *W. Roux' Arch. f. Entw. d. Organism. u. mikrosk. Anat.* **100**: 599-638.
- Srinivas, S., T. Watanabe, C. S. Lin, C. M. Williams, Y. Tanabe, T. M. Jessell & F. Costantini, (2001) Cre reporter strains produced by targeted insertion of EYFP and ECFP into the ROSA26 locus. *BMC Dev Biol* **1**: 4.
- Stenman, J. M., B. Wang & K. Campbell, (2003) Tlx controls proliferation and patterning of lateral telencephalic progenitor domains. *J Neurosci* **23**: 10568-10576.
- Stocker, A. M. & A. Chenn, (2006) Differential expression of alpha-E-catenin and alpha-N-catenin in the developing cerebral cortex. *Brain Res* **1073-1074**: 151-158.
- Stocker, A. M. & A. Chenn, (2009) Focal reduction of alphaE-catenin causes premature differentiation and reduction of beta-catenin signaling during cortical development. *Dev Biol* **328**: 66-77.
- Stoykova, A., M. Götz, P. Gruss & J. Price, (1997) Pax6-dependent regulation of adhesive patterning, R-cadherin expression and boundary formation in developing forebrain. *Development* **124**: 3765-3777.
- Stuhmer, T., L. Puelles, M. Ekker & J. L. Rubenstein, (2002) Expression from a Dlx gene enhancer marks adult mouse cortical GABAergic neurons. *Cereb Cortex* **12**: 75-85.
- Tachibana, K., H. Nakanishi, K. Mandai, K. Ozaki, W. Ikeda, Y. Yamamoto, A. Nagafuchi, S. Tsukita & Y. Takai, (2000) Two cell adhesion molecules, nectin and cadherin, interact through their cytoplasmic domain-associated proteins. *J Cell Biol* **150**: 1161-1176.

- Takahashi, T., J. P. Misson & V. S. Caviness, Jr., (1990) Glial process elongation and branching in the developing murine neocortex: a qualitative and quantitative immunohistochemical analysis. *J Comp Neurol* **302**: 15-28.
- Takaishi, K., T. Sasaki, H. Kotani, H. Nishioka & Y. Takai, (1997) Regulation of cell-cell adhesion by rac and rho small G proteins in MDCK cells. *J Cell Biol* **139**: 1047-1059.
- Takekuni, K., W. Ikeda, T. Fujito, K. Morimoto, M. Takeuchi, M. Monden & Y. Takai, (2003) Direct binding of cell polarity protein PAR-3 to cell-cell adhesion molecule nectin at neuroepithelial cells of developing mouse. *J Biol Chem* **278**: 5497-5500.
- Tamai, K., M. Semenov, Y. Kato, R. Spokony, C. Liu, Y. Katsuyama, F. Hess, J. P. Saint-Jeannet & X. He, (2000) LDL-receptor-related proteins in Wnt signal transduction. *Nature* **407**: 530-535.
- Tarabykin, V., A. Stoykova, N. Usman & P. Gruss, (2001) Cortical upper layer neurons derive from the subventricular zone as indicated by Svet1 gene expression. *Development* **128**: 1983-1993.
- Tavazoie, M., L. Van der Veken, V. Silva-Vargas, M. Louissaint, L. Colonna, B. Zaidi, J. M. Garcia-Verdugo & F. Doetsch, (2008) A specialized vascular niche for adult neural stem cells. *Cell Stem Cell* **3**: 279-288.
- Togashi, H., K. Abe, A. Mizoguchi, K. Takaoka, O. Chisaka & M. Takeichi, (2002) Cadherin regulate s dendritic spine morphogenesis. *Neuron* **35**: 77-89.
- Toida, K., K. Kosaka, Y. Aika & T. Kosaka, (2000) Chemically defined neuron groups and their subpopulations in the glomerular layer of the rat main olfactory bulb--IV. Intraglomerular synapses of tyrosine hydroxylase-immunoreactive neurons. *Neuroscience* **101**: 11-17.
- Toresson, H. & K. Campbell, (2001) A role for Gsh1 in the developing striatum and olfactory bulb of Gsh2 mutant mice. *Development* **128**: 4769-4780.
- Tramontin, A. D., J. M. Garcia-Verdugo, D. A. Lim & A. Alvarez-Buylla, (2003) Postnatal development of radial glia and the ventricular zone (VZ): a continuum of the neural stem cell compartment. *Cereb Cortex* **13**: 580-587.
- Tripathi, P., (2009) Isolation of multipotent astroglia from the adult stem cell niche and the injured brain, Dissertation *Digitale Hochschulschriften der LMU*: 1-141.
- Tripathi, P., R. Beckervordersandforth-Bonk, J. Ninkovic, E. Bayam, A. Lepier, F. Kirchoff, J. Hirrlinger, A. Haslinger, D. C. Lie, J. Beckers, M. Irmler & M. Götz, (in preparation) *In vivo* fate mapping and expression analysis of prospectively isolated adult neural stem cells from the mouse subependymal zone.
- Uchida, N., K. Shimamura, S. Miyatani, N. G. Copeland, D. J. Gilbert, N. A. Jenkins & M. Takeichi, (1994) Mouse alpha N-catenin: two isoforms, specific expression in the nervous system, and chromosomal localization of the gene. *Dev Biol* **163**: 75-85.
- Uemura, M. & M. Takeichi, (2006) Alpha N-catenin deficiency causes defects in axon migration and nuclear organization in restricted regions of the mouse brain. *Dev Dyn* **235**: 2559-2566.
- Vasioukhin, V., C. Bauer, L. Degenstein, B. Wise & E. Fuchs, (2001) Hyperproliferation and defects in epithelial polarity upon conditional ablation of alpha-catenin in skin. *Cell* **104**: 605-617.
- Ventura, R. E. & J. E. Goldman, (2007) Dorsal radial glia generate olfactory bulb interneurons in the postnatal murine brain. *J Neurosci* **27**: 4297-4302.
- Waclaw, R. R., Z. J. Allen, 2nd, S. M. Bell, F. Erdelyi, G. Szabo, S. S. Potter & K. Campbell, (2006) The zinc finger transcription factor Sp8 regulates the generation and diversity of olfactory bulb interneurons. *Neuron* **49**: 503-516.

References

Watabe-Uchida, M., N. Uchida, Y. Imamura, A. Nagafuchi, K. Fujimoto, T. Uemura, S. Vermeulen, F. van Roy, E. D. Adamson & M. Takeichi, (1998) alpha-Catenin-vinculin interactions to organize the apical junctional complex in epithelial cells. *J Cell Biol* **142**: 847-857.

Watabe, M., A. Nagafuchi, S. Tsukita & M. Takeichi, (1994) Induction of polarized cell-cell association and retardation of growth by activation of the E-cadherin-catenin adhesion system in a dispersed carcinoma line. *J Cell Biol* **127**: 247-256.

Weickert, C. S., M. J. Webster, S. M. Colvin, M. M. Herman, T. M. Hyde, D. R. Weinberger & J. E. Kleinman, (2000) Localization of epidermal growth factor receptors and putative neuroblasts in human subependymal zone. *J Comp Neurol* **423**: 359-372.

Weigmann, A., D. Corbeil, A. Hellwig & W. B. Huttner, (1997) Prominin, a novel microvilli-specific polytopic membrane protein of the apical surface of epithelial cells, is targeted to plasmalemmal protrusions of non-epithelial cells. *Proc Natl Acad Sci U S A* **94**: 12425-12430.

Wichterle, H., J. M. Garcia-Verdugo & A. Alvarez-Buylla, (1997) Direct evidence for homotypic, glia-independent neuronal migration. *Neuron* **18**: 779-791.

Wichterle, H., D. H. Turnbull, S. Nery, G. Fishell & A. Alvarez-Buylla, (2001) In utero fate mapping reveals distinct migratory pathways and fates of neurons born in the mammalian basal forebrain. *Development* **128**: 3759-3771.

Willaime-Morawek, S., R. M. Seaberg, C. Batista, E. Labbe, L. Attisano, J. A. Gorski, K. R. Jones, A. Kam, C. M. Morshead & D. van der Kooy, (2006) Embryonic cortical neural stem cells migrate ventrally and persist as postnatal striatal stem cells. *J Cell Biol* **175**: 159-168.

Williams, R. W., (2000) Mapping genes that modulate mouse brain development: a quantitative genetic approach. *Results Probl Cell Differ* **30**: 21-49.

Wiznerowicz, M. & D. Trono, (2003) Conditional suppression of cellular genes: lentivirus vector-mediated drug-inducible RNA interference. *J Virol* **77**: 8957-8961.

Woodgett, J. R., (2001) Judging a protein by more than its name: GSK-3. *Sci STKE* **2001**: re12.

Woodhead, G. J., C. A. Mutch, E. C. Olson & A. Chenn, (2006) Cell-autonomous beta-catenin signaling regulates cortical precursor proliferation. *J Neurosci* **26**: 12620-12630.

Worthington, W. C., Jr. & R. S. Cathcart, 3rd, (1963) Ependymal cilia: distribution and activity in the adult human brain. *Science* **139**: 221-222.

Wu, S. X., S. Goebbels, K. Nakamura, K. Kometani, N. Minato, T. Kaneko, K. A. Nave & N. Tamamaki, (2005) Pyramidal neurons of upper cortical layers generated by NEX-positive progenitor cells in the subventricular zone. *Proc Natl Acad Sci U S A* **102**: 17172-17177.

Wu, X., F. Quondammatteo, T. Lefever, A. Czuchra, H. Meyer, A. Chrostek, R. Paus, L. Langbein & C. Brakebusch, (2006) Cdc42 controls progenitor cell differentiation and beta-catenin turnover in skin. *Genes Dev* **20**: 571-585.

Yamada, S., S. Pokutta, F. Drees, W. I. Weis & W. J. Nelson, (2005) Deconstructing the cadherin-catenin-actin complex. *Cell* **123**: 889-901.

Yamanaka, T., Y. Horikoshi, Y. Sugiyama, C. Ishiyama, A. Suzuki, T. Hirose, A. Iwamatsu, A. Shinohara & S. Ohno, (2003) Mammalian Lgl forms a protein complex with PAR-6 and aPKC independently of PAR-3 to regulate epithelial cell polarity. *Curr Biol* **13**: 734-743.

Yamanaka, T., Y. Horikoshi, A. Suzuki, Y. Sugiyama, K. Kitamura, R. Maniwa, Y. Nagai, A. Yamashita, T. Hirose, H. Ishikawa & S. Ohno, (2001) PAR-6 regulates aPKC activity in a novel way and mediates cell-cell contact-induced formation of the epithelial junctional complex. *Genes Cells* **6**: 721-731.

- Yin, T. & K. J. Green, (2004) Regulation of desmosome assembly and adhesion. *Semin Cell Dev Biol* **15**: 665-677.
- Yoshida, M., Y. Suda, I. Matsuo, N. Miyamoto, N. Takeda, S. Kuratani & S. Aizawa, (1997) Emx1 and Emx2 functions in development of dorsal telencephalon. *Development* **124**: 101-111.
- Young, K. M., M. Fogarty, N. Kessaris & W. D. Richardson, (2007) Subventricular zone stem cells are heterogeneous with respect to their embryonic origins and neurogenic fates in the adult olfactory bulb. *J Neurosci* **27**: 8286-8296.
- Yu, J. M., J. H. Kim, G. S. Song & J. S. Jung, (2006) Increase in proliferation and differentiation of neural progenitor cells isolated from postnatal and adult mice brain by Wnt-3a and Wnt-5a. *Mol Cell Biochem* **288**: 17-28.
- Zhong, C., M. S. Kinch & K. Burridge, (1997) Rho-stimulated contractility contributes to the fibroblastic phenotype of Ras-transformed epithelial cells. *Mol Biol Cell* **8**: 2329-2344.
- Zhong, W. & W. Chia, (2008) Neurogenesis and asymmetric cell division. *Curr Opin Neurobiol* **18**: 4-11.
- Zhou, C. J., U. Borello, J. L. Rubenstein & S. J. Pleasure, (2006) Neuronal production and precursor proliferation defects in the neocortex of mice with loss of function in the canonical Wnt signaling pathway. *Neuroscience* **142**: 1119-1131.
- Zhou, J., J. Qu, X. P. Yi, K. Graber, L. Huber, X. Wang, A. M. Gerdes & F. Li, (2007) Upregulation of gamma-catenin compensates for the loss of beta-catenin in adult cardiomyocytes. *Am J Physiol Heart Circ Physiol* **292**: H270-276.
- Zimmerman, L. B., J. M. De Jesus-Escobar & R. M. Harland, (1996) The Spemann organizer signal noggin binds and inactivates bone morphogenetic protein 4. *Cell* **86**: 599-606.
- Zufferey, R., D. Nagy, R. J. Mandel, L. Naldini & D. Trono, (1997) Multiplication of self-replicating lentiviral vectors achieves efficient gene delivery in vivo. *Nat Biotechnol* **15**: 871-875.

7 Acknowledgements

Without question, this work would not have been accomplished without the assistance and advises of many people. I am indebted to the whole Götz lab for their intelligence, experience, and willingness to share their knowledge.

In particular, I would like to deeply thank **Prof. Dr. Magdalena Götz** for guiding, supporting and encouraging me during the last few years. I appreciate her many useful comments, all her time that she spend to discuss my projects and her keen-witted advices on this work. I have grown a lot as a scientist during my time in Munich, and Magdalena and her lab environment have been greatly responsible.

I furthermore have to thank, **Dr. Marie-Theres Schmid**, who introduced me to the field of developmental neurobiology and trained me especially at the beginning of this work.

I am very grateful to my intellectual guide, **Dr. Jovica Nincovic**, with whom I've shared many interesting conversations about science, that have been essential to the development of my thought process during the past few years. I am thankful that he always had an ear for my questions and prevented me from overdoing some experiments.

A very, very big thank-you goes to our technicians in the lab: **Andrea Steiner, Angelika Waiser, Timo Öztürk, Detlef Franzen** and **Emily Baumgart Violette**. They take care of every need, problem, empty buffer bottle, and all the details that we tend to forget. Without your technical help, especially in the last months, I never would have managed all the tissue culture experiments, genotypings and cryostat cuttings.

Furthermore, I want to thank my great colleagues that have become also very good friends during my time in the Götz lab. **Christian Böhlinger**, who started with me this marathon and went with me through this bumpy road until reaching the final goal. I am very grateful to my girls at the Helholtz Zentrum: **Dr. Ruth Beckervordersandforth, Tessa Walcher, Dr. Maki Asami, Dr. Pia Johansson, Joana Barbosa, Dr. Silvia Capello** and **Lena Beilschmidt**. You all made my life much happier, provided a warm working atmosphere, interesting scientific discussions and also good nights outside the lab. Special thanks also to **Gregor Pilz** and **Ronny Stahl**.

Administrative life in the Götz Lab runs smoothly thanks to the diligent work of our secretaries **Elsa Melo** and **Donna Thomson**.

Außerdem danke ich von ganzem Herzen meiner Familie, besonders meinen Großeltern und meinem Freund Dirk, für ihre Liebe, Geduld und Unterstützung.

CURRICULUM VITAE

Persönliche Daten

Name: Franziska Weinandy
Geburtsdatum: 9. April 1980
Geburtsort: Jena
Staatsangehörigkeit: Deutsch
Dienstanschrift: Helmholtz-Zentrum München, ISF, Ingolstädter Landstraße 1,
D-85764 Neuherberg, Deutschland
E-Mail: weinandy_franziska@web.de

Wissenschaftliche Erfahrung

2006 - heute **Doktorarbeit** im Labor von Prof. Dr. Magdalena Götz am Institut für Stammzellforschung, Helmholtz Zentrum München, Deutschland
Towards an Understanding of the Role of Apical Polarity Molecules in Neural Stem Cells and Neurogenesis
Technische Universität München, Lehrstuhl für Entwicklungsgenetik, Deutschland

2004 – 2005 **Diplomarbeit** im Labor von Prof. Dr. Isabelle Mansuy am Brain Research Institute, Universität von Zürich, Schweiz
Comprehensive Phosphoproteomic Analyses in Mouse Cortex by Nano-Flow Liquid Chromatography-Tandem Mass Spectrometry

2002 – 2004 **Wissenschaftliche Hilfskraft** im Labor von Prof. Dr. Otto Witte Klinik für Neurologie, Friedrich Schiller Universität Jena, Deutschland

Bildungsgang

16.12. 2005 Erwerb des akademischen Grads Diplombiologin

1999 – 2005 Biologiestudium an der Friedrich Schiller Universität Jena, Deutschland

1998 – 1999 Beginn der Krankenschwesterlehre im Universitätsklinikum der Friedrich Schiller Universität Jena, Deutschland

09. Juli 1998 Erwerb der Allgemeinen Hochschulreife

1992 – 1998 Friedrich Schiller Gymnasium Eisenberg, Deutschland

1986 – 1992 Staatliche Regelschule Eisenberg-West, Deutschland

Publikationen

Munton R.P., Tweedie-Cullen R., Livingstone-Zatchej M., **Weinandy F.**, Waidelich M., Longo D., Gehrig P., Potthast F., Rutishauser D., Gerrits B., Panse C., Schlapbach R., Mansuy I.M. (2007). Qualitative and quantitative analyses of protein phosphorylation in naive and stimulated mouse synaptosomal preparations. *Mol Cell Proteomics*. 6(2):283-93.

Frahm C., Haupt C., **Weinandy F.**, Siegel G., Bruehl C., Witte OW.(2004). Regulation of GABA transporter mRNA and protein after photothrombotic infarct in rat brain. *J. Comp. Neurol.* 478(2), 176-88.